Algebraic Methods for Chemical Reaction Networks with Extrinsic Noise



Michael Felix Adamer

Merton College

University of Oxford

A thesis submitted for the degree of

Doctor of Philosophy in Mathematics

Trinity 2019

To my parents,
for their endless support, patience, and encouragement.

Acknowledgements

First and foremost I would like to express my gratitude to my supervisors, Eamonn Gaffney, Heather Harrington, and Thomas Woolley. I am eternally grateful for their guidance in academic matters and beyond. I would also like to thank Martin Helmer, who was my collaborator on a substantial part of this thesis, for his tireless effort to explain elementary concepts to me. Not to be missed from the list is also Philip Maini who, through his kindness and wittiness, makes the Wolfson Centre of Mathematical Biology such a fantastic place to do research.

I am thankful for the many people who provided intellectual stimulation, in particular, the wider chemical reaction networks community and the organisers of various conferences I had the opportunity to attend. Many a hard working day has been brightened by my group mates and I will miss Thursday cake and group lunches. I am grateful to have had such great office mates, who always listened to my rants. The Doctoral Training Centre did many great things for me, but most importantly, it provided a community and I am thankful for all the amazing people I met through it, in particular Bartosz, Jared, Daniel, and Simone.

My time at Oxford has been greatly enriched by all the people who spent part of this journey with me. Special thanks goes to the Oxford University Mountaineering Club, the Oxford Austrian Society, and their members. I would like to thank my parents, Rosemarie Adamer and Rudolf Haller for their tireless support. Special mention should also go to the rest of my family, in particular, my brother Paul. I am grateful for the support of my friends Christoph, Fabian, Manuel, and Stefan back home in Austria who, despite me being on a cold, rainy island for most of the year, have always provided company and support when I needed it. I will also never forget the rock gigs Joel and I attended. Neither will I stop being grateful for all the support of Alannah Burns and her incredible life insights.

Finally, I would like to thank Merton College for providing a fixed point during my entire time at Oxford. Despite its reputation, to me it was never the place "where fun goes to die", but the setting of many good memories.

Abstract

Many biological mechanisms can be understood as a complex interaction of chemical reactions. In order to explain the wealth of biochemical phenomena in systems biology, a sophisticated analytic framework for these chemical reaction networks is needed. This thesis investigates the role of extrinsic fluctuations in biochemical reaction mechanisms and develops mathematical tools for the systematic study of extrinsic noise.

The first part of this thesis studies variability in biological processes which manifests itself as randomised rate constants. This variability can stem from many sources, such as different cellular environments, or upstream stochastic effects, which directly influence the reaction network under study. As variability is often modelled as constant, but unknown parameters, parameter-free algebraic methods are developed in this thesis to study large classes of chemical reaction networks named families. In particular, these methods allow for parameter-free model rejection, or model testing and give upper bounds on the algebraic complexity of these tasks. Further, a parameter-free result on the capability of multistationarity in infinite classes of networks is proved.

The second part of this thesis studies time-varying extrinsic noise, such as fluctuating experimental conditions, which directly influences the reaction rates. A particular focus is on upstream stochastic networks, propagating their stochasticity into the main network under study. Crucially, as the stochasticity in the system is imposed externally, the analysis of such models is not subject to the constraints of stochastic methods. While intrinsic noise imposes rigid restrictions on the modelling process, it is shown how in extrinsic noise models the deterministic model structure stays intact. Consequently, in this thesis, algebraic methods for deterministic networks are extended to be applied to networks subject to extrinsic noise in order to find oscillations and preclude stochastic switching. The effects of intrinsic stochasticity are also compared to the effects of extrinsic noise and the framework is extended to correlated (coloured) noise.

Contents

1 Introduction **1**

1.1 Spatial vs. Non-spatial Models 5

1.2 Deterministic vs. Stochastic Models 8

1.3 Extrinsic vs. Intrinsic Noise 12

1.4 Contributions 14

2 Mathematical Background **17**

2.1 Deterministic Models 18

2.1.1 Algebraic Methods for Deterministic Models 26

2.1.1.1 Toric Geometry 34

2.2 Stochastic Models 35

2.2.1 The Chemical Master Equation and the Gillespie Algorithm . 35

2.2.2 The Fokker-Planck and Chemical Langevin Equation 38

2.2.2.1 Power Spectral Methods 41

2.3 Deterministic Networks and Extrinsic Noise 42

3 Steady State Invariants and Multistationarity for Families of Toric Reaction Networks **47**

3.1 Families of Reaction Networks 50

3.1.1 Definitions 50

3.1.2 Toric Families 56

3.2 Matroid Theory for Toric Chemical Reaction Networks 63

3.2.1 Experimental Design and Compatibility 68

3.3 Inheritance of Multistationarity for Toric Families 71

3.4 Conclusion 76

4 Complexity of Model Testing of Chemical Reaction Networks with Toric Steady States **78**
4.1 Methods . . . 81
4.1.1 Steady State Varieties in Projective Space . . . 83
4.1.2 Toric Models and Euclidean Distance Degree . . . 85
4.1.3 Real Closest Points . . . 91
4.1.4 Computational Methods . . . 92
4.2 Results . . . 93
4.2.1 Multi-site Phosphorylation Networks . . . 94
4.2.1.1 Processive Networks . . . 94
4.2.1.2 Distributive Networks . . . 96
4.2.2 Sequestration Networks . . . 100
4.2.3 Kinetic Proofreading Networks (McKeithan Model) . . . 102
4.2.4 Multimeric Pore-Forming Toxins . . . 106
4.3 Discussion . . . 108
4.3.1 Restrictions and Extensions . . . 109
4.4 Conclusion . . . 111

5 Graph-Theoretic Methods for Finding Quasi-Cycles in Non-spatial Models with Stochastic Inflow **113**
5.1 Power Spectra for Systems with Intrinsic or Extrinsic Noise . . . 115
5.1.1 The Intrinsic Noise Case . . . 116
5.1.2 The Extrinsic Noise Case . . . 116
5.2 Sturm Chains and Digraphs . . . 118
5.2.1 Sturm Chains for Counting the Maxima of Power Spectra . . . 118
5.2.1.1 Application to the Three-Species Autocatalytic Network 121
5.2.2 Graph Theoretic Approach . . . 124
5.3 Application to Larger Networks . . . 128
5.4 Conclusion . . . 134

6 Coloured Noise From Stochastic Inflows in Reaction-Diffusion Systems **136**
6.1 Theoretical Results . . . 140
6.1.1 Sign Conditions for Monostationarity . . . 140
6.1.2 Stochastic Inflow in Chemical Reaction Networks . . . 141
6.2 Power Spectra for Stochastic Inflows . . . 145
6.2.1 Application to the Schnakenberg System . . . 149

6.3 Computational Results 151
6.3.1 Numerical Methods 151
6.3.2 White Noise 152
6.3.3 Ornstein-Uhlenbeck Noise 153
6.3.4 Power Law Noise 155
6.3.5 Stochastic Auxiliary Networks 158
6.3.6 Mixed Noise 161
6.3.7 Reduced Stochastic Inflows 163
6.4 Conclusion 163

7 Discussion and Future Research **167**
7.1 Summary of Thesis Results 167
7.2 Further Work 169

References **172**

List of Figures

1.1 A road map for the thesis. 14

2.1 The trefoil curve, a plane quartic curve. 28
2.2 The Michaelis-Menten steady state variety. 30
2.3 Simulations of the stochastic production-degradation network. 38
2.4 The power spectrum of the stochastic production-degradation network. 42
2.5 The Brusselator network and its dynamical regimes. 45
2.6 The truncated Gaussian distribution. 46

3.1 A schematic of the family construction 51
3.2 The two-site ladder graph 52

4.1 The polytope $P = \mathrm{conv}(A)$ 90
4.2 Computational run times for multi-site phosphorylation. 99
4.3 The polytope associated to the sequestration network. 102
4.4 Computational run times for the sequestration network. 103
4.5 The polytope associated to the McKeithan network. 105
4.6 Computational run times for the McKeithan network. 105
4.7 Computational run times for the pore network. 108

5.1 The directed graph of the stochastic three species autocatalytic network. 126
5.2 The stochastic phase diagram of the three species autocatalytic network. 128
5.3 Intrinsic and extrinsic noise in the three species autocatalytic network. 129
5.4 The directed graph of the stochastic five species autocatalytic network. 132
5.5 Intrinsic and extrinsic noise in the five species autocatalytic network. 133

6.1 The mechanisms of stochastic inflows. 143
6.2 Deterministic behaviour and white noise in the Schnakenberg system. 154
6.3 The Schnakenberg system with Ornstein-Uhlenbeck noise. 156
6.4 The Schnakenberg system with red noise. 159
6.5 The Schnakenberg system with violet noise. 160

6.6 An example auxiliary network. 160
6.7 The Schnakenberg system with noise generated by an auxiliary network. 162
6.8 The Schnakenberg system with Ornstein-Uhlenbeck and white noise. . 164

List of Tables

4.1 A summary of the computed ED degrees for chemical reaction networks. 80
4.2 Run times of the distributive network. 99
4.3 Reaction network theory metrics for the models. 109

5.1 Factors of the three species autocatalytic network graph. 127

6.1 The main results on various noise colours. 151
6.2 The noise colours of power law noise. 157

List of Symbols

Algebraic Symbols

$\mathbb{K}$	a field
$\mathbb{C}$	the complex numbers
$\mathbb{R}$	the real numbers
$\mathbb{Q}$	the rational numbers
$\mathbb{K}^*$	an algebraic torus
$\overline{\mathbb{K}}$	the algebraic closure of $\mathbb{K}$
$\mathbb{P}^n$	projective n-space
x_i	a variable
R, $\mathbb{K}[x]$	a polynomial ring over $\mathbb{K}$
I	an ideal of R
P	$\begin{cases}\text{prime ideal}\\ \text{polytope (Chapter 4)}\end{cases}$
$\sqrt{I}$	the radical of I
$I : J^\infty$	saturation of I with respect to J
$\mathbb{K}(x)$	the fraction field of $\mathbb{K}[x]$
$\succ$	a term ordering
$\mathtt{LT}$	the leading term
$V(I)$	the variety of I
$\overline{V(I)}$	the projective closure of $V(I)$
π_ℓ	the projection map
$\pi(\kappa)$	the evaluation map
A	the A-matrix (Chapters 2, 3 and 4)
B	binomial exponent matrix (Chapters 3 and 4)
ψ_A	the toric map
ϕ_A	the parameterisation map
X_A	projective toric variety
$\tilde{X}_A$	affine cone of X_A
$\mathcal{G}$	a graph
$\mathbb{V}$	the vertex set of $\mathcal{G}$
$\mathcal{M}$	a matroid
E	$\begin{cases}\text{the edge set of } \mathcal{G}\\ \text{the ground set of } \mathcal{M}\end{cases}$
$\mathcal{I}$	the independent sets of $\mathcal{M}$
$\mathcal{B}$	the matroid bases
ρ	rank function of a matroid
C	a matroid circuit
$\Phi(C)$	Laurent binomial of C
$\overline{\Phi(C)}$	binomial of C
$\boldsymbol{e}$	canonical basis vector of $\mathbb{R}^n$
σ	sign function
$\boldsymbol{I}$	identity matrix

Chemical Reaction Symbols

$\mathfrak{N}$	a chemical reaction network
$\mathcal{N}$	a family of reaction networks
$\mathcal{N}_i$	the i^{th} member of $\mathcal{N}$
$\mathcal{S}$	the set of species
$\mathcal{C}$	the set of complexes
$\mathcal{R}$	the set of species
$\emptyset$	the zero complex
$\boldsymbol{r}_i$	reaction vectors
X_i	chemical species
x_i	chemical concentrations
C_i	a complex
$\boldsymbol{\kappa}$	the vector of reaction rates
$\boldsymbol{\nu}$	the flux vector
Γ	the stoichiometric matrix
A_κ	negative weighted Laplacian
$\psi(\boldsymbol{x})$	map from species to complexes
α	map from complexes to species
$\boldsymbol{z}$	a conservation relation
δ	network deficiency

Dynamical and Stochastic Systems Symbols

$\boldsymbol{x}^*$	a steady state
$\boldsymbol{\delta x}$	a perturbation to the steady state
J	Jacobian matrix
dt	time interval
D	diffusion coefficient
$\mathcal{K}$	number of compartments
Δ_s	compartment size
U_i	number of molecule X_i
u_i	stochastic system state
Ω	system size
η	stochastic process
ξ	normal Gaussian process
B	correlation matrix (Chapters 2, 5 and 6)
$\hat{f}$	Fourier transform of f
P_x	power spectrum of x
k	spatial frequency
ω	(angular) frequency

Chapter Specific Symbols

M	unlabelled digraph (Chapter 3)
μ	weight assignment function (Chapter 3)
J	exponent and conservation relation matrix (Chapter 3)
$\bar{A}$	the projective closure of A (Chapter 4)
u_i	a data point (Chapter 4)
λ_i	generic, real weights (Chapter 4)
EDdegree(X)	the ED degree of X (Chapter 4)
A	Jacobian plus lattice Laplacian matrix (Chapter 6)

Chapter 1

Introduction

> *"My mind", he said, "rebels at stagnation. Give me problems, give me work, give me the most abstruse cryptogram or the most intricate analysis, and I am in my own proper atmosphere. I can dispense then with artificial stimulants. But I abhor the dull routine of existence. I crave for mental exaltation. That is why I have chosen my own particular profession, or rather created it, for I am the only one in the world."*
>
> – Sir Arthur Conan Doyle, The Sign of Four

The emergence of complex biological behaviour, such as oscillations and switches, from simple chemical reactions and how these reactions interact to govern the operation and decision making of cells is one of the fundamental questions in cellular biology [Alberts et al., 2007; Murray, 2002, 2008]. In experimental systems the situation is usually more challenging than in a purely theoretical context, as not only are the parameters unknown (see e.g. Harrington et al. [2012]), often the reaction mechanism itself is poorly understood (e.g. Gross et al. [2016a]). The aim of the mathematical modelling of chemical reaction networks is, therefore, three-fold:

(i) to provide techniques for identifying model parameters for a given reaction mechanism and data set,

(ii) to show which models in a set of candidate mechanisms have the ability to describe the data, independent of the parameter values,

(iii) to suggest new mechanisms which leads to new models or novel model behaviour.

While the first question can be answered with techniques from statistics or computer science [Ashyraliyev et al., 2009], questions (ii) and (iii) require a modelling

approach. Typically, this modelling is implemented in a bottom-up manner where biological insights are used to construct a mathematical model. The model dynamics are then analysed by using parameters sweeps, and numerical or analytical bifurcation analysis to establish the validity of the modelling assumptions [Murray, 2002, 2008]. By contrast, the second approach is a top-down approach in which the features and structure of existing models are highlighted and general mathematical theorems are sought. This can be applied to simplify the bottom-up modelling of new biological mechanisms [Conradi et al., 2005]. In particular, question (ii) requires sophisticated mathematical tools to establish claims about a model which hold for all positive parameter values (e.g. see Feinberg [1987]), rather than a bounded, often discrete, set of parameter values. Question (iii) often uses a hybrid approach of using biological insight to suggest a new mechanism and anticipate its behaviour. Then the mechanism is tested in well-established models to highlight the feasibility of the approach (e.g. see Woolley et al. [2011c]).

The subfield of chemical reaction network theory seeks to provide methods to answer all three questions using mathematical abstraction and rigorous techniques from fields as diverse as commutative algebra [Gross et al., 2016b], geometry [Millán et al., 2012], graph theory [Mincheva and Roussel, 2007] and dynamical systems theory [Craciun et al., 2013b]. Chemical reaction network theory started in the 1970s with the pioneering work of Horn, Jackson and Feinberg [Horn and Jackson, 1972; Horn, 1972; Feinberg, 1987, 1988], who made the first connections between the graphical structure of a chemical reaction network and its dynamical properties. They relied on techniques of linear algebra and graph theory and were motivated mainly by the questions arising in the chemical engineering of tank reactors. Hence, many factors which play a role in systems biology, such as spatial dependence or noisy behaviour, were not considered in the original theory. With the growing importance of systems biology and the mathematical modelling of biological processes, the pioneering work of Feinberg et al. [Feinberg, 1987; Horn and Jackson, 1972; Horn, 1972] has been adapted and expanded to study a range of questions arising in biology. In particular, in the recent years algebraic geometry has been applied successfully to chemical reaction networks due to the polynomial structure of many of the models studied in systems biology [Dickenstein, 2016].

Previous research in chemical reaction network theory can also be roughly divided to address one of the questions outlined above. Question (i) has been addressed from an algebraic and combinatorial viewpoint, often in combination with statistical modelling [Craciun et al., 2009b, 2013a]. Particularly fruitful is the study of the long

term behaviour of the models such as steady states and, occasionally, oscillations. Recent research highlights the mathematical (algebraic) dependencies of the variables which represent the chemical concentrations at steady state and show how these can be used in parameter estimation [Harrington et al., 2012; MacLean et al., 2015]. To do this, polynomial equations in the measured chemical concentrations are sought and, combined with a data set, a combinatorial object known as a matroid is studied. In order to account for noisy measurements, an optimisation problem minimising the Euclidean distance (ED) using numerical algebraic geometry is investigated in Gross et al. [2016a]. For complicated models, however, standard numerical algebraic geometry methods require extensive knowledge about the intrinsic geometry of the system under study, otherwise solutions might be missed. Further, the complexity of solving for points that minimise the ED can rise exponentially with the number of solutions to be found. The research presented in Chapter 4 addresses these issues and suggests biological features responsible for model complexity. The study of polynomial equations, which have to hold for a given steady state is bridging the gap between question (i) and question (ii). In particular, model rejection can be performed by studying the singular values of a data matrix [MacLean et al., 2015].

A question tangential to question (i), and of fundamental theoretical and practical importance, concerns the identifiability of a model. While statistical and algebraic methods can be employed to find model parameters, it is often possible that the model parameters can have an infinite number of values and still be optimal with respect to the parameter identification procedure chosen [Craciun and Pantea, 2008]. Such models are called unidentifiable and models for which every parameter can only take a finite number of values at the optimum is called identifiable. There exists a large body of previous research on identifiability [Craciun and Pantea, 2008; Chis et al., 2011; Farina et al., 2006; Meshkat et al., 2009; Meshkat and Sullivant, 2014; Meshkat et al., 2011]. In contrast to other areas of chemical reaction network theory, the techniques used are differential algebra methods [Harrington et al., 2016] which allow for the consideration of time series data.

The study of question (ii) has a long tradition dating back to the original work of Feinberg, Horn and Jackson [Horn and Jackson, 1972; Horn, 1972; Feinberg, 1987, 1988]. In particular, early results use close connections between graphical structure of the network and linear algebra to give conditions when a network only has one biologically viable steady state, i.e. a steady state where all species concentrations are positive, for any parameters and any initial concentration of the chemicals. Despite many important models obeying the conditions for one biologically viable steady

state, for example simple diffusion and some immune reaction or cellular signalling models, most mathematically interesting and biologically relevant systems do not fall in this category (e.g. see Holstein et al. [2013]). Hence, much previous work focused on finding models which have the capability of multistationarity [Joshi and Shiu, 2015; Banaji and Pantea, 2016], that is, finding models, which, for some parameter values, have more than one positive steady state. Some recent results include finding smallest chemical reaction networks which are multistationary [Joshi and Shiu, 2013], a Jacobian criterion for finding multistationarity [Joshi and Shiu, 2012], multistationarity for chemical reaction networks with favourable steady state geometry [Millán et al., 2012], inheritance of multistationarity [Banaji and Pantea, 2018], methods for finding parameter regions of multistationarity, finding lower bounds on the number of positive steady states [Bihan et al., 2018], graph theoretical approaches [Mincheva and Roussel, 2007; Mincheva and Craciun, 2008] and case studies of particular multistationary networks [Holstein et al., 2013]. Although there is a sizeable body of literature on multistationarity, many approaches choose one model at a time to illustrate decision criteria which, in theory, could be generalised to other models. Some biological networks, however, such as kinetic proofreading [Mckeithan, 1995] can be extended to an infinite amount of variables and Chapter 3 gives combinatorial results on the multistationarity structure of these models. Combinatorial and perturbation theory approaches have also been proposed to guarantee or rule out dynamical behaviours such as oscillations [Mincheva and Roussel, 2007; Angeli et al., 2013; Banaji, 2018].

Question (iii) is to some degree the hardest question to answer as it not only requires extensive use of the methods for model validation and parameter estimation developed in answering the first two questions, it further requires extensive biological insight to suggest origins of novel mechanisms. Due to this fact the body of previous research, which investigates new model mechanisms from an algebraic viewpoint is not as large as the amount of previous work done on question (i) and (ii). However, the techniques arising from numerical algebraic geometry [Gross et al., 2016a], polyhedral geometry [Craciun et al., 2009b], oriented matroids [Gerstl et al., 2018] and graph theory [Diego et al., 2018] can be applied to select models from a range of candidate network structures. As the set of candidate structures can be expanded arbitrarily, these techniques provide methods to suggest new model behaviour. Recent work by Gross et al. [2016a] uses numerical algebraic geometry and parameter homotopy for model testing. Chapters 3 and 4 also build on the idea of constructing candidate models and testing them, however, they use symbolic rather than numerical

methods. In Craciun et al. [2009b] a combinatorial approach is outlined which uses the polyhedra associated with a set of candidate models in order to infer the most likely network that describes the data. Further, metabolic networks have been studied using oriented matroids to identify elementary flux modes which could be used to construct new enzyme networks [Gerstl et al., 2018]. In Mincheva and Roussel [2007] and Mincheva and Craciun [2008] it is shown how network motifs can generate oscillations and multistability. In Diego et al. [2018] it was highlighted how graph theoretical methods can be used to identify network topologies leading to a desired model behaviour, namely spatial patterning. If this approach could be extended to a predictive tool for an arbitrary number of species, then this could lead to a wealth of new patterning mechanisms.

Despite the numerous results and tools of chemical reaction network theory, many possible extensions of the framework, such as models with spatial structure or noisy systems, are still largely unexplored. In the following subsections some results of the modelling of spatial and noisy systems are summarised and contributions of chemical reaction network theory to the respective areas are highlighted.

1.1 Spatial vs. Non-spatial Models

Most research in chemical reaction network theory has been concerned with the properties of so-called *well-mixed* models, that is, models which have no spatial dependency. Well-mixed models can be described by a set of ordinary differential equations (ODEs). Whereas this assumption can be justified for chemical tank reactors, as was the case in the original work of Feinberg et al., the well mixed approximation is often not applicable in biological systems. Non-spatial models cannot, by construction, explain the wealth of spatial organisation seen in biology, such as animal fur patterning [Murray, 2008], hair placodes [Sick et al., 2006], whiskers [Nagase et al., 2007] or feather formation [Lin et al., 2009]. The focus of chemical reaction network theory on non-spatial systems can be attributed to three factors. First, historically chemical reaction network theory was developed to describe the dynamics of chemical reactions in tank reactors in which the spatial heterogeneity can be eliminated by stirring. Secondly, the techniques of chemical reaction network theory are often tools coming from commutative algebra and algebraic geometry, fields of mathematics concerned with polynomial equations. While sometimes the requirement for polynomial equations can be relaxed to rational functions or generalised polynomial maps as the right hand side of ODEs, the modelling of spatial systems requires the use of partial

differential equations (PDEs) and algebraic tools are often not applicable to answer research questions about systems of PDEs. The third reason is also that, similar to the choice of dynamical law in non-spatial chemical reaction networks (see Chapter 2), there exist different models for incorporating spatial heterogeneity, from simple diffusion [Murray, 2008] to the response of chemicals to nutrient gradients (chemotaxis) [Murray, 2008], or haptotaxis, in which cells move due to gradients in the density of the extracellular matrix [Murray and Oster, 1984], or the response to electric signals (galvanotaxis) [Mycielska and Djamgoz, 2004], or light (phototaxis) [Drescher et al., 2010]. Further, the fluid through which the chemicals travel can be subject to flows and, hence, convective transport can be considered too. A related complication is the choice of the domain in which chemicals can move. Its geometry, dimensionality and boundary conditions can drastically influence the model behaviour [Murray, 2008].

Despite the difficulty of modelling spatial chemical systems, there exists a wealth of results, not necessarily from an algebraic viewpoint, on spatial organisation of chemical species, so-called patterns. Probably the most famous and widely used theory is the one of two diffusing species which can react with each other to form stripes or spots, so-called Turing patterns. Turing patterns are named after Alan Turing whose seminal work [Turing, 1952] founded the field of reaction-diffusion patterns. In [Turing, 1952] it was postulated that a stable, inhomogeneous state could be created by a diffusive mechanism leading to symmetry breaking of a near homogeneous state.

Despite the generality and elegant simplicity of Turing's theory, it is still an open question whether Turing systems exist in biology. Although there exist chemical systems which form Turing patterns [De Kepper et al., 1982; Míguez et al., 2006] and many biological mechanisms which have been theorised to be Turing mechanisms, experimental evidence at the level of molecular detail has yet to be found. Nevertheless, Turing's theory has been successfully used in predictive modelling of biochemical systems [Sage et al., 2009; Yochelis et al., 2008]. Another problem with Turing's theory is that often the parameter ranges for Turing systems are small and extensive fine-tuning of the parameters is needed to observe patterning [Murray, 1982]. Further, perturbations to initial conditions, or domain geometry, or boundary conditions can have major effects on the patterns obtained [Baker et al., 2008]. However, it seems that in nature most patterning processes are robust towards extrinsic perturbation and this robustness problem [Maini et al., 2012] is one of biggest challenges of Turing's theory.

While a large number of theoretical models have been shown to be Turing systems, there exist a few canonical models which form a basis for many proof-of-principle

studies in reaction-diffusion systems. The simplest such system is the Schnakenberg model [Schnakenberg, 1979] which was developed in search of a simple network which still has periodic solutions. As can be shown, the model is also capable of forming spatial patterns and there exists a large body of literature studying different features of the model. The Gierer-Meinhardt system [Gierer and Meinhardt, 1972] provides a seminal patterning mechanism which relies on a chemical, the activator, which triggers its own production and the production of a second chemical, the inhibitor. The inhibitor slows down the production of the activator and this short-range-activation-long-range-inhibition model motivates a large body of biochemical research on pattern formation. The most generic two-species patterning mechanism up to cubic terms was introduced in Barrio et al. [1999] and is commonly referred to as the BVAM model. Due to the generality it can be mapped onto other networks such as the Schnakenberg system.

Despite the complications of spatial heterogeneity, in contrast to well-mixed systems, there are nevertheless opportunities for chemical reaction network theory to make statements about Turing systems. The first observation is that Turing systems require a stable steady state and, hence, the search for Turing systems can be connected to research in multistationarity and multistability [Mincheva and Craciun, 2008]. Additionally, graph theoretical methods have yielded novel insight, especially in Mincheva and Roussel [2006] a formula was presented, which generalises the conditions for Turing instabilities to an arbitrary number of species. The graph theoretical results in chemical reaction network theory often use particular bipartite graphs, for example the species-reaction (SR) graph in Domijan [2008], to derive necessary conditions for Turing instabilities. More recent research [Diego et al., 2018] uses the properties of a Jacobian digraph to characterise minimal Turing patterns on three species, that is directed graph with a minimal number of edges to give a Turing system; removal of any of the edges would also remove the Turing instability. Further results of Diego et al. [2018] give conditions on the directed graph of a network which guarantee a Turing instability.

An approach combining analysis and chemical reaction network theory to study the convergence of reaction-diffusion systems to the homogeneous steady state was outlined in Mincheva and Siegel [2004]. Unlike most research outlined so far [Mincheva and Siegel, 2004] study systems that do not pattern, but converge to the (homogeneous) steady state predicted by the non-spatial theory. Another possible handle for the use of chemical reaction network theory is the discretisation of space (method of lines) which transforms a PDE to a set of coupled ODEs. If the right hand side of

these ODEs is given by polynomial or rational functions, their steady states can be studied directly with algebraic techniques. However, due to the generally non-linear nature of the equations it is non-trivial to prove the convergence of solutions of the method of lines to the solutions of the PDE, although, there exist results on simple networks [Mohamed et al., 2018].

1.2 Deterministic vs. Stochastic Models

A further complication in the modelling of biological systems is that often the number of reacting particles is small and, therefore, a simple ODE formalism breaks down. If the particle number is small, then the stochastic nature of chemical reactions needs to be considered [Gillespie, 1976]. This intrinsic stochasticity of chemical reactions is often called intrinsic noise. In the case of intrinsic noise different modelling techniques are used and, instead of ODEs, a stochastic system can be modelled by a (normally infinite) set of linear ODEs, or a single PDE, or a set of stochastic differential equations (SDEs) [van Kampen, 1983]. Due to the breakdown of the ODE description, algebraic methods can often not be used to analyse stochastic systems. Common approaches to study stochastic models include finding approximations to the stochastic description, which allow for analytic methods to be used [van Kampen, 1983], and the adaption of tools from theoretical physics [Weber and Frey, 2017]. A common tool for investigating the behaviour of stochastic chemical reaction networks is exact numerical simulation via the Gillespie algorithm [Gillespie, 1976].

The reason why stochastic systems are interesting to study is that their behaviour can sometimes drastically diverge from the ODE model, which describes the large particle number limit of the system [Kurtz, 1972] and cannot capture the impact or extent of fluctuations. In particular, it is often the case that the mean of a stationary distribution of the stochastic system is not equal to the steady state value predicted by the ODE system [Erban et al., 2007]. Further, in enzymatic reactions, such as the Michaelis-Menten scheme [Michaelis and Menten, 1913], when the enzyme number is very low, effects such as stochastic focusing can appear. When stochastic focusing is present, a chemical species has an abnormally large reaction to the noise in another species [Gürsoy et al., 2016]. Another example of the difference between deterministic and stochastic behaviour is that stochastic systems can exhibit limit-cycle-like oscillations, often called quasi-cycles [McKane and Newman, 2005], whereas their deterministic counterpart is stable. These quasi-cycles are important in practice as they provide a stochastic analogue of limit cycles in deterministic systems. In a similar

fashion to limit cycles, the existence and number of quasi-cycles in a system is highly dependent on the parameter range. While there are some approximations and heuristics [Dauxois et al., 2009], there is no easy way of deciding how many quasi-cycles are present in a stochastic trajectory. Chapter 5 addresses this problem using real algebraic geometry and graph theory. Often, in bistable systems, stochastic fluctuations can drive the system from one deterministic stable steady state to another [Matheson et al., 1975]. Another interesting effect in stochastic systems is that sometimes the stationary distribution can be unimodal, meaning that the system fluctuates mainly about a single value, even though the deterministic system is bistable and, hence, stochastic switching or, equivalently, a bimodal distribution is expected [Vlysidis and Kaznessis, 2018]. The converse effect is also known [Plesa et al., 2018]. Further, chemical species can become extinct in stochastic systems even when the solutions of the corresponding deterministic ODE system remain positive at all times [Anderson et al., 2014].

Intrinsic stochasticity also has effects on spatial systems where, in addition to providing stochastic perturbations in Turing patterns, they can induce spatio-temporal patterns in deterministically stable and spatially homogeneous solutions [Schumacher et al., 2013]. Further, [Biancalani et al., 2010] demonstrated that stochasticity can also induce stable patterning outside the deterministic Turing regime and the results of Woolley et al. [2011c] show that the patterns in stochastic systems emerge much faster than the patterns of their deterministic counterparts. Hence, stochasticity can induce patterning and may be a mechanism to make Turing systems more robust.

Although the effect of stochasticity is seemingly positive for the patterning mechanism, care needs to be taken, as reported effects often depend on the exact modelling mechanism. Many approaches of modelling stochastic Turing systems start with a reaction-diffusion master equation (RDME) and either simulate this equation directly using exact numerical algorithms or coarse grain the RDME to obtain simpler SDEs which are more amenable to analytic techniques. Either approach, however, assumes that space is discretised into compartments (lattice models) and often the results obtained depend on the discretisation [Cao and Erban, 2014]. The compartment size for correct simulation is bounded from below and above [Erban and Chapman, 2009; Kang et al., 2012; Cao and Erban, 2014] and, crucially, the RDME approach gives answers different to the continuum model in the limit of the compartment size converging to zero [Isaacson, 2009]. More accurate formulations of stochastic Turing mechanisms are off-lattice Brownian models which are computationally expensive and analytically virtually intractable [Erban et al., 2007]. Hence, despite the limitations

of the RDME method it is still one of the most widely used reaction-diffusion models. Further complications are the fact that simple reaction-diffusion PDEs are often not an accurate description of the PDEs obtained by coarse graining the RDME [Biancalani et al., 2010]. Coarse grained models often contain cross diffusion terms, that is diffusion of one species influenced by the presence of another, not modelled in the reaction-diffusion PDE.

Despite the difference in dynamics and long term behaviour of stochastic systems when compared to deterministic systems and the different mathematical formulation of the models, recent results extend the framework of chemical reaction network theory and applied algebra to stochastic systems. The most prominent result uses methods from deficiency theory [Feinberg, 1987] to derive steady state distributions for a large class of chemical reaction networks [Anderson et al., 2010]. These stationary distributions are products of Poisson and binomial distributions and are termed product-form distributions. In Cappelletti and Wiuf [2016] the assumptions on the networks were relaxed to a balancing condition called complex balancing which concerns a flow on the graph of the chemical reaction network. Crucially, stochastic versions of Feinberg's results [Feinberg, 1987] on steady states and stability of a deterministic system were proved. Hence, the long time behaviour of some deterministic systems can be extended trivially to their stochastic counterparts and the only parameters needed are the deterministic steady state values of the chemical species. A connection between another network balancing condition called detailed balance and the different notion of its Markov chain detailed balance was investigated in Joshi [2013]. In particular, it was shown that network detailed balance always implies Markov chain detailed balance, but for some specific classes of examples, such as birth-dearth processes, the converse is not true. For other balancing conditions, which are often used in chemical reaction network theory, the relations between the deterministic and stochastic formulations, and a hierarchy of balancing conditions were established in Cappelletti and Joshi [2018]. The aim of all these results is to establish network properties which guarantee a closed form analytic, usually product-from Poisson, stationary distribution of the network and to prove stochastic versions of the pioneering results of Feinberg, Horn and Jackson.

Further stochastic analogues of deterministic properties were found in Anderson et al. [2018] and Hansen and Wiuf [2018]. In Anderson et al. [2018] it was shown that when stochastic systems have a product-form stationary distribution, then the trajectory is non-explosive, i.e. the species concentrations have a finite value at infinite times. This non-explosivity property can be thought of as the stochastic analogue

to boundedness of a solution of a system of ODEs. A stochastic analogue of quasi steady states was derived in Hansen and Wiuf [2018] and existence conditions for quasi steady state distributions were given.

Since the seminal work of Michaelis and Menten an approximation for deterministic enzymatic reaction mechanisms is known and in Cappelletti and Wiuf [2017] a stochastic version was developed. In Cappelletti and Wiuf [2017] it was shown how stochastic reaction networks involving a short lived intermediate species can be described by a simpler mechanism without the intermediate. Some deterministic chemical reaction networks can have steady states whose values are independent of the amount of chemical present initially and these systems are said to exhibit absolute concentration robustness [Shinar and Feinberg, 2010]. While a fascinating property in deterministic systems, recent extensions to stochastic systems show that the stochastic behaviour of systems with absolute concentration robustness can be considerably different to the deterministic one. In particular, given a number of assumptions on the network outlined in Anderson et al. [2014], then, eventually at least one species goes extinct. Further, it was shown in Anderson et al. [2017] that by rescaling time a quasi stationary distribution can be found for the times before the extinction event and that this distribution is also product-form Poisson.

Inverse problems have also been considered, namely, it was found in Cappelletti et al. [2018] that any probability distribution on the positive integer lattice can be arbitrarily approximated by a chemical reaction network. These approximations are ergodic and, hence, robust to finitely many perturbations in particle numbers. Naturally, the findings of Cappelletti et al. [2018] could have large implications in the design of biological circuits aimed at performing certain tasks in vivo.

Geometric techniques have been considered in Van Vu and Hasegawa [2019a] to find parameter regions in which the means and variances of the chemical species obey given constraints. These techniques are useful in inverse problems, where parameter regions are sought in which a network has a given behaviour. This is a problem analogous to finding a deterministic phase diagram of a system. However, similar to the algebraic approaches to stochastic systems presented in this thesis, the methods of Van Vu and Hasegawa [2019a] can only be applied to unimodal distributions originating from monostationary networks.

Spatial stochastic systems have been explored in Van Vu and Hasegawa [2019b]. It was shown that in RDME models diffusion can often be neglected when the steady state distribution is calculated. In particular, if the steady state distribution is a product-form Poisson distribution then, surprisingly, diffusion can be neglected.

1.3 Extrinsic vs. Intrinsic Noise

Unlike intrinsic noise, which originates from the physical process by which chemicals react, extrinsic noise is an experimental parameter which either originates from biological variability, imperfect experimental conditions, measurement error [Sagués et al., 2007], or, it can even be used as a driving force to achieve certain model behaviour [Barajas-Solano and Tartakovsky, 2016]. Due to the control that an experimenter has over the noise in the system, it is more amenable to theoretical study than the stringent conditions put on the dynamics of chemical reaction networks by intrinsic noise. However, there are surprisingly few theoretical studies on extrinsic noise in chemical reaction network theory.

A simple manifestation of extrinsic noise is cell-to-cell variability [Swain et al., 2002; Filippi et al., 2015]. With the emergence of single cell and high-throughput methods in biology, it has become possible to obtain time series data at single cell level [Filippi et al., 2015]. From this data the reaction parameters for every single cell can be estimated and it is often the case that the network has drastically different reaction parameters in different cells. This difference is often called cell-to-cell variability [Elowitz et al., 2002; Snijder and Pelkmans, 2011] and it can have its origin in the different micro-environments present in different cells. In recent research the variability in phosphorylation networks was investigated and Bayesian methods were used in conjunction with high throughput data to highlight the variation of the responses to signal in single cells [Filippi et al., 2015; Lenive et al., 2016]. In particular, it was shown that the variation in input to the phosphorylation cascades is the main source of noise in the system. In Lenive et al. [2016] approximate Bayesian methods were used to distil the effect of extrinsic noise present in single-cell gene expression mechanisms. It is important to note that cell-to-cell variability or variability in input can be translated into the language of chemical reaction network theory by stating that "a result holds for all possible parameter values" (cell-to-cell variability in reaction rates) and "for all possible initial conditions" (variability in the input). Hence, the notion of extrinsic noise as variability is to some extent an inbuilt feature of chemical reaction network theory and this may be an explanation why chemical reaction network theory papers do not explicitly mention extrinsic noise.

Extrinsic noise in spatial systems has often been studied in the context of single species, or order parameter, systems such as Ginzburg-Landau model or the Swift-Hohenberg equation. Often the correlations in the noise were considered to be in space and time. In García-Ojalvo and Sancho [1996] a Swift-Hohenberg model subject to

extrinsic white noise with spatial correlations was studied and extensions to temporal correlations in a Ginzburg-Landau model were presented in García-Ojalvo and Sancho [1994]. The possible behaviour of a general single species model subject to white extrinsic noise was presented in Scarsoglio et al. [2011] and single species models on growing domains were studied in Escudero [2009]. While one variable models are the most tractable analytically and are useful to gain insight into the effect of noise, they are often far removed from biological scenarios in which usually many-species models need to be considered. A recent example of extrinsic noise in a Turing system is [Hochberg et al., 2003] where renormalization group techniques were used to highlight the effect of correlated noise in the Gray-Scott model. Despite this initial case study of the Gray-Scott model, a systematic discussion of Turing systems subject to extrinsic noise has not been published in previous work. Chapter 6 presents a first study of extrinsic-noise reaction-diffusion systems with a particular focus on temporally correlated noise.

An introduction to systems with extrinsic noise is also presented in the review paper of Sagués et al. [2007]. In contrast to the research mentioned in the previous paragraph, this paper not only briefly covers order parameter equations subject to noise, it further contrasts extrinsic and intrinsic noise and suggests possible origins of extrinsic noise such as the photosensibility of certain chemical reactions. The idea of letting parameters fluctuate in space and time provides a second major source of extrinsic noise which is seldom mentioned explicitly and actively investigated in this thesis in Chapter 5 and Chapter 6. In particular, a framework for the study of chemical reaction networks modelled by ODEs in conjunction with the parameter noise outlined in Sagués et al. [2007] is developed.

Although not explicitly developed for, or applied to, chemical reaction networks or biological systems in general, there are many approaches for deriving effective PDEs from SDEs with white and correlated noise. A general overview of methods extending the derivation of a PDE describing the evolution of the probability density of a stochastic system to correlated noise is given in Hänggi and Jung [1994]. As discussed in Hänggi and Jung [1994] it is often not possible to obtain an exact PDE and approximation or closure procedures need to be used. Functional calculus approaches are studied in Fox [1986a] and the convergence of the commonly used small noise approximation is presented in Fox [1986b]. Besides the small noise approximation, moment closure approximations such as outlined in Barajas-Solano and Tartakovsky [2016] are used to obtain analytically tractable PDEs. However, from a chemical reaction network viewpoint, the analytical progress presented by converting a system of SDEs

to a single PDE is compensated by the loss of network information. Crucially, the connection of the network structure to the ODE system is lost, and the network-ODE connection will be shown to play a major role in networks with parameter noise in the sense of Sagués et al. [2007].

1.4 Contributions

In the following I give a road map to this thesis and discuss my contributions to the field. The aim of this thesis is to show how extrinsic noise affects chemical reaction networks. In particular, algebraic results on model testing and multistationarity are proved for constant, arbitrary, positive rate constants. Further, the temporal dynamics of reaction models subject to time-varying extrinsic noise is studied with methods of graph theory and applied algebra.

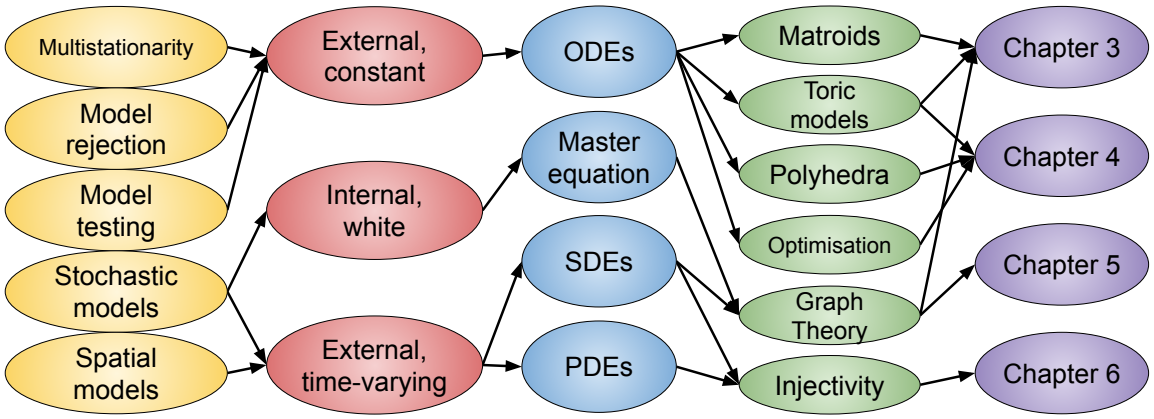


Figure 1.1: The structure of this thesis. In the first layer are the research topics addressed, followed by the types of noise modelled, the modelling framework, the mathematics used and the corresponding chapters.

Chapter 2 covers the preliminaries of mathematical biology and relevant mathematical techniques. In particular, Chapter 2 covers essential mathematical notions of chemical reaction network theory, commutative algebra and algebraic geometry. The main tools for stochastic modelling are also introduced. Further, the mathematical formulation of extrinsic noise as studied in this thesis and its application in each chapter is outlined.

Chapters 3 and 4 consider systems with constant, extrinsic noise. Chapter 3 is based on the paper *"Steady state invariants for families of chemical reaction networks"* [Adamer and Helmer, 2019b] and studies systems with constant, but arbitrary parameters. In particular, it extends to the current framework of chemical reaction

network theory by developing tools for classes of reaction models that can be constructed algorithmically. Critically, the results do not depend on the exact parameter values of the model. To this end, the steady state geometry is studied and a novel method to find relations between the steady state geometries of different models is introduced by setting certain model parameters to zero. These relations are used to find invariant binomial equations and applied to study multistationarity and model selection. Other invariants, in particular the dimension of the steady state variety, are considered too.

In Chapter 4, which is based on the paper *"Complexity of model testing for dynamical systems with toric steady states"* [Adamer and Helmer, 2019a], the Euclidean Distance (ED) degree is introduced as a parameter-independent steady state invariant that can be associated to a chemical reaction network. The ED degree is then used to give a new measure of the complexity of model fitting and model rejection. In particular, it is assumed that a (set of) candidate model(s) is proposed and steady state data is measured. Then, the ED degree can give information about the complexity of finding a real, positive point that is a steady state solution of the model and which is closest to the data point. It is shown that such a point exists and methods for finding this real, positive point are highlighted. Possible biological origins of the different model complexities are discussed.

Chapters 5 and 6 cover systems with time-varying, so-called parameter noise. In Chapter 5, which is based on the paper *"Graph-facilitated resonant mode counting in stochastic interaction networks"* [Adamer et al., 2017], a novel graph theoretic method is presented for calculating the number of different quasi-cycle frequencies in a stochastic network. Further, it also outlines a new method to incorporate extrinsic noise into chemical reaction networks. The behaviour of systems subject to intrinsic noise is contrasted with the behaviour subject to extrinsic noise. It is shown that the difference between the two modelling paradigms is only quantitative, but not qualitative in the case of white, i.e. uncorrelated, noise. The graph theoretic method used in Chapter 5 has previously been shown to be insightful when finding deterministic oscillations. The extension to stochastic systems is a first use of chemical reaction network theory in stochastic systems subject to time-varying extrinsic noise.

Chapter 6, based on *"Coloured noise from stochastic inflows in reaction-diffusion systems"* [Adamer et al., 2020], covers the extension of parameter noise to spatial systems. Again, it is shown that in the white noise case the difference between intrinsic and extrinsic noise is quantitative rather than qualitative. A further novelty introduced in this chapter is the use of injectivity criteria based on the concept of

oriented matroids for finding appropriate models in an extrinsic noise framework. Effectively, this is a restriction to unimodal distributions. The main goal of Chapter 6, however, is to give a first insight into the effect of temporally correlated, or coloured, noise on spatial chemical reaction networks. It is shown that, depending on the type of noise correlation, patterns can be formed or destroyed and even oscillations can be induced. Another particular focus is on a sound justification of the origin of extrinsic noise in chemical reaction networks.

Chapter 2

Mathematical Background

> *"I think that mathematics can benefit by acknowledging that the creation of good models is just as important as proving deep theorems."*
>
> – David Mumford

This chapter introduces essential mathematical notions and theorems. Furthermore, it highlights established methods in chemical reaction network theory, both deterministic and stochastic. In Section 2.1 the mathematical notions and central theorems of chemical reaction network theory are laid out. In Subsection 2.1.1 the algebraic techniques for analysing the steady states of reaction models are introduced.

Section 2.2 introduces essential notions of stochastic modelling of chemical reactions, starting from microscopic models and coarse graining to mesoscopic models. Subsection 2.2.1 discusses the Chemical Master Equation approach and the Gillespie algorithm as a continuous time Markov chain approximation to the dynamics of a stochastic system. In Subsection 2.2.2 commonly used approximation schemes for the Chemical Master Equation and, moreover, power spectral methods as a tool to analyse stochastic behaviour are discussed.

The last section in this chapter, Section 2.3, discusses how deterministic models with parameters drawn at random from an underlying distribution can be viewed as networks subject to extrinsic noise. It also lays out the main hypotheses of this thesis, namely the connection between extrinsic noise and deterministic models. The background presented here will form either explicit or implicit assumptions of the following chapters.

2.1 Deterministic Models

There exist many equivalent definitions of a chemical reaction network and in this thesis two of the most common ones are used; namely, the description as a multiset of "species", "complexes" and "reactions" [Feinberg, 1995] which leads to the representation as a directed graph [Craciun et al., 2009a]. Both descriptions can easily be converted into each other and, depending on the situation, the most convenient definition is used. Another common definition of chemical reaction networks not used in this thesis is the description as Petri nets [Baez and Pollard, 2017] or the Species-Reaction (SR) graph [Angeli et al., 2007]. The main focus of this section is on systems which are homogeneous in space, such as reactions happening in chemical tank reactors [Feinberg, 1987]. Hence, all the chemical concentrations will be functions of time, but not space. A brief excursion into spatial systems is given in Remark 2.1.18

The definition of a chemical reaction network as multiset goes back to Horn and Jackson who first introduced this notion in Horn and Jackson [1972]. A restatement of their definition is the following.

Definition 2.1.1. *A chemical reaction network is a multiset* $\mathfrak{N} = \{\mathcal{S}, \mathcal{C}, \mathcal{R}\}$ *where the sets are,*

- $\mathcal{S}$*, the set of chemical species present in the network,*
- $\mathcal{C}$*, the set of complexes, which are non-negative linear combinations of species,*
- $\mathcal{R}$*, the set of reactions from one complex to another, which can be represented as ordered pairs of complexes.*

Example 2.1.2 (Autocatalytic network)**.**

$$X_1 + X_2 \to X_2 \quad X_1 \rightleftharpoons \emptyset \rightleftharpoons X_2$$

The autocatalytic network is a system with species set $\mathcal{S} = \{X_1, X_2\}$*, complexes* $\mathcal{C} = \{X_1, X_2, X_1 + X_2, \emptyset\}$ *and reactions* $\mathcal{R} = \{X_1 + X_2 \to X_2, X_1 \to \emptyset, \emptyset \to X_1, X_2 \to \emptyset, \emptyset \to X_2\}$*. Note that the empty set,* $\emptyset$*, is used to describe the generation and degradation of chemical species through a mechanism not explicitly modelled. In an experimental setup this could correspond to an inflow or outflow of species. The empty set is named "zero complex" and* $\emptyset \notin \mathcal{S}$*.*

To make a connection between the *structure* of a network and its *dynamics*, a model for the reaction kinetics is needed. There are many different models used in the literature and the choice of model depends on the proposed reaction mechanism. A few examples are mass action [Horn and Jackson, 1972], Michaelis-Menten [Michaelis and Menten, 1913], Hill function kinetics [Kim and Gelenbe, 2012] or rational functions [Wei, 1999]. In this thesis mass action kinetics are used as they are the simplest and most widely studied reaction kinetics. A brief glimpse into the use of other kinetic models is given in Example 2.1.17.

The law of mass action rests on the physical observation that the rate at which a chemical reaction proceeds is proportional to the amount of chemical species present in a system. In particular, as deterministic systems measure "amount" in species concentration, e.g. mmol/L, the speed of a reaction is proportional to the concentration of a species. If there are combinations of species, then their concentrations are multiplied. In a network with $\mathcal{S} = \{X_1, \ldots, X_n\}$ and their respective concentrations $\boldsymbol{x} = \{x_1, \ldots, x_n\}$, a generic reaction can be modelled by

$$\sum_{j=1}^{n} \alpha_j X_j \to \sum_{j=1}^{n} \beta_j X_j, \tag{2.1}$$

and the corresponding reaction rate is therefore $\nu \propto x_1^{\alpha_1} \cdots x_n^{\alpha_n} = \boldsymbol{x}^{\boldsymbol{\alpha}}$ with $\boldsymbol{\alpha} = (\alpha_1, \ldots, \alpha_n)^T$. The non-negative integer coefficients $\alpha_j,\ \beta_j \in \mathbb{Z}_{\geq 0}$ are the *stoichiometric coefficients*. The reaction speed is dependent on the *reactant complex* which is the complex on the left hand side of equation (2.1). The complex on the right hand side of (2.1) is called the *product complex*.

The constant of proportionality is denoted by $\kappa \in \mathbb{R}_{>0}$ and, hence, $\nu = \kappa \boldsymbol{x}^{\boldsymbol{\alpha}} = \kappa x_1^{\alpha_1} \cdots x_n^{\alpha_n}$. The *rate constant*, κ, is a positive model parameter which is usually left to be determined. As there is one parameter per reaction, it is apparent that the number of parameters can be very large in biochemical networks.

To formulate a system of ordinary differential equations (ODEs) describing the dynamics of the system a *flux vector*, $\boldsymbol{\nu}$, consisting of the reaction rates of every reaction in the system is built first [Palsson, 2006]. Then, the *stoichiometric matrix*, Γ, is formulated which gives information about how many molecules of each species are produced or consumed in each reaction [Palsson, 2006]. Let $\boldsymbol{\alpha}_i = (\alpha_{i_1}, \ldots, \alpha_{i_n})^T$ and $\boldsymbol{\beta}_i = (\beta_{i_1}, \ldots, \beta_{i_n})^T$ be the column vectors corresponding to the stoichiometric coefficients of the reactant and product complexes for the i^{th} reaction respectively. Then, the i^{th} column of the stoichiometric matrix is given by $\boldsymbol{r}_i = \boldsymbol{\beta}_i - \boldsymbol{\alpha}_i$ and, hence,

in a network with m reactions

$$\Gamma = (\boldsymbol{r}_1, \ldots, \boldsymbol{r}_m) = (\boldsymbol{\beta}_1 - \boldsymbol{\alpha}_1, \ldots, \boldsymbol{\beta}_m - \boldsymbol{\alpha}_m). \tag{2.2}$$

The dynamical system which describes the evolution of the concentrations, $\boldsymbol{x}$, is given by

$$\frac{d\boldsymbol{x}}{dt} = \dot{\boldsymbol{x}} = \Gamma\boldsymbol{\nu} = \boldsymbol{f}(\boldsymbol{x}). \tag{2.3}$$

Example 2.1.3 (Autocatalytic network continued)**.** *The flux vector for the autocatalytic network is given by* $\boldsymbol{\nu} = (\kappa_1 ab, \kappa_2 a, \kappa_3, \kappa_4 b, \kappa_5)^T$ *and the stoichiometric matrix is*

$$\Gamma = \begin{array}{c} \begin{matrix} \boldsymbol{r}_1 & \boldsymbol{r}_2 & \boldsymbol{r}_3 & \boldsymbol{r}_4 & \boldsymbol{r}_5 \end{matrix} \\ \begin{pmatrix} -1 & -1 & 1 & 0 & 0 \\ 0 & 0 & 0 & -1 & 1 \end{pmatrix} \end{array} \begin{matrix} x_1 \\ x_2 \end{matrix}$$

Hence, the dynamical system describing the time evolution of the chemical concentrations a *and* b *is*

$$\frac{d}{dt}\begin{pmatrix} a \\ b \end{pmatrix} = \Gamma\boldsymbol{\nu} = \begin{pmatrix} -\kappa_1 x_1 x_2 - \kappa_2 x_1 + \kappa_3 \\ -\kappa_4 x_2 + \kappa_5 \end{pmatrix}.$$

Of great importance are the left and right kernels of the matrix Γ. It is a trivial statement that, if $\ker(\Gamma) = \{0\}$, then there exists no positive species concentration vector $\boldsymbol{x}$ such that $\Gamma\boldsymbol{\nu} = 0$. The left kernel of Γ, $\ker(\Gamma^T)$, defines the *conservation relations*.

Lemma 2.1.4. *Let* $\mathfrak{N}$ *be a chemical reaction system with stoichiometric matrix* Γ*. Then there exist* $\dim(\ker(\Gamma^T))$ *conserved quantities, up to linear dependencies, which are defined by*

$$\{\boldsymbol{z}^T \cdot \boldsymbol{x} = c \mid \boldsymbol{z} \in \ker(\Gamma^T)\}.$$

Proof. Multiply both sides of (2.3) by $\boldsymbol{z}^T$. Hence,

$$\boldsymbol{z}^T \cdot \frac{d\boldsymbol{x}}{dt} = \frac{d}{dt}\left(\boldsymbol{z}^T \cdot \boldsymbol{x}\right) = \boldsymbol{z}^T\Gamma\boldsymbol{\nu} = 0.$$

This implies that $\boldsymbol{z}^T \cdot \boldsymbol{x} = c$ and $\boldsymbol{z} \in \ker(\Gamma^T)$. The fact that the left kernel of Γ is a vector space of dimension $d = \dim(\ker(\Gamma^T))$ implies that any choice of basis for this vector space gives exactly d independent conserved quantities. □

Remark 2.1.5. *Let* $Z = (\boldsymbol{z}_1, \ldots, \boldsymbol{z}_d)^T$ *denote the matrix of conservation relations and* $\boldsymbol{c} = (c_1, \ldots, c_d)^T$ *any vector of conserved quantities. The conservation relations of a given system can therefore be written compactly as* $Z\boldsymbol{x} - \boldsymbol{c} = 0$*.*

The effect of the conserved quantities on a system is to confine its dynamics to the cosets of the *stoichiometric subspace* [Feinberg, 1987], a subspace of $\mathbb{R}^{|\mathcal{S}|}$, where $|\mathcal{S}|$ is the number of chemical species. Due to the fact that the linear relations $Z\boldsymbol{x} - \boldsymbol{c} = 0$ have to hold for all times the constants $\boldsymbol{c} = \{c_1, \ldots, c_d\}$ are fixed by the initial conditions.

Sometimes it is preferable to define a reaction system by putting more emphasis on its graph structure. In the next paragraphs chemical reaction networks are introduced in terms of their directed graphs (digraphs).

Definition 2.1.6. *A chemical reaction network is a weighted directed graph (digraph) $\mathcal{G}$ with the complex set as vertex set, $\mathcal{C} = \{C_1, \ldots, C_{|\mathcal{C}|}\}$ and edge set $(C_i, C_j) \in E(\mathcal{G})$ if and only if $C_i \to C_j \in \mathcal{R}$. The edge weights are the rate constants $\boldsymbol{\kappa} = \{\kappa_1, \ldots, \kappa_m\}$.*

To translate the static digraph definition to a dynamical system three maps [Gunawardena, 2003] are defined,

1. a linear map A_κ from complexes to complexes,
2. a linear map α from complexes to species, and,
3. a nonlinear map $\psi(\boldsymbol{x})$ from the species to complexes.

The linear map A_κ is the negative transposed Laplacian matrix of the digraph [Craciun et al., 2009a]. The ij^{th} entry of A_κ for $i \neq j$ is the edge weight of the edge $C_j \to C_i$ and the diagonal entries are the negative sums of the column entries. The linear map α^T is precisely the transpose of the matrix of stoichiometric coefficients of each complex such that $\alpha = (\boldsymbol{\alpha}_1, \ldots, \boldsymbol{\alpha}_{|\mathcal{C}|})$. The map ψ assigns a monomial to each vertex using the law of mass action. In particular, each complex C_i can be converted to a monomial via $\boldsymbol{x}^{\boldsymbol{\alpha}_i}$, hence, $\psi_i(\boldsymbol{x}) = x_1^{\alpha_{i_1}} \cdots x_n^{\alpha_{i_n}} = \boldsymbol{x}^{\boldsymbol{\alpha}_i}$. By combining these maps the dynamical system,

$$\frac{d\boldsymbol{x}}{dt} = \Gamma \boldsymbol{\nu} = \alpha A_\kappa \psi(\boldsymbol{x}), \tag{2.4}$$

is obtained.

Example 2.1.7 (Michaelis-Menten [Michaelis and Menten, 1913])**.** *The Michaelis-Menten network is a widely used model for enzyme catalysis. The network is given by* $\mathfrak{N} = \{\{E, S, ES, P\}, \{E+S, ES, E+P\}, \{E+S \to ES, ES \to E+S, ES \to E+P\}\}$ *which translates into the reaction graph*

$$E + S \underset{\kappa_{-1}}{\overset{\kappa_1}{\rightleftharpoons}} ES \xrightarrow{\kappa_2} E + P, \quad \Rightarrow \quad C_1 \underset{\kappa_{-1}}{\overset{\kappa_1}{\rightleftharpoons}} C_2 \xrightarrow{\kappa_2} C_3.$$

From the graph description the dynamical system can be formulated. The negative graph Laplacian of the network is

$$A_\kappa = \begin{pmatrix} -\kappa_1 & \kappa_{-1} & 0 \\ \kappa_1 & -\kappa_{-1} - \kappa_2 & 0 \\ 0 & \kappa_2 & 0 \end{pmatrix}.$$

The linear map of complexes, α, is given by

$$\alpha^T = \begin{array}{c} \begin{matrix} E & S & ES & P \end{matrix} \\ \begin{pmatrix} 1 & 1 & 0 & 0 \\ 0 & 0 & 1 & 0 \\ 1 & 0 & 0 & 1 \end{pmatrix} \end{array} \begin{array}{l} E+S \\ ES \\ E+P \end{array}.$$

Denote the concentration of the species as $[E] = x_1$, $[S] = x_2$, $[ES] = x_3$, $[P] = x_4$, then, the non-linear map from species to complexes is $\psi(\boldsymbol{x}) = (x_1x_2, x_3, x_1x_4)^T$. Hence, the system of equations

$$\frac{d}{dt}\begin{pmatrix} x_1 \\ x_2 \\ x_3 \\ x_4 \end{pmatrix} = \alpha A_\kappa \psi(\boldsymbol{x}) = \Gamma \boldsymbol{\nu} = \begin{pmatrix} -\kappa_1 x_1 x_2 + \kappa_{-1} x_3 + \kappa_2 x_3 \\ -\kappa_1 x_1 x_2 + \kappa_{-1} x_3 \\ \kappa_1 x_1 x_2 - \kappa_{-1} x_3 - \kappa_2 x_3 \\ \kappa_2 x_3 \end{pmatrix},$$

is obtained. The stoichiometric matrix is given by

$$\Gamma = \begin{pmatrix} -1 & 1 & 1 \\ -1 & 1 & 0 \\ 1 & -1 & -1 \\ 0 & 0 & 1 \end{pmatrix},$$

and, hence, conservation relations may be chosen as $[E] + [ES] = x_1 + x_3 = c_1$ and $[S]+[ES]+[P] = x_2+x_3+x_4 = c_2$. Note that the differential equation for the product P is driven by the first three ODEs, but P leaves the first three equations unaffected. Hence, the fourth ODE can be neglected in the analysis.

The dynamical systems governing the evolution of mass action networks are described by polynomial differential equations and, therefore, techniques of algebraic geometry and commutative algebra can be applied to study their steady state behaviour. Before turning to the algebraic geometry of polynomial systems of the form of (2.3), some additional definitions and central theorems of chemical reaction network theory are presented. First, steady states of a dynamical system associated to a chemical reaction system are formally defined.

Definition 2.1.8. *Let $\mathfrak{N}$ be a chemical reaction network whose dynamics is described by equation (2.3). A* steady state *is a vector $\boldsymbol{x}^* \in \mathbb{R}^{|\mathcal{S}|}$ such that $\Gamma\boldsymbol{\nu}(\boldsymbol{x}^*) = 0$. A* positive steady state *is a vector $\boldsymbol{x}^* \in \mathbb{R}^{|\mathcal{S}|}_{>0}$ such that $\Gamma\boldsymbol{\nu}(\boldsymbol{x}^*) = 0$. A chemical reaction network is said to be* multistationary *if, for some fixed parameters, there exist two distinct vectors $\boldsymbol{x}^*$, $\boldsymbol{y}^* \in \mathbb{R}^{|\mathcal{S}|}_{>0}$ such that $\Gamma\boldsymbol{\nu}(\boldsymbol{x}^*) = \Gamma\boldsymbol{\nu}(\boldsymbol{y}^*) = 0$. Further, it is required that the conservation relations hold, that is $\boldsymbol{x}^* - \boldsymbol{y}^* \in \ker(Z)$.*

Remark 2.1.9. *Non-negative steady states, these are steady state vectors $\boldsymbol{x}^* \in \mathbb{R}_{\geq 0}$, in which some species concentrations are zero (extinction states) are also biologically allowed. However, the convention in this thesis is to define steady states as positive vectors. Extinction steady states are biologically very important and a systematic investigation of extinction states and their relation to the analysis in this thesis could form part of future work (see Chapter 7).*

As will be shown in Subsection 2.1.1 the equations describing the steady states of mass action networks form an ideal in a polynomial ring. Hence, they are directly amenable for the study under the lens of algebraic geometry. Positive steady states are usually the focus of much work in chemical reaction network theory, as outlined in Chapter 1. Positive steady states describe an important subset of the biologically realistic, non-negative, steady state solutions to the dynamical systems.

Example 2.1.10 (Phosphorylation Networks)**.** *Phosphorylation networks play a major role in many cellular signalling pathways. This example introduces the phosphorylation network for only one phosphorylation site on the substrate S, however, in Chapter 3 multi-site mechanisms are introduced. The phosphorylation network is given by* $\mathfrak{N} = \{\{E, F, S_0, S_1, ES_0, FS_1\}, \{E+S_0, ES_0, E+S_1, F+S_1, FS_1, F+S_0\}, \{E+S_0 \to ES_0, ES_0 \to E+S_0, ES_0 \to E+S_1, F+S_1 \to FS_1, FS_1 \to F+S_1, FS_1 \to F+S_0\}\}$ *and its reaction graph is*

$$E + S_0 \underset{\kappa_2}{\overset{\kappa_1}{\rightleftharpoons}} ES_0 \xrightarrow{\kappa_3} E + S_1, \quad F + S_1 \underset{\kappa_5}{\overset{\kappa_4}{\rightleftharpoons}} FS_1 \xrightarrow{\kappa_6} F + S_0.$$

With mass action, the dynamics of the network are governed by the ODE system

$$\frac{d}{dt}\begin{pmatrix} x_1 \\ x_2 \\ x_3 \\ x_4 \\ x_5 \\ x_6 \end{pmatrix} = \begin{pmatrix} -\kappa_1 x_1 x_3 + \kappa_2 x_5 + \kappa_3 x_5 \\ -\kappa_4 x_2 x_4 + \kappa_5 x_6 + \kappa_6 x_6 \\ -\kappa_1 x_1 x_3 + \kappa_2 x_5 + \kappa_6 x_6 \\ -\kappa_4 x_2 x_4 + \kappa_3 x_5 + \kappa_5 x_6 \\ \kappa_1 x_1 x_3 - \kappa_2 x_5 - \kappa_3 x_5 \\ \kappa_4 x_2 x_4 - \kappa_5 x_6 - \kappa_6 x_6 \end{pmatrix}.$$

Hence, the stoichiometric matrix is

$$\Gamma = \begin{pmatrix} -1 & 1 & 1 & 0 & 0 & 0 \\ 0 & 0 & 0 & -1 & 1 & 1 \\ -1 & 1 & 0 & 0 & 0 & 1 \\ 0 & 0 & 1 & -1 & 1 & 0 \\ 1 & -1 & -1 & 0 & 0 & 0 \\ 0 & 0 & 0 & 1 & -1 & -1 \end{pmatrix}$$

and the flux vector $\nu = (\kappa_1 x_1 x_3, \kappa_2 x_5, \kappa_3 x_5, \kappa_4 x_2 x_4, \kappa_5 x_6, \kappa_6 x_6)^T$. *The linear space generated by left kernel of* Γ *is three dimensional, corresponding to the conservation relations of the substrate and the two enzymes, and* $\boldsymbol{z}_1 = (0, 0, 1, 1, 1, 1,)$, $\boldsymbol{z}_2 = (1, 0, 0, 0, 1, 0)$ *and* $\boldsymbol{z}_3 = (0, 1, 0, 0, 0, 1)$ *are a basis. In Goldbeter and Koshland [1981, 1984] it was shown that the one-site phosphorylation system has one positive steady state for any choice of parameters.*

Much previous work focused on the connection between dynamics and graph structure of reaction networks, see Chapter 1. Its central concept is the *Deficiency Zero Theorem*, as detailed below. Before stating the theorem, the notions of reversibility and deficiency in a chemical reaction model are discussed. First, some nomenclature of graph theory is introduced.

Definition 2.1.11 ([Harary, 2005])**.** *A connected component of a directed graph is strongly connected if, whenever there exists a directed path from vertex* i *to vertex* j*, then there also exists a directed path from* j *to* i*.*

The analogous feature in chemical reaction network theory is the notion of *weak reversibility.*

Definition 2.1.12 ([Feinberg, 1987])**.** *A network is weakly reversible if every component of the reaction digraph is strongly connected. A reaction network is reversible if every reaction is reversible, i.e. the unweighted graph is undirected.*

The next technical notion needed is the concept of deficiency.

Definition 2.1.13 ([Gunawardena, 2003])**.** *The deficiency of a chemical reaction network is*

$$\delta = \dim(\ker(\alpha^T) \cap \operatorname{im}(A_\kappa)) \geq 0.$$

Another formula used to calculate network deficiency is

$$\delta = |\mathcal{C}| - \ell - \dim(\operatorname{span}\{\boldsymbol{r}_1, \ldots, \boldsymbol{r}_m\}),$$

where ℓ is the number of connected components of the reaction graph [Gunawardena, 2003, Proposition 5.1]. Both formulas agree under the conditions laid out in Gunawardena [2003] and in general $0 \leq \dim(\ker(\alpha^T) \cap \mathrm{im}(A_\kappa)) \leq |\mathcal{C}| - \ell - \dim(\mathrm{span}\{\boldsymbol{r}_1, \ldots, \boldsymbol{r}_m\})$. Further, the notion of a stoichiometric compatibility class is needed.

Definition 2.1.14 ([Feinberg, 1987]). *Given a stoichiometric subspace S and a vector of initial conditions $\boldsymbol{x}_0$, the stoichiometric compatibility class is given by the set $(\boldsymbol{x}_0 + S) \cap \mathbb{R}^{|\mathcal{S}|}_{\geq 0}$.*

The Deficiency Zero Theorem which makes a fundamental connection between dynamics and structure of chemical reaction systems is now stated below.

Theorem 2.1.15 (Deficiency Zero [Feinberg, 1987]). *Let $\mathfrak{N}$ be a weakly-reversible reaction network with deficiency zero. Then, with mass action kinetics, $\mathfrak{N}$ has exactly one positive steady state on each stoichiometric compatibility class and any choice of positive rate constants. Further, the steady state is locally stable relative to its stoichiometric compatibility class.*

Example 2.1.16 (Production-Degradation). *The production-degradation network is probably the simplest model which is weakly reversible and deficiency zero. The network is given by $\mathfrak{N} = \{\{A\}, \{A, \emptyset\}, \{A \to \emptyset, \emptyset \to A\}\}$ which translates into the reaction graph*

$$A \underset{\kappa_{-1}}{\overset{\kappa_1}{\rightleftharpoons}} \emptyset.$$

It can trivially be seen that the network is not only weakly reversible, but reversible and has two complexes, one connected component and the span of its reaction vectors, $\boldsymbol{r}_1 = 1$ and $\boldsymbol{r}_2 = -1$ is one dimensional. Hence the network has deficiency zero and one stable steady state is expected. Using the law of mass action, the dynamical system is given by a single ODE, $\dot{x_1} = -\kappa_1 x_1 + \kappa_{-1}$. Due to its simplicity, the ODE can be solved exactly to give

$$x_1(t) = x_1(0)e^{-\kappa_1 t} + \frac{\kappa_{-1}}{\kappa_1}\left(1 - e^{-\kappa_1 t}\right).$$

Hence, provided $\kappa_1 > 0$, and independent of the initial conditions and (positive) rate constants, the system will always converge on the steady state κ_{-1}/κ_1, which is a stable steady state.

The next example shows how non-mass action kinetics can arise in reaction networks.

Example 2.1.17 (Michaelis-Menten continued)**.** *In the Michaelis-Menten system it is often assumed that the concentration of the intermediate complex ES does not vary in time and, hence,* $x_3 \approx \kappa_1/(\kappa_{-1}+\kappa_2)x_1x_2$*. Combining this expression with the conservation law* $c_1 = x_1 + x_3$ *yields the equation*

$$x_3 = \frac{c_1 x_2}{\frac{\kappa_{-1}+\kappa_2}{\kappa_1} + x_2}.$$

Substituting this expression into the governing differential equations gives a network with Michaelis-Menten kinetics, a special case of Hill function kinetics.

The next remark gives a brief insight into spatial systems, which are discussed in more detail in Chapter 6

Remark 2.1.18 (Spatial Systems)**.** *If concentrations are not spatially uniform, the spatial heterogeneity needs to be taken into account. On* ℓ*-dimensional static domains this is most easily motivated by allowing the species to diffuse. Diffusion transforms the ODE system (2.3) into a system of partial differential equations (PDEs) [Murray, 2002],*

$$\frac{\partial \boldsymbol{x}(\boldsymbol{s},t)}{\partial t} = D\frac{\partial^2}{\partial \boldsymbol{s}^2}\boldsymbol{x} + \boldsymbol{f}(\boldsymbol{x}),$$

where $D = \operatorname{diag}(D_1,\dots,D_n)$ *is a matrix of diffusion coefficients and* $\partial^2/\partial \boldsymbol{s}^2 = \partial^2/\partial s_1^2 + \cdots + \partial^2/\partial s_\ell^2)$ *is the* ℓ*-dimensional Laplacian operator. To make the PDE system more tractable to algebraic methods, the Laplacian can be discretised which is exploited in Chapter 6.*

2.1.1 Algebraic Methods for Deterministic Models

To gain insight into the dynamics of a given reaction network, one investigates the steady states of its associated dynamical system. However, as a chemical reaction network is described by nonlinear polynomial equations, finding all positive steady states is a highly nontrivial task requiring sophisticated mathematical tools. Commutative algebra and algebraic geometry provide the framework to compute the steady states of reaction models. In this subsection some notions of algebraic geometry used in this thesis, either explicitly or as an implicit assumption, are discussed. Proofs and more detail can be found in Cox et al. [2013] or Cox et al. [2006].

Let $\mathbb{K}$ be a field and $R = \mathbb{K}[x_1,\dots,x_n]$ a polynomial ring with coefficients in $\mathbb{K}$. The most common fields used in the theory of chemical reactions are the complex numbers $\mathbb{C}$, the real numbers, $\mathbb{R}$, the rational numbers, $\mathbb{Q}$, or the field of rational functions in the rate constants $\mathbb{K}(\kappa_1,\dots,\kappa_m)$.

Remark 2.1.19. *For most of the proofs in this subsection, the field $\mathbb{K}$ is required to be* algebraically closed*, that is, every polynomial with coefficients in $\mathbb{K}$ needs to have all of its roots in $\mathbb{K}$. The algebraic closure is denoted by $\overline{\mathbb{K}}$. Since every field has an algebraic closure [Lang, 2002], this assumption is not a strong restriction.*

The central elements that are studied in this thesis are the ideals of R.

Definition 2.1.20. *Let $R = \mathbb{K}[x_1, \ldots, x_n]$ be a polynomial ring. An ideal I of R, $I \subseteq R$ is a subset of elements of R such that*

1. $0 \in I$,
2. $i_1 + i_2 \in I$ *for* $i_1, i_2 \in I$,
3. $ri \in I$ *for* $r \in R$ *and* $i \in I$.

A collection of polynomials in R can generate an ideal.

Definition 2.1.21. *An ideal $I \subseteq R$ is generated by a set of polynomials $\{f_1, \ldots, f_s\}$ such that*

$$I = \langle f_1, \ldots, f_s \rangle = \left\{ \sum_{i=1}^{s} h_i f_i \ : \ h_1, \ldots, h_s \in R \right\}.$$

An ideal is said to be finitely generated if the number of generators is finite. In fact, every ideal of a polynomial ring over $\mathbb{K}$ is finitely generated, a property summarised in Hilbert's Basis Theorem.

Theorem 2.1.22 (Basis Theorem)**.** *Every ideal of a polynomial ring $\mathbb{K}[x_1, \ldots, x_n]$, where $\mathbb{K}$ is any field, is finitely generated.*

Remark 2.1.23. *The statement of Hilbert's basis theorem used in this thesis is weaker than the original theorem which only requires the coefficients of the polynomials to be elements of a Noetherian ("small") ring rather than a field $\mathbb{K}$. However, any field is also a Noetherian ring.*

Often the generators of an ideal are compared to bases in linear algebra and this comparison is used where appropriate. However, generators do not fulfil the requirements of uniqueness and minimality. There is, however, a set of generators which is unique and minimal, a *reduced Gröbner basis*. To build a Gröbner basis a term ordering needs to be fixed. The term ordering needs to be an unambiguous, or total, ordering on the terms of a polynomial.

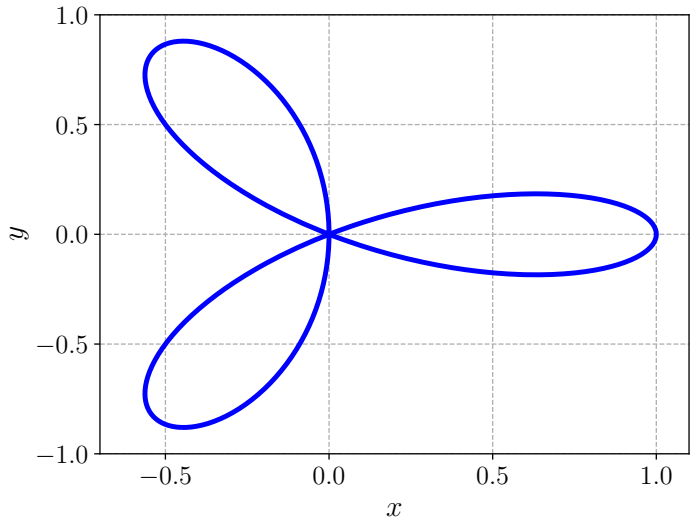


Figure 2.1: The trefoil curve, a plane quartic curve.

Definition 2.1.24. *A monomial ordering is a relation* $\succ$ *on the set of monomials* $\boldsymbol{x}^\alpha$, $\alpha \in \mathbb{Z}^n_{\geq 0}$ *such that:*

1. $\succ$ *is a total ordering on* $\mathbb{Z}^n_{\geq 0}$.
2. *If* $\alpha \succ \beta$ *and* $\gamma \in \mathbb{Z}^n_{\geq 0}$, *then* $\alpha + \gamma \succ \beta + \gamma$.
3. *Every non-empty subset of* $\mathbb{Z}^n_{\geq 0}$ *has a smallest element under* $\succ$.

Common monomial orderings are the lexicographic, "lex", graded lexicographic, "glex" or graded reverse lexicographic, "grevlex", order and further details can be found in Cox et al. [2006]. A monomial ordering allows one to find the leading term of a polynomial $f \in R$, $\mathtt{LT}(f)$.

Example 2.1.25 (Trefoil Curve)**.** *The trefoil curve, Figure 2.1, is defined by the quartic equation*

$$f(x, y) = x^4 + 2x^2y^2 + y^4 - x^3 + 3xy^2 = 0.$$

Various term orderings with leading term underlined are:

(i) Lexicographic: $\underline{x^4} - x^3 + 2x^2y^2 + 3xy^2 + y^4$,

(ii) Graded lexicographic: $\underline{x^4} + 2x^2y^2 + y^4 - x^3 + 3xy^2$,

(iii) Graded reverse lexicographic: $\underline{x^4} + 2x^2y^2 + y^4 - x^3 + 3xy^2$.

Definition 2.1.26 (Gröbner Basis)**.** *Let $I \subseteq R$ be an ideal of a polynomial ring, different to $\{0\}$. A Gröbner basis, $G = \{g_1, \dots, g_m\}$, is a subset of I such that*

$$\langle \mathtt{LT}(g_1), \dots, \mathtt{LT}(g_m) \rangle = \langle \mathtt{LT}(I) \rangle.$$

Further, $\langle g_1, \dots, g_m \rangle = I$.

Remark 2.1.27. *Note that for* every *$I \subseteq R$ a Gröbner basis can be computed [Cox et al., 2013].*

Remark 2.1.28. *Gröbner bases are at the heart of many algorithms and computations in nonlinear algebra. They are commonly used to find the solutions to nonlinear polynomial equations, count the number of solutions of systems of polynomials, obtain intersections of ideals or compute implicit representations of geometric objects.*

A minimal and unique set of generators of an ideal with respect to a monomial ordering $\succ$ is a *reduced Gröbner Basis.*

Definition 2.1.29 (Reduced Gröbner Basis)**.** *Fix an ideal $I \subseteq R$ and a monomial ordering $\succ$, then G is a reduced Gröbner basis of I if*

1. *the leading coefficient of every $g \in G$ is 1,*
2. *for any $g \neq h$ and $g, h \in G$ no monomial of g is a multiple of $\mathtt{LT}(h)$.*

Example 2.1.30 (Lotka-Volterra)**.** *The Lotka-Volterra model is an example of the oscillatory dynamics of a system with one non-zero steady state. It is one of the most commonly used examples of predator-prey dynamics. The Lotka-Volterra network incorporates the essential dynamics of a predator-prey interaction, birth of the prey, death by predation, predator growth due to predation and predator death [Murray, 2002]. The Lotka-Volterra model can be described as a chemical reaction network $\mathfrak{N} = \{\{X_1, X_2\}, \{X_1 + X_2, 2X_2, X_1, 2X_1, X_2, \emptyset\}, \{X_1 + X_2 \to 2X_2, X_1 \to 2X_1, X_2 \to \emptyset\}\}$ and its reaction graph is*

$$X_1 + X_2 \xrightarrow{\kappa_1} 2X_2, \quad X_1 \xrightarrow{\kappa_2} 2X_1, \quad X_2 \xrightarrow{\kappa_3} \emptyset.$$

The stoichiometric matrix is given by

$$\Gamma = \begin{pmatrix} -1 & 1 & 0 \\ 1 & 0 & -1 \end{pmatrix},$$

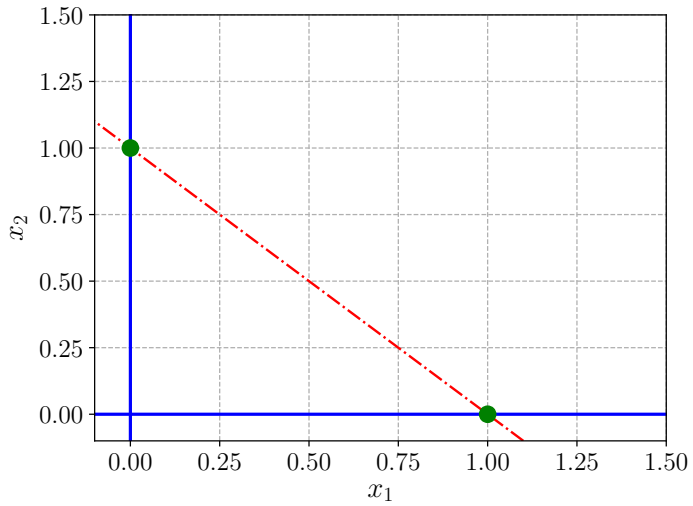


Figure 2.2: The steady state variety of the Michaelis-Menten system with parameters $\kappa_1 = \kappa_2 = \kappa_{-1} = c_1 = 1$ is simply the union of the coordinate axes. Species x_3 is zero at any steady state and therefore not shown in the figure. The stoichiometric compatibility class is simply a line connecting the two steady states $(1, 0)$ and $(0, 1)$.

and combining Γ *with the flux vector* $\boldsymbol{\nu} = (\kappa_1 x_1 x_2, \kappa_2 x_1, \kappa_3 x_2)^T$ *gives the dynamical system*

$$\frac{d}{dt}\begin{pmatrix} x_1 \\ x_2 \end{pmatrix} = \begin{pmatrix} -\kappa_1 x_1 x_2 + \kappa_2 x_1 \\ \kappa_1 x_1 x_2 - \kappa_3 x_2 \end{pmatrix}.$$

There are no linear conserved quantities and, the ideal describing the steady states is generated by $I = \langle -\kappa_1 x_1 x_2 + \kappa_2 x_1, \kappa_1 x_1 x_2 - \kappa_3 x_2 \rangle$. *A reduced lexicographic Gröbner basis of the system is* $G = \{x_1 - (\kappa_3/\kappa_2)x_2, x_2^2 - (\kappa_2/\kappa_1)x_2\}$. *It is easy to see that the reduced lexicographic Gröbner basis is a triangularised system, i.e.* g_1 *is a function of* (x_1, x_2) *and* g_2 *is a univariate polynomial. Hence, by solving the polynomials one by one the solutions to the steady state equations can be found.*

Next, essential notions of algebraic geometry are introduced by translating the language of ideals into geometric statements. Further details can be found in Cox et al. [2006].

The basic object of study in classical algebraic geometry are *algebraic varieties* which are the common zero sets of collections of polynomials.

Definition 2.1.31 (Variety)**.** *Let* $\boldsymbol{f} = \{f_1, \ldots, f_m\} \in R$. *Then, the set*

$$X = V(\boldsymbol{f}) = \{(x_1^*, \ldots, x_n^*) \in \overline{\mathbb{K}}^n \mid f_i(x_1^*, \ldots, x_n^*) = 0,\ \forall i = 1, \ldots, m\}$$

is called an algebraic variety.

Clearly, if $f_1(x_1^*, \ldots, x_n^*) = \cdots = f_m(x_1^*, \ldots, x_n^*) = 0$, then

$$\sum_{i=1}^{m} h_i(x_1^*, \ldots, x_n^*) f_i(x_1^*, \ldots, x_n^*) = 0 \tag{2.5}$$

for arbitrary $h_i \in R$. Hence, a variety can be defined in terms of an ideal $I = \langle f_1, \ldots, f_m \rangle$ such that $X = V(I)$.

Example 2.1.32 (Michaelis-Menten (continued))**.** *The steady state ideal of the Michaelis-Menten system is generated by*

$$I = \langle -\kappa_1 x_1 x_2 + \kappa_{-1} x_3 + \kappa_2 x_3, -\kappa_1 x_1 x_2 + \kappa_{-1} x_3 \rangle.$$

The corresponding steady state variety lies $\mathbb{C}^3$ *and has dimension* $\dim(V(I)) = 1$*. As can be seen in Figure 2.2, intersecting* $V(I) \cap V(\boldsymbol{z}_1^T \cdot \boldsymbol{x} - c_1)$ *gives the steady states of the system.*

Varieties translate ideals into geometric objects which is the start to building an algebra-geometry dictionary. The next obvious question to ask is: "Given a variety $X \subset \overline{\mathbb{K}}^n$ what are the polynomials vanishing on it?" This is answered by the central theorem of algebraic geometry which is Hilbert's Nullstellensatz. To state the Nullstellensatz the notion of a radical ideal is needed.

Definition 2.1.33 (Radical Ideal)**.** *Let* $I \subset R$ *be an ideal of the ring* R *then*

$$\sqrt{I} = \{r \in R \mid r^N \in I \text{ for some } N \in \mathbb{Z}_{>0}\}.$$

Theorem 2.1.34 (Nullstellensatz)**.** *Given an ideal* $J \subseteq R$ *then the relation*

$$I(V(J)) = \sqrt{J}$$

holds.

The Nullstellensatz therefore gives a bijection between radical ideals and varieties. This is a useful fact when converting from an algebraic description of a system to a geometric one. In particular, in most applications the varieties under study can be decomposed into several distinct components, called *irreducible components.*

Definition 2.1.35. *A variety* X *is irreducible if whenever* $X = X_1 \cup X_2$*, where* X_1 *and* X_2 *are varieties, then either* $X_1 = X$ *or* $X_2 = X$*.*

The definition of an irreducible variety can used to characterise reducible varieties.

Theorem 2.1.36. *Every variety X has a unique (up to ordering) decomposition into irreducible components,*

$$X = X_1 \cup X_2 \cup \cdots \cup X_m,$$

such that $X_i \not\subseteq X_j$ for $i \neq j$.

The decomposition of varieties into its irreducible components can be translated back to algebraic notions via *prime ideals*.

Definition 2.1.37. *An ideal $I \subseteq R$ is prime if, for $f, g \in R$, then whenever $fg \in I$ either $f \in I$ or $g \in I$.*

With the definition of a prime ideal the following proposition holds.

Proposition 2.1.38 ([Cox et al., 2013])**.** *A variety $X \subset \overline{\mathbb{K}}^n$ is irreducible if and only if $I(X)$ is a prime ideal.*

Example 2.1.39 (Lotka-Volterra (continued))**.** *The steady state ideal of the Lotka-Volterra model is $I = \langle -\kappa_1 x_1 x_2 + \kappa_2 x_1, \kappa_1 x_1 x_2 - \kappa_3 x_2 \rangle$. The steady state variety has dimension $\dim(V(I)) = 0$ and, therefore, consists of points in $\mathbb{C}^2$. The ideal can be decomposed into prime ideals $I = \langle x_1, x_2 \rangle \cap \langle x_1 - \kappa_3/\kappa_1, x_2 - \kappa_2/\kappa_1 \rangle$ from which it can be seen that the variety $V(I)$ is a union of the points $(0, 0)$ and $(\kappa_3/\kappa_1, \kappa_2/\kappa_1) \in \mathbb{R}^2_{\geq 0}$.*

Note that every prime ideal is a radical ideal. By the Nullstellensatz, there is a bijection between prime ideals and irreducible varieties. Varieties can be seen as closed sets and, therefore, they also induce a topology on the affine space $\overline{\mathbb{K}}^n$. This topology is coarse and highly non-Hausdorff. However, closed sets in this topology are vital for the study of projections of varieties [Cox et al., 2013].

Definition 2.1.40 (Zariski Topology)**.** *The closed sets $V(I)$ for $I \subseteq R$ induce the Zariski topology on $\overline{\mathbb{K}}^n$. The Zariski closure of a subset $S \subseteq \overline{\mathbb{K}}^n$, $\overline{S}$ is the smallest variety containing S. Further, a subset $Q \subseteq V(I)$ is Zariski dense if $\overline{Q} = V(I)$.*

The Zariski topology and Zariski closed sets are extremely important in many applications of algebraic geometry. For example, suppose there is a chemical reaction network for which there are measurements for the concentrations $x_{\ell+1}, \ldots, x_n$, however, no measurements could be obtained for the first ℓ variables. In this case the steady variety needs to be projected from $\overline{\mathbb{K}}^n$ to $\overline{\mathbb{K}}^{n-\ell}$ in order to fit the data to the model. Generically, projections of varieties are not varieties, but Zariski dense sets. To compute the closure the following theorem is needed.

Theorem 2.1.41. *Let $V(I) \in \overline{\mathbb{K}}^n$ and let $\pi_\ell : \overline{\mathbb{K}}^n \to \overline{\mathbb{K}}^{n-\ell}$ be the projection map onto the last $n-\ell$ coordinates. Then, the Zariski closure of $\pi_\ell(V(I))$ is equal to the variety of the ℓ^{th} elimination ideal $I_\ell = I \cap \mathbb{K}[x_{\ell+1}, \ldots, x_n]$.*

In practice, the elimination ideals can be obtained from a lex Gröbner basis.

Example 2.1.42 (Michaelis-Menten (continued))**.** *A reduced lex Gröbner basis of the Michaelis-Menten system in the ring $\mathbb{K}[x_3, x_2, x_1]$ is $G = \{x_1x_2, x_3\}$. Hence, projecting onto last two coordinates, $\mathbb{C}^3 \to \mathbb{C}^2$, gives $I_1 = \pi_1(I) = \langle x_1x_2\rangle = \langle x_1\rangle \cap \langle x_2\rangle$. This corresponds to the coordinate axes shown in Figure 2.2.*

A special case of elimination ideals is *implicitization*. Suppose the d-dimensional variety is parameterised by the variables $t_1, \ldots, t_d$ and this parameterisation is given in an explicit form

$$\begin{aligned} x_1 &= \phi_1(t_1, \ldots, t_d), \\ &\vdots \\ x_n &= \phi_n(t_1, \ldots, t_d). \end{aligned} \tag{2.6}$$

The functions ϕ_i are rational functions of the variables $t_1, \ldots, t_d$. Then, the implicit equations for the variety are given by the intersection ideal

$$I = \langle x_1 - \phi_1(t_1, \ldots, t_d), \ldots, x_n - \phi_n(t_1, \ldots, t_d)\rangle \cap \mathbb{K}[x_1, \ldots, x_n]. \tag{2.7}$$

The conversion between implicit and explicit representation of varieties will be very important in Subsection 2.1.1.1.

To conclude this subsection, a procedure for removing components of a variety, called *saturation*, is introduced. In chemical reaction network theory one is often only interested in positive solutions and, therefore, all components of a variety contained in the coordinate axes can be removed. Saturation often renders the studied system more manageable and sometimes reveals the underlying geometric structure of the system.

Definition 2.1.43 (Saturation)**.** *Let $I, J \subseteq R$ be ideals of R, then $I : J^\infty$ is the set*

$$\{f \in R \mid \text{for all } g \in J, \text{ there exists an integer } N \geq 0 \text{ such that } fg^N \in I\}.$$

The ideal $I : J^\infty$ is called the saturation ideal of I with respect to the ideal J.

The following theorem illustrates the effect of saturation on a variety.

Proposition 2.1.44. *Let $I, J \subseteq R$, then $V(I : J^\infty) = \overline{V(I) \setminus V(J)}$.*

Hence, saturating with respect to $J = \langle \prod_i x_i \rangle$ removes any component contained in the coordinate axes of $\overline{\mathbb{K}}^n$.

Example 2.1.45 (Lotka-Volterra (continued))**.** *The saturation of the steady state ideal I of the Lotka-Volterra system is*

$$I : \langle x_1 x_2 \rangle^\infty = \langle x_1 - (\kappa_3/\kappa_1), x_2 - (\kappa_2/\kappa_1) \rangle.$$

As expected, the component $(0, 0)$ of the steady state variety was removed and only the non-zero steady state is left.

2.1.1.1 Toric Geometry

Toric geometry appears in many applications of algebraic geometry to biology, statistics, engineering and computer science. In this subsection essential definitions of toric geometry are given and it is briefly explained how toric varieties relate to chemical reaction networks.

Extensive use is made of the notation $\mathbb{K}^* = \mathbb{K} \setminus \{0\}$ where $\mathbb{K} = \mathbb{C}$ or, more rarely $\mathbb{R}$. The set $\mathbb{C}^*$ is known as the *complex (algebraic) torus* and varieties which can be parameterised by monomial functions with the torus as their domain are called toric varieties. Toric varieties have a rich combinatorial structure.

Definition 2.1.46 (Toric Variety)**.** *A toric variety is the Zariski closure of the image of the monomial map*

$$\psi_A : (\mathbb{K}^*)^d \to \mathbb{K}^n,$$

such that,

$$\boldsymbol{t} \to (\boldsymbol{t}^{\boldsymbol{a}_1}, \ldots, \boldsymbol{t}^{\boldsymbol{a}_n}),$$

where $\boldsymbol{t}^{\boldsymbol{a}_i} = t_1^{a_{i_1}} \cdots t_d^{a_{i_d}}$.

The exponent vectors $\boldsymbol{a}_i$ are integer vectors and are often referred to as characters of a torus. The monomials $\boldsymbol{t}^{\boldsymbol{a}_i}$ are Laurent monomials [Lang, 2002] in the ring $\mathbb{K}[t_1^\pm, \ldots, t_d^\pm]$, where $t_i^\pm$ denotes the variable t_i and its inverse t_i^{-1} respectively. The exponent vectors can be collected into a rank d, $d \times n$ matrix $A = (\boldsymbol{a_1}, \ldots, \boldsymbol{a_n})$ which is commonly referred to as *A-matrix*. The A-matrix carries a lot of a priori information about the toric variety, such as its dimension, d. Taking its columns as vertices of convex sets ("polytopes") in $\mathbb{Z}^n$, other geometric invariants of the variety can be calculated purely from the information given by the polytope. Polyhedral geometry

will only play a minor role in this thesis and more information can be found in Ziegler [2012].

Is was shown in Eisenbud and Sturmfels [1996] that the implicit equations of a toric variety are given by *prime binomial ideals* and the connection between binomiality of the ideal and monomial maps play a central role in this thesis. In particular, the positive steady states of many chemical reaction networks are described by toric varieties [Millán et al., 2012; Craciun et al., 2009a]. Especially, the steady state varieties of deficiency zero, weakly reversible networks are always toric [Craciun et al., 2009a].

Example 2.1.47 (Phosphorylation Networks (continued))**.** *The steady state variety of the Phosphorylation network is three dimensional and, after saturating out the coordinate axes, it is generated by the binomials* $I : \langle x_1 \cdots x_6 \rangle^\infty = \langle \kappa_3 x_5 - \kappa_6 x_6, \kappa_4 x_2 x_4 - (\kappa_5 + \kappa_6) x_6, \kappa_1 \kappa_3 x_1 x_3 - (\kappa_2 \kappa_6 + \kappa_3 \kappa_6) x_6 \rangle$*. The binomials generating* $I : \langle x_1 \cdots x_6 \rangle^\infty$ *are prime in the ring* $\mathbb{R}(\kappa_1, \ldots, \kappa_6)[x_1, \ldots, x_6]$*. A linear algebra calculation further described in Chapter 3 reveals that the steady states of the phosphorylation network are given by a toric variety with A-matrix*

$$A = \begin{pmatrix} -1 & 0 & 1 & 0 & 0 & 0 \\ 0 & -1 & 0 & 1 & 0 & 0 \\ 1 & 1 & 0 & 0 & 1 & 1 \end{pmatrix}.$$

2.2 Stochastic Models

In this section an overview of the methods of stochastic modelling of chemical reactions is given. Chapters 5 and 6 are motivated by problems and techniques arising from the modelling of stochastic chemical reaction networks, although, due to the extrinsic stochasticity, a different modelling framework is used.

This subsection is divided into two parts, the first part introduces continuous time Markov chain models of stochastic networks, the second covers approximations to the Markov description and useful analytical tools for predicting model behaviour.

2.2.1 The Chemical Master Equation and the Gillespie Algorithm

In this section the fundamental statistical theory of describing systems of interacting chemical species is laid out and an algorithm to numerically simulate such systems is described. As in the previous section any spatial aspect is ignored and it is assumed that the system is "well mixed". A system is well mixed if the majority of particle

collisions are non-reactive and, therefore, the distribution of positions is uniform in space. The well mixed assumption allows one to only consider reactive collisions and develop a local statistical theory of the reaction system [Gillespie, 2007].

As in Section 2.1 a chemical reaction network is defined as the multiset $\mathfrak{N} = \{\mathcal{S}, \mathcal{C}, \mathcal{R}\}$. Let $\mathcal{S} = \{X_1, \ldots, X_n\}$ and, in analogy to the deterministic case, let $\mathcal{R} = \{\boldsymbol{r}_1, \ldots, \boldsymbol{r}_{|\mathcal{R}|}\}$ be represented by the reaction vectors defined in (2.2). In the deterministic case the dynamics are expressed in terms of the chemical concentrations, $\boldsymbol{x}(t)$, whereas in the stochastic setting, the evolution of the system is determined by the *number* of molecules, $\boldsymbol{U}(t) = (U_1, \ldots, U_n)^T \in \mathbb{Z}^n_{\geq 0}$, where the random variables $U_i(t)$ are the number of molecules of species X_i at time t. Further, let $\boldsymbol{u} \in \mathbb{Z}^n_{\geq 0}$ be a non-negative vector describing a single realisation of $\boldsymbol{U}$ [Gillespie, 1992]. Consequently, a reaction $\boldsymbol{r}_i \in \mathcal{R}$ changes the state of the system $\boldsymbol{u} \to \boldsymbol{u} + \boldsymbol{r}_i$. To develop a full probabilistic theory, first, the probability density of a reaction to occur needs to be found.

Definition 2.2.1 (Reaction Propensity [Gillespie, 1992])**.** *Let $a_i(\boldsymbol{u})$ be a probability density such that $a_i(\boldsymbol{u})dt$ is the probability of reaction $\boldsymbol{r}_i$ to occur in the time interval $[t, t + dt)$. The function $a_i(\boldsymbol{u})$ is called the* reaction propensity *and the collection of all propensities in the network is the propensity vector $\boldsymbol{a}(\boldsymbol{u}) = (a_1(\boldsymbol{u}), \ldots, a_{|\mathcal{R}|}(\boldsymbol{u}))^T$.*

Remark 2.2.2. *Note that the expressions used in this subsection, $a_i(\boldsymbol{u})$, are* functions *of the state vector $\boldsymbol{u}$, whereas the vectors $\boldsymbol{a}_i$ defined in 2.1.1.1 are* integer vectors.

The choice of the appropriate propensity function for a stochastic reaction network is a similar modelling choice to selecting the reaction kinetics in deterministic systems. The most commonly used propensity function is the probabilistic law of mass action [Anderson et al., 2010], which simplifies to the deterministic law of mass action in the appropriate limit.

Definition 2.2.3 (Probabilistic Mass Action)**.** *Let $\boldsymbol{r}_i = \boldsymbol{\beta}_i - \boldsymbol{\alpha}_i$ be a reaction of the stochastic chemical reaction network from complex $C_{\boldsymbol{\alpha}_i}$ defined by the stoichiometric coefficients $\boldsymbol{\alpha}_i$ to complex $C_{\boldsymbol{\beta}_i}$ with stoichiometric coefficients $\boldsymbol{\beta}_i$. Then the propensity function according to the probabilistic law of mass action is*

$$a_i(\boldsymbol{u}) = \kappa_i \prod_{l=1}^{n} \frac{u_l!}{(u_l - \alpha_{i_l})!} \mathbb{1}_{u_l \geq \alpha_{i_l}},$$

where $\mathbb{1}$ is the indicator function.

According to [Gillespie, 1992], which states that only one reaction occurs in the time interval $[t, t+dt)$ as $dt \to 0$, a Kolmogorov backward equation can be formulated [Gardiner, 1985],

$$\frac{\partial}{\partial t} p(\boldsymbol{u}, t|\boldsymbol{u}_0, t_0) = \sum_i^m p(\boldsymbol{u} - \boldsymbol{r}_i, t|\boldsymbol{u}_0, t_0) a_i(\boldsymbol{u} - \boldsymbol{r}_i) - p(\boldsymbol{u}, t|\boldsymbol{u}, t_0) a_i(\boldsymbol{u}). \tag{2.8}$$

Equation (2.8) is known as the *Chemical Master Equation* (CME) and fully describes the time evolution of a stochastic chemical reaction network. In most cases, the state space of the system is infinite and exact analytical expressions for the probability density $p(\boldsymbol{u}, t|\boldsymbol{u}_0, t_0)$ do not exist. One is often interested in the stationary distribution, $\phi(\boldsymbol{u})$, such that, as $t \to \infty$, $\partial p(\boldsymbol{u}, t|\boldsymbol{u}_0, t_0)/\partial t \approx 0$ and $p(\boldsymbol{u}, t|\boldsymbol{u}_0, t_0) \to \phi(\boldsymbol{u})$. This is the stochastic analogue to solving for the steady states of a deterministic system. Due to the infinite state space of many reaction networks, exact analytic solutions often do not exist. However, approximations to arbitrary order of precision can sometimes be found [van Kampen, 1983].

Common approaches for solving the CME are computational simulations. An exact algorithm for the solving the CME computationally is the *Gillespie Algorithm* [Gillespie, 2007]. Approximate solutions to the CME in the presence of low noise can be found analytically via van Kampen's *weak noise expansion* which is covered in the next subsection.

Example 2.2.4 (Production-Degradation)**.** *The stochastic version of the production-degradation network encountered in Example 2.1.16 is one of the few exactly solvable stochastic networks. It is described by the CME*

$$dp(a, t|a_0, t_0)/dt = \kappa_1 p(a-1, t|a_0, t_0) + \kappa_2(a+1)p(a+1, t|a_0, t_0) - \kappa_2 a p(a, t|a_0, t_0) - \kappa_1 p(a, t|a_0, t_0).$$

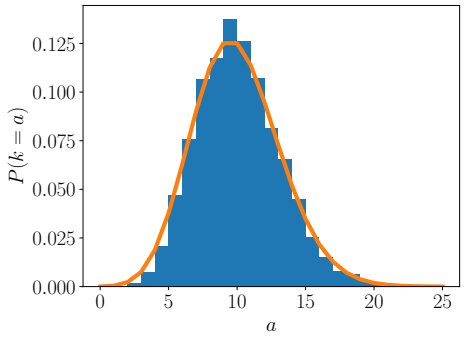
Hence, the stationary distribution can be found from

$$\kappa_1\phi(a-1) + \kappa_2(a+1)\phi(a+1) - \kappa_1\phi(a) - \kappa_2 a\phi(a) = 0.$$

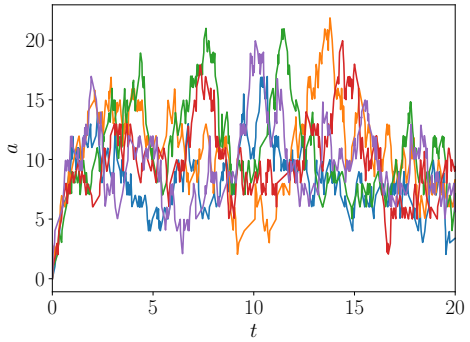
Solving this recurrence relation gives the stationary distribution

$$\phi(a) = \frac{1}{a!}\left(\frac{\kappa_2}{\kappa_1}\right)^a e^{-\frac{\kappa_2}{\kappa_1}},$$

which is a Poisson distribution with mean κ_2/κ_1, which is the deterministic steady state. A comparison of the analytic stationary distribution and a simulation can be found in Figure 2.3a and sample paths generated from the CME via the Gillespie algorithm are plotted in Figure 2.3b.



(a) A comparison of the steady state distribution of the production-degradation network. The bars are the stationary distribution obtained from a Gillespie simulation and the orange line is the analytic solution.



(b) Five sample paths generated of the production-degradation network via the Gillespie algorithm with initial condition $a_0 = 0$. The trajectories fluctuate around the deterministic steady state of $a = 10$.

Figure 2.3: Simulations and analytic results of the stationary distribution and trajectories of the production-degradation network with parameters $\kappa_1 = 1$ and $\kappa_2 = 10$.

2.2.2 The Fokker-Planck and Chemical Langevin Equation

As mentioned in the previous section, the CME cannot be solved exactly in most cases and often computational methods are used to gain insight into the stochastic behaviour of chemical reaction networks. To make analytic progress, various approximation methods have been used [van Kampen, 1983; Munsky and Khammash, 2006; Engblom, 2009].

In this subsection the system size, or *weak noise*, expansion [van Kampen, 1983] is introduced, which reduces the high dimensional CME to a systematic expansion around the mean field. In particular, this expansion relies on the existence of a so-called system size parameter Ω. The parameter Ω is often identified with "representative system size" such as the maximum number of animals that an ecosystem can support in ecological models, the number of molecules at steady state of a chemical reaction network, or the volume of a tank in a chemical reactor. Stochastic effects play a role in chemical reaction models due to the finite amount of molecules in a system [McKane and Newman, 2005]. Hence, stochastic networks which are modelled by a CME are examples of systems with *intrinsic noise*. Intrinsic noise is a type of noise which is part of the physical process by which a system evolves and it cannot be circumvented in a perfect experiment. If, for example, the number of molecules were infinite, then all stochastic effects would disappear, a consequence of the central limit theorem [Grimmet and Stirzaker, 1982]. Therefore, the first step to approximating

equation (2.8) is a change of variables

$$U_i = x_i\Omega + \delta x_i\sqrt{\Omega}. \tag{2.9}$$

Note, that the variable x_i is a deterministic variable, whereas the variable δx_i is a continuous random variable. Under the assumption of (2.9) the limit $\Omega \to \infty$ is given by

$$\lim_{\Omega\to\infty} \frac{\boldsymbol{U}}{\Omega} = \boldsymbol{x}. \tag{2.10}$$

By van Kampen [1983] the distribution $p(\boldsymbol{U}, t)$ is the same as the translated distribution $\Pi(\boldsymbol{\delta x}, t)$. Hence, the CME (2.8) can be Taylor expanded around the new distribution and the deterministic variables $\boldsymbol{x}$ in terms of Ω. Expanding the various terms of the CME gives

$$\frac{\partial p}{\partial t} = \frac{\partial \Pi}{\partial t} - \sqrt{\Omega}\sum_{i=1}^{n} \frac{dx_i}{dt}\frac{\partial \Pi}{\partial \delta x_i}, \tag{2.11a}$$

$$a_i(\boldsymbol{u} - \boldsymbol{r}_i) \approx \Omega\left(a_i(\boldsymbol{x}) + \frac{1}{\sqrt{\Omega}}\sum_{j=1}^{n}\frac{\partial a_i(\boldsymbol{x})}{\partial x_j}\delta x_j + \mathcal{O}\left(\frac{1}{\Omega}\right)\right), \tag{2.11b}$$

$$\begin{aligned} p(\boldsymbol{u} - \boldsymbol{r}_i, t) &= \Pi\left(\boldsymbol{\delta x} - \frac{\boldsymbol{r}_i}{\sqrt{\Omega}}, t\right) \approx \\ &\approx \left(1 - \frac{1}{\sqrt{\Omega}}\sum_{j=1}^{n}\Gamma_{ij}\frac{\partial}{\partial \delta x_j} + \frac{1}{2\Omega}\sum_{j=1}^{n}\sum_{l=1}^{n}\Gamma_{ij}\Gamma_{il}\frac{\partial^2}{\partial \delta x_j \partial \delta x_l} + \mathcal{O}\left(\frac{1}{\Omega^{\frac{3}{2}}}\right)\right)\Pi(\boldsymbol{\delta x}, t). \end{aligned} \tag{2.11c}$$

Hence, substituting (2.11a)-(2.11c) into (2.8) and ignoring terms of order $\mathcal{O}(1/\sqrt{\Omega})$, an expansion of the CME in terms of the system size is obtained

$$\begin{aligned} &\frac{\partial \Pi}{\partial t} - \sqrt{\Omega}\sum_{i=1}^{n}\frac{dx_i}{dt}\frac{\partial \Pi}{\partial \delta x_i} = \\ &= \sum_{i=1}^{m}\left(-\sqrt{\Omega}\sum_{j=1}^{n}\Gamma_{ij}\frac{\partial}{\partial \delta x_j} + \frac{1}{2}\sum_{j=1}^{n}\sum_{k=1}^{n}\Gamma_{ij}\Gamma_{il}\frac{\partial^2}{\partial \delta x_j \partial \delta x_l}\right)\left(a_i(\boldsymbol{x}) + \frac{1}{\sqrt{\Omega}}\sum_{j=1}^{n}\frac{\partial a_i(\boldsymbol{x})}{\partial x_j}\right)\Pi(\boldsymbol{\delta x}). \end{aligned} \tag{2.12}$$

The approximation $\Omega \gg 1$ is the weak noise approximation, which assumes that the system size Ω is large enough, such that all terms of order smaller than unity can be ignored [van Kampen, 1983]. By collecting all terms of order $\mathcal{O}(\sqrt{\Omega})$ the equation

$$\sum_{i=1}^{n}\frac{dx_i}{dt}\frac{\partial \Pi}{\partial \delta x_i} = \sum_{i=1}^{n}\sum_{j=1}^{n}\Gamma_{ij}a_i(\boldsymbol{x})\frac{\partial \Pi}{\partial \delta x_i}, \tag{2.13}$$

is obtained. Further, in the limit $\Omega \to \infty$, an expansion of the stochastic law of mass action yields the deterministic law of mass action [Anderson et al., 2010] to give, $\boldsymbol{a}(\boldsymbol{x}) = \boldsymbol{\nu}$. Hence, the deterministic equations are recovered,

$$\frac{d\boldsymbol{x}}{dt} = \Gamma \boldsymbol{a}(\boldsymbol{x}). \tag{2.14}$$

At order $\mathcal{O}(1)$ a Fokker-Planck equation describing the time evolution of Π can be found [van Kampen, 1983],

$$\begin{aligned}\frac{\partial \Pi}{\partial t} &= \sum_{i=1}^{m} \left(- \sum_{j,k=1}^{n} \frac{\partial a_i}{\partial x_k} \Gamma_{ij} \frac{\partial (\delta x_j \Pi)}{\partial \delta x_k} + \frac{1}{2} a_i \sum_{j,k=1}^{n} \Gamma_{ij} \Gamma_{ik} \frac{\partial^2 \Pi}{\partial \delta x_j \partial \delta x_k} \right), \\ &= - \sum_{j,k=1}^{n} J_{jk} \frac{\partial (\delta x_k \Pi)}{\partial \delta x_j} + \frac{1}{2} \sum_{j,k=1}^{n} B_{jk} \frac{\partial^2 \Pi}{\partial \delta x_j \partial \delta x_k}. \end{aligned} \tag{2.15}$$

where

$$J = \{J_{ij}\} = \{\partial (\Gamma \boldsymbol{\nu})_i / \partial x_j\}, \tag{2.16a}$$

$$B = \Gamma \mathrm{diag}(\boldsymbol{\nu}) \Gamma^T = \{B_{ij}\}_{i,j=1\ldots,n}, \tag{2.16b}$$

and $\mathrm{diag}(\boldsymbol{\nu})$ is a diagonal matrix with the entries of $\boldsymbol{\nu}$ on its diagonal. Notice that the matrix J is just the Jacobian matrix of the deterministic system (2.14).

Example 2.2.5 (Production-Degradation (continued))**.** *The noise in the production-degradation network can be described by the Fokker-Planck equation*

$$\frac{\partial \Pi}{\partial t} = \kappa_1 \frac{\partial \delta a \Pi}{\partial \delta a} + \frac{1}{2} (\kappa_1 a + \kappa_2) \frac{\partial^2 \Pi}{\partial (\delta a)^2}.$$

Substituting for the deterministic steady state, $a = \kappa_2/\kappa_1$, gives

$$\frac{\partial \Pi}{\partial t} = \kappa_1 \frac{\partial \delta a \Pi}{\partial \delta a} + \kappa_2 \frac{\partial^2 \Pi}{\partial (\delta a)^2}.$$

Using Itô's Lemma [Gardiner, 1985] an equivalent Langevin equation, the *Chemical Langevin Equation* (CLE) can be formulated which describes the time evolution of the noise

$$d\boldsymbol{\delta x} = J \boldsymbol{\delta x} dt + \boldsymbol{\eta} dt, \tag{2.17}$$

where $\boldsymbol{\eta}$ is a vector of Gaussian stochastic processes, such that

$$\langle \eta_i(t) \rangle = 0, \tag{2.18a}$$

$$\langle \eta_i(t) \eta_j(t') \rangle = B_{ij} \delta(t - t'). \tag{2.18b}$$

Equivalently, the noise term in equation (2.17), $\boldsymbol{\eta}\, dt$, can be written as $b\sqrt{dt}\,\boldsymbol{\xi}$, where $\boldsymbol{\xi}$ is a vector of standard Gaussian processes, $N(0,1)$, and b is a matrix such that $bb^T = B$. The CLE is a system of stochastic differential equations (SDEs) and, when the deterministic system converges to a steady state, the system is linear. Due to this linearity, analytic methods, such as Fourier transforms, can be used to obtain information about the noise in a stochastic chemical reaction network. One of the most important analytic tools is the computation of the power spectrum.

Remark 2.2.6. *Non well-mixed systems can also be modelled in the CME framework [Woolley et al., 2011c]. It is assumed that the space can be discretised into locally well-mixed compartments. To model diffusion a set of reactions describing the inflow and outflow of each species in each compartment is added.*

2.2.2.1 Power Spectral Methods

The power spectrum is an important analytic tool in signal processing and the study of stochastic processes [Woolley et al., 2011b]. In analogy to spectral theory in linear algebra, where principal component analysis considers the spectrum of data matrices to find features of data sets [Jolliffe, 2011], spectral theory for time dependent signals can be used to find prominent temporal frequencies in the data [Woolley et al., 2011b].

The power spectrum of an input δx is defined by Gardiner [1985] and Miller and Childers [2012],

$$P_{\delta x} = \langle |\widehat{\delta x}|^2 \rangle, \tag{2.19}$$

where $\langle \cdot \rangle$ denotes the average over realisations and $\hat{\cdot}$ is the Fourier transform,

$$\widehat{\delta x} = \int_{-\infty}^{\infty} \delta x e^{-i\omega t} dt. \tag{2.20}$$

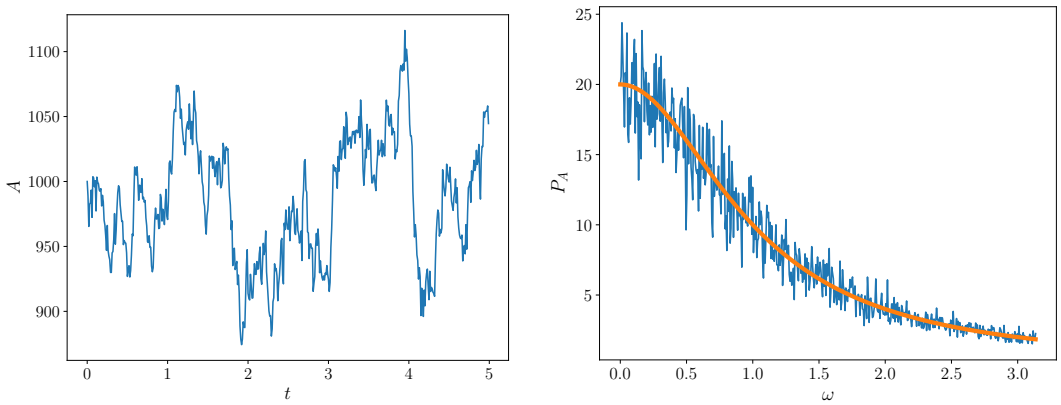
The power spectrum is a function of frequency, namely $\widehat{\delta x} = \widehat{\delta x}(\omega)$.

For stochastic chemical reaction networks the power spectrum can be computed trivially from the CLE, if the network has a stable steady state. In this case, the CLE is linear and can be Fourier transformed to give

$$\begin{aligned} \int_{-\infty}^{\infty} \frac{d\boldsymbol{\delta x}}{dt} e^{-i\omega t} dt &= \int_{-\infty}^{\infty} (J\boldsymbol{\delta x} + \boldsymbol{\eta}) e^{-i\omega t} dt, \\ -i\omega \widehat{\boldsymbol{\delta x}} &= J\widehat{\boldsymbol{\delta x}} + \hat{\boldsymbol{\eta}}, \\ \widehat{\boldsymbol{\delta x}} &= -\left(J + i\omega \boldsymbol{I}\right)^{-1} \hat{\boldsymbol{\eta}}, \end{aligned}$$

where $\boldsymbol{I}$ is the identity matrix. Hence, the power spectrum is given by

$$P_{\boldsymbol{\delta x}} = \langle \widehat{\boldsymbol{\delta x}} \widehat{\boldsymbol{\delta x}}^{\dagger} \rangle = \left(J + i\omega \boldsymbol{I}\right)^{-1} \langle \hat{\boldsymbol{\eta}} \hat{\boldsymbol{\eta}}^{\dagger} \rangle \left[\left(J + i\omega \boldsymbol{I}\right)^{-1}\right]^{\dagger}, \tag{2.21}$$



(a) A trajectory of the Chemical Langevin Equation of the production-degradation network.

(b) The analytic and simulated power spectrum of the production-degradation network. The power spectrum was averaged over 100 simulations.

Figure 2.4: The CLE trajectory and power spectrum of the production-degradation network. The parameters are $\kappa_1 = 1$ and $\kappa_2 = 10$ as before.

where † denotes the hermitian conjugate.

Example 2.2.7 (Production-Degradation (continued))**.** *The CLE of the production-degradation can be derived from the Fokker-Planck equation to give*

$$d\delta a = -\kappa_1 \delta a dt + \sqrt{2\kappa_2}\sqrt{dt}\xi,$$

where $\xi \sim N(0,1)$ is a standard normal Gaussian process. A trajectory of the CLE is plotted in Figure 2.4a. The power spectrum is given by

$$P_{\delta a} = \frac{2\kappa_2}{\kappa_1^2 + \omega^2}.$$

The power spectrum of the production-degradation network is plotted in Figure 2.4b.

Peaks in the power spectrum highlight stochastic oscillations, so-called quasi-cycles. Power spectra are used extensively in Chapter 5 and 6.

2.3 Deterministic Networks and Extrinsic Noise

So far it has been an implicit assumption that the rate constant, κ, is a constant with one unique, known value and does not fluctuate in time. Often, however, the rate constants are sensitive to their environments and they can vary considerably [Picco et al., 2017]. There are various mechanisms responsible for the variation of the rate

constants such as cell to cell variability [Filippi et al., 2015], or varying experimental conditions [Sato et al., 2003] such as varying temperature. Both are examples of *extrinsic noise* in biological or chemical systems. In Chapter 5 it is shown how extrinsic noise can create stochastic trajectories of deterministic models and induce drastically new behaviour. Some of this new behaviour is studied in this thesis. In this section, the main framework and mathematical assumptions that underlie the study of extrinsic noise in this thesis are introduced, starting from the rate constants κ as constant but random parameters and generalising to rate constants as stochastic processes.

Let $\mathfrak{N}$ be a deterministic chemical reaction network with n species and m reactions and $I \subseteq \mathbb{K}(\kappa_1, \ldots, \kappa_m)[x_1, \ldots, x_n]$ its steady state ideal. The ideal I actually represents a family of ideals parameterised by the rate constants $\kappa_1, \ldots, \kappa_m$. Whenever a particular set of rate constants is chosen, then a member of the family of ideals is picked. Algebraically, choosing a set of parameters amounts to the evaluation map $\pi : \mathbb{K}(\kappa_1, \ldots, \kappa_m) \to \mathbb{K}$. In particular, due to the fact that the variables $\boldsymbol{\kappa}$ represent rate constants, the evaluation is restricted to $\pi(\kappa_i) \to \mathbb{R}_{\geq 0}$, as negative values are nonphysical. For constant rate constants, the evaluation map is restricted further to $\pi(\kappa_i) \to \mathbb{R}_{>0}$, as rate constants evaluated to zero imply that no reaction happens, which is incompatible with the network $\mathfrak{N}$.

Another way to view the evaluation map π is a graph theoretic one. Let $\mathcal{G}(\mathcal{C}, E)$ be the directed graph associated to $\mathfrak{N}$. Then π is a function that assigns a random, but positive edge weight to each edge. Again, edges of zero weight would imply that the edge does not exist and, hence, turns $\mathcal{G}$ into the digraph associated to a different model. Extensive use of this fact is made in Chapter 3.

By definition, the map π assigns a positive value to each rate constant, κ, and the value assigned to this rate constant can stem from either:

(i) a specific value measured in an experiment or found in the literature, or,

(ii) can be drawn from distribution of parameter values, which takes biological variability into account.

Picking different members of a family can result in different model behaviour. For example, a member of a family can have multiple steady states, whereas another cannot, or some family members may be in a regime where a Hopf bifurcation has occurred, whereas others are stable, or unstable. This is illustrated in the example below.

Example 2.3.1 (Brusselator)**.** *The Brusselator is a model for an autocatalytic reaction which is capable of having oscillating solutions. It was proposed by Ilya Prigogine and his collaborators of the Université Libre de Bruxelles as a model for the Belousov–Zhabotinsky reaction (BZ reaction). The reaction scheme is*

$$\begin{aligned} X_1 &\underset{\kappa_1}{\overset{\kappa}{\rightleftharpoons}} \emptyset \\ 2X_1 + X_2 &\xrightarrow{\kappa} 3X_1 \\ X_1 &\xrightarrow{\kappa_2} X_2 + D, \end{aligned}$$

which translates into the dynamical system

$$\frac{d}{dt}\begin{pmatrix} x_1 \\ x_2 \end{pmatrix} = \begin{pmatrix} \kappa_1 + x_1^2 x_2 - \kappa_2 x_1 - x_1 \\ \kappa_2 x_1 - x_1^2 x_2 \end{pmatrix},$$

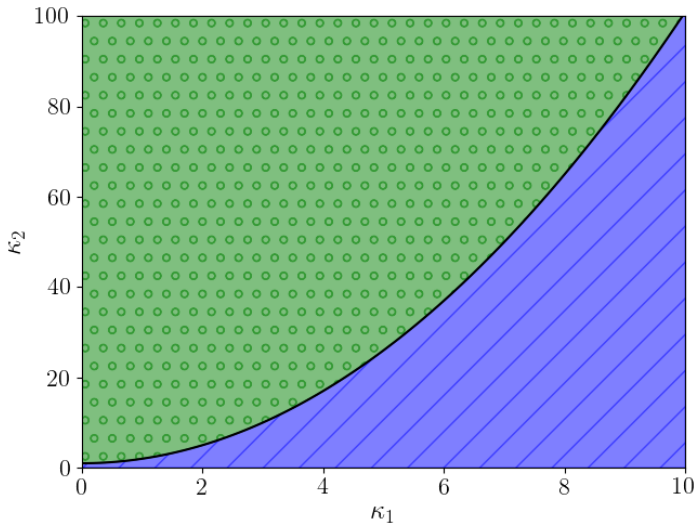
where all rate constants κ have been set to one. The model has one steady state, $\boldsymbol{x}^* = (\kappa_1, \kappa_1/\kappa_2)^T$, which is unstable, if $\kappa_2 > 1 + \kappa_1^2$. Hence, fixing $\kappa_1 = 1$ and $\kappa_2 = 2 + \delta\kappa_2$, where $\delta\kappa_2$ is an arbitrary perturbation of κ_2 drawn from a standard normal distribution, the sensitive dependence of the model behaviour on the constants κ_1, κ_2 can be shown. A phase diagram of the Brusselator is plotted in Figure 2.5a and a stable and an oscillatory trajectory is shown in Figure 2.5b and 2.5c respectively.

It is of great importance to account for extrinsic noise when deciding whether a model fits the data or not [Filippi et al., 2015]. Often, in order to circumvent the influence of noise, it is best to find parameter-free criteria to distinguish models [Harrington et al., 2012] or find model properties that are independent of the parameter values chosen [MacLean et al., 2015]. Chapter 3 and 4 highlight two such model properties, namely the Euclidean Distance (ED) degree and the algebraic matroids associated to prime binomial steady state ideals.

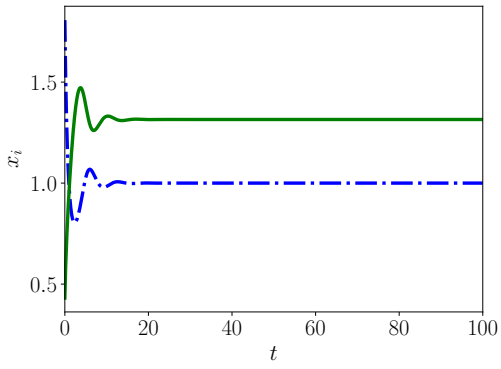
When the extrinsic influence is not constant, but varies in time, such as varying temperature, then the rate constants become time dependent. Hence, at any time, t, a rate constant is chosen from a given distribution. In this thesis the underlying distribution is modelled as a *truncated Gaussian*, see Figure 2.6, as a proof of principle model. The choice of distribution is further motivated by the central limit theorem and the fact that the truncated Gaussian is a non-negative distribution. The stochastic process governing the evolution of a single rate constant κ is given by

$$K(t) = \kappa + \frac{1}{\sqrt{\Omega}}\sqrt{B}\,\eta, \tag{2.22}$$

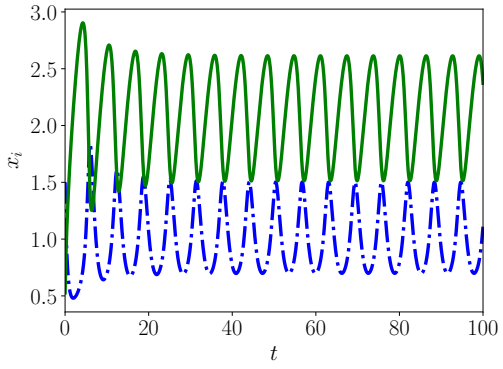
where B is positive constant and η is a stochastic process following a normal Gaussian distribution truncated at zero.



(a) The phase plane of the Brusselator model. The green, dotted region is the oscillatory regime, whereas the blue, striped region is the region of stability.



(b) The Brusselator in the stable regime with $\kappa_1 = 1$ and $\kappa_2 = 1.31$.



(c) The Brusselator in the oscillatory regime with parameters $\kappa_1 = 1$ and $\kappa_2 = 2.11$.

Figure 2.5: The Brusselator network and its dynamical regimes.

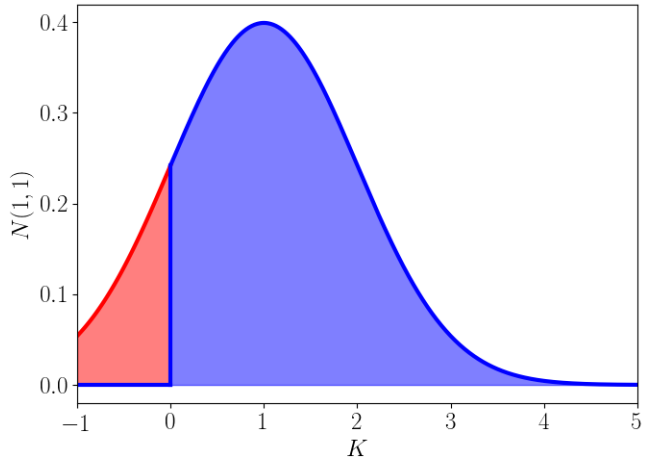


Figure 2.6: An unnormalised truncated Gaussian distribution centred at $\mu = 1$ and variance $\sigma^2 = 1$, i.e. $f(x) = H(x)/\sqrt{2\pi} \times e^{-(x-1)^2/2}$, where $H(x)$ is the Heaviside function. The blue area represents the truncated Gaussian distribution and the red shaded area symbolises the truncation.

Under certain circumstances, the description of a reaction network with extrinsic noise matches the intrinsic noise description of the same network. For simplicity, consider a network with one species only, such as the production-degradation network. Suppose a reaction network of one species is deterministically stable with one steady state for any choice of rate constants and has one inflow reaction $\emptyset \to X$. Let κ be the rate constant for this inflow reaction. Hence, if the inflow reaction is the only reaction subject to extrinsic noise, then the ODE governing the evolution of X is $dx/dt = f(x) + \eta$, where η is a Gaussian stochastic process of zero mean and variance B. Linearising around the steady state gives $d\delta x/dt = J\delta x + \eta$, where $J = df(x)/dx$. This is precisely the CLE, if the variances of η match.

Rendering the rate constants as stochastic processes drastically increases the model complexity, since one has to solve the underlying deterministic equations of the model and simultaneously a stochastic process governing the evolution of the rate constants. In Chapter 5 a multivariate generalisation of the stochastic process (2.22) is introduced and in Chapter 6 it is further generalised to spatial systems. Additionally, in 6 an extension to temporally correlated noise, $B = B(t, t')$, is considered.

Chapter 3

Steady State Invariants and Multistationarity for Families of Toric Reaction Networks

"If people do not believe that mathematics is simple, it is only because they do not realise how complicated life is."
– John von Neumann

This chapter is based on work by Adamer and Helmer published in Adamer and Helmer [2019b].

In this chapter the positive steady states for algorithmically constructed reaction networks, called *families*, whose positive steady states may be parameterised by monomials are investigated. Further, the algebraic dependencies of the variables representing the chemical concentrations are used to investigate experimental design and model identification for entire families. In particular, all of the methods in this chapter require no prior additional assumption on the parameter values other than positivity. Hence, the methods of this chapter are ideal for the study of constant extrinsic noise as outlined in Section 2.3. In fact, the results of Section 3.2.1 only require measurements of a subset of chemical concentrations for model selection and, although parameters could be estimated, knowing the model parameters is not necessary for applying the model rejection criterion of Lemma 3.2.15. Hence, the novel tools developed in this chapter can be applied to models for which parameters are unknown or unmeasurable.

Families of networks are formally defined in Definition 3.1.2. To obtain an intuition for what could be described as a family, consider a simple Michaelis-Menten enzymatic reaction [Michaelis and Menten, 1913],

$$E + S \rightleftharpoons ES \to E + P_1, \tag{3.1}$$

in which a substrate, S, binds to an enzyme, E, to form an enzyme-substrate complex, which enables the substrate to be modified into a product P_1. Now, suppose that the product P_1 acts as a substrate for the same enzyme, and is modified further,

$$E + S \rightleftharpoons ES \to E + P_1 \rightleftharpoons EP_1 \to E + P_2. \tag{3.2}$$

It is clear that the Michaelis-Menten reaction graph given by (3.1) can be embedded into the larger network (3.2) and this chain of modifications can be continued to P_N. Therefore, networks (3.1) and (3.2) are members of the same family. One aim of this chapter is to study steady states and related properties of the whole family by focusing only on members with a small number of products N; in this framework, for $N = 1$, the network (3.1) is obtained.

One of the central goals of this chapter is to develop criteria to distinguish which families have members with multiple positive steady states, so-called multistationary networks. Establishing if a network is multistationary and finding the associated parameter regions is highly non-trivial; a range of different approaches have been applied previously (see Joshi and Shiu [2015] for a summary). A number of necessary and occasionally necessary and sufficient conditions for multistationarity have been developed relying on mathematical techniques such as degree theory [Conradi et al., 2017], graph theory [Mincheva and Roussel, 2007], deficiency theory [Feinberg, 1988] or steady state parameterisations [Millán et al., 2012]. In particular, monomial positive steady state parameterisations proved fruitful due to their relations to toric varieties which are well understood in algebraic geometry [Fulton, 1993]. For a more comprehensive literature review on the topic of multistationarity the reader is referred to Chapter 1.

Often these conditions come with algorithms to construct witnesses to multistationarity, that is, a set of parameters, $\boldsymbol{\kappa}$, for which the network is multistationary. Recent results extend the techniques for identifying multistationarity to highly structured networks [Dickenstein et al., 2019] and networks with intermediates [Sadeghimanesh and Feliu, 2018].

Previous work relating to the concept of families introduced in this chapter considers so-called atoms of multistationarity, which are the smallest multistationary subnetworks that can induce multistationarity in their parent networks [Joshi and Shiu, 2013]. Network properties resulting from the gluing of networks are investigated in Gross et al. [2018]. Other network modifications which preserve or destroy multistationarity are studied in Banaji and Pantea [2018]. Recent results extend the

techniques for identifying multistationarity to highly structured networks [Dickenstein et al., 2019] and networks with intermediates [Sadeghimanesh and Feliu, 2018; Feliu and Wiuf, 2013].

In this chapter a concept of families of networks is developed which unifies the notion of highly structured networks, subnetworks and networks with intermediates. It is shown in Theorem 3.3.2 that if one member of a family is multistationary for some parameter values then so are all larger networks obtained by the recursive construction of Definition 3.1.2. A family of networks can in certain cases (see Example 3.1.5) be a sequence of nested subnetworks, where subnetworks are defined in Joshi and Shiu [2013]. In other cases it is a sequence of networks that can be built by adding intermediate species into reactions (see Example 3.1.6). Some have the additional structure of MESSI systems as studied in Pérez-Millán and Dickenstein [2018] and in such cases the additional MESSI structure can be used to study the family.

Going beyond multistationarity, necessary conditions for model rejection among members of a family are also investigated. These conditions can even be applied if there is only limited steady state data available. In particular, in Section 3.2, algebraic dependencies between the variables at a positive steady state are encoded using a combinatorial object called an algebraic matroid [Rosen, 2015; Oxley, 2006]. From the algebraic matroid, in Lemma 3.2.15, binomial relations are found that have to be satisfied by the chemical concentrations at any positive steady state, the so-called steady state invariants [Karp et al., 2012]. The results in Section 3.2.1 extend the previous research of Harrington et al. [2012], and MacLean et al. [2015], and the application of matroids in experimental design presented in Gross et al. [2016b]; MacLean et al. [2015]. Using these previous results, it is possible to give necessary conditions for the distinguishability of two members of a family of reaction networks with respect to a data set of measured chemical concentrations. Consequently, in this chapter conditions are constructed that inform which species have to be measured to be able to reject a family member.

In summary, the biological questions addressed in this chapter are:

1. What conditions are needed to define families of chemical reaction networks and what is the relation between their steady states? (Section 3.1)

2. Can the family construction be used in model selection or parameter estimation for the entire family? (Section 3.2)

3. Is it possible to find conditions such that multistationarity of one family member implies multistationarity for all subsequent members? (Section 3.3)

This biological motivation translates into the following algebraic questions which are answered using techniques from toric geometry and matroid theory:

1. What are the relations between the toric varieties defined by recursively constructed reaction graphs?

2. What is the connection between the circuit polynomials of matroids associated to different family members?

3. What is the relation between the positive parts of the steady state varieties of subsequent family members?

This chapter is organised as follows. In Section 3.1 a rigorous definition of a family of (reaction network) graphs and some preliminary results are given. Section 3.2 focuses on Question 3 using matroid theory. Some new terminology, which simplifies the proofs in the remainder of the chapter, is also introduced. In Section 3.3 the main result on multistationarity is proved using the matroidal language developed in the previous section. The results of this chapter are discussed in Section 3.4 and further directions are also suggested.

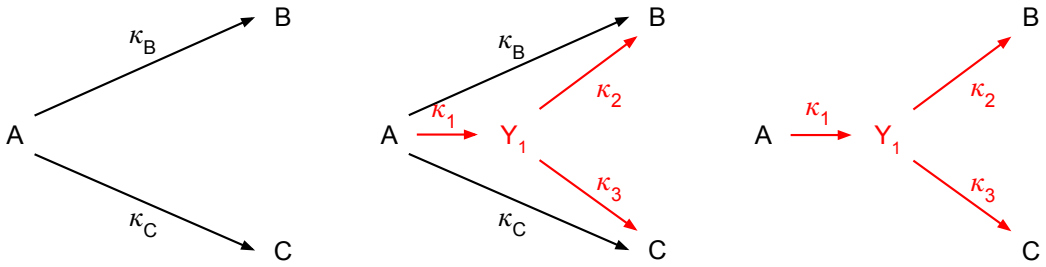
3.1 Families of Reaction Networks

In this chapter results which hold for a range of networks rather than a single network are obtained. When the properties studied (such as multistationarity) are present in a "small network", these properties lift to all larger networks constructed by the procedure outlined below. The collection of all such networks is called a family $\mathcal{N}$ with members $\mathcal{N}_i$. A formal definition is now given for families of graphs, and, by extension, of families of chemical reaction networks.

3.1.1 Definitions

Families of networks can be found in a wide range of biological settings such as multi-site phosphorylation [Conradi and Shiu, 2015] (e.g. cellular signalling, DNA transcription, cell death), kinetic proofreading [Mckeithan, 1995] (immune response), or compartmentalised diffusion [Woolley et al., 2011b] (spatial models).

A family is identified by the properties of its reaction graphs. If the graph of another network can be constructed from a given network by a fixed set of procedures, the networks are in the same family; an example of such a construction is given in Figure 3.1.



(a) The graph $\mathcal{G}_0$.

(b) Adding a species Y_1 to form the intermediate network.

(c) Deleting edges to form the graph $\mathcal{G}_1$.

Figure 3.1: Starting from the graph in 3.1a, first new vertices and edges are added in 3.1b and, second, some edges of the original graph are deleted in 3.1c. Note that Figures 3.1a and 3.1c can be obtained from the intermediate network 3.1b by setting the edge weights $\{\kappa_1, \kappa_2, \kappa_3\}$ or, respectively, $\{\kappa_A, \kappa_B\}$ to zero.

Remark 3.1.1 (Informal Construction of Families of Graphs)**.** *Fix a labelled digraph $\mathcal{G}_n$ and an unlabelled digraph M; from these build new family members step-by-step. At each step assign a new set of labels to M, rendering M a labelled digraph. The vertices of $\mathcal{G}_{n+1}$ are the union of those of $\mathcal{G}_n$ and of M. The edges of the graph $\mathcal{G}_{n+1}$ are obtained from $\mathcal{G}_n$ as follows:*

1. *Add a set $\mathcal{E}$ of edges adjacent to both some vertices of M and some vertices of $\mathcal{G}_n$; the resulting graph $\mathcal{G}_n^{\text{int}}$ is referred to as the* intermediate graph *(see also Definition 3.1.8).*

2. *Delete some subset of the edges of $\mathcal{G}_n$ from the graph $\mathcal{G}_n^{\text{int}}$ to form $\mathcal{G}_{n+1}$.*

A definition from graph theory [Noy and Ribó, 2004] is used to formalise this construction. Graphs constructed as in Remark 3.1.1 form a family if they satisfy the conditions of Definition 3.1.2 below.

Definition 3.1.2. *For a reaction graph $\mathcal{G} = (\mathcal{C}, \mathcal{R})$ and for $U \subseteq \mathcal{C}$ let $\mathcal{G}[U]$ be the subgraph induced by U and $N_{\mathcal{G}}(U)$ the set of vertices adjacent to some vertex in U. Consider a set of graphs $\{\mathcal{G}_i\}_{i\geq 0}$ where $\mathcal{G}_i = (\mathcal{C}_i, \mathcal{R}_i)$. Set $\mathcal{W}_0 = \mathcal{C}_0$ and $\mathcal{E}_0 = \mathcal{R}_0$; additionally let $\mathcal{W}_{i+1} = \mathcal{C}_{i+1} - \mathcal{C}_i$, and $\mathcal{E}_{i+1} = \mathcal{R}_{i+1} - \mathcal{R}_i$ for $i \geq 0$. Further, there exists a positive integer n, a labelled graph M and a set of reactions Y, such that the set $\{\mathcal{G}_i\}_{i\geq 0}$ is called a family of graphs if the following properties hold:*

1. $N_{\mathcal{G}_n}(\mathcal{W}_n) \subseteq \mathcal{W}_0 \cup (\bigcup_{i=0}^{r} \mathcal{W}_{n-i})$ *for* $n > r$,

2. $\mathcal{R}_n = (\mathcal{R}_{n-1} - Y) \cup \mathcal{E}_n$, *where* $Y \subseteq \bigcup_{i=1}^{r} \mathcal{E}_{n-i}$,

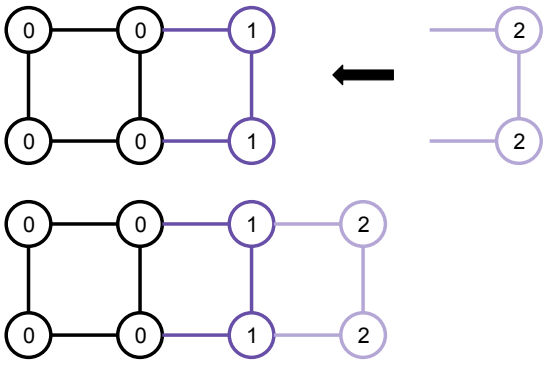


Figure 3.2: An illustration of building a two-site ladder graph. The vertices are labelled according to the sets $\mathcal{W}_i$ and the edge colours highlight the sets $\mathcal{E}_i$. It can be seen that the labelled graph M added to $\mathcal{G}_i$ is always the same.

3. *the graph* $\mathcal{G}_n\left[\mathcal{W}_0 \cup \left(\bigcup_{i=0}^{r} \mathcal{W}_{n-i}\right)\right]$ *is equal to* M *for* $n > r$. *In addition,* $\mathcal{G}_n[\mathcal{W}_n]$ *is always the same graph.*

Put simply, the last condition says that the graph "added" to the previous graph must be the same for each step throughout the family; this is illustrated in Figure 3.2 and further elucidated in Noy and Ribó [2004]. In the context of chemical reaction networks another condition is added, namely, that in every new family member there appears at least one new chemical species:

4. $\mathcal{S}_M \subsetneq \mathcal{S}_N$ for $M < N$

This condition is equivalent to the condition that in a smaller network every set of chemical species for which their chemistry allows for the formation of a complex has formed a complex. Therefore, to give rise to a larger network new species have to be added.

Remark 3.1.3. *Note that not every infinite sequence of networks is a family as defined in Definition 3.1.2. For a non-example see Example 3.1.7.*

Remark 3.1.4. *For ease of notation, the unlabelled graph M is drawn in a "dot and arrow" representation; e.g. the graph $M = \{\cdot, \cdot \to \cdot\}$ corresponds to a graph with two connected components, an isolated vertex and a component with two unlabelled vertices and a directed edge between them.*

Example 3.1.5 (Distributive Phosphorylation)**.** *Distributive phosphorylation with $N = 1$ phosphorylation sites follows the reaction scheme*

$$E + S_0 \rightleftharpoons ES_0 \to E + S_1,$$
$$F + S_1 \rightleftharpoons FS_1 \to F + S_0.$$

The reaction scheme is a digraph $\mathcal{G}_1 = (\mathcal{W}_1, \mathcal{E}_1)$ *with* $\mathcal{W}_1 = \{E + S_0, ES_0, E + S_1, F + S_1, FS_1, F + S_0\}$ *and* $\mathcal{E}_1 = \{(E + S_0, ES_0), (ES_0, E + S_0), (ES_0, E + S_1), (F + S_1, FS_1), (FS_1, F + S_1), (FS_1, F + S_0)\}$.

To construct $\mathcal{G}_2$*, the sets* $\mathcal{W}_2 = \{ES_1, E + S_2, F + S_2, FS_2\}$ *and*

$$\mathcal{E}_2 = \{(E+S_1, ES_1), (ES_1, E+S_1), (ES_1, E+S_2), (F+S_2, FS_2), (FS_2, F+S_2), (FS_2, F+S_1)\}$$

are used. Defining $\mathcal{G}_2 = (\mathcal{W}_1 \cup \mathcal{W}_2, \mathcal{E}_1 \cup \mathcal{E}_2)$ *gives*

$$\begin{aligned} E + S_0 \rightleftharpoons ES_0 \to E + S_1 &\rightleftharpoons ES_1 \to E + S_2, \\ F + S_2 \rightleftharpoons FS_2 \to F + S_1 &\rightleftharpoons FS_1 \to F + S_0. \end{aligned}$$

Hence (in the notation of Definition 3.1.2), $M = \{\cdot \to \cdot, \cdot \rightleftharpoons \cdot\}$ *and* $r = 1$*. The digraphs* $\mathcal{G}_1$ *and* $\mathcal{G}_2$ *define the family members* $\mathcal{N}_1$ *and* $\mathcal{N}_2$*. Inductively, this procedure can be continued to member* $\mathcal{N}_N$*. By inspection of the green subgraph it can be seen that Condition 3 of Definition 3.1.2 is fulfilled for any* $N > 0$ *and, therefore, the distributive phosphorylation networks form a family. Further,* $\mathcal{N}_1$ *is a subnetwork of* $\mathcal{N}_2$ *as defined in Joshi and Shiu [2013, Definition 2.2].*

Example 3.1.6 (Processive Phosphorylation)**.** *Processive phosphorylation of a substrate with* $N = 1$ *phosphorylation sites follows the reaction scheme*

$$\begin{aligned} E + S_0 &\rightleftharpoons ES_0 \to E + P, \\ F + P &\rightleftharpoons FS_1 \to F + S_0. \end{aligned}$$

For $N = 1$ *this is the same reaction scheme as for distributive phosphorylation, except for the relabelling of the fully phosphorylated substrate as product* P*. However, to construct the next family member from the digraph* $\mathcal{G}_1$ *the sets* $\mathcal{W}_2 = \{ES_1, FS_2\}$ *and* $\mathcal{E}_2 = \{(ES_0, ES_1), (ES_1, E + P), (F + P, FS_2), (FS_2, F + P), (FS_2, FS_1)\}$ *are used. Next, the edges* $Y_1 = \{(ES_0, E + P), (F + P, FS_1), (FS_1, F + P)\}$ *are deleted which results in the graph* $\mathcal{G}_2 = (\mathcal{W}_1 \cup \mathcal{W}_2, (\mathcal{E}_1 \cup \mathcal{E}_2) - Y_1)$ *to give*

$$\begin{aligned} E + S_0 \rightleftharpoons ES_0 &\to ES_1 \to E + P, \\ F + P &\rightleftharpoons FS_2 \to FS_1 \to F + S_0. \end{aligned}$$

Where the vertices, $M = \{\cdot, \cdot\}$*, were added and* $r = 1$ *as in Definition 3.1.2. Again, the digraphs* $\mathcal{G}_1$ *and* $\mathcal{G}_2$ *define the family members* $\mathcal{N}_1$ *and* $\mathcal{N}_2$*. Condition 3 of Definition 3.1.2 is fulfilled for any* $N > 1$ *and, therefore, the processive phosphorylation networks form a family.*

Example 3.1.7 (Non-example)**.** *As mentioned in Remark 3.1.3 not every infinite sequence of graphs forms a family. Consider the autocatalytic networks*

$$X_i + X_{i+1} \to 2X_{i+1},$$
$$X_i \rightleftharpoons \emptyset \qquad \text{for } i = 1, \ldots, N \text{ and setting } X_{N+1} = X_1.$$

In the reaction above $\emptyset$ represents production and degradation of a molecule by a mechanism not further studied. Without loss of generality consider $\mathcal{N}_7$ and $\mathcal{N}_8$; it can be seen that $\mathcal{C}_8$ is not a union of $\mathcal{C}_7$ and another graph as $X_7 + X_1 \in \mathcal{C}_7 \not\subseteq \mathcal{C}_8$.

This subsection is concluded by considering the polynomial equations arising from the reaction graphs of successive members of a family. First, it can be seen from Section 2.1 that every reaction has a unique rate constant, κ_i, which is the edge weight of the reaction digraph. Therefore, in the dynamical system given by the equations (2.3) every monomial, which represents a reaction, is multiplied by a constant κ_i. Note that isolated vertices in the reaction graph do not contribute to the dynamics of the network. Hence, for families of networks which satisfy Definition 3.1.2 with $Y = \emptyset$, the equations of the N^{th} member of a family can be derived from the $(N+1)^{\text{th}}$ member by setting all the edge weights of the edges added to the reaction graph to zero. Formally, the evaluation map π is defined by

$$\pi : \mathbb{K}[\kappa_1, \ldots, \kappa_{m+m'}][x_1, \ldots, x_n] \to \mathbb{K}[\kappa_1, \ldots, \kappa_m][x_1, \ldots, x_n]$$
$$\pi(\kappa_i) = \begin{cases} \kappa_i \text{ if } i \leq m, \\ 0 \text{ otherwise.} \end{cases} \tag{3.3}$$

For networks which require the deletion of a set of edges, Y, the concept of an *intermediate network* is needed.

Definition 3.1.8 (Intermediate Network)**.** *The intermediate network $\mathcal{G}_n^{\text{int}}$ is the network constructed by only adding reactions to join the newly labelled graph M to $\mathcal{G}_n$ and before any edges are deleted from the reaction graph. See Step 1 of Remark 3.1.1.*

Remark 3.1.9. *The next member of a family is a subnetwork of the intermediate network. Hence, for families in which the next family member coincides with the intermediate network (i.e. when $Y = \emptyset$ in Definition 3.1.2), this terminology is not required.*

The dynamical equations of the N^{th} and $(N+1)^{\text{th}}$ member can be constructed from their intermediate network by defining the appropriate evaluation maps. As can be seen from Condition 2 of Definition 3.1.2 the reaction (edge) set of the $(N+1)^{\text{th}}$ member of a family is given by $\mathcal{R}_{N+1} = (\mathcal{R}_N - Y) \cup \mathcal{E}_N$. The edge sets for the N^{th} and intermediate network are given by $\mathcal{R}_N$ and $\mathcal{R}_N \cup \mathcal{E}_N$ respectively. Define a function μ which associates a unique edge weight, $\kappa_{i,j}$, to every edge of the reaction graph,

$$\begin{aligned} \mu :\ & \mathcal{C} \times \mathcal{C} \to \mathbb{R}[\boldsymbol{\kappa}], \\ & \mu\left((C_i, C_j)\right) = \kappa_{i,j}. \end{aligned} \tag{3.4}$$

This gives the rate constants $\mu(\mathcal{R}_N) = \{\kappa_1, \ldots, \kappa_m\}$, $\mu(\mathcal{E}_N) = \{\kappa_{m+1}, \ldots, \kappa_{m+m'}\}$ and $\mu(Y) = \{\kappa_1, \ldots, \kappa_{m''}\}$ (where the rate constants produced by (3.4) are relabelled as required). By construction, an edge is not present in the reaction graph if it has an edge weight of 0. Hence, two evaluation maps can be defined to map the edge sets of the intermediate network to the $(N+1)^{\text{th}}$ and N^{th} network respectively,

$$\begin{aligned} \pi^+ : \mathbb{K}[\kappa_1, \ldots, \kappa_{m+m'}][x_1, \ldots, x_n] &\to \mathbb{K}[\kappa_{m''+1}, \ldots, \kappa_{m+m'}][x_1, \ldots, x_n] \\ \pi(\kappa_i) &= \begin{cases} \kappa_i \text{ if } i > m'', \\ 0 \text{ otherwise}, \end{cases} \end{aligned} \tag{3.5}$$

and

$$\begin{aligned} \pi^- : \mathbb{K}[\kappa_1, \ldots, \kappa_{m+m'}][x_1, \ldots, x_n] &\to \mathbb{K}[\kappa_1, \ldots, \kappa_m][x_1, \ldots, x_n] \\ \pi(\kappa_i) &= \begin{cases} \kappa_i \text{ if } i \leq m, \\ 0 \text{ otherwise}. \end{cases} \end{aligned} \tag{3.6}$$

This results in the edge weights

$$\pi^+\left(\mu\left(\mathcal{R}_N \cup \mathcal{E}_N\right)\right) = \{\kappa_{m''+1}, \ldots, \kappa_{m+m'}\} = \mu\left((\mathcal{R}_N - Y) \cup \mathcal{E}_N\right)$$

and

$$\pi^-\left(\mu\left(\mathcal{R}_N \cup \mathcal{E}_N\right)\right) = \{\kappa_1, \ldots, \kappa_m\} = \mu\left(\mathcal{R}_N\right),$$

which, after taking the inverse of μ, can be associated to the reaction sets of the $(N+1)^{\text{th}}$ and N^{th} network respectively. In particular, if $\mathcal{G}_N^{\text{int}}$ is the intermediate graph associated to $\mathcal{G}_N$ then applying π^- to (the edge set of) $\mathcal{G}_N^{\text{int}}$ will yield $\mathcal{G}_N$ and applying π^+ to (the edge set of) $\mathcal{G}_N^{\text{int}}$ will yield $\mathcal{G}_{N+1}$.

3.1.2 Toric Families

Extending the discussion of Subsection 2.1.1.1, toric varieties and their connection to chemical reaction networks are introduced. A toric variety is an algebraic variety which can be defined by binomial equations generating a prime ideal. The primality of the ideal ensures that the corresponding algebraic variety is irreducible. Chemical reaction networks whose steady state ideal is generated by such prime ideals have been studied in the literature, e.g. Millán et al. [2012]. To simplify notation the following definition is made.

Definition 3.1.10. *A chemical reaction network whose steady state ideal has an associated prime that is binomial is a toric chemical reaction network.*

Showing whether a chemical reaction network is toric is a non-trivial task; previous results have used deficiency theory [Craciun et al., 2009a] or network structure based methods [Millán et al., 2012]. Formally, the associated primes of a steady state ideal need to be found and a Gröbner basis of each computed. If the reduced Gröbner basis is binomial then the ideal is a prime binomial ideal [Eisenbud and Sturmfels, 1996]. However, as every toric variety has non-zero components removing any components of the steady state variety contained in the coordinate axes is often a first step towards identifying the toric components. Algebraically this removal is accomplished by computing the saturation $I^\infty = I : (x_1 \cdots x_n)^\infty$, [Cox et al., 2013].

The analysis of the remainder of this chapter is restricted to toric networks as a monomial parameterisation can be found for the positive part of the associated (steady state) variety. Consider a prime binomial steady state ideal defined by ν equations

$$I = \langle \boldsymbol{x}^{\boldsymbol{b}_i^+} - \boldsymbol{x}^{\boldsymbol{b}_i^-} \mid i \in 1, \ldots, \nu \rangle \subseteq \mathbb{K}[x_1, \ldots, x_n].$$

The vectors $\boldsymbol{b}_i^+$ and $\boldsymbol{b}_i^-$ are positive column vectors with disjoint support and let $B = (\boldsymbol{b}_1, \ldots, \boldsymbol{b}_\nu)$ be the matrix with columns $\boldsymbol{b}_i = \boldsymbol{b}_i^+ - \boldsymbol{b}_i^-$, called the exponent matrix of I. Then there exists a matrix A such that $\boldsymbol{b}_i \in \ker(A)$, $\forall i \in 1, \ldots, \nu$. The matrix A is a $d \times n$ integer matrix where d is the dimension of the toric variety and n is the dimension of the ambient affine space. Note that, since the dimension of a variety cannot exceed the dimension of its ambient space, $\operatorname{rank}(A) \leq d \leq n$

Remark 3.1.11. *Note that there is some freedom in the choice of the matrix A, as integer row operations on rows of A will not change its kernel and, hence, the variety it parameterises is left unaltered. Therefore,* any *matrix A is informally referred to as* the *A-matrix associated to a toric variety $V(I)$.*

From this A-matrix another definition of a toric variety can be found.

Definition 3.1.12. *Given an $\boldsymbol{x}^* = (x_1^*, \ldots, x_n^*) \in \mathbb{K}^n$ define a (Laurent) monomial map $\psi_A^{(\boldsymbol{x}^*)} := \psi_A$ with*

$$\psi_A : (\mathbb{K}^*)^d \to \mathbb{K}^n,$$

where

$$\boldsymbol{t} \mapsto (x_1^* \boldsymbol{t}^{\boldsymbol{a}_1}, \ldots, x_n^* \boldsymbol{t}^{\boldsymbol{a}_n}),$$

with $\boldsymbol{a}_i$ being a column of A. The (Zariski) closure of the image of this monomial map defines a toric variety, $X_{A,\boldsymbol{x}^*} = \overline{\psi_A((\mathbb{K}^*)^d)}$.

The monomial map ψ_A also induces a parameterisation map.

Definition 3.1.13. *The parameterisation map defined by the A-matrix is the $\mathbb{K}$-algebra homomorphism*

$$\phi_A : \mathbb{K}[x_1, \ldots, x_n] \to \mathbb{K}[t_1^{\pm}, \ldots, t_d^{\pm}]$$
$$\phi_A(x_i) = x_i^* \boldsymbol{t}^{\boldsymbol{a}_i} = x_i^* t_1^{a_{i_1}} \cdots t_d^{a_{i_d}}$$

with $x_i^* \in \mathbb{K}$. Note as above, the map ϕ_A depends on $\boldsymbol{x}^* \in \mathbb{K}^n$.

Example 3.1.14. *The steady state ideal of the network $X_1 + X_2 \underset{\kappa_2}{\overset{\kappa_1}{\rightleftharpoons}} X_3$ is $I = \langle -\kappa_1 x_1 x_2 + \kappa_2 x_3 \rangle$. By inspection this ideal is prime and binomial. A parameterization $x_1 = x_1^* t_1$, $x_2 = x_2^* t_2$, $x_3 = x_3^* t_1 t_2$ can be found corresponding to the A-matrix*

$$A = \begin{pmatrix} 1 & 0 & 1 \\ 0 & 1 & 1 \end{pmatrix}.$$

Remark 3.1.15. *Consider $\mathbb{K} = \mathbb{R}(\kappa_1, \ldots, \kappa_m)$. By definition the entries of $\boldsymbol{x}^*$ are given by algebraic functions in $\boldsymbol{\kappa}$. In practice the choices of κ should be restricted to those such that when $\boldsymbol{x}^*$ is evaluated at some fixed $(\kappa_1, \ldots, \kappa_m)^T \in \mathbb{R}^m_{>0}$ it holds that $\boldsymbol{x}^* \in \mathbb{R}^n_{>0}$.*

Before proceeding to prove a series of small results which establish the notion of toric steady state ideals of families of toric networks, a toric family is formally defined.

Definition 3.1.16 (Toric family)**.** *If every member of a family of networks is a toric chemical reaction network, the family is called a toric family.*

Remark 3.1.17. *Prominent examples of toric families are multi-site phosphorylation networks or compartmentalised diffusion networks.*

The proposition below is straightforward, however, a proof is included as no explicit proof could be found in the literature.

Proposition 3.1.18. *Consider a chemical reaction network with steady state ideal* $I = \langle \alpha^T A_k \boldsymbol{x}^\alpha \rangle$ *in the polynomial ring* $\mathbb{R}[x_1, \ldots, x_n]$. *Let* $V = \overline{V(\alpha^T A_\kappa \boldsymbol{x}^\alpha) \cap (\mathbb{R}^*)^n}$ *be the real steady state variety and let the linear equations* $\ell_1, \ldots, \ell_d$ *be the corresponding conservation relations. Suppose that* $\dim(V \cap V(\ell_1, \ldots \ell_d)) = d'$. *Then* $\dim(V) = d + d'$. *Further if* V *is a toric variety it holds that* $\dim(V \cap (\mathbb{R}_{>0})^n) = d + d'$.

Proof. Each linear form ℓ_j contains a constant term $c_j \in \mathbb{R}$ which can be chosen freely. For a sufficiently general choice of $c_1, \ldots, c_d$ the intersection $V \cap V(\ell_1, \ldots \ell_d)$ is transverse (see e.g. Hartshorne [2013]), it follows that $d' = \dim(V \cap V(\ell_1, \ldots \ell_d)) = \dim(V) - \dim(V(\ell_1, \ldots \ell_d)) = \dim(V) - d$. Because V is toric it is parameterised by monomials, and hence its dimension in the positive orthant is the same as its dimension over $\mathbb{R}^n$. □

Example 3.1.19 (Example 3.1.14 cont.)**.** *In the network of Example 3.1.14 there are two independent conservation relations* $x_1 + x_3 = c_1$ *and* $x_2 + x_3 = c_2$ *which implies that the dimension of the steady state variety,* $V(I)$, *is* $\dim(V(I)) \geq 2$. *Indeed, the dimension of the (toric) variety* $V(I)$ *is* 2, *implying that* $d' = 0$.

Remark 3.1.20. *In the notation of Proposition 3.1.18* $d' > 0$ *implies that there is an infinite number of steady states on each general stoichiometric compatibility class, defined by general choices of* $c_1, \ldots, c_d$. *Remember that in the general case the intersection of the stoichiometric compatibility class with the steady state variety is transverse, however, there may be special choices of* $c_1, \ldots, c_d$ *where this is not the case. The case* $d' > 0$ *renders the discussion of multistationarity irrelevant. Therefore, for the remainder of this chapter it is assumed that* $d' = 0$, *meaning that the dimension of the toric variety is equal to the number of conservation relations.*

Proposition 3.1.18 shows that the dimension of a toric steady state variety only depends on the network property of the conservation relations provided that the assumption of 3.1.20 holds. Hence, dimension is a model invariant robust to the effect of noise. In Chapter 4 another model invariant with this property, the Euclidean Distance degree, will be studied.

Lemma 3.1.21 states that saturation and evaluation can be interchanged and, hence, the network operation of deleting edges in the reaction graph can be carried out before, or after, finding the prime binomial ideal in the steady state ideal.

Lemma 3.1.21. *Let $L = \langle \kappa_{m+1}, \ldots, \kappa_{m+m'} \rangle$ be an ideal corresponding to the evaluation map π^- and let $X_{N+1} \subset \mathbb{C}_\kappa^{m+m'} \times \mathbb{C}_x^{n+n'}$ be the steady state variety of the $(N+1)^{th}$ family member. It holds that*

1. $\overline{X_{N+1} \cap V(L) - V(x_1 \cdots x_{n+n'})} = \overline{X_{N+1} - V(x_1 \cdots x_{n+n'})} \cap V(L)$,
2. $\overline{X_{N+1} - V(x_1 \cdots x_{n+n'})} \cap V(L) = \overline{X_N - V(x_1 \cdots x_n)}$

Proof. Note that $\overline{V(L) - V(x_1 \cdots x_{n+n'})} = V(L)$. Hence,

$$\begin{aligned}
\overline{X_{N+1} \cap V(L) - V(x_1 \cdots x_{n+n'})} &= \overline{(X_{N+1} - V(x_1 \cdots x_{n+n'})) \cap (V(L) - V(x_1 \cdots x_{n+n'}))} \\
&= \overline{(X_{N+1} - V(x_1 \cdots x_{n+n'}))} \cap \overline{(V(L) - V(x_1 \cdots x_{n+n'}))} \\
&= \overline{(X_{N+1} - V(x_1 \cdots x_{n+n'}))} \cap V(L),
\end{aligned}$$

which proves the first statement. For the second statement note that, by construction of the evaluation map, $X_{N+1} \cap V(L) = X_N \subset \mathbb{C}_\kappa^m \times \mathbb{C}_x^n \times \mathbb{C}^{n'}$. Hence,

$$\begin{aligned}
\overline{X_{N+1} - V(x_1 \cdots x_{n+n'})} \cap V(L) &= \overline{X_{N+1} \cap V(L) - V(x_1 \cdots x_{n+n'})} \\
&= \overline{X_N - V(x_1 \cdots x_{n+n'})} \\
&= \overline{X_N - V(x_1 \cdots x_n)}.
\end{aligned}$$

□

Suppose that $\mathcal{N}$ is a toric family of reaction networks with the $(N+1)^{th}$ member of the family having toric steady states specified by the binomial ideal I_{N+1}. Lemma 3.1.21 establishes a useful connection between species (corresponding to variables x), and reactions (corresponding to κ), or, equivalently, between species and edges of a reaction graph. By the extra Condition 4 of Definition 3.1.2 every new edge must either originate or end on a complex containing a new species. Hence, by applying the evaluation map π^- an ideal of an intermediate network I_N^{int} $(= I_{N+1}$ for nested subnetworks) is automatically mapped from $\mathbb{K}[x_1, \ldots, x_{n+n'}]$ (corresponding to a network with $n+n'$ chemical species) to an ideal in the ring $\mathbb{K}[x_1, \ldots, x_n]$ (corresponding to a network with n species).

Proposition 3.1.22 below shows that the image of a binomial ideal under π is either the constant ideal (corresponding to an empty variety) or another binomial ideal.

Proposition 3.1.22. *Work in the ring $R = \mathbb{R}(\kappa_1, \ldots, \kappa_{m+m'})[x_1, \ldots, x_{n+n'}]$ and define the partial evaluation map $\pi : R \to \mathbb{R}(\kappa_1, \ldots, \kappa_m)[x_1, \ldots, x_{n+n'}]$ specified by $\pi(f) = f(\kappa_1, \ldots, \kappa_m, 0, \ldots, 0, x_1, \ldots, x_{n+n'})$. Suppose that $I_{N+1} : (x_1 \cdots x_{n+n'})^\infty \subset R$*

is a binomial ideal. Then $I_N = \pi(I_{N+1}) : (x_1 \cdots x_n)^\infty \cap \mathbb{R}(\kappa_1, \ldots, \kappa_m)[x_1, \ldots, x_n]$ *is either a binomial ideal or the ideal* (1)*. Further, if a choice of rate constants is fixed and* $I_{N+1} : (x_1 \cdots x_{n+n'})^\infty$ *is thought of as an ideal in* $\mathbb{R}[x_1, \ldots, x_{n+n'}]$ *then if* $V(I_{N+1} : (x_1 \cdots x_{n+n'})^\infty) \subset \mathbb{R}^n$ *is a toric variety and if* $V(I_N : (x_1 \cdots x_n)^\infty) \cap \mathbb{R}^n_{>0} \neq \emptyset$ *then* $\overline{V(I_N) \cap \mathbb{R}^n_{>0}}$ *is a toric variety.*

Proof. By assumption $I_{N+1} : (x_1 \cdots x_{n+n'})^\infty$ is a binomial ideal, hence,

$$I_{N+1} : (x_1 \cdots x_{n+n'})^\infty = (\Xi_1^+ x^{\boldsymbol{b}_1^+} - \Xi_1^- x^{\boldsymbol{b}_1^-}, \ldots, \Xi_\nu^+ x^{\boldsymbol{b}_\nu^+} - \Xi_\nu^- x^{\boldsymbol{b}_\nu^-}),$$

where $\Xi_j^\pm$ are polynomial functions of the rate constants. For each term $\beta_j = \Xi_j^+ x^{b_j^+} - \Xi_j^- x^{b_j^-}$ it holds that $\pi(\beta_j) = \pi(\Xi_j^+) x^{b_j^+} - \pi(\Xi_j^-) x^{b_j^-}$, hence either:

- $\pi(\beta_j) = 0$, this happens if $\pi(\Xi_j^+) = \pi(\Xi_j^-) = 0$;
- $\pi(\beta_j)$ is a monomial, this happens if one of $\pi(\Xi_j^+)$ or $\pi(\Xi_j^-)$ evaluates to zero and the other does not;
- $\pi(\beta_j) = \beta_j'$ and still binomial, this happens when both $\pi(\Xi_j^+) \neq 0$ and $\pi(\Xi_j^-) \neq 0$.

If $\pi(\beta_j)$ is a monomial for some j then the ideal $\pi(I_{N+1}) : (x_1 \cdots x_{n+n'})^\infty = (1)$, otherwise, it must be a binomial ideal generated by the β_j such that $\pi(\beta_j) = \beta_j'$. By Lemma 3.1.21 this ideal is the binomial ideal $I_N : (x_1 \cdots x_n)^\infty$.

Since for a fixed choice of rate constants $I_N : (x_1 \cdots x_n)^\infty$ is a binomial ideal in $\mathbb{R}[x_1, \ldots, x_n]$ and it is assumed that $V(I_N)$ has a nonempty intersection with the positive orthant $\mathbb{R}^n_{>0}$ then the last statement follows by Conradi et al. [2018, Proposition 5.2]. This Proposition states that if I is a binomial ideal with variety $V(I)$ at most one of its irreducible components intersects $\mathbb{R}^n_{>0}$. □

Hence, by Proposition 3.1.22, if the intermediate network of the $(N+1)^{\text{th}}$ and the N^{th} member of a family is toric, then both, the N^{th} and $(N+1)^{\text{th}}$ members are either toric or have empty positive steady state varieties. A relationship between the A-matrices of successive members of toric families is now found by considering the binomial ideals and their Gale duals. Further details on Gale duality can be found in [Gelfand et al., 2008, §7.1.F].

Definition 3.1.23 (Gale Dual Matrices)**.** *A matrix A is Gale dual to a matrix B if the columns of B form a basis for the kernel of A, that is if* $\operatorname{im}(B) = \ker(A)$ *and* $\ker(B) = \{0\}$.

Theorem 3.1.24. *Let $I_{N+1} : (x_1 \cdots x_{n+n'})^\infty \subset \mathbb{R}(\kappa_1, \ldots, \kappa_{m+m'})[x_1, \ldots, x_{n+n'}]$ be a binomial ideal defining the positive steady states of the $(N+1)^{th}$ member of a family of reaction networks. Also let π be the evaluation map which sends $\kappa_{m+1} = \cdots = \kappa_{m+m'} = 0$ and assume that $I_N = \pi(I_{N+1}) \subset \mathbb{R}(\kappa_1, \ldots, \kappa_m)[x_1, \ldots, x_n]$. Then $I_N : (x_1 \cdots x_n)^\infty$ is binomial. Further, for a choice of generators, let B_{N+1}, B_N be the matrices associated to the exponents of the binomial ideals I_{N+1} and I_N. Similarly let A_{N+1} and A_N be Gale dual to B_{N+1} and B_N. Then:*

1. *B_N is a submatrix of B_{N+1} and,*
2. *A_N is a submatrix of A_{N+1}, if the submatrix of B_{N+1} formed by the columns which have at least one non-zero entry in the last n' rows has rank at most n'.*

Proof. First statement 1 is proved. By assumption $I_{N+1} : (x_1 \cdots x_{n+n'})^\infty$ is a binomial ideal, hence,

$$I_{N+1} : (x_1 \cdots x_{n+n'})^\infty = (\Xi_1^+ x^{\boldsymbol{b}_1^+} - \Xi_1^- x^{\boldsymbol{b}_1^-}, \ldots, \Xi_\nu^+ x^{\boldsymbol{b}_\nu^+} - \Xi_\nu^- x^{\boldsymbol{b}_\nu^-}).$$

By Proposition 3.1.22 it follows that if $I_N : (x_1 \cdots x_n)^\infty$ is not empty, then it is also a binomial ideal and its set of generators must appear in $\pi(\Xi_1^+ x^{\boldsymbol{b}_1^+} - \Xi_1^- x^{\boldsymbol{b}_1^-}, \ldots, \Xi_\nu^+ x^{\boldsymbol{b}_\nu^+} - \Xi_\nu^- x^{\boldsymbol{b}_\nu^-})$. Hence, its matrix of exponents can be obtained by choosing a subset (of size $\mu \leq \nu$) of the exponent vector pairs $(\boldsymbol{b}_1^+, \boldsymbol{b}_1^-), \ldots, (\boldsymbol{b}_\nu^+, \boldsymbol{b}_\nu^-)$. By definition of the matrix B, it follows that B_N is a submatrix of B_{N+1}, proving 1.

Note that no variables in $x_{n+1}, \ldots, x_{n+n'}$ appear in I_N and, hence, the subset of exponent vectors $\boldsymbol{b}_i = \boldsymbol{b}_i^+ - \boldsymbol{b}_i^-$ defining $I_N : (x_1 \cdots x_n)^\infty$ have the general form $\boldsymbol{b}_i = (b_{i_1}, \ldots, b_{i_n}, 0, \ldots, 0)^T$. Further, the entries of the remaining $\nu - \mu$ exponent vectors have at least one non-zero entry in the last n' rows and these vectors can be collected into a matrix $\tilde{B}$. Hence, B_{N+1} may be written in block form as

$$B_{N+1} = \left(\begin{array}{c|c} B_N & \tilde{B} \\ \hline 0_{n' \times \mu} & \end{array} \right).$$

It is clear that the first n entries of any basis vector of the left kernel of B_{N+1} must form a vector in the left kernel of B_N. Hence, the left kernel of B_{N+1} has a basis of the form $\tilde{\boldsymbol{a}}_i = (\boldsymbol{a}_i, \bar{\boldsymbol{a}}_i)$, where $\boldsymbol{a}_i$ is an element of a given basis of the left kernel of B_N or the zero vector and $\bar{\boldsymbol{a}}_i \in \mathbb{Z}^{n'}$ is a vector of variables to be determined. From the rank condition it is clear that the matrix $\tilde{B}$ has a rank of at most n' and, for any given i, a system of linear equations is obtained, $\tilde{\boldsymbol{a}}_i \tilde{\boldsymbol{b}} = 0$, for all columns $\tilde{\boldsymbol{b}}$ of $\tilde{B}$. Due to the rank condition, this system has always at least one (rational) solution

and, hence, the collection of all solutions form a basis of the left kernel of B_{N+1} to give the matrix A_{N+1} (after clearing the denominators by multiplications of rows with scalars). Therefore, A_N can be chosen as a submatrix of A_{N+1}, proving 2. □

An interesting Corollary of the above Theorem occurs if the number of conservation relations is constant.

Corollary 3.1.25. *Suppose the assumption of Remark 3.1.20 holds and that the number of conservation relations remains constant. Then, the matrix A_N is obtained from A_{N+1} by deleting the last n' of its columns.*

Proof. When the dimensions of the varieties of the networks $\mathcal{N}_{N+1}$ and $\mathcal{N}_N$ are the same, then so do the dimensions of the left kernels of their B-matrices. Hence, by Theorem 3.1.24 this is the case if and only if $\text{rank}(\tilde{B}) = n'$ and the result follows by the Rouché-Capelli Theorem. □

This section is concluded by relating the mathematical insights of the above theorems to families of toric chemical reaction networks.

Theorem 3.1.26. *The A-matrices of members of a family of chemical reaction networks are submatrices of each other when the assumption of Remark 3.1.20 is valid, all networks considered have the same number of conservation relations and one of the following conditions hold:*

(i) The family consists of a sequence of subnetworks with toric steady states.

(ii) The family is toric with toric intermediates.

Proof. Part (i) follows immediately from Theorem 3.1.24. To prove (ii), suppose I_N and I_{N+1} are the (binomial) steady state ideals of two members of a family and I'_{N+1} is the steady state ideal of their intermediate network. It follows from Theorem 3.1.24 that the A-matrices of I_N and I_{N+1} are submatrices of the A-matrix of the intermediate. Each column of the A-matrix corresponds to a variable x_i. Since both I'_{N+1} and I_{N+1} are ideals with species $\{x_1, \ldots, x_{n+n'}\}$ then their associated A-matrices have the same number of columns. Further, by assumption, the number of conservation relations stays constant. Therefore, by Proposition 3.1.18 the A matrices associated to I'_{N+1} and I_{N+1} are the same, since the ideals have the same dimension, meaning the A-matrices must have the same number of rows. Hence, the A-matrices associated to I_N and I_{N+1} are submatrices; i.e. A_N is a submatrix of A_{N+1}. □

3.2 Matroid Theory for Toric Chemical Reaction Networks

In this section the biological and algebraic Questions 2 and 3 are addressed. Recall that these questions regard the possibility of constructing the positive steady state locus of *all* members of a family by only measuring a fixed subset of species (e.g. the species of the $N = 1$ member of the family). Further, the problems of parameter estimation and model rejection are considered. This section uses the techniques presented in Harrington et al. [2012], MacLean et al. [2015], and Gross et al. [2016b], however, by exploiting the toric geometry of the steady states, predictions can be made for entire families of models.

One of the focuses of this chapter is to find independent subsets of the chemical species. Independent subsets can give valuable information about which species concentrations have to be measured in order to be able to reject a model and which concentrations can be determined from measurements. A simple example of linear independence is the set of three vectors $\boldsymbol{v}_1 = (1, 0)^T$, $\boldsymbol{v}_2 = (0, 1)^T$, $\boldsymbol{v}_3 = (2, 1)^T$. The set of vectors $\{\boldsymbol{v}_1, \boldsymbol{v}_2\}$ is linearly *independent*, whereas $\boldsymbol{v}_3 = \boldsymbol{v}_1 + \boldsymbol{v}_2$ and $\{\boldsymbol{v}_1, \boldsymbol{v}_2, \boldsymbol{v}_3\}$ is therefore *dependent*. The vectors $\boldsymbol{v}_1$ and $\boldsymbol{v}_2$ are said to from a *basis* of the set $\{\boldsymbol{v}_1, \boldsymbol{v}_2, \boldsymbol{v}_3\}$ which is a familiar notion of linear algebra. The set $\{\boldsymbol{v}_1, \boldsymbol{v}_2, \boldsymbol{v}_3\}$ is minimally dependent as it contains only a single element other than a basis and is a *circuit*. Matroid theory extends the notion of independence to polynomials rings. First, a matroid is defined.

Definition 3.2.1 (Matroid)**.** *A matroid $\mathcal{M}((E, \mathcal{I}))$ is a pair of two finite sets $(E, \mathcal{I})$ where E is the ground set and $\mathcal{I}$ is a set of subsets of E, called independent sets, satisfying the following conditions [Oxley, 2006].*

1. *The empty set, $\emptyset$, is independent such that $\emptyset \in \mathcal{I}$ and, hence, $\mathcal{I} \neq \emptyset$.*
2. *If $i \in \mathcal{I}$ and $i' \subseteq i$ then $i' \in \mathcal{I}$. This is called the* hereditary property*.*
3. *If i_1, $i_2 \in \mathcal{I}$ and $|i_1| < |i_2|$ then there exists an element $x \in i_2 - i_1$ such that $i_1 \cup x \in \mathcal{I}$. This is the* exchange property*.*

The notions of matroid *basis*, *rank* and *circuit* will also be useful.

Definition 3.2.2. *Matroid bases, rank and circuits are defined as follows:*

- *A* basis S *of a matroid* $\mathcal{M}$ *is a maximally independent subset, i.e. a subset* $S \in \mathcal{I}$ *such that* $S \cup k$ *is a dependent set for all* $k \in E - S$*. Define the set of all bases to be* $\mathcal{B}$*.*

- *The* rank ρ *is a function on a subset of* E *which takes a set* $e \subseteq E$ *and returns the cardinality of the largest subset* $i \subseteq e$ *which also satisfies* $i \in \mathcal{I}$*.*

- *The* circuits C *are minimally dependent sets, i.e. subsets of* E *which satisfy* $C \notin \mathcal{I}$ *and* $(C - z) \in \mathcal{I}$ *for any* $z \in C$*.*

In particular for a matroid $\mathcal{M}$ it holds that all bases of $\mathcal{M}$ are equicardinal. An important notion in matroid theory is also the rank of a matroid.

Definition 3.2.3 (Rank of a matroid)**.** *The* rank *of a matroid* $\mathcal{M}$*,* $\rho(\mathcal{M})$*, is the cardinality of a basis.*

Due to the general definition of a matroid, many mathematical objects have a matroid structure such as sets of vectors in a vector space or graphs. One class of matroids relevant for chemical reaction networks are *algebraic matroids*. Algebraic matroids encode the algebraic dependencies between the variables of a polynomial ring $R = \mathbb{K}[x_1, \ldots, x_n]$ in a prime ideal P. In a chemical reaction network setting the variables of a polynomial ring are the concentrations of the chemical species and the prime ideals which encode dependence of the chemical species are the associated primes of the steady state ideal. For information on how to compute algebraic matroids the reader is referred to [Oxley, 2006; Rosen, 2014]. Since the focus of this chapter is on the relation between the matroids of families of reaction networks, the notion of a submatroid is introduced.

Definition 3.2.4 (Submatroid)**.** *Given a subset* $E' \subset E$*, a matroid* $\mathcal{M}'(E', \mathcal{I}')$ *is a submatroid of* $\mathcal{M}(E, \mathcal{I})$ *if* $\mathcal{I}' = \mathcal{I} \cap \mathcal{P}(E')$*, where* $\mathcal{P}(E')$ *is the power set of* E'*. The rank function of* $\mathcal{M}'$ *is the restriction* $\rho_{\mathcal{M}'}(S) = \rho_{\mathcal{M}}(S)$ *for* $S \subseteq E'$*.*

Submatroids of algebraic matroids contain a subset of the polynomial relations between the variables of circuits of the original matroid. The relations between the variables of circuits are referred to as *circuit polynomials*. In particular, this chapter considers algebraic matroids of toric networks and the relations of matroids within a family of networks.

Proposition 3.2.5. *Let $E = \{x_1, \ldots, x_n\}$, $S = \{x_{i_1}, \ldots, x_{i_j}\} \subseteq E$ and define $\phi_A(S)$ by $\phi_A(S) = \{\phi_A(x_{i_1}), \ldots, \phi_A(x_{i_j})\}$, where ϕ_A is the parameterisation map of Definition 3.1.13. The ground set E with the set*

$$\mathcal{I} = \{S \subseteq E : \text{the monomials in } \phi_A(S) \text{are algebraically independent}\}$$

is a matroid $\mathcal{M}(E, \mathcal{I})$. Further, this matroid is isomorphic to the matroid defined by the column vectors of the A-matrix.

Proof. Consider the image of E under ϕ_A; this is a set of monomials. A set S of monomials is algebraically independent if and only if there exists no polynomial $p \in k[t_1^{\pm}, \ldots, t_d^{\pm}]$ such that $p(S) = 0$. This is exactly the condition to give an independent set $i \in \mathcal{I}$. Further, by Mittmann [2013, Lemma 4.2.10], a set of monomials is independent if and only if their exponent vectors are linearly independent. Hence, algebraic independence of $\phi_A(S)$ is equivalent to linear independence of the columns of the matrix A corresponding to S. □

Definition 3.2.6. *The matroid $\mathcal{M}(A)$ defined by the column vectors, $\boldsymbol{a}_i$, of a full rank integer matrix A encodes the algebraic dependencies of the concentrations at a non-zero (usually positive) steady state of a chemical reaction network and is therefore called the* positive steady state (PSS) matroid.

The PSS matroid is defined by the parameterisation of the positive steady states of a toric chemical reaction network. The parameterisation (A-matrix) only depends on the polynomial structure of the steady state ideal and not the parameters $\boldsymbol{\kappa}$. Hence, the PSS matroids for any two positive choices of $\boldsymbol{\kappa}$ of the same network $\mathfrak{N}$ are equivalent. Therefore, PSS matroids can be used to study systems subject to extrinsic noise.

Definition 3.2.7 (Laurent Binomial Associated to a PSS matroid circuit)**.** *Let $X_{A,\boldsymbol{x}^*}$ be the toric variety defined by a full rank matrix A and a positive vector $\boldsymbol{x}^*$ as in Definition 3.1.12. Let $\mathcal{M}(A)$ be the associated PSS matroid (Definition 3.2.6). Consider a circuit $C = \{\boldsymbol{a}_{i_1}, \ldots, \boldsymbol{a}_{i_{j-1}}\} \cup \{\boldsymbol{a}_{i_j}\} \subseteq E$ of the matroid $\mathcal{M}(A)$, where $\{\boldsymbol{a}_{i_1}, \ldots, \boldsymbol{a}_{i_{j-1}}\} \in \mathcal{I}$. The Laurent polynomial is defined by*

$$\Phi(C) = x_{i_j}^{\lambda_{i_j}} - \left(x_{i_j}^*\right)^{\lambda_{i_j}} \left(\prod_{l=1}^{j-1} \left(x_{i_l}^*\right)^{-\lambda_{i_l}}\right) \prod_{l=1}^{j-1} x_{i_l}^{\lambda_{i_l}} \in \mathbb{K}[x_1^{\pm 1}, \ldots, x_n^{\pm 1}]$$

with $\lambda_{i_l} \in \mathbb{Z}$ chosen such that $\sum_{l=1}^{j-1} \lambda_{i_l} \boldsymbol{a}_{i_l} = \lambda_{i_j} \boldsymbol{a}_{i_j}$ and λ_{i_j} is positive (this is possible since C is a circuit). The expression $\Phi(C)$ is called the Laurent binomial associated to C.

Definition 3.2.8 (Binomial Associated to a PSS matroid circuit)**.** *Let $\Phi(C)$ be a Laurent binomial of a circuit C of a PSS matroid as in Definition 3.2.7. The binomial associated to C is $\overline{\Phi(C)}$ which is $\Phi(C)$ with the denominator cleared, i.e.*

$$\overline{\Phi(C)} = x_{i_j}^{\lambda_{i_j}} x^{\boldsymbol{\lambda}^-} - \left(x_{i_j}^*\right)^{\lambda_{i_j}} \left(\prod_{l=1}^{j-1} \left(x_{i_l}^*\right)^{-\lambda_{i_l}}\right) x^{\boldsymbol{\lambda}^+} \in \mathbb{K}[x_1, \ldots, x_n],$$

where $\lambda_j^+ = \lambda_j$ if $\lambda_j > 0$ and zero otherwise and where $\lambda_j^- = |\lambda_j|$ if $\lambda_j < 0$ and zero otherwise.

Lemma 3.2.9. *Let $X_{A,\boldsymbol{x}^*}$ be the toric variety defined by a full rank matrix A and a positive vector $\boldsymbol{x}^*$ as in Definition 3.1.12 and let $\mathcal{M}(A)$ be the associated PSS matroid. If C is a circuit in $\mathcal{M}(A)$ then $\Phi(C)(\boldsymbol{x}) = 0$ if $\boldsymbol{x} \in (\mathbb{C}^*)^n \cap X_{A,\boldsymbol{x}^*}$.*

Proof. Given a linearly dependent set of vectors it holds that, without loss of generality, $\sum_{l=1}^{j-1} \lambda_{i_l} \boldsymbol{a}_{i_l} = \lambda_{i_j} \boldsymbol{a}_{i_j}$ for some integers $\lambda_{i_l} \in \mathbb{Z}$ and $\lambda_{i_j} \in \mathbb{Z}_{>0}$. It follows that

$$t^{\sum_i^{j-1} \lambda_{i_l} \boldsymbol{a}_{i_l}} = t^{\lambda_{i_j} \boldsymbol{a}_{i_j}}.$$

Taking the preimage under ϕ_A this can be rewritten as

$$(x_{i_j}^*)^{\lambda_{i_j}} \prod_{l=1}^{j-1} (x_{i_l})^{\lambda_{i_l}} \prod_{l=1}^{j-1} (x_{i_l}^*)^{-\lambda_{i_l}} = x_{i_j}^{\lambda_{i_j}}.$$

□

Lemma 3.2.10. *Let $\mathcal{M}(A)$ be the matroid associated to a toric chemical reaction network $\mathfrak{N}$ Choose a basis S and $n-d$ circuits C_i such that $\bigcap_i C_i = S$. Then, the following holds*

$$V(\overline{\Phi(C_1)}, \ldots, \overline{\Phi(C_{n-d})}) \cap \mathbb{R}^n_{>0} = V(I_{\mathfrak{N}}) \cap \mathbb{R}^n_{>0}.$$

Hence, proving that the variety $V(\langle \overline{\Phi(C_1)}, \ldots, \overline{\Phi(C_{n-d})} \rangle)$, when intersected with the subspace spanned by the conservation relations, contains at least two positive points is necessary for proving multistationarity of the original toric network given by $I_{\mathfrak{N}}$.

Proof. Let $F_k(x_1, \ldots, x_n) = \overline{\Phi(C_k)}$ to give $W = V(F_1, \ldots, F_{n-d})$ and also let

$$X_{A,\boldsymbol{x}^*} = \overline{\{(x_1^* t^{a_1}, \ldots, x_n^* t^{a_n}) \mid t \in (\mathbb{C}^*)^d\}}.$$

The containment $X_{A,\boldsymbol{x}^*} \cap \mathbb{R}^n_{>0} \subseteq W \cap \mathbb{R}^n_{>0}$ follows from Lemma 3.2.9. Now prove the other containment. For a positive real point $\boldsymbol{w} \in W \cap \mathbb{R}^n_{>0}$ it must hold that, for each $k = 1, \ldots, n-d$, $F_k(\boldsymbol{w}) = 0$. Hence, by Definition 3.2.8,

$$w_{i_j}^{\lambda_{i_j}} \boldsymbol{w}^{\boldsymbol{\lambda}_- - \boldsymbol{\lambda}_+} = \left(x^*_{i_j}\right)^{\lambda_{i_j}} \left(\prod_{l=1}^{j-1} \left(x^*_{i_l}\right)^{-\lambda_{i_l}}\right).$$

For each circuit define the vector $\tilde{\boldsymbol{\lambda}} \in \mathbb{Z}^n$ as the vector with non-zero entries i_ℓ corresponding to the values of the coefficients of $\lambda_{i_j}\boldsymbol{a}_{i_j} - \sum_{y=1}^{j-1} \lambda_{i_y}\boldsymbol{a}_{i_y} = 0$. and let Λ be the matrix with rows $\tilde{\boldsymbol{\lambda}}_k$; note that the rows of Λ form a basis of $\ker(A)$. Set $\tilde{\boldsymbol{w}} = (w_{i_1}, \ldots, w_{i_j})$ and set $\tilde{\boldsymbol{x}^*} = (x^*_{i_1}, \ldots, x^*_{i_j})$; then

$$\left(\frac{\tilde{\boldsymbol{w}}}{\tilde{\boldsymbol{x}^*}}\right)^{\tilde{\boldsymbol{\lambda}}_k} = 1, \quad \text{which gives,} \quad \tilde{\boldsymbol{\lambda}}_k \cdot \log(\tilde{\boldsymbol{w}}/\tilde{\boldsymbol{x}^*}) = 0.$$

Further, $\log(\tilde{\boldsymbol{w}}/\tilde{\boldsymbol{x}^*}) \in \ker(\Lambda)$ and, hence, $\tilde{\boldsymbol{w}}/\tilde{\boldsymbol{x}^*}$ is in the image of $\boldsymbol{x}^* t^A$. □

The theorem below relates the algebraic matroid defined by the ideal of a toric variety $X_{A,\boldsymbol{x}^*}$ to the PSS matroid $\mathcal{M}(A)$.

Theorem 3.2.11. *Let $I_b \subseteq R = \mathbb{K}[x_1, \ldots, x_n]$ be a prime binomial ideal defining a toric variety $X_{A,\boldsymbol{x}^*} = V(I_b)$ where $A \in \mathbb{Z}^{d\times n}$ is the exponent matrix of the corresponding monomial parameterisation. Denote the algebraic matroid defined by I_b as $\mathcal{M}(I_b)$ and the matroid defined by the linear independence of the columns of A by $\mathcal{M}(A)$. Then $\mathcal{M}(I_b) = \mathcal{M}(A)$.*

Proof. The variables of the ground set of $\mathcal{M}(A)$ have algebraic dependencies as defined in Proposition 3.2.5. Hence, their algebraic dependencies can be found by solving the implicitisation problem $I = J \cap \mathbb{K}[x_1, \ldots, x_n]$ where $J = \langle x_1 - x_1^* t^{\boldsymbol{a}_1}, \ldots, x_n - x_n^* t^{\boldsymbol{a}_n}\rangle$. However, the same ideal defines the implicit equations of a toric variety defined by $\psi_A : t \to (x_1^* t^{\boldsymbol{a}_1}, \ldots, x_n^* t^{\boldsymbol{a}_n})$. Hence, the algebraic relations between the monomials $\phi_A(x)$ are identical to the algebraic relations defined by the binomial ideal I_b. This implies that $\mathcal{M}(A) = \mathcal{M}(I_b)$. □

Remark 3.2.12. *Theorem 3.2.11 shows that the algebraic matroid defined by the binomial ideal and the PSS matroid are identical and, therefore, the algebraic matroid can be studied directly using linear algebra operations on the columns of the A-matrix defining the PSS matroid. This way bases, circuits and even circuit polynomials can be inferred trivially.*

As the binomial equations constructed using Definition 3.2.8 vanish on the positive steady states and the PSS matroid encodes all the relations between chemical concentrations at positive steady state, the study of matroids associated to families of reaction networks with toric steady states can be restricted to the PSS matroids. The next proposition establishes a connection between the matroids of all members of a family.

Proposition 3.2.13. *Fix a family of toric reaction networks $\mathcal{N}$ and let $\mathcal{N}_M, \mathcal{N}_N \in \mathcal{N}$ with $M < N$. If both members of the family have the same number of conservation relations then $\mathcal{M}(A_M)$ is a submatroid of $\mathcal{M}(A_N)$.*

Proof. If the dimensions of the varieties are the same, then, by Theorem 3.1.24 the A-matrix of $\mathcal{N}_M$ is a submatrix of the A-matrix of $\mathcal{N}_N$. Therefore, $E_M \subset E_N$ and, trivially, any set of linearly independent columns of any matrix is also linearly independent set of columns in any submatrix containing these. Hence, $\mathcal{I}_M = \mathcal{I}_N \cap \mathcal{P}(E_M)$. □

3.2.1 Experimental Design and Compatibility

In this subsection it is studied how steady state matroids and submatroids can be employed in experimental design and model rejection. For the remainder of this subsection it is assumed that the number of conservation relations within a family is fixed. Hence, by Proposition 3.2.13 the matroids of smaller family members are submatroids of the matroids of larger family members.

Previous related work includes the study of "complex-linear steady state invariants" [Karp et al., 2012] and data coplanarity [Harrington et al., 2012]. A study using the language of algebraic matroids explicitly can be found in Gross et al. [2016b]. In this section results similar to [Harrington et al., 2012; MacLean et al., 2015] are obtained using the PSS matroid and the circuit-like polynomials of Definition 3.2.8 and it is shown how they can be used in model rejection and experimental design for entire toric families.

First, the focus lies on the minimum number of species that need to be measured to be able to construct the steady state locus for an entire family (if the rate constants are known).

Proposition 3.2.14. *Fix a family of chemical reaction networks $\mathcal{N}$ for which the rate constants $\boldsymbol{\kappa}$ associated to every family member are known. There exists a subset of species of the smallest family member which is sufficient to measure at steady state in order to construct a corresponding positive steady state for every subsequent family member.*

Proof. Recall that $\boldsymbol{x}^*$ is a positive vector for known constants. Choose a basis S of the PSS matroid of the smallest family member $\mathcal{N}_1$. Hence, by Definition 3.2.8 binomial relations can be constructed to determine the steady state concentrations of the chemical species not in the basis. By Proposition 3.2.13 any basis of $\mathcal{N}_1$ is a basis of the subsequent family members and, hence, Definition 3.2.8 applies. □

Hence, by Proposition 3.2.14, measuring the concentrations of all the species in a basis of the smallest network in a family is sufficient to determine the steady states of the entire family.

Next, the PSS matroids are used for model selection or model rejection by applying techniques from Harrington et al. [2012] and Gross et al. [2016b]. For simplicity, the results focus on the case of perfect, that is noise-free, data. However the result of Lemma 3.2.15 can also be applied to noisy data by following the construction in MacLean et al. [2015]. To determine whether a model is compatible with observed data it is necessary to determine whether there exists a set of parameters $\{\kappa_1, \ldots, \kappa_m\} > 0$ such that a measured data point $\{\xi_{i_1}, \ldots, \xi_{i_j}\}$ is an element of the steady state variety. To proceed, a condition for model compatibility of perfect data is formulated.

Lemma 3.2.15. *Let $\mathfrak{N}$ be a reaction network with PSS matroid $\mathcal{M}(A)$. Assume that the rate constants are fixed but unknown, but the initial conditions are varied. Fix a circuit C corresponding to the linear relations among the columns of A via $\sum_{l=1}^{j-1} \lambda_{i_l} \boldsymbol{a}_{i_l} = \lambda_{i_j} \boldsymbol{a}_{i_j}$. Given a pair of steady state measurements $\{\xi_{i_1}, \ldots, \xi_{i_j}\}$ and $\{\zeta_{i_1}, \ldots, \zeta_{i_j}\}$ of the concentrations of C, the corresponding model is compatible only if*

$$\xi_{i_j}^{\lambda_{i_j}} \prod_{l=1}^{j-1} \xi_{i_l}^{-\lambda_{i_l}} = \zeta_{i_j}^{\lambda_{i_j}} \prod_{l=1}^{j-1} \zeta_{i_l}^{-\lambda_{i_l}}.$$

Proof. As in Remark 3.1.15 fix rate constants $\boldsymbol{\kappa} = (\kappa_1, \ldots, \kappa_m)^T \in \mathbb{R}^m_{>0}$ such that $\boldsymbol{x}^* \in \mathbb{R}^n_{>0}$. Rearrange $\Phi(C)$ of Definition 3.2.7 to give

$$x_{i_j}^{\lambda_{i_j}} \prod_{l=1}^{j-1} x_{i_l}^{-\lambda_{i_l}} = \left(x_{i_j}^*\right)^{\lambda_{i_j}} \left(\prod_{l=1}^{j-1} \left(x_{i_l}^*\right)^{-\lambda_{i_l}} \right) = \theta \in \mathbb{R}_{>0}.$$

For the measurements to be compatible it must be true that when the expression above is evaluated at $x_{i_l} = \xi_{i_l}$ and at $x_{i_l} = \zeta_{i_l}$ the same value, θ, is obtained. The conclusion follows. □

Remark 3.2.16. *For PSS matroids not only circuits can be used to form invariants similar to the one presented in Lemma 3.2.15, although circuits are the simplest case. Using a PSS matroid, any dependent set of the PSS matroid can be converted into a binomial equation and, hence, an invariant.*

Due to the additional structure provided by the PSS matroid the condition of Lemma 3.2.15 is much simpler than the linear algebra condition of Harrington et al. [2012]. By Proposition 3.2.13 it is easy to see that if Lemma 3.2.15 holds for a given PSS matroid it holds for all of its submatroids. Hence, measuring only a subset of species which belongs to a smaller member of the family is sufficient to conclude that the measurements of this subset of species is compatible for the whole family. In particular, this allows one to say that a given data set is compatible with a family of networks, but it cannot be specified which network in the family is 'most' compatible with the data.

Identifying model parameters for perfect data has been studied extensively in previous work [Meshkat et al., 2018; Chis et al., 2011; Walter, 2014] and, therefore, the discussion in this chapter is restricted to the novel methods obtained by using the PSS matroid of a family of networks. In particular, the PSS matroid allows for straightforward conversion of a variety in the space of species to a variety in the space of parameters. First, it is shown that, in the case of toric steady states, biologically viable parameter sets $\boldsymbol{\kappa} = (\kappa_1, \ldots, \kappa_m)^T \in \mathbb{R}^m_{>0}$ are the positive part of an algebraic variety and, then, this result is generalised to the entire family.

Proposition 3.2.17. *Let A be a full rank $d \times n$ integer matrix and let $C_1, \ldots, C_{n-d}$ be a collection of circuits of the matroid $\mathcal{M}(A)$, each containing the same basis S. Using Definition 3.2.7 to obtain the ideal $J = \langle \overline{\Phi(C_1)}, \ldots, \overline{\Phi(C_{n-d})} \rangle \subseteq R = \mathbb{K}[x_1, \ldots, x_n]$ and denoting the variables present in a circuit as $\boldsymbol{x}(C_1) \subseteq \{x_1, \ldots, x_n\}$, then the intersection ideal $J_{C_i} = J \cap \mathbb{K}[\boldsymbol{x}(C_i)]$ is principal (generated by one element) with generator $\overline{\Phi(C_i)}$.*

Proof. By construction both, the numerator and the denominator of $\Phi(C_i)$ contain only variables in C_i and, hence, after clearing the denominator the resulting polynomial $\overline{\Phi(C_i)}$ also only contains variables in C_i. Since C_i is a circuit, the ideal J_{C_i} has codimension 1 in $R \cap \mathbb{K}[x(C_i)]$ and, hence, by Mumford [1999, I.,§7, Proposition 4] it is principal. Further, $J \cap \mathbb{K}[\boldsymbol{x}(C_i)] = \langle \overline{\Phi(C_i)} \rangle$ and, therefore, $J_{C_i} = \langle \overline{\Phi(C_i)} \rangle$. □

Proposition 3.2.17 shows that the positive part of the steady state variety can easily be projected onto coordinate subspaces by dropping circuits. Hence, the PSS

matroid allows for some freedom to "pick and mix" variables according to measurements. The picking and mixing corresponds to the geometric operation of projection of the variety $X = V(\langle\overline{\Phi(C_1)}, \ldots, \overline{\Phi(C_{n-d})}\rangle) \subseteq \mathbb{K}^n$. Next, suppose there exists a measurement $\xi = \{\xi_{i_1}, \ldots, \xi_{i_\ell+d}\}$ containing measurements for the species in a basis S of the PSS and the species in the circuits $C_1, \ldots, C_\ell$, all containing S. Combining the idea of projection and measurement (evaluation) leads to the definition of a *parameter variety*.

Definition 3.2.18. *Keeping the same notation as above and, by choosing an appropriate set of generators, i.e. "clearing the denominators", let* $J = \langle\overline{\Phi(C_1)}, \ldots, \overline{\Phi(C_\ell)}\rangle \subseteq \mathbb{R}[\kappa_1, \ldots, \kappa_m, x_1, \ldots, x_n]$ *and, hence,* $V(J) \subset \mathbb{R}^m \times \mathbb{R}^n$. *The parameter variety,* X_m, *is obtained from* $V(J)$ *by the evaluation*

$$X_m = V(J) \cap V(\langle x_{i_1} - \xi_{i_1}, \ldots, x_{i_{\ell+d}} - \xi_{i_{\ell+d}}\rangle) \subseteq \mathbb{R}^m.$$

The parameter variety is obtained by the selective projection and evaluation of the binomials obtained from Definition 3.2.8 and is a variety in the space of parameters only. Every parameter vector compatible with the measurement ξ is on the parameter variety. Every set of measurements gives rise to a parameter variety and, in order to be compatible with a model, their intersection needs to be non empty, in fact, their intersection needs to be non empty in the positive orthant. In order to uniquely identify a model based on a given measurement the positive orthant of X_m needs to consist of a single point only. Various algebraic techniques can be applied to show when this is the case, e.g. Cox et al. [2013] or Müller et al. [2016].

The parameter varieties of families of toric networks can be related by applications of projections (selective application of Definition 3.2.8) and the partial evaluation map π. Suppose J_N and J_{int} are the ideals of the N^{th} member of a family and the intermediate model between the N^{th} and $(N+1)^{\text{th}}$ member, respectively. Let both ideals (or a projection of them) contain the same circuits $C_1, \ldots, C_\ell$. Then, by Proposition 3.1.22, $J_N = \pi(J_{\text{int}})$

3.3 Inheritance of Multistationarity for Toric Families

In this section the inheritance of multistationarity among members of families of toric chemical reaction networks is investigated. The main result of this section is Theorem 3.3.2, where results of Sadeghimanesh and Feliu [2018], and Müller et al.

[2016] are applied to show that if a multistationary member of a family (satisfying certain conditions) can be identified, then every larger member of the same family is multistationary for some parameter values. First, some additional notation is introduced.

Definition 3.3.1. *Let $I_B \subset \mathbb{K}[x_1, \ldots, x_n]$ be a prime binomial ideal defining a complete intersection of codimension $n - d$ and let the matrix B be an exponent matrix of a minimal generating set of I_B. Define*

$$J = \begin{pmatrix} Z \\ B^T \end{pmatrix}$$

where Z is an integer matrix. Further, let

$$J^\lambda = \begin{pmatrix} Z \\ \left(B^T\right)^\lambda \end{pmatrix},$$

where $\left(B^T\right)^\lambda = (\boldsymbol{b}_1\lambda_1, \ldots, \boldsymbol{b}_n\lambda_n)$ for the columns b_i of B^T. A matrix J^λ is called regular if $\det(J^\lambda) \neq 0$ for some values of $(\lambda_1, \ldots, \lambda_n)$.

Now, the main theorem of this section is stated.

Theorem 3.3.2. *Fix a family of toric chemical reaction networks. Suppose that the family obeys the following conditions*

(C1) The family has toric intermediates.

(C2) The number of conservation relations stays constant.

(C3) The matrix J^λ for the N^{th} network is regular.

Then, if the N^{th} member of the family is capable of multistationarity, every member of the family for which $M \geq N$ is also capable of multistationarity.

Before proving the theorem above, the following lemma is proved.

Lemma 3.3.3. *Fix a family of reaction networks, where each member of the family and each intermediate network have the same number of conservation relations. Let Z_N be a conservation relation matrix of the N^{th} network. Then, Z_{N+1} is obtained by adding columns to Z_N, i.e. Z_N is a submatrix of Z_{N+1}.*

Proof. First, build the stoichiometric matrix of the intermediate network by adding n' species and m' reactions to the N^{th} network. Hence, the stoichiometric matrix of the intermediate network, Γ_N^{int}, has the form

$$\Gamma_N^{\text{int}} = \left(\begin{array}{c|c} \Gamma_N & \\ \hline 0_{n' \times m} & \tilde{\Gamma}_N \end{array} \right),$$

where $\Gamma_N = (\boldsymbol{r}_1, \ldots, \boldsymbol{r}_m)$ is the $n \times m$ stoichiometric matrix of the N^{th} network and, $\tilde{\Gamma}_N = (\boldsymbol{r}_{m+1}, \ldots, \boldsymbol{r}_{m+m'})$ is the $(n+n') \times m'$ matrix of new reactions. Hence, any basis of the left kernel of Γ_N^{int} can be written as $\tilde{\boldsymbol{z}}_i = (\boldsymbol{z}_i \ , \ \boldsymbol{z}_i')$, where $\boldsymbol{z}_i$ is an element of a basis of the left kernel of Γ_N or zero and $\boldsymbol{z}_i'$ is a vector to be determined by $\tilde{\Gamma}_N$. The assumption of equidimensionality of the left kernels of Γ_N and Γ_N^{int} can be satisfied only if $\operatorname{rank}(\tilde{\Gamma}_N) = n'$ and, in the same fashion as Corollary 3.1.25, it follows, that Z_N is a submatrix of Z_N^{int}. Now, delete m'' of the first m columns of Γ_N^{int} to form Γ_{N+1}. By the equidimensionality assumption it follows, that the rows of Z_N^{int} form a basis of the left kernel of Γ_{N+1}. Hence, $Z_N^{\text{int}} = Z_{N+1}$ and Z_N is a submatrix of Z_{N+1}. □

From Lemma 3.3.3 and Lemma 3.2.10 it becomes apparent why (C2) and toric steady states are required. Namely, toric steady states are needed to construct a matrix B and, hence, J_N^λ and (C2) is required to ensure that the conservation relation matrices are submatrices. The proof of Theorem 3.3.2 is now stated.

Proof. Fix a vector $\boldsymbol{x}^* \in \mathbb{R}^n_{>0}$ as in Definition 3.2.7 and choose a basis S and $n-d$ circuits $\{C_1, \ldots, C_{n-d}\}$ of the PSS matroid associated to the N^{th} member of a family such that $\bigcap_i C_i = S$. Consider the polynomial system

$$\overline{\Phi(C_1)}(\boldsymbol{x}) = \cdots = \overline{\Phi(C_{n-d})}(\boldsymbol{x}) = Z_N \boldsymbol{x} - \boldsymbol{c} = 0. \tag{3.7}$$

Further, let B_N denote the exponent matrix of the binomials $\overline{\Phi(C_1)}, \ldots, \overline{\Phi(C_{n-d})}$ as in Definition 3.1.23. Hence, following the construction of Definition 3.3.1 the square matrix

$$J_N^\lambda = \begin{pmatrix} Z_N \\ (B_N^T)^\lambda \end{pmatrix},$$

is obtained. By construction (see Lemma 3.2.10), $V(\overline{\Phi(C_1)}(x), \cdots, \overline{\Phi(C_{n-d})}(x)) \cap \mathbb{R}^n_{>0} \neq \emptyset$. By Sadeghimanesh and Feliu [2018, Theorem 2.7] the system (3.7) is multistationary if and only if either $\det(J_N^\lambda) = 0$ or $\det(J_N^\lambda) \neq 0$ and the polynomial $\det(J_N^\lambda)$ in $\lambda_1, \ldots, \lambda_n$ has a positive and a negative term. Suppose the N^{th} network is multistationary and, by condition (C3), $\det(J_N^\lambda) \neq 0$. Next, build the $(N+1)^{\text{th}}$ network by adding n' new species and consider its matrix J_{N+1}^λ. To obtain this matrix

consider the new circuit binomials $\overline{\Phi(C_{n-d+1})}(\boldsymbol{x}) = \cdots = \overline{\Phi(C_{n+n'-d})}(\boldsymbol{x}) = 0$, where each circuit contains the basis S and one new variable x_{n+i} with its corresponding positive exponent b_{n+i}, where $i = 1, \ldots, n'$. The exponent vectors will therefore have exactly one non-zero element (namely the positive integer b_{n+i}) in the last n' rows. Therefore, the matrix J^{λ}_{N+1} has the block form

$$J^{\lambda}_{N+1} = \left(\begin{array}{c|c} J^{\lambda}_{N} & Z_{N+1}|_{[(1\ldots d)\times(n+1\ldots n+n')]} \\ & 0_{(n-d)\times l} \\ \hline \left(B^{T}_{N+1}\right)^{\lambda}|_{[(n-d+1\ldots n+n'-d)\times(1\ldots n)]} & \operatorname{diag}(b_{n+1}\lambda_{n+1}, \ldots, b_{n+n'}\lambda_{n+n'}) \end{array} \right)$$

where $A|_{[y_1\ldots y_m \times a_1 \ldots a_n]}$ denotes the restriction of a matrix A to the rows $y_1 \ldots y_m$ and columns $a_1 \ldots a_n$. The matrix $\operatorname{diag}(b_{n+1}\lambda_{n+1}, \ldots, b_{n+n'}\lambda_{n+n'})$ is a diagonal matrix with diagonal elements $b_{n+1}\lambda_{n+1}, \ldots, b_{n+n'}\lambda_{n+n'}$. Hence, the expression $T = \left(\prod_{i=n+1}^{n+n'} b_i\lambda_i\right) \det(J^{\lambda}_{N}) \neq 0$ must appear in $\det(J^{\lambda}_{N+1})$ and, in particular, no term in T can be cancelled by any other term appearing in $\det(J^{\lambda}_{N+1})$. Hence, if $\det(J^{\lambda}_{N})$ has coefficients of opposite sign so does $\det(J^{\lambda}_{N+1})$ and, therefore the network is multistationary. The proof is completed by induction. □

Remark 3.3.4. *Note that, since it is allowed to choose different bases of the PSS matroid, and, hence, different binomial systems, it may be possible to satisfy Condition (C3) of Theorem 3.3.2 for one particular choice of basis but not for a different choice of basis.*

The results are illustrated using the two and three site distributive phosphorylation networks.

Example 3.3.5. *The PSS matroid of the one-site and two-site distributive phosphorylation networks are represented respectively by the A-matrices*

$$A_1 = \begin{pmatrix} 1 & 0 & 0 & 1 & 1 & 1 \\ 1 & 1 & 0 & 0 & 1 & 1 \\ 0 & 0 & 1 & 1 & 1 & 1 \end{pmatrix} \text{ and } A_2 = \begin{pmatrix} 1 & 0 & 0 & 1 & 1 & 1 & 2 & 2 & 2 \\ 1 & 1 & 0 & 0 & 1 & 1 & 0 & 1 & 1 \\ 0 & 0 & 1 & 1 & 1 & 1 & 1 & 1 & 1 \end{pmatrix},$$

respectively. Hence, choosing a basis of $a_1 = (1,1,0)^T$, $a_2 = (0,1,0)^T$ *and* $a_3 = (0,0,1)^T$ *a parameterisation for the one-site network can be found to give*

$$\begin{aligned} x_2x_4 - x_2^*x_4^*\left(x_1^*x_3^*\right)^{-1}x_1x_3 &= 0, \\ x_5 - \left(x_1^*x_3^*\right)^{-1}x_5^*x_1x_3 &= 0, \\ x_6 - \left(x_1^*x_3^*\right)^{-1}x_6^*x_1x_3 &= 0. \end{aligned}$$

The two-site model has three additional equations, namely

$$\begin{aligned} x_2^2 x_7 - (x_1^*)^{-2} (x_3^*)^{-1} (x_2^*)^2 x_7^* x_1^2 x_3 = 0, \\ x_2 x_8 - (x_1^*)^{-2} (x_3^*)^{-1} x_2^* x_8^* x_1^2 x_3 = 0, \\ x_2 x_9 - (x_1^*)^{-2} (x_3^*)^{-1} x_2^* x_9^* x_1^2 x_3 = 0. \end{aligned}$$

Hence, the B-matrices,

$$B_1^T = \begin{pmatrix} -1 & 1 & -1 & 1 & 0 & 0 \\ -1 & 0 & -1 & 0 & 1 & 0 \\ -1 & 0 & -1 & 0 & 0 & 1 \end{pmatrix},$$

and

$$B_2^T = \begin{pmatrix} -1 & 1 & -1 & 1 & 0 & 0 & 0 & 0 & 0 \\ -1 & 0 & -1 & 0 & 1 & 0 & 0 & 0 & 0 \\ -1 & 0 & -1 & 0 & 0 & 1 & 0 & 0 & 0 \\ -2 & 2 & -1 & 0 & 0 & 0 & 1 & 0 & 0 \\ -2 & 1 & -1 & 0 & 0 & 0 & 0 & 1 & 0 \\ -2 & 1 & -1 & 0 & 0 & 0 & 0 & 0 & 1 \end{pmatrix},$$

are obtained. The conservation relations can be chosen as

$$Z_2 = \begin{pmatrix} -1 & -1 & 1 & 1 & 0 & 0 \\ 1 & 0 & 0 & 0 & 1 & 0 \\ 0 & 1 & 0 & 0 & 0 & 1 \end{pmatrix},$$

and

$$Z_2 = \begin{pmatrix} -1 & -1 & 1 & 1 & 0 & 0 & 1 & 0 & 0 \\ 1 & 0 & 0 & 0 & 1 & 0 & 0 & 1 & 0 \\ 0 & 1 & 0 & 0 & 0 & 1 & 0 & 0 & 1 \end{pmatrix}.$$

This leads to

$$det\,(J_1^\lambda) = \lambda_3\lambda_4\lambda_5 + \lambda_1\lambda_4\lambda_6 + \lambda_3\lambda_4\lambda_6 + \lambda_3\lambda_5\lambda_6 + \lambda_4\lambda_5\lambda_6.$$

Note that this determinant is square-free and homogeneous as investigated in Dickenstein et al. [2019] and that it has only coefficients equal to +1. Indeed, it is a well known fact the the one-site distributive network is monostationary [Flockerzi et al., 2014].

The determinant of J_2^λ *is equal to*

$$\begin{aligned}det(J_2^\lambda) = &-\lambda_2\lambda_3\lambda_4\lambda_5\lambda_7\lambda_8 - \lambda_1\lambda_2\lambda_3\lambda_6\lambda_7\lambda_8 - \lambda_1\lambda_2\lambda_4\lambda_6\lambda_7\lambda_8 - \lambda_1\lambda_3\lambda_4\lambda_6\lambda_7\lambda_8\\ &-\lambda_2\lambda_3\lambda_4\lambda_6\lambda_7\lambda_8 - \lambda_2\lambda_4\lambda_5\lambda_6\lambda_7\lambda_8 + \lambda_3\lambda_4\lambda_5\lambda_6\lambda_7\lambda_8 - \lambda_1\lambda_2\lambda_3\lambda_4\lambda_5\lambda_9\\ &-\lambda_1\lambda_2\lambda_3\lambda_5\lambda_6\lambda_9 - 2\lambda_1\lambda_2\lambda_4\lambda_5\lambda_6\lambda_9 - \lambda_2\lambda_3\lambda_4\lambda_5\lambda_6\lambda_9 + \lambda_1\lambda_3\lambda_4\lambda_5\lambda_7\lambda_9\\ &+\lambda_1\lambda_3\lambda_5\lambda_6\lambda_7\lambda_9 + 2\lambda_1\lambda_4\lambda_5\lambda_6\lambda_7\lambda_9 + \lambda_3\lambda_4\lambda_5\lambda_6\lambda_7\lambda_9 - 2\lambda_2\lambda_3\lambda_4\lambda_5\lambda_8\lambda_9\\ &-\lambda_1\lambda_2\lambda_3\lambda_6\lambda_8\lambda_9 - 2\lambda_1\lambda_2\lambda_4\lambda_6\lambda_8\lambda_9 - \lambda_1\lambda_3\lambda_4\lambda_6\lambda_8\lambda_9 - 2\lambda_2\lambda_3\lambda_4\lambda_6\lambda_8\lambda_9\\ &-\lambda_2\lambda_3\lambda_5\lambda_6\lambda_8\lambda_9 - 2\lambda_2\lambda_4\lambda_5\lambda_6\lambda_8\lambda_9 + \lambda_3\lambda_4\lambda_5\lambda_6\lambda_8\lambda_9 + \lambda_7\lambda_8\lambda_9\ det(J_1^\lambda),\end{aligned}$$

and, therefore, contains a term $T = \lambda_7\lambda_8\lambda_9 det(J_1^\lambda)$. *The determinant of the two-site network has coefficients of opposite signs and, hence, the network is multistationary and so are all larger networks in the family. In particular, it is known that the* N*-site distributive network has a maximum of* $2N-1$ *positive steady states [Flockerzi et al., 2014].*

This section is ended with a conjecture motivated by Theorem 3.3.2 and the results of Flockerzi et al. [2014].

Conjecture 3.3.6. *Consider a family of reaction networks* $\mathcal{N}$ *and a member* $\mathcal{N}_N$ *such that the assumption of Remark 3.1.20 holds. If the* N^{th} *member of this family has a maximum of* ℓ *positive steady states, then the network* $\mathcal{N}_{N+M}$ *has a maximum of at least* ℓ *positive steady states for* $M \geq 0$.

3.4 Conclusion

In this chapter families of chemical reaction networks with toric steady states, called toric families, were studied. First, the dimensions and parameterisations of the toric steady state varieties were investigated and these geometric properties were connected to network properties whenever possible. In particular, if there is a finite number of positive steady states in all stoichiometric compatibility classes, then the number of conservation relations determines the dimension of the toric steady state variety and, with certain restrictions, the monomial parameterisation of a chemical species X_i is preserved throughout the family.

Furthermore, the matroid defined by the parameterisation of the positive steady states were studied. In particular, it was shown that the algebraic matroid defined by the binomial steady state ideal is equivalent to the PSS matroid. It was shown how binomials reminiscent of circuit polynomials can be constructed from the PSS matroid

and how they can be used for model selection, experimental design or even parameter identification. Except for the result on parameter identification, in which the parameters were treated as variables, all results hold for generic, positive parameters.

The final section investigated the multistationarity structure of toric families. The main result of the section was proved, namely, that if a member of a family is capable of multistationarity, then, under some mild restrictions, all larger members are too. This result was proved by using the circuit-like binomials constructed from the PSS matroids. The results were illustrated by example of the multi-site distributive phosphorylation network.

The methods in this chapter used algebraic objects such as matroids and A-matrices which depend on the polynomial structure of the reaction network, but not on the coefficients (the rate constants $\boldsymbol{\kappa}$). Hence, most methods presented in this chapter can be employed when there is complete ignorance of the parameter values. When rate constants had to be fixed, the choice was sufficiently generic with mild restrictions usually automatically satisfied in biological systems, e.g. $\boldsymbol{x}^* \in \mathbb{R}^n_{>0}$ when $\boldsymbol{\kappa}$ are fixed.

Further research could include applying the results of this chapter to other meaningful biological families such as different models for immune system reactions, e.g. [Mckeithan, 1995; Dushek and van der Merwe, 2014]. Another direction could be to study the parameter varieties defined in this paper in the context of previous identifiability research and aim to include noisy data. Finally, a proof of Conjecture 3.3.6 would be highly desirable.

Chapter 4

Complexity of Model Testing of Chemical Reaction Networks with Toric Steady States

> *"Algebraic geometry seems to have acquired the reputation of being esoteric, exclusive, and very abstract, with adherents who are secretly plotting to takeover all the rest of mathematics. In one respect this last point is accurate."*
>
> – David Mumford

This chapter is based on work published in Adamer and Helmer [2019a].

In this chapter chemical reaction networks subject to constant extrinsic noise are studied. In particular, it is assumed that any rate constant can have any positive value. Hence, as complete ignorance of parameter values makes it impossible to quantitatively predict model behaviour, methods which are robust to perturbations in the parameter values need to be employed. To this end, a range of algebraic and geometric invariants to study the long term behaviour of chemical reaction networks are available, such as the dimension of the steady state variety and its degree. In this chapter the Euclidean Distance degree (ED degree) is studied, which is a geometric invariant measuring the complexity of a model. As shown in Proposition 4.1.6, the ED degree is independent of parameters. The computation of the ED degree in this chapter is restricted to toric varieties due to the additional combinatorial structure which greatly simplifies the computations [Helmer and Sturmfels, 2016] and allows for closed form formulas.

Dynamical systems with toric steady states [Millán et al., 2012; Craciun et al., 2009a] are ubiquitous in the modelling of natural phenomena. While the analysis will focus on examples arising from systems biology, the techniques used could be

applied to study any dynamical system with toric steady states (see Definition 4.1.2 and Section 2.1.1.1 in Chapter 2).

Due to the inherent complexity of the biological world it is often unknown which models best capture the biological mechanism. Therefore, many candidate models are often constructed to focus on a particular aspect of a biological system. When a set of candidate reaction mechanisms (i.e. a set of models) has been developed, the optimal values of the parameters need to be identified. Hence, two important questions arising in modelling of biological systems are:

1. *Model Selection:* Which mathematical model most accurately describes the biological system?

2. *Model Testing:* To what extent is the chosen model capable of explaining the observed data?

This chapter focuses on the latter question of model testing by giving an upper bound on the complexity of finding the optimal parameter values. The results are complimentary to the model selection approach presented in Gross et al. [2016a] and independent of the actual model parameters. In Gross et al. [2016a] numerical algebraic geometry based algorithms for selecting the best fitting model were developed. The aim of this chapter is to quantify the computational complexity of the model selection task *without* solving the underlying equations. This "model complexity", although inherent in all approaches which solve the underlying equations, has not been studied in the literature. Numerical algebraic geometry tools, however, are used to show the validity of the claims.

The main quantities needed for a practical answer to the model testing question are the steady state concentrations of a chemical reaction network which extremise the squared Euclidean distance to a given data point. Constrained Euclidean distance (ED) optimisation problems of various types occur commonly in many applications. When the constraints are given by polynomial equations, these problems may be solved using methods from algebraic geometry and techniques for this have been developed by several authors [Draisma et al., 2016; Ottaviani et al., 2014]. In applications, the algebraic geometric ED problems have been studied in the contexts of low rank tensor and low rank matrix approximation, see for example [Ottaviani et al., 2014; Stegeman and Friedland, 2017]. In systems biology, as discussed above, the ED problem has been used to study the model selection problem in Gross et al. [2016a]. Other areas where the algebraic geometric ED problem arises include phylogenetics [Casanellas et al., 2017], computer vision [Trager et al., 2015; Fløystad et al.,

2018], signal processing [Condat and Hirabayashi, 2014], and sensor data analysis [Compagnoni et al., 2015, 2014]. In the setting of this chapter, the ED optimisation problem considered is to find the points on the steady state locus of chemical reaction networks which are closest to a given data point. The difficulty of solving this problem can be measured by an invariant called the Euclidean Distance degree [Draisma et al., 2016].

The focus of this chapter will be on computing exact formulas for the ED degree of the steady states of several chemical reaction networks with toric steady states. These formulas will be independent of the choice of rate constants $\boldsymbol{\kappa}$ and will be entirely determined by the graph of the chemical reaction network. The formulas will be found *without* solving the associated polynomial system of critical equations. Below, in Table 4.1, the ED degrees for the chemical reaction models considered in this chapter are tabulated. The ED degrees provide the (relative) computational cost of solving the model testing and model selection problems for the different reaction networks. In particular, it can be seen that three of the models, Processive Phosphorylation [Conradi and Shiu, 2015] (Section 4.2.1.1), the Sequestration network [Conradi and Shiu, 2018] (Section 4.2.2) and the McKeithan model [Mckeithan, 1995] (Section 4.2.3) have a small and constant ED degree relative to the number of reactions; meaning the testing and selection problems for these models can be solved in a practical time for an arbitrary number of reactions. On the other hand, Distributive Phosphorylation [Conradi and Shiu, 2015] (Section 4.2.1.2) and Pore Forming models [Lee et al., 2016] (Section 4.2.4) have an ED degree which grows linearly with the number of reactions; this will in practice yield an approximately exponential growth in the run time for the computation of the solutions of the testing and selection problems for these models.

Processive (§4.2.1.1)	Distributive (§4.2.1.2)	Sequestration (§4.2.2)	McKeithan (§4.2.3)	Pore (§4.2.4)
28	$23N + 5$	1	6	$3N - 2$

Table 4.1: The ED degree for several chemical reaction models with varying number of reactions, given by N.

The chapter is organised as follows. In Section 4.1 relevant mathematical notions that will be used to study the ED degree are reviewed. In Section 4.2 the ED degree of the models listed in Table 4.1 is computed for an arbitrary number of reactions. In Section 4.3 a biological interpretation of the results computed in Section 4.2 is outlined. A summary of the work is given in Section 4.4.

4.1 Methods

In this section the algebraic techniques that will be used to investigate the complexity of the models discussed in Section 4.2 are outlined and several small results used in their analysis are given. The required mathematical tools are given in Section 4.1.1 and Section 4.1.2 and they build on the methods introduced in Section 2.1.1. In Section 4.1.3 it is shown that for the models considered here it is guaranteed that at least one biologically relevant (i.e. positive and real) local minimum can be found. A brief overview of the computational tools available for solving the ED problem is also given in Section 4.1.4.

For studying the ED problem, chemical reaction networks, denoted by $\mathfrak{N}$, with mass action kinetics are chosen and, as in Chapter 2, the system of ODEs governing their evolution is given by

$$\dot{\boldsymbol{x}} = \boldsymbol{f}(\boldsymbol{x}, \boldsymbol{\kappa}), \tag{4.1}$$

where $\boldsymbol{f}(\boldsymbol{x}, \boldsymbol{\kappa})$ is a system of polynomial equations in $\boldsymbol{x} = (x_1, \ldots, x_n)$ with the $\boldsymbol{\kappa} = (\kappa_1, \ldots, \kappa_m)$ being fixed, but arbitrary, positive reaction constants. When measuring the concentrations, $\boldsymbol{x}$, experimentally, often it is only possible to measure the steady state concentrations of species but not the rate constants. Therefore, only the steady states of (4.1) are considered in this chapter. As already discussed in Chapter 2 the steady state ideal $I = \langle f_1(\boldsymbol{x}, \boldsymbol{\kappa}), \cdots, f_n(\boldsymbol{x}, \boldsymbol{\kappa}) \rangle$ gives rise to the *steady state variety*, which is the algebraic variety

$$V_{\mathfrak{N}} = V(I) \subset \mathbb{C}^n. \tag{4.2}$$

With a fixed list of rate constants $\boldsymbol{\kappa} = (\kappa_1, \ldots, \kappa_m)$ in (4.2), a main goal of chemical reaction network theory is to analyse steady state behaviour of (4.1) and of central importance are steady states in which every single chemical species has positive concentration. Hence, points in $V_{\mathfrak{N}}$ which are also in $(\mathbb{R}_{>0})^n = \{(x_1, \ldots, x_n) \in \mathbb{R}^n \mid x_i > 0 \ \forall i\}$ are studied. To this end the *non-zero closure* of $V_{\mathfrak{N}}$ is defined to be the variety $V_{\mathfrak{N}}^{\neq 0} = \overline{V_{\mathfrak{N}} \cap (\mathbb{C}^*)^n}$, where the Zariski closure is taken in $\mathbb{C}^n$. For a given variety $V_{\mathfrak{N}}$ in $\mathbb{C}^n$ taking the non-zero closure, $V_{\mathfrak{N}}^{\neq 0}$, of $V_{\mathfrak{N}}$ has the effect of removing any irreducible component W of $V_{\mathfrak{N}}$ such that every point in W has at least one zero coordinate, i.e. the steady state ideal is saturated with respect to $\langle x_1 \cdots x_n \rangle$.

The study of the two problems of model testing and model selection can now be framed in relation to the steady state variety [Gross et al., 2016b]. For the model testing problem a chemical reaction network $\mathfrak{N}$ with steady state variety $V_{\mathfrak{N}}$ is taken together with some observed steady state data $\boldsymbol{u} \in \mathbb{R}^n$. Often it is necessary to test

whether there exists a point $\boldsymbol{x} \in V_{\mathfrak{N}}$ which is within some distance ϵ of the observed data. If such a point exists, then the model describes the observed data, i.e. it is necessary to test if there exists a $\boldsymbol{x} \in V_{\mathfrak{N}}$ such that $\|\boldsymbol{x} - \boldsymbol{u}\| < \epsilon$, where $\epsilon > 0$.

A related problem is the one of model selection [Gross et al., 2016b]; given some observed data point u and a collection of candidate models $\mathfrak{N}^{(\ell)}$, where (ℓ) denotes the ℓ^{th} model, it is important to know which model most closely approximates the data, i.e. for which model is the minimum value of $\left\|\boldsymbol{x}^{(\ell)} - u\right\|$ minimised for some point $\boldsymbol{x}^{(\ell)} \in V_{\mathfrak{N}^{(\ell)}}$? To solve both these problems the set of points $\boldsymbol{x} \in V_{\mathfrak{N}}$ which minimise the expression $\|\boldsymbol{x} - \boldsymbol{u}\|$ for some data $\boldsymbol{u} \in \mathbb{R}^n$ must be computed. Such an optimisation problem is referred to as an Euclidean distance (ED) problem [Draisma et al., 2016]. The main goal of this chapter is to apply the concept of the ED problem [Draisma et al., 2016; Helmer and Sturmfels, 2016] to chemical reaction networks.

Formally, the points $\boldsymbol{x} \in V_{\mathfrak{N}} \subset \mathbb{R}^n$ which minimise the (weighted) Euclidean distance between the observed data $\boldsymbol{u}$ and the model values $\boldsymbol{x}$ are sought, given a data point $\boldsymbol{u} = (u_1, \ldots, u_n) \in \mathbb{R}^n$ with weights $\boldsymbol{\lambda} = (\lambda_1, \ldots, \lambda_n)$. More precisely, for $\lambda_i \in \mathbb{R}_{>0}$, the following constrained optimisation problem is considered

$$\text{Minimise} \quad d^2 = \sum_{i=1}^{n} \lambda_i (u_i - x_i)^2 \text{ subject to } \boldsymbol{x} \in V_{\mathfrak{N}}. \tag{4.3}$$

In practice it is often necessary to find all local solutions to (4.3) to find the global minimum of the ED problem. Hence, the difficulty of solving the optimization problem (4.3) for generic $\boldsymbol{u}$ and generic $\boldsymbol{\lambda}$ is governed by the number of complex optima of the optimization problem, called (complex) critical points, which are the solutions of the critical equations. The critical equations for a radical ideal $I = \langle g_1, \ldots, g_s \rangle$ are the elements of the critical ideal, which is generated by Draisma et al. [2016]

$$I_{\text{crit}} = \left(I + \left\langle (c+1) \times (c+1) \text{ - minors of } \begin{pmatrix} (\boldsymbol{\lambda} \star (\boldsymbol{u} - \boldsymbol{x}))^T \\ J(\boldsymbol{g}) \end{pmatrix} \right\rangle \right) : I_{\text{sing}}^{\infty}, \tag{4.4}$$

where $J(\boldsymbol{g})$ is the Jacobian matrix, $\star$ denotes the component-wise (Hadamard) product, c is the codimension of $V(I)$, and I_{sing} is the ideal of the singular locus of $V(I)$ defined by

$$I_{\text{sing}} = I + \langle c \times c \text{ - minors of } J(\boldsymbol{g}) \rangle \,. \tag{4.5}$$

Fixing a choice of rate constants, $\boldsymbol{\kappa}$ and specifying a steady state variety $V_{\mathfrak{N}}$ (as in (4.2)), the *(generic) Euclidean distance degree* of $V_{\mathfrak{N}}$, written as EDdegree($V_{\mathfrak{N}}$), is defined as the number of complex critical points of (4.3). This number will be the same for any generic choice of $\boldsymbol{\lambda}$ and $\boldsymbol{u}$. For special choices of $\boldsymbol{\lambda}$ there may be

fewer critical points associated to (4.3), such cases are denoted by $\text{EDdegree}_{\boldsymbol{\lambda}}(V_{\mathfrak{N}})$; similarly for special choices of $\boldsymbol{u}$. For any choice of $\boldsymbol{\lambda}, \boldsymbol{u}$ (even non-generic choices), the $\text{EDdegree}(V_{\mathfrak{N}})$ will be an upper bound on the number of critical points of (4.3) (see Draisma et al. [2016]), that is

$$\text{EDdegree}_{\boldsymbol{\lambda},\boldsymbol{u}}(V_{\mathfrak{N}}) \leq \text{EDdegree}(V_{\mathfrak{N}}).$$

As above let $V_{\mathfrak{N}}^{\neq 0}$ denote the non-zero closure of the steady state variety $V_{\mathfrak{N}}$ (i.e. $V_{\mathfrak{N}}^{\neq 0}$ is the result of removing irreducible components of $V_{\mathfrak{N}}$ with zero coordinates) associated to a chemical reaction network $\mathfrak{N}$. In what follows the (generic) Euclidean distance degree of $V_{\mathfrak{N}}^{\neq 0}$ will be studied. This number will provide a (reasonably sharp) estimate for the computational complexity of solving the model testing problem associated to (4.3). In particular the ED degree measures the difficulty of finding and representing *all* solutions (and hence all real solutions) to the ED problem (4.3). Additionally knowledge of the number of expected solutions to the ED problem (4.3) (i.e. knowing the ED degree) could be used to aid the design of specialized symbolic or numeric methods to solve these problems rapidly.

Remark 4.1.1 (A note on generic values)**.** *As mentioned above, the number of critical points will be constant for "most" (generic) choices of $\boldsymbol{u}$ and $\boldsymbol{\lambda}$. Results of Helmer and Sturmfels [2016] and Draisma et al. [2016] give conditions when the data point, $\boldsymbol{u}$, and the weights, $\boldsymbol{\lambda}$, are not generic. This is the case, when either the data point or the weights lie on an algebraic variety (further details can be found in Helmer and Sturmfels [2016]). Most importantly, the algebraic conditions of when data and weights are not generic induce a Zariski topology on $\mathbb{C}^n$ and, therefore, this shows that there exist dense, Zariski open sets, for which $\boldsymbol{u}$ and $\boldsymbol{\lambda}$ are generic.*

4.1.1 Steady State Varieties in Projective Space

For chemical reaction networks the steady state variety, and hence the associated variety defined by the critical equations of (4.3), are objects in an affine space such as $\mathbb{R}^n$ or $\mathbb{C}^n$. To effectively derive the exact formulas for the ED degree presented below the ambient space needs to be changed slightly. To intuitively understand the need for this consider, for example, the intersection of a parabola and a line in the real affine space $\mathbb{R}^2$. In an affine space such an intersection may be empty, i.e. the parabola could be above or below the line. The possibility of two such curves failing to intersect in an affine ambient space such as $\mathbb{C}^n$ makes it impractical to compute exact expressions for the number of points in the intersection of curves and surfaces in

these spaces without resorting to direct computational methods (such as computing a Gröbner basis of the ideal of critical points). To avoid this problem and to allow for the derivation of exact expressions for the ED degree without using the equations for the variety of critical points an ambient projective space, $\mathbb{P}^n$, is often found useful to work in. In a projective space it is certain that, for example, a parabola and a line will have a non-empty intersection. A dimension n complex projective space $\mathbb{P}^n$ can be thought of as the closure of the affine space $\mathbb{C}^n$ obtained by adding 'points at infinity', the effect of this being that if the projective closure of two affine curves that do not intersect in affine space is taken, they will have intersections in projective space at the added points at infinity, for more details on affine and projective spaces see Mumford [1995]. As a consequence of the discussion above the exact expressions obtained for the ED degrees of the projective closures of the steady state varieties will be upper bounds on the the number of solutions of the associated affine ED problem.

In what follows it is often desirable to work with the projective closure of the affine steady state variety $V_{\mathfrak{N}}$. Let $\mathbb{K}$ be a field (such as $\mathbb{C}$ or $\mathbb{R}$) and suppose X is an affine variety in $\mathbb{K}^n$, let $\overline{X} \subset \mathbb{P}^n$ denote the projective closure of X. Recall that projective varieties are defined by homogeneous polynomial equations. To obtain the projective closure of an affine variety, every polynomial in its defining ideal needs to be homogenised. In Cox et al. [2013] it is outlined, that this can be achieved if the equations of a Gröbner basis for the defining ideal are *homogenised*. More explicitly, consider an affine variety $X = V(f_1, \ldots, f_r) \subset \mathbb{K}^n$ and suppose the polynomials $f_1, \ldots, f_r$ form a Gröbner basis for an ideal $I = (f_1, \ldots, f_r)$ in $\mathbb{K}[x_1, \ldots, x_n]$. The ideal I is homogenised by homogenising all of the f_i with respect to x_0 to obtain polynomials f_i^h in $\mathbb{K}[x_0, \ldots, x_n]$. The projective closure $\overline{X} \subset \mathbb{P}^n$ is then defined by the ideal $I^h = (f_1^h, \ldots, f_r^h) \subset \mathbb{K}[x_0, \ldots, x_n]$, i.e. $\overline{X} = V(f_1^h, \ldots, f_r^h) \subset \mathbb{P}^n$.

Let $W_X \subset \mathbb{C}^{n+1}$ denote the affine cone over $\overline{X}$. Recall that a projective variety and its affine cone are defined by the same homogeneous ideal. In Draisma et al. [2016] it is shown that

$$\text{EDdegree}(\overline{X}) = \text{EDdegree}(W_X).$$

All solutions to the optimisation problem (4.3) for an affine variety X will have a corresponding solution in the affine cone over X, W_X, hence the relation holds that

$$\text{EDdegree}(X) \leq \text{EDdegree}(W_X) = \text{EDdegree}(\overline{X}).$$

4.1.2 Toric Models and Euclidean Distance Degree

In this subsection projective toric varieties are briefly defined and a combinatorial method to compute the Euclidean distance degree of a toric model is summarised. A more detailed discussion of this topic can be found in Helmer and Sturmfels [2016].

A toric model is an algebraic variety defined as follows. First, fix an integer $d \times n$-matrix $\bar{A}$, with columns $\boldsymbol{a}_1, \boldsymbol{a}_2, \ldots, \boldsymbol{a}_n$, and rank d such that the vector $(1, 1, \ldots, 1)$ lies in the row space of $\bar{A}$ over $\mathbb{Q}$. In particular, $\bar{A}$ is allowed to have negative entries. Each column vector $\boldsymbol{a}_i$ defines a (Laurent) monomial $\boldsymbol{t}^{\boldsymbol{a}_i} = t_1^{a_{1i}} t_2^{a_{2i}} \cdots t_d^{a_{di}}$ where $\boldsymbol{t} \in (\mathbb{C}^*)^d$, and $\mathbb{C}^* = \mathbb{C} \backslash \{0\}$ denotes the non-zero complex numbers ($\mathbb{C}^*$ is often referred to as the complex torus). The *affine toric variety* defined by $\bar{A}$ is

$$\tilde{X}_{\bar{A}} = \overline{\{(\boldsymbol{t}^{\boldsymbol{a}_1}, \ldots, \boldsymbol{t}^{\boldsymbol{a}_n}) : \boldsymbol{t} \in (\mathbb{C}^*)^d\}} \subset \mathbb{C}^n,$$

that is, $\tilde{X}_{\bar{A}}$ is the (Zariski) closure in $\mathbb{C}^n$ of the image of the monomial parameterisation specified by $\bar{A}$. The implicit equations for $\tilde{X}_{\bar{A}}$ will always be homogeneous binomials, that is $\tilde{X}_{\bar{A}} = V(I)$ where I is an ideal defined by homogeneous binomial equations. More precisely [Sturmfels, 1996, Corrollary 4.3] states that

$$I = \left(x^{\boldsymbol{b}^+} - x^{\boldsymbol{b}^-} \mid \boldsymbol{b} \in \ker(\bar{A}) \right), \tag{4.6}$$

where b_i^+ is equal to b_i if $b_i > 0$ and 0 otherwise, and where b_i^- is equal to $|b_i|$ if $b_i < 0$ and 0 otherwise. Conversely, any prime polynomial ideal $(f_1, \ldots, f_m)$ in $\mathbb{K}[x_0, \ldots, x_{n-1}]$, where each f_i is a homogeneous binomial, will define an affine toric variety $\tilde{X}_{\bar{A}}$ in $\mathbb{C}^n$. Note that (4.6) defines a simple way to transition between the parametric and implicit descriptions of a toric variety (and vice versa), namely by computing a basis for the kernel of $\bar{A}$ to obtain a list of vectors defining the implicit equations. Conversely, a suitable matrix $\bar{A}$ can be computed from a prime binomial ideal, since the exponents of the binomials, interpreted as in (4.6), will define $\ker(\bar{A})$, from which $\bar{A}$ may be computed. Note that this procedure may generate an isomorphic variety rather than equal variety, i.e. the embedding may have changed, however, the ED degree, the degree of the variety, etc. are invariant under isomorphism and do not depend on the embedding.

The affine toric variety $\tilde{X}_{\bar{A}}$ is the affine cone [Cox et al., 2006] over the *projective toric variety* $X_{\bar{A}} \subset \mathbb{P}^{n-1}$, that is $X_{\bar{A}}$ is the (Zariski) closure in $\mathbb{P}^{n-1}$ of the same parameterisation. The projective toric variety $X_{\bar{A}}$ is defined implicitly to be the zeros of the same set of homogeneous binomials that define $\tilde{X}_{\bar{A}}$, that is $X_{\bar{A}} = V(f_1, \ldots, f_m)$ in $\mathbb{P}^{n-1}$. It can be seen that that $\dim(X_{\bar{A}}) = d-1$ and $\dim(\tilde{X}_{\bar{A}}) = d$. To the projective

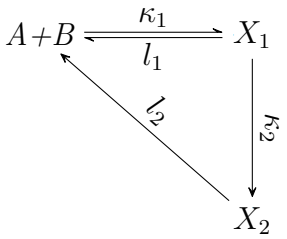
toric variety $X_{\bar{A}}$ a polytope $P = \mathrm{Conv}(\bar{A})$ is associated, which is the convex hull of the lattice points specified by the columns of the matrix $\bar{A}$. The polytope P is contained in $\mathbb{R}^d$ and has dimension $\dim(P) = \dim(X_{\bar{A}}) = d - 1$; the degree of $X_{\bar{A}}$ may also be read from the polytope, namely $\deg(X_{\bar{A}}) = \mathrm{Vol}(P)$ where Vol denotes the normalised $d-1$ dimensional volume. Further background on affine and projective toric varieties can be found in Cox et al. [2011], Sturmfels [1996], Gelfand et al. [2008], and Fulton [1993].

Definition 4.1.2 (Dynamical System with Toric Steady States)**.** *Consider a dynamical system $\dot{\boldsymbol{x}} = \boldsymbol{f}(\boldsymbol{x})$ where $\boldsymbol{f}(\boldsymbol{x})$ is a system of polynomial equations in variables $x_1, \ldots, x_n$. If the non-zero closure $(V(\boldsymbol{f}))^{\neq 0}$ is a toric variety then the dynamical system $\dot{\boldsymbol{x}} = \boldsymbol{f}(\boldsymbol{x})$ is defined to be a dynamical system with toric steady states.*

Remark 4.1.3. *Networks which satisfy the Deficiency Zero Theorem (see Chapter 2, Section 2.1) are toric dynamical systems as studied in Craciun et al. [2009a] and are sometimes also called complex balanced systems. The steady state varieties of these dynamical systems are toric [Craciun et al., 2009a, Theorem 7], hence these dynamical systems are dynamical systems with toric steady states in the sense of Definition 4.1.2. Since the toric dynamical systems of Craciun et al. [2009a] are defined in terms of the reaction graph it is possible that a dynamical system with toric steady states (in the sense of Definition 4.1.2) is not a toric dynamical system (in the sense of Craciun et al. [2009a]). For example, one can check that the two-site distributive phosphorylation model (see Section 4.2.1.2 or Millán et al. [2012, Example 3.13]) is not complex balanced, meaning the associated ODE system is not a toric dynamical system in the sense of Craciun et al. [2009a]. On the other hand, the non-zero closure of the steady state variety is a toric variety, hence the associated ODE system is a dynamical system with toric steady states in the sense of Definition 4.1.2. In addition to satisfying the Deficiency Zero Theorem, another nice property of toric dynamical systems in the sense of Craciun et al. [2009a] is that they may be identified from properties of a Euclidean embedding of the reaction graph, see Yu and Craciun [2018, §2.1].*

Definition 4.1.2 is further illustrated by example of a kinetic proofreading network and the Michaelis Menten system introduced in Chapter 2.

Example 4.1.4 (Two-site kinetic proofreading)**.** *A simple model of kinetic proofreading in T-cells follows the reaction scheme [Mckeithan, 1995]:*



The dynamics of the network is governed by the ODE system

$$\frac{d}{dt}\begin{pmatrix} a \\ b \\ x_1 \\ x_2 \end{pmatrix} = \underbrace{\begin{pmatrix} -1 & 0 & 1 & 1 \\ -1 & 0 & 1 & 1 \\ 1 & -1 & -1 & 0 \\ 0 & 1 & 0 & -1 \end{pmatrix}}_{\Gamma} \underbrace{\begin{pmatrix} \kappa_1 ab \\ \kappa_2 x_1 \\ l_1 x_1 \\ l_2 x_2 \end{pmatrix}}_{\boldsymbol{\nu}(\boldsymbol{x})}.$$

It is easy to check the that the deficiency of this network is zero. The network is also clearly weakly reversible. Following the construction for the complex balancing ideal in Craciun et al. [2009a] it can be shown that the toric component of the steady state variety is generated by the implicit equations

$$0 = \kappa_1 ab - (l_1 + \kappa_2)x_1,$$
$$0 = \kappa_2 x_1 - l_2 x_2.$$

Hence, the steady state ideal is prime and binomial and, therefore, defines a toric variety.

Example 4.1.5 (Michaelis-Menten Kinetics)**.** *The standard [Michaelis and Menten, 1913] enzyme catalysis follows the reaction scheme*

$$E + S \rightleftharpoons ES \to E + P. \tag{4.7}$$

Hence, the governing ODE system can be formulated

$$\frac{dx}{dt} = \underbrace{\begin{pmatrix} -1 & 1 & 1 \\ -1 & 1 & 0 \\ 1 & -1 & -1 \\ 0 & 0 & 1 \end{pmatrix}}_{\Gamma} \underbrace{\begin{pmatrix} \kappa_1 x_1 x_2 \\ \kappa_2 x_3 \\ \kappa_3 x_3 \end{pmatrix}}_{\boldsymbol{\nu}(\boldsymbol{x})}. \tag{4.8}$$

It can be shown that the deficiency is zero, however, the system is not weakly reversible. Therefore, Michaelis-Menten kinetics does not have a steady state ideal with a toric irreducible component. In particular the steady state ideal is $I = \langle -\kappa_1 x_1 x_2 + \kappa_2 x_3 + \kappa_3 x_3,\ -\kappa_1 x_1 x_2 + \kappa_2 x_3,\ \kappa_1 x_1 x_2 - \kappa_2 x_3 - \kappa_3 x_3,\ \kappa_3 x_3 \rangle$*, the primary decomposition of this ideal contains no components whose radical is a prime binomial ideal; hence the steady state variety cannot be written as a union of toric varieties.*

Next, it is shown that when studying the generic ED degree of a chemical reaction network with toric steady states the result is independent of the rate constants. In all that follows only the ED problem as stated in (4.9) is considered.

Proposition 4.1.6. *Let $X_{\bar{A}}$ be the (toric part of the) steady state variety of a chemical reaction network with toric steady states. The ED degree of $X_{\bar{A}}$ is independent of the choice of reaction coefficients and is equal to the number of complex critical points of the unconstrained optimisation problem:*

$$\text{Minimise } \sum_{i=1}^{n} \lambda_i (u_i - t^{a_i})^2 \ \textit{over all} \ \ t = (t_1, \ldots, t_d) \in (\mathbb{C}^*)^d. \tag{4.9}$$

Proof. Consider the ED problem for a chemical reaction network $\mathfrak{N}$ with toric steady states and a positive steady state $\boldsymbol{x}^* = (x_1^*, \ldots, x_n^*) \in \mathbb{R}^n_{>0}$, which is a function of the rate constants κ. Then the steady state variety $(V_{\mathfrak{N}})_A$ can be parameterised by a $d \times n$ matrix A (with $(1, \ldots, 1)$ in its row space) as

$$(V_{\mathfrak{N}})_A = \overline{\{(x_1^* t^{a_1}, \ldots, x_n^* t^{a_n}) \,:\, t \in (\mathbb{C}^*)^d\}} \subset \mathbb{C}^n.$$

The unconstrained version of the corresponding Euclidean distance minimisation problem for $(V_{\mathfrak{N}})_A$ is:

$$\text{Minimise } \sum_{i=1}^{n} \lambda_i^* (u_i^* - x_i^* t^{a_i})^2 \ \text{ over all } \ \ t = (t_1, \ldots, t_d) \in (\mathbb{C}^*)^d, \tag{4.10}$$

for generic u^* and λ^* (more precisely, generic u^* and λ^* are chosen from Zariski dense sets D_{u^*} and D_{λ^*} further studied in Helmer and Sturmfels [2016]). Observe that for any choice of $\boldsymbol{x}^* = (x_1^*, \ldots, x_n^*) \in (\mathbb{C}^*)^n$ the sets

$$D_u = \left\{ (u_1, \ldots, u_n) \mid u_i = \frac{u_i^*}{x_i^*} \right\}, \quad D_\lambda = \{ (\lambda_1, \ldots, \lambda_n) \mid \lambda_i = x_i^* \lambda_i^* \},$$

are in one to one correspondence with the Zariski dense sets D_{u^*} and D_{λ^*} and, therefore, also Zariski dense. Hence, the ED problem may be stated as in (4.9) for generic $\lambda \in D_\lambda$ and $u \in D_u$. From this it follows that the generic ED degree does not depend on the positive steady state $(x_1^*, \ldots, x_n^*)$, nor on the rate constants $\boldsymbol{\kappa} = (\kappa_1, \ldots, \kappa_n)$, which determine $x_1^*, \ldots, x_n^*$. □

In Helmer and Sturmfels [2016] an exact formula for the ED degree for toric varieties was derived. Let $\bar{A}$ be an integer $d \times n$ matrix with $(1, \ldots, 1)$ in its row space,

parameterising the toric component of the steady state variety, as above. It is shown in Helmer and Sturmfels [2016] that for the associated projective toric variety $X_{\bar{A}} \subset \mathbb{P}^{n-1}$ the Euclidean distance degree of $X_{\bar{A}}$ can be computed combinatorially from the polytope $P = \text{Conv}(\bar{A})$. Specifically in Helmer and Sturmfels [2016, Theorem 1.1] it is shown that

$$\text{EDdegree}(X_{\bar{A}}) = \sum_{i=0}^{\dim(X_{\bar{A}})} (-1)^{d-i-1} \cdot \left(2^{d-1} - 1\right) \cdot V_i \,, \tag{4.11}$$

where V_i denotes the sum of all *Chern-Mather* volumes of all dimension i faces of the polytope P. When P is a smooth polytope (so that $X_{\bar{A}}$ is a smooth variety) V_i is simply the sum of all the normalised i dimensional volumes of all dimension i faces of P. In the singular case the normalised volumes are weighted by the *Euler obstruction* of a face, which is an integer that accounts for the singularities of $X_{\bar{A}}$ associated to a face β of the polytope P. The *Euler obstruction* of a face β of P is denoted $\text{Eu}(\beta)$ and is defined recursively:

1. $\text{Eu}(P) \;=\; 1$,
2. $\text{Eu}(\beta) \;=\; \sum_{\substack{\alpha \text{ s.t. } \beta \text{ is a} \\ \text{proper face of } \alpha}} (-1)^{\dim(\alpha)-\dim(\beta)-1} \cdot \mu(\alpha/\beta) \cdot \text{Eu}(\alpha).$

Here $\mu(\alpha/\beta)$ is the normalized relative subdiagram volume (see Helmer and Sturmfels [2016, Definition 2.1] or [Gelfand et al., 2008, Definition 3.8]). Using this the *Chern-Mather volume* of a face, β, is defined to be the product of the normalised volume $\text{Vol}(\beta)$ and the Euler obstruction $\text{Eu}(\beta)$. With this notation the Chern-Mather of all dimension i faces of P is:

$$V_i \;=\; \sum_{\substack{\beta \text{ face of } P \\ \dim(\beta)=i}} \text{Vol}(\beta)\text{Eu}(\beta), \tag{4.12}$$

see Helmer and Sturmfels [2016, §2] for more details. These definitions with an example are now illustrated with an example.

Example 4.1.7. *Consider the* 3×6 *integer matrix*

$$\bar{A} = \begin{pmatrix} 1 & 0 & 1 & 2 & 3 & 1 \\ 0 & 1 & 1 & 1 & 1 & 2 \\ 1 & 1 & 1 & 1 & 1 & 1 \end{pmatrix}.$$

The monomial parameterisation of the associated projective toric variety $X_{\bar{A}} \subset \mathbb{P}^{6-1}$ *is*

$$X_{\bar{A}} \;=\; \overline{\{(t_1t_3 : t_2t_3 : t_1t_2t_3 : t_1^2t_2t_3 : t_1^3t_2t_3 : t_1t_2^2t_3) \,|\, t \in (\mathbb{C}^*)^3\}} \subset \mathbb{P}^5.$$

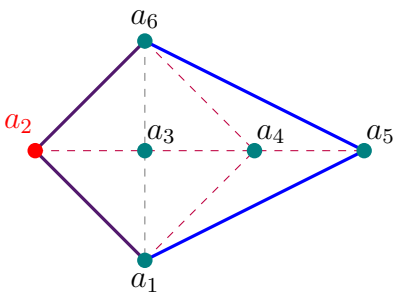


Figure 4.1: The polytope $P = \text{conv}(A)$. The columns of A define the lattice points drawn above, note that this polytope, P, may be drawn in two dimensions since the third coordinate of all vectors is one, i.e. they are all contained in the same plane in $\mathbb{R}^3$.

Written as the common vanishing set of implicit homogeneous binomial equations

$$X_{\bar{A}} = V(x_3^2 - x_2x_4, x_2x_3 - x_1x_4, x_1x_3 - x_0x_5, x_2^2 - x_0x_5).$$

From the matrix $\bar{A}$ *it can be seen that* $\dim(X_{\bar{A}}) = 3-1 = 2$. *The polytope* $P = \text{conv}(\bar{A})$ *associated to* $X_{\bar{A}}$ *is given in Figure 4.1. From the triangulation in Figure 4.1 it can be seen that* $\deg(X_{\bar{A}}) = \text{Vol}(P) = 6$. *The computation of* $\text{EDdegree}(X_{\bar{A}})$ *is now illustrated by computing the Chern-Mather volumes* V_0, V_1, V_2 *and applying* (4.11). *Note that since the only dimension two face is the whole polytope* P, *and since by definition* $\text{Eu}(P) = 1$, *it holds that* $V_2 = \text{Vol}(P) = \deg(X_{\bar{A}}) = 6$. *Now compute* V_1. *It can be verified that* $X_{\bar{A}}$ *has singularities only in dimension zero, hence all dimension one faces, i.e. all edges* $\mathbf{e}$ *of* P, *will have Euler obstruction* $\text{Eu}(\mathbf{e}) = 1$. *From this it can be computed that* V_1 *is equal to the number of edges of* P, *that is* $V_1 = 4 \cdot \text{Vol}(\mathbf{e}) = 4$; *it remains to compute* V_0.

Let $\mathbf{v}$ *be a vertex contained in an edge* $\mathbf{e}$ *of the polytope* P, *to find* $\text{Eu}(\mathbf{v})$ *the subdiagram volumes* $\mu(P/\mathbf{v})$ *and* $\mu(\mathbf{e}/\mathbf{v})$ *must be considered. The subdiagram volume* $\mu(\mathbf{e}/\mathbf{v})$ *is equal to the one dimensional volume of an edge (which is one) minus the one dimensional volume of an edge with the vertex* $\boldsymbol{v}$ *removed (which is zero), hence it always holds that* $\mu(\mathbf{e}/\mathbf{v}) = 1 - 0 = 1$. *Consider the vertex* a_2 *of* P, *the subdiagram volume* $\mu(P/a_2)$ *is equal to the two dimensional volume of* P *minus the two dimensional volume of the convex hull of the points* a_1, a_3, a_4, a_5, a_6 *(that is the remaining points after* a_2 *is removed). Hence* $\mu(P/a_2) = \mathbf{6} - \mathbf{4} = 2$, *this gives*

$$\text{Eu}(a_2) = 2 \cdot \text{Eu}(\mathbf{e}) \cdot \mu(\mathbf{e}/a_2) - \text{Eu}(P) \cdot \mu(P/a_2) = 2 \cdot \mathbf{1} - 1 \cdot 2 = 0.$$

Similarly $\text{Eu}(a_5) = 0$, *and* $\text{Eu}(a_1) = \text{Eu}(a_6) = -1$, *giving*

$$V_0 = 0 \cdot \text{Vol}(a_2) + 0 \cdot \text{Vol}(a_5) - \text{Vol}(a_1) - \text{Vol}(a_6) = -2.$$

Plugging these values into (4.11) *the ED degree is obtained,*

$$\text{EDdegree}(X_{\bar{A}}) \;=\; 7V_2 - 3V_1 + V_0 \;=\; 7\cdot 6 - 3\cdot 4 + (-2) \;=\; 28.$$

4.1.3 Real Closest Points

In the applications considered here, real solutions of the optimisation problem (4.3) are particularly important. In Friedland and Stawiska [2013, 2014] it is shown that a finite, and non-zero, number of real solutions to (4.3) always exist. The relevant results are briefly summarised below.

For this discussion let $V = V(f_1, \ldots, f_m) \subset \mathbb{R}^n$ be a real variety, and, without loss of generality, is is assumed that V is irreducible. For a general point $\boldsymbol{u} \in \mathbb{R}^n$ and a general point $\boldsymbol{\lambda} \in \mathbb{R}^n_{>0}$ the optimisation problem

$$\text{Minimise} \quad \sum_{i=1}^{n} \lambda_i (u_i - x_i)^2 \;\; \text{subject to } \boldsymbol{x} \in V, \tag{4.13}$$

is studied.

The (positive weighted) square of the Euclidean norm is convex and differentiable. It follows by Theorem 2.2 of Friedland and Stawiska [2014] that for general $\boldsymbol{u} \in \mathbb{R}^n$ and general (positive) $\boldsymbol{\lambda} \in \mathbb{R}^n_{>0}$ there exists a unique real global minimum $\boldsymbol{x}^*$ for the problem (4.13). Further, since $\boldsymbol{x}^*$ is a minimum it must be a solution to the critical equations (4.4). Let the critical points variety be the variety in $\mathbb{C}^n$ defined by (4.4). All critical points in $\mathbb{R}^n$ must appear in the critical points variety. In particular, the critical points variety in $\mathbb{C}^n$ will contain the real global minimum $\boldsymbol{x}^*$. It may also be shown (see Lemma 4.3 of Friedland and Stawiska [2013]) that all real minima are smooth critical points. Computing any global algorithmic solution to (4.13) in practice will require the computation of all complex critical points.

For the case where $V = \tilde{X}_{\bar{A}}$ is the affine cone over a projective toric variety $X_{\bar{A}}$ a slightly stronger statement regarding the existence of a *positive* real local minimum can be made.

Proposition 4.1.8. *Let $V = \tilde{X}_A$ be the affine cone over a projective toric variety X_A. Let $\mathbb{R}_+$ denote the positive reals and suppose that $V \cap (\mathbb{R}_+)^n$ is non-empty, then there exists a at least one real local minimum $x^* = (x_1^*, \ldots, x_n^*) \in \mathbb{R}^n$ for* (4.13) *such that $x_i^* \geq 0$, $\forall i$.*

Proof. Fix a general real data point $u \in \mathbb{R}^n$. The (positive weighted) squared Euclidean distance

$$f(x_1, \ldots, x_n) = \sum_{i=1}^{n} \lambda_i (x_i - u_i)^2, \quad \lambda_i \in \mathbb{R}_{>0}$$

is strictly convex in $\mathbb{R}^n$. By Fulton [1993, §4.2] (see also [Cox et al., 2011, §12.2]) there exists a map $\mu : X_A \to \mathbb{R}^d$ (called the algebraic *moment map*) which is a homeomorphism from the nonnegative part of X_A, $(X_A)_{\geq 0}$, onto the polytope $P = \text{conv}(A)$. Further it is shown in Fulton [1993, §4.2] that the map μ induces a real analytic isomorphism between all points of $X_A \cap (\mathbb{R}^*)^d$ and the relative interior of P, $\text{int}(P)$. Similarly, the isomorphism induced by μ also gives an isomorphism between the torus orbit of a face and the relative interior of the face for any face of P. Since the set of real points in the polytope P is a closed compact set it follows that $(X_A)_{\geq 0}$ is also a closed compact set with interior $(X_A)_{>0}$. Let $\tilde{f} = f|_{(X_A)_{\geq 0}}$. The domain of $\tilde{f}$ is a closed compact set, therefore there exists at least one point $x^* \in (X_A)_{\geq 0}$ that minimizes $\tilde{f}$. Since x^* is a minimum of $\tilde{f}$ on $(X_A)_{\geq 0}$, and f is defined by the same polynomial, then x^* is both a critical point and a local minimum of f. □

4.1.4 Computational Methods

In this subsection several standard methods for solving systems of polynomial equations are briefly reviewed. It should be emphasised that when studying the ED problem the complexity of the computational methods used corresponds primarily to the ED degree of the variety X and not to $\deg(X)$. This is because when the optimisation problem (4.3) is solved, the zero dimensional variety consisting of the smooth points in X which satisfy the critical equations of (4.3) is considered. While these points form a subvariety of X, the degree of this subvariety may be substantially different from that of X, and all computational methods will compute the solutions to (4.3) by finding the points in this subvariety of X defined by the critical equations.

Gröbner bases: Gröbner basis methods have been shown to be very useful in the context of systems biology [Gross et al., 2016b; Joshi and Shiu, 2015], especially due to the fact that they allow the user to find exact, symbolic expressions for the varieties concerned. Where possible, the Gröbner basis of the models is computed in lexicographical (lex) monomial order to generate a triangular system. Then, all real solutions of the system can be found by iteratively applying a numerical or symbolic solver. While highly useful, Gröbner basis methods can be computationally expensive, particularly when computing a Gröbner basis in the lex term ordering (to obtain a triangular system). More explicitly, effective methods to compute all points in a zero dimensional variety W in a dimension n ambient space using Gröbner basis often have two steps. First the Gröbner basis in some other term order (which is faster to compute in) is found using some efficient Gröbner basis algorithm. Second the

FGLM algorithm (or another reordering scheme) [Faugere et al., 1993] is applied to transform this into a lex Gröbner basis. In practice, the second step, namely the reordering step, is often the bottle neck. In the zero dimensional case the FGLM algorithm has complexity $\mathcal{O}(n \deg(W)^3)$ [Faugere et al., 1993], and in particular its complexity is primarily determined by the degree of W. In the case of the Euclidean distance problem, $\deg(W)$ is the degree of the variety defined by the critical equations of (4.3), i.e. the ED degree.

Numerical Algebraic Geometry (NAG): NAG methods have recently been used for model selection and optimisation problems [Gross et al., 2016a]. In this chapter two commonly applied NAG packages, PHCpack [Verschelde, 1999] and Bertini [Bates et al., 2006], are used to solve the ED problem for the chemical reaction networks studied. The advantage of parameter homotopy or NAG methods is that they can be much faster than current Gröbner basis algorithms in some cases. However, realising this benefit sometimes requires specially programmed methods tailored to a given system. This can be aided by knowing, a priori, more details about the system to be solved, for example its degree. When knowing the ED degree ahead of time, this could be used in the construction of specialised NAG methods since this would represent the number of solution paths that would need to be tracked to solve the problem; hence this knowledge could improve both the performance and reliability of NAG methods in specific cases of interest. Implementations of NAG methods also provide black box solvers, however these may not be well suited for the particular problem at hand. In this chapter PHCpack is used to compute the solutions to the ED problem for several examples. Test computations using Bertini [Bates et al., 2006] were also carried out, however, Bertini did not perform well on the toric varieties studied in this chapter and solutions could not be found for any but the smallest ED degrees due to computational timeout. Practical experience shows that PHCpack is often quite effective when applied to highly structured systems, such as those arising from toric varieties. However, as with all numeric methods, numerical stability and precision can pose challenges, making it hard to be certain all solutions have been computed, especially for larger ED degrees (see Section 4.2.1.2 for details).

4.2 Results

In this section novel closed form formulas for the Euclidean distance degree of five commonly studied chemical reaction networks are computed. To highlight the use-

fulness of the ED degree as a new model metric, for each model the computational time of the ED problem is also computed.

4.2.1 Multi-site Phosphorylation Networks

Phosphorylation is a ubiquitous mechanism in cell biology [Salazar and Höfer, 2009] and the most widely studied protein modification [Cohen, 2001]. Phosphorylation controls the production of new proteins as well as their degradation and the transmission of intra- and intercellular signals. Abnormal phosphorylation is connected with a vast number of diseases such as cancer, diabetes, hypertension, heart attacks and rheumatoid arthritis [Cohen, 2001]. In particular, abnormal myotonin phosphorylation leads to myotonic muscular dystrophy [Roberts et al., 1997] and similarly, disturbed phosphorylation of the insulin receptor is a cause of diabetes [Gual et al., 2005].

A simple phosphorylation network consists of a substrate (a protein), kinases which phosphorylate the substrate and phosphatases to dephosphorylate. Phosphorylation can be thought of as an on/off switch for cellular mechanisms in which the presence of multiple sites enables fine tuning [Salazar and Höfer, 2009]. For an N site protein there exists, in principle, a maximum of 2^N states, which indicates a large redundancy in biological function.

While a protein with multiple sites can be phosphorylated in an arbitrary manner, there are two extreme mechanisms in multi-site phosphorylation. On the one hand, there is processive phosphorylation, where the kinase binds to the substrate and phosphorylates all sites before unbinding, and on the other hand we have distributive phosphorylation in which a binding-unbinding event is required for each phosphorylation. Experiments have highlighted the existence of kinases falling in each category, but also a whole spectrum of intermediate 'processivity' [Rubinstein et al., 2016].

4.2.1.1 Processive Networks

Whilst purely processive systems are rarely found, there exist a number of cellular processes which exhibit a high degree of processivity [Salazar and Höfer, 2009; Velazquez-Dones et al., 2005; Aoki et al., 2011] such as the phosphorylation of the splicing factor ASF/SF2 which has a role in heart development, cell motility and tissue formation [Aubol et al., 2003; Ma et al., 2008; Burack and Sturgill, 1997].

The processive multi-site phosphorylation network as studied in Conradi and Shiu [2015] is considered, which, for N sites, is described by the reaction scheme

$$S_0 + E \underset{\kappa_2}{\overset{\kappa_1}{\rightleftharpoons}} S_0E \underset{\kappa_4}{\overset{\kappa_3}{\rightleftharpoons}} S_1E \underset{\kappa_6}{\overset{\kappa_5}{\rightleftharpoons}} \cdots \underset{\kappa_{2N}}{\overset{\kappa_{2N-1}}{\rightleftharpoons}} S_{N-1}E \xrightarrow{\kappa_{2N+1}} S_N + E,$$

$$S_N + F \underset{l_{2N}}{\overset{l_{2N+1}}{\rightleftharpoons}} S_NF \underset{l_{2N-2}}{\overset{l_{2N-1}}{\rightleftharpoons}} \cdots \underset{l_4}{\overset{l_5}{\rightleftharpoons}} S_2F \underset{l_2}{\overset{l_3}{\rightleftharpoons}} S_1F \xrightarrow{l_1} S_0 + F.$$

To translate this reaction network into a system of ordinary differential equations variables representing the concentrations of the chemical species are assigned in the following way:

x_1	x_2	x_3	x_4	x_5	x_6	x_7	x_8	$\cdots$	x_{2N+3}	x_{2N+4}
E	F	S_0	S_N	S_0E	S_1F	S_1E	S_2F	$\cdots$	$S_{N-1}E$	S_NF

The assignment identifies the variable x_i with $\boldsymbol{e}_i$, the i^{th} basis vector of $\mathbb{R}^{2N+4}$. The system can now be formulated as a system of ordinary differential equations via defining the stoichiometric matrix Γ for the processive network,

$$\begin{aligned}\Gamma = (&\boldsymbol{e}_5 - (\boldsymbol{e}_1 + \boldsymbol{e}_3), \cdots, \boldsymbol{e}_{2i+5} - \boldsymbol{e}_{2i+3}, \cdots, \boldsymbol{e}_4 + \boldsymbol{e}_1 - \boldsymbol{e}_{2N+3}, \\ &\boldsymbol{e}_2 + \boldsymbol{e}_3 - \boldsymbol{e}_6, \cdots, \boldsymbol{e}_{2i+4} - \boldsymbol{e}_{2i+6}, \cdots, \boldsymbol{e}_{2N+4} - (\boldsymbol{e}_2 + \boldsymbol{e}_4)),\end{aligned} \tag{4.14}$$

where $i = 1, \cdots, N-1$. Similarly the flux vector $\boldsymbol{\nu}(\boldsymbol{x})$ can be formulated

$$\boldsymbol{\nu}(\boldsymbol{x}) = \begin{pmatrix} \kappa_1 x_1 x_3 - \kappa_2 x_5 \\ \kappa_3 x_5 - \kappa_4 x_7 \\ \kappa_5 x_7 - \kappa_6 x_9 \\ \vdots \\ \kappa_{2N-1} x_{2N+1} - \kappa_{2N} x_{2N+3} \\ \kappa_{2N+1} x_{2N+3} \\ l_1 x_6 \\ l_3 x_8 - l_2 x_6 \\ \vdots \\ l_{2N-3} x_{2N+2} - l_{2N-4} x_{2N} \\ l_{2N-1} x_{2N+4} - l_{2N-2} x_{2N+2} \\ l_{2N+1} x_2 x_4 - l_{2N} x_{2N+4} \end{pmatrix}. \tag{4.15}$$

In (2.3) it was shown that the generators of the steady state ideal of the processive model are given by $\Gamma\boldsymbol{\nu}(\boldsymbol{x})$. By considering the family of affine varieties generated by the steady state ideal of the processive model the ED degree of the non-zero closure can be found.

Theorem 4.2.1. *Let $V_{\mathfrak{N}}$ denote the steady state variety of the N-site processive phosphorylation network. Then, the ED degree is given by*

$$\text{EDdegree}\left(\overline{V_{\mathfrak{N}}^{\neq 0}}\right) = 28.$$

Proof. In Conradi and Shiu [2015, (5.11)] it is shown that $V_{\mathfrak{N}}^{\neq 0} = \lambda \cdot \tilde{X}_A$ where $\lambda \in (\mathbb{C}^*)^{2N+2}$ and where $\tilde{X}_A$ is the affine toric variety defined by the $3 \times (2N+2)$ integer matrix

$$A = \begin{pmatrix} 0 & 1 & 0 & -1 & 0 & 0 & \cdots & 0 \\ -1 & 0 & 1 & 0 & 0 & 0 & \cdots & 0 \\ 1 & 0 & 0 & 1 & 1 & 1 & \cdots & 1 \end{pmatrix}.$$

Taking the projective closure of $V_{\mathfrak{N}}^{\neq 0}$ gives $\overline{V_{\mathfrak{N}}^{\neq 0}} = (1, \lambda) \cdot X_{\bar{A}}$ where $X_{\bar{A}}$ is the projective toric variety given by the $4 \times (2N+3)$ integer matrix

$$\bar{A} = \begin{pmatrix} 1 & 1 & 1 & 0 & 0 & 0 & 0 & \cdots & 0 \\ 0 & -1 & 0 & 1 & 0 & 0 & 0 & \cdots & 0 \\ 1 & 1 & 0 & 0 & 1 & 0 & 0 & \cdots & 0 \\ 1 & 1 & 1 & 1 & 1 & 1 & 1 & \cdots & 1 \end{pmatrix},$$

where the last $2n-2$ columns are $(0,0,0,1)^T$. For any choice of the integer $n \geq 1$ it can be seen that the matrix $\bar{A}$ will have six unique column vectors, from this it is straightforward to show that the polytope $P = \text{conv}(\bar{A})$ has exactly six vertices with none of the columns of $\bar{A}$ specifying interior lattice points. Since the Chern-Mather volumes are determined by the polytope P and by the interior lattice points corresponding to columns of $\bar{A}$ it follows immediately that only the six vertices of the polytope P need to be considered. These are given as the columns of the matrix

$$P^{\text{vertex}} = \begin{pmatrix} 1 & 1 & 1 & 0 & 0 & 0 \\ 0 & -1 & 0 & 1 & 0 & 0 \\ 1 & 1 & 0 & 0 & 1 & 0 \\ 1 & 1 & 1 & 1 & 1 & 1 \end{pmatrix} = \begin{pmatrix} \boldsymbol{v}_1 & \boldsymbol{v}_2 & \boldsymbol{v}_3 & \boldsymbol{v}_4 & \boldsymbol{v}_5 & \boldsymbol{v}_6 \end{pmatrix},$$

where $\boldsymbol{v}_i$ denotes vertex i.

Computing with this polytope is can be shown that the Chern-Mather volumes of P are $V_0 = 12$, $V_1 = 12$, $V_2 = 8$ and $V_3 = 4$. Applying (4.12) gives $\text{EDdegree}\left(\overline{V_{\mathfrak{N}}^{\neq 0}}\right) = 28$.

□

4.2.1.2 Distributive Networks

Distributive phosphorylation is an important mechanism in many cellular processes [Salazar and Höfer, 2009; Ferrell and Bhatt, 1997; Waas et al., 2001; Nash et al., 2001; Deshaies and Ferrell Jr, 2001], most prominently, the ERK2 MAP kinase, which is responsible for basic cellular functions such as cell proliferation, differentiation and cell death, is phosphorylated and dephosphorylated distributively [Ferrell and Bhatt,

1997; Burack and Sturgill, 1997]. In contrast to processive systems distributive multi-site phosphorylation networks can admit multiple steady states [Conradi and Shiu, 2015; Holstein et al., 2013]. Intuitively, one would therefore expect the distributive mechanism to be 'more complex' than its processive counterpart. The results of this subsection quantify its complexity using the ED degree.

The reaction mechanism for the N-site distributive network from Conradi and Shiu [2015] is

$$S_0 + E \underset{l_1}{\overset{\kappa_1}{\rightleftharpoons}} S_0E \xrightarrow{\kappa_1'} S_1 + E \underset{l_2}{\overset{\kappa_2}{\rightleftharpoons}} S_1E \xrightarrow{\kappa_2'} \cdots \xrightarrow{\kappa_{N-1}'} S_{N-1} + E \underset{l_N}{\overset{\kappa_N}{\rightleftharpoons}} S_{N-1}E \xrightarrow{\kappa_N'} S_N + E,$$

$$S_N + F \underset{\bar{l}_N}{\overset{\bar{\kappa}_N}{\rightleftharpoons}} S_NF \xrightarrow{\bar{\kappa}_N'} \cdots \xrightarrow{\bar{\kappa}_{N-2}'} S_2 + F \underset{\bar{l}_2}{\overset{\bar{\kappa}_2}{\rightleftharpoons}} S_2F \xrightarrow{\bar{\kappa}_2'} S_1 + F \underset{\bar{l}_1}{\overset{\bar{\kappa}_1}{\rightleftharpoons}} S_1F \xrightarrow{\bar{\kappa}_1'} S_0 + F.$$

As in subsection 4.2.1.1 the chemical species are identified with the variables to give:

x_1	x_2	x_3	$\cdots$	x_{N+3}	x_{N+4}	$\cdots$	x_{2N+3}	x_{2N+4}	$\cdots$	x_{3N+3}
E	F	S_0	$\cdots$	S_N	S_0E	$\cdots$	$S_{N-1}E$	S_1F	$\cdots$	S_NF

From the reaction scheme the stoichiometric matrix Γ can be derived in terms of the matrices Γ_1, Γ_2, Γ_3, Γ_4, the zero matrix $\mathbf{0}_{N\times N}$ and the identity matrix $\boldsymbol{I}_{N\times N}$,

$$\Gamma_1 = \left(\begin{array}{ccc} -1 & \cdots & -1 \\ 0 & \cdots & 0 \\ \hline \multicolumn{3}{c}{-\boldsymbol{I}_{N\times N}} \\ \hline 0 & \cdots & 0 \\ \hline \multicolumn{3}{c}{\boldsymbol{I}_{N\times N}} \\ \hline \multicolumn{3}{c}{\mathbf{0}_{N\times N}} \end{array}\right), \quad \Gamma_2 = \left(\begin{array}{ccc} 1 & \cdots & 1 \\ 0 & \cdots & 0 \\ \hline 0 & \cdots & 0 \\ \hline \multicolumn{3}{c}{\boldsymbol{I}_{N\times N}} \\ \hline \multicolumn{3}{c}{-\boldsymbol{I}_{N\times N}} \\ \hline \multicolumn{3}{c}{\mathbf{0}_{N\times N}} \end{array}\right), \quad \Gamma_3 = \left(\begin{array}{ccc} 0 & \cdots & 0 \\ -1 & \cdots & -1 \\ \hline 0 & \cdots & 0 \\ \hline \multicolumn{3}{c}{-\boldsymbol{I}_{N\times N}} \\ \hline \multicolumn{3}{c}{\mathbf{0}_{N\times N}} \\ \hline \multicolumn{3}{c}{\boldsymbol{I}_{N\times N}} \end{array}\right), \quad \Gamma_4 = \left(\begin{array}{ccc} 0 & \cdots & 0 \\ 1 & \cdots & 1 \\ \hline \multicolumn{3}{c}{\boldsymbol{I}_{N\times N}} \\ \hline 0 & \cdots & 0 \\ \hline \multicolumn{3}{c}{\mathbf{0}_{N\times N}} \\ \hline \multicolumn{3}{c}{-\boldsymbol{I}_{N\times N}} \end{array}\right),$$

to give $\Gamma = (\Gamma_1 \,|\, -\Gamma_1 \,|\, \Gamma_2 \,|\, \Gamma_3 \,|\, -\Gamma_3 \,|\, \Gamma_4)$. Analogously, the flux vector can be derived to give:

$$\begin{aligned}\boldsymbol{\nu}(\boldsymbol{x}) = (&\kappa_1 x_1 x_3, \ldots, \kappa_N x_1 x_{N+2}, l_1 x_{N+4}, \ldots, l_N x_{2N+3}, \kappa_1' x_{N+4}, \ldots, \kappa_N' x_{2N+3}, \\ &\bar{\kappa}_1 x_2 x_4, \ldots, \bar{\kappa}_N x_2 x_{N+3}, \bar{l}_1 x_{2N+4}, \ldots, \bar{l}_N x_{3N+3}, \bar{\kappa}_1' x_{2N+4}, \ldots, \bar{\kappa}_N' x_{3N+3})^T.\end{aligned} \tag{4.16}$$

Now, closed form expressions for the ED degree of the family of toric varieties, which corresponds to the non-zero closure of the steady state variety of the N-site distributive phosphorylation network, can be given.

Theorem 4.2.2. *Let $V_{\mathfrak{N}}$ denote the steady state variety of the distributive N-site phosphorylation network. Then, the ED degree is given by*

$$\text{EDdegree}\left(\overline{V_{\mathfrak{N}}^{\neq 0}}\right) = 23N + 5.$$

Proof. In Theorem 4.3 of Millán et al. [2012] it is shown that $V_{\mathfrak{N}}^{\neq 0} = \lambda \cdot X_A$ where $\lambda \in (\mathbb{C}^*)^{3N+3}$ and where X_A is the affine toric variety defined by

$$A = \begin{pmatrix} 1 & 0 & 0 & 1 & 2 & \cdots & N & 1 & 2 & \cdots & N & 1 & 2 & \cdots & N \\ 1 & 1 & 0 & 0 & 0 & \cdots & 0 & 1 & 1 & \cdots & 1 & 1 & 1 & \cdots & 1 \\ 0 & 0 & 1 & 1 & 1 & \cdots & 1 & 1 & 1 & \cdots & 1 & 1 & 1 & \cdots & 1 \end{pmatrix}.$$

Taking the projective closure of $V_{\mathfrak{N}}^{\neq 0}$ gives $\overline{V_{\mathfrak{N}}^{\neq 0}} = (1, \lambda) \cdot X_{\bar{A}}$ where $(1, \lambda) \in (\mathbb{C}^*)^{3N+4}$ and $X_{\bar{A}}$ is the projective toric variety defined by the matrix

$$\bar{A} = \begin{pmatrix} 0 & 0 & 0 & 1 & 1 & \cdots & 1 & 1 & 1 & \cdots & 1 & 1 & 1 & \cdots & 1 \\ 1 & 0 & 0 & 1 & 1 & \cdots & 1 & 0 & 0 & \cdots & 0 & 0 & 0 & \cdots & 0 \\ 0 & 1 & 0 & 0 & 1 & \cdots & N & 1 & 2 & \cdots & N & 1 & 2 & \cdots & N \\ 1 & 0 & 1 & N & N-1 & \cdots & 0 & N-1 & N-2 & \cdots & 0 & N-1 & N-2 & \cdots & 0 \end{pmatrix}.$$

$P_N = \text{conv}(\bar{A})$ is the polytope of the convex hull of the column vectors of $\bar{A}$. Note that P_N has exactly 7 vertices for any N. Given this is straightforward to see that for any N the polytope P_N always has the 7 vertices given as the columns of the matrix

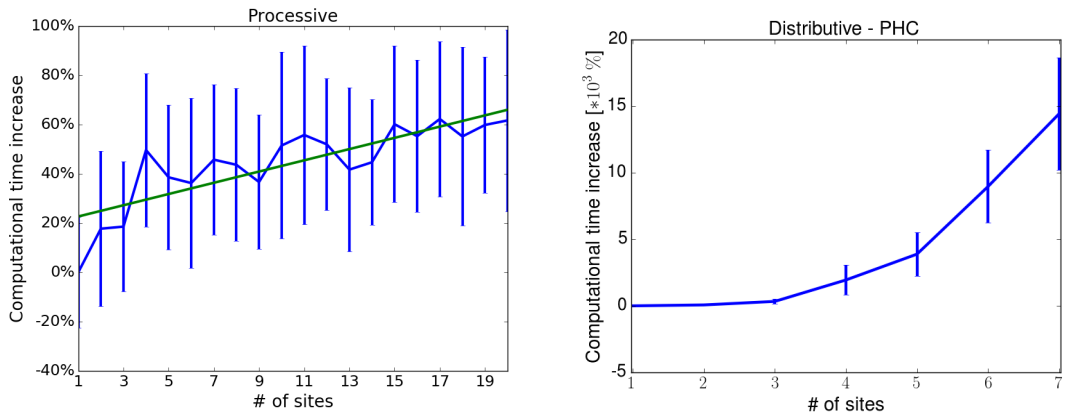
$$P_N^{\text{vertex}} = \begin{pmatrix} 0 & 0 & 0 & 1 & 1 & 1 & 1 \\ 1 & 0 & 0 & 1 & 1 & 0 & 0 \\ 0 & 1 & 0 & N & 0 & N & 1 \\ 1 & 0 & 1 & 0 & N & 0 & N-1 \end{pmatrix} = \begin{pmatrix} \boldsymbol{v}_1 & \boldsymbol{v}_2 & \boldsymbol{v}_3 & \boldsymbol{v}_4 & \boldsymbol{v}_5 & \boldsymbol{v}_6 & \boldsymbol{v}_7 \end{pmatrix},$$

where $\boldsymbol{v}_i$ denotes vertex i. The Chern-Mather volumes of the faces of the polytope P_N can now be computed by applying (4.12). In dimension three it can be shown that the Chern-Mather volume of P_N is $V_3 = \text{Vol}(P_N) = 3N + 1$. P_N has 8 dimension two faces; totalling the Chern-Mather volumes of these faces gives $V_2 = 4 \cdot (N + 1)$. P_N has 13 dimension one faces; totalling the Chern-Mather volumes of these faces gives $V_1 = 2N + 10$. Finally, totalling the Chern-Mather volumes of the vertices gives $V_0 = 12$. Applying (4.11) gives

$$\begin{aligned} \text{EDdegree}\left(\overline{V_{\mathfrak{N}}^{\neq 0}}\right) &= 15V_3 - 7V_2 + 3V_1 - V_0 = \\ &= 45N + 15 - (28N + 28) + (6N + 30) - 12 = 23N + 5. \end{aligned}$$

□

For small N the ED problem can be solved for the multi-site phosphorylation networks computationally in SageMath [Sage Developer Team, 2016] by computing the Gröbner basis of the non-zero closures of the models' steady varieties in lex order. This is usually the bottleneck in solving systems of non-linear polynomial equations. After a lex Gröbner basis has been computed numerical solvers can then



(a) Processive (b) Distributive

Figure 4.2: Comparing the run times to solve the ED problem for the processive and the distributive multi-site phosphorylation networks. For the processive model the Gröbner basis were computed whereas for the distributive NAG methods were used, because the run time was considerably shorter than for computing the Gröbner basis.

be used iteratively as each generator is a polynomial in one new variable only (if the number of solutions to the polynomial system defined by the Gröbner basis is finite). In Figure 4.2a it is shown that the wall time for computations of the Gröbner basis is approximately constant for the processive network. The run times for the computation of the Gröbner bases of the distributive network prove very large (>1 day for $N = 2$ phosphorylation sites), hence, for efficiency, PHCpack [Verschelde, 1999] is used. Despite the NAG method being orders of magnitude faster, the problem of PHCpack missing solutions is encountered, especially as the number of sites increases. Since there is no guarantee that the global minimum is in the solutions that are found, many runs are needed to find all solutions to the ED problem (see Table 4.2). Thus, in particular, the ED degree aids in determining whether all solutions have been found. This, combined with a method to certify numerical solutions, can give a certain answer to when all solutions have been found using NAG methods.

Number of Sites	Avg. # of runs for solution	Avg. time per run	Avg. total run time per solution
1	1.2	0.47s	0.57s
2	1.1	0.90s	0.95s
3	1.3	1.90s	2.46s
4	2.6	4.41s	11.57s
5	4	5.75s	23.00s
6	4.6	11.24s	51.36s
7	6.17	13.33s	82.20s

Table 4.2: Run time results for the Distributive network using PHCpack, the total time to find all solutions is listed in the last column.

4.2.2 Sequestration Networks

Sequestration reactions are chemical reactions in which a molecule is rendered inactive by binding to a second molecule [Joshi and Shiu, 2015]. A classic example would be the inhibition of a substrate by an enzyme,

$$E + S \to \emptyset. \tag{4.17}$$

Following [Joshi and Shiu, 2015] a sequestration network of N species is constructed by allowing for $N-1$ sequestration reactions and one synthesis reaction. Let $\mathfrak{N}_m$ denote the N species sequestration network and let X_i denote the species occurring in $\mathfrak{N}_m$, the reaction scheme is given below:

$$\begin{aligned} X_1 + X_2 &\xrightarrow{\kappa_1} \emptyset, \\ X_2 + X_3 &\xrightarrow{\kappa_2} \emptyset, \\ &\vdots \\ X_{N-1} + X_N &\xrightarrow{\kappa_{N-1}} \emptyset, \\ X_1 &\xrightarrow{\kappa_N} mX_N. \end{aligned} \tag{4.18}$$

Denoting the concentration of X_i as x_i the flux vector is

$$\boldsymbol{\nu}(\boldsymbol{x}) = \left(\kappa_1 x_1 x_2, \kappa_2 x_2 x_3, \ldots, \kappa_{N-1} x_{N-1} x_N, \kappa_N x_1\right)^T. \tag{4.19}$$

From the reaction scheme the matrix Γ can be found which is given by

$$\boldsymbol{\Gamma} = (-\boldsymbol{e}_1 - \boldsymbol{e}_2, -\boldsymbol{e}_2 - \boldsymbol{e}_3, \cdots, -\boldsymbol{e}_{N-1} - \boldsymbol{e}_N, -\boldsymbol{e}_1 + m\, \boldsymbol{e}_N). \tag{4.20}$$

After closer inspection one finds that not every $\mathfrak{N}_m$ has a non-empty non-zero closure or a toric steady state variety. In the proof of Theorem 4.2.3 it is shown that the model has toric steady states only for certain choices of N and m and the ED degree is calculated for the case where $m = 1$ and N is an odd integer.

Theorem 4.2.3. *Let $V_{\mathfrak{N}_m}$ be the steady state variety of the N-site sequestration network $\mathfrak{N}_m$ with m being the coefficient of the synthesis reaction in the reaction network as in (4.18). If $m = 1$ and N is an odd integer then the ED degree is given by*

$$\text{EDdegree}\left(\overline{V_{\mathfrak{N}_m}^{\neq 0}}\right) = 1.$$

For all other choices of m and N the variety $V_{\mathfrak{N}_m}^{\neq 0}$ is empty.

Proof. First let N be an odd integer and treat m as a variable. Examining the matrix Γ in (4.20) it can be seen that each row of Γ has only two non-zero entries. Also note that each entry of the vector $\boldsymbol{\nu}(\boldsymbol{x})$ in (4.19) is a monomial, hence the ideal $I_N = \Gamma \cdot \boldsymbol{\nu}(\boldsymbol{x})$ is generated by binomials. By definition the steady state variety is $V_{\mathfrak{N}_m} = V(I_N)$, the variety $V_{\mathfrak{N}_m}^{\neq 0}$ consists of all points in $V(I_N)$ which have no zero coordinates, hence in particular,

$$V_{\mathfrak{N}_m}^{\neq 0} = \overline{V(I_N) \backslash V(x_1 x_2 \cdots x_N)} = V(I_N : (x_1 x_2 \cdots x_N)^\infty).$$

Computing the ideal $I^{\neq 0} = I_N : (x_1 x_2 \cdots x_N)^\infty$ a prime ideal generated by binomials is obtained and one of these binomials is $m - 1$. Hence $V_{\mathfrak{N}_m}^{\neq 0}$ is empty whenever $m \neq 1$. Setting $m = 1$ in $I^{\neq 0}$ a new ideal $I_{m=1}^{\neq 0}$ is obtained and again generated by binomials. Interpreting the exponents of these binomials as in (4.6) the generators of the kernel of the matrix which defines a parameterisation of a variety isomorphic to $V_{\mathfrak{N}_{m=1}}^{\neq 0} = V(I_{m=1}^{\neq 0})$ is obtained. The resulting toric variety is called X_A; the defining matrix of X_A is the $2 \times (N+1)$ integer matrix

$$A = \begin{pmatrix} 1 & 0 & 0 & 0 & 0 & \cdots & 0 & 0 & 0 \\ 0 & 1 & 0 & 1 & 0 & \cdots & 1 & 0 & 1 \end{pmatrix}.$$

Now suppose that N is an even integer and again treat m as a variable. Computing $I^{\neq 0} = I_N : (x_1 x_2 \cdots x_N)^\infty$ in this case again yields a prime ideal generated by binomials, among these binomials is the polynomial $m + 1$. However, $m = -1$ is not valid for the model (m must be positive by construction), hence $V_{\mathfrak{N}_m}^{\neq 0}$ is empty in this case.

Now consider the case where $V_{\mathfrak{N}_m}^{\neq 0}$ is non-empty, namely set $m = 1$ and let N be an odd integer. By the arguments above the non-zero closure of $V_{\mathfrak{N}_m}$ is given by $V_{\mathfrak{N}_m}^{\neq 0} = X_A$. Taking the projective closure of X_A yields the projective toric variety $X_{\bar{A}}$ defined by the $3 \times (N+2)$ integer matrix

$$\bar{A} = \begin{pmatrix} 1 & 0 & 0 & 0 & \cdots & 0 & 0 & 0 \\ 0 & 1 & 0 & 1 & \cdots & 0 & 1 & 0 \\ 1 & 1 & 1 & 1 & \cdots & 1 & 1 & 1 \end{pmatrix}.$$

The polytope $P = \text{conv}(\bar{A})$ is a triangle of dimension 2 (see Figure 4.3). The three vertices of P are given as the columns of the matrix

$$P_m^{\text{vertex}} = \begin{pmatrix} 1 & 0 & 0 \\ 0 & 1 & 0 \\ 1 & 1 & 1 \end{pmatrix} = \begin{pmatrix} \boldsymbol{v}_1 & \boldsymbol{v}_2 & \boldsymbol{v}_3 \end{pmatrix},$$

where $\boldsymbol{v}_i$ denotes vertex i.

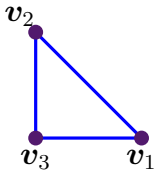


Figure 4.3: The polygon $P = \text{conv}(\bar{A})$.

This polytope P (see Figure 4.3) is smooth (i.e. the associated toric variety is smooth), hence V_j, the sum of all Chern-Mather volumes of all faces of dimension j, is equal to the sum of all normalized volumes of dimension j faces. P is a triangle, and hence has normalized volume one, has three edges (dimension one faces) each of with normalized volume one, and has three vertices. This gives $V_2 = 1$, $V_1 = 3$, $V_0 = 3$, respectively. Applying (4.11) gives

$$\text{EDdegree}(X_{\bar{A}}) = \sum_{j=0}^{2} (-1)^{2-j}(2^{j+1} - 1) \cdot V_j = 1.$$

□

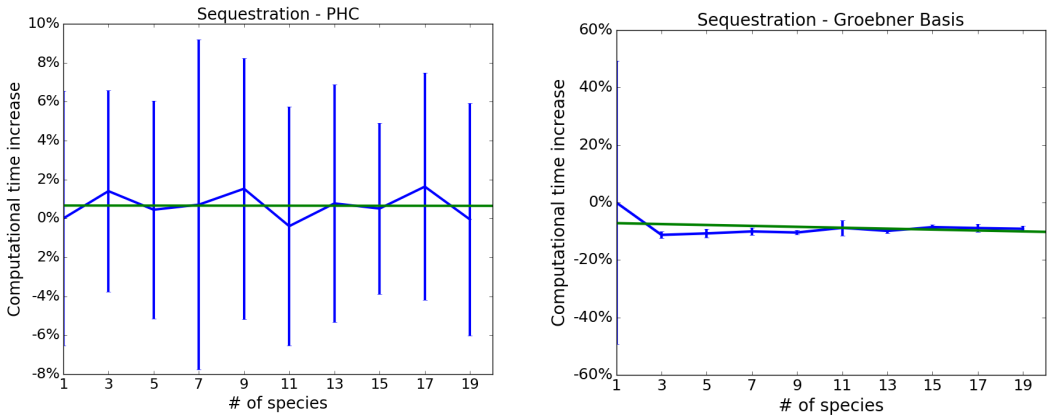
Remark 4.2.4. *Theorem 4.2.3 is rather remarkable as it states that for any parameter vector and any measurement there will always be exactly one local minimum for the Euclidean distance problem associated to the sequestration network (4.18). However, it can be shown that $V_{\mathfrak{N}_{m=1}}^{\neq 0}$ does not intersect the positive orthant and, therefore, while sequestration networks are biologically important, the study of their positive steady states is futile.*

Due to its minimal complexity the ED problem for sequestration networks can be solved by computing the Gröbner basis from which the solution can be read off immediately; see Figure 4.4.

4.2.3 Kinetic Proofreading Networks (McKeithan Model)

Kinetic proofreading networks are vital components in cell biology that enhance binding selectivity [Blanchard et al., 2004; Mckeithan, 1995; Hopfield, 1974; Sontag, 2001]. The first mathematical models for kinetic proofreading were developed to explain the astonishing accuracy of DNA replication and protein synthesis. The model presented in this chapter was initially proposed by McKeithan [Mckeithan, 1995] to understand the simultaneous high sensitivity and high selectivity of antigen recognition in T cells.

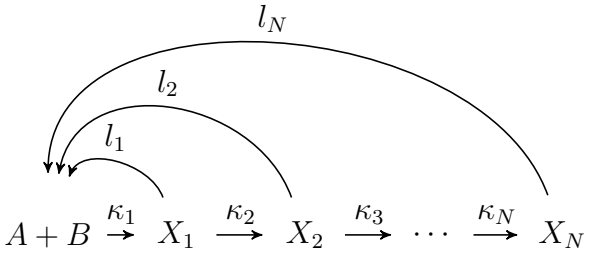
In the model a ligand (A) binds to T-cell receptor (B) which is transformed via intermediate stages to a final stage X_N. The product X_N initiates the T-cell



(a) Direct computation with PHCpack (b) Gröbner basis only

Figure 4.4: A comparison of the run times for finding the solution to the ED problem for the Sequestration networks (4.18). NAG and Gröbner basis methods give an approximately constant run time for any number of species as expected from the constant ED degree.

reaction. There is time-delay between the initial antigen binding and T-cell activation. Therefore, ligands, which are not tailored to a specific T-cell receptor, will dissociate before X_N is formed in significant quantities. The *McKeithan model* follows the reaction scheme:



Denoting the concentrations of the species as $\{a, b, x_1, \cdots, x_N\}$ the flux vector can be formulated

$$\boldsymbol{\nu}(\boldsymbol{x}) = (\kappa_1 ab, \kappa_2 x_1, \kappa_3 x_2, \ldots, \kappa_N x_{N-1}, l_1 x_1, l_2 x_2, \ldots, l_N x_N)^T . \tag{4.21}$$

As in the previous models the stoichiometric matrix can be constructed from the reaction network

$$\boldsymbol{\Gamma} = (-\boldsymbol{e}_1 - \boldsymbol{e}_2 + \boldsymbol{e}_3, -\boldsymbol{e}_3 + \boldsymbol{e}_4, \cdots, -\boldsymbol{e}_{N+1} + \boldsymbol{e}_{N+2}, \boldsymbol{e}_1 + \boldsymbol{e}_2 - \boldsymbol{e}_3, \cdots, \boldsymbol{e}_1 + \boldsymbol{e}_2 - \boldsymbol{e}_{N+2}). \tag{4.22}$$

By using (2.3) the affine steady state variety of the model and its parameterisation can be found.

The projective closure and, hence, the ED degree can now be calculated.

Theorem 4.2.5. *Let $V_{\mathfrak{N}}$ be the steady state variety of the N-site McKeithan Model. Then the ED degree is given by*

$$\text{EDdegree}\left(\overline{V_{\mathfrak{N}}^{\neq 0}}\right) = 6.$$

Proof. Let I_N be the ideal in $\mathbb{K}[x_1, \ldots, x_N, a, b]$ generated by $\Gamma\boldsymbol{\nu}(\boldsymbol{x})$. It can be shown inductively, that I_N is a prime ideal generated by binomials (for $N \geq 1$). Finding a matrix with kernel given by the set of exponents of I_N (interpreted as in (4.6)) it can be shown that the steady state variety of the N-site McKeithan Model is isomorphic to the affine toric variety X_A defined by the $2 \times (N+2)$ integer matrix

$$A = \begin{pmatrix} 1 & 1 & 1 & \cdots & 1 & 1 & 0 \\ 1 & 1 & 1 & \cdots & 1 & 0 & 1 \end{pmatrix}.$$

Since any toric variety is its own non-zero closure it is true that $V_{\mathfrak{N}}^{\neq 0} \cong X_A$. Taking the projective closure of X_A it can be found that $\overline{X_A} = X_{\bar{A}}$ is the projective toric variety defined by the $3 \times (N+3)$ integer matrix

$$\bar{A} = \begin{pmatrix} 1 & 0 & 0 & 0 & \cdots & 0 & 1 & 0 \\ 1 & 0 & 0 & 0 & \cdots & 0 & 0 & 1 \\ 1 & 1 & 1 & 1 & \cdots & 1 & 1 & 1 \end{pmatrix}.$$

For any choice of the integer $N \geq 1$ the polytope $P = \text{conv}(\bar{A})$ has exactly four vertices with none of the columns of $\bar{A}$ specifying interior lattice points. Since the Chern-Mather volumes are determined by the polytope P and by the interior lattice points corresponding to columns of $\bar{A}$ it follows immediately that only consider the four vertices of the polytope P need to be considered, as P has no interior points. These are given as the columns of the matrix

$$P^{\text{vertex}} = \begin{pmatrix} 1 & 0 & 1 & 0 \\ 1 & 0 & 0 & 1 \\ 1 & 1 & 1 & 1 \end{pmatrix} = \begin{pmatrix} \boldsymbol{v}_1 & \boldsymbol{v}_2 & \boldsymbol{v}_3 & \boldsymbol{v}_4 \end{pmatrix},$$

where $\boldsymbol{v}_i$ denotes vertex i.

This polytope P (see Figure 4.5) is smooth (i.e. the associated toric variety is smooth). Hence V_j, the sum of all Chern-Mather volumes of all faces of dimension j, is equal to the sum of all normalized volumes of dimension j faces. The normalized

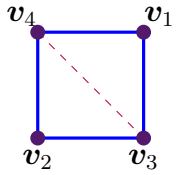
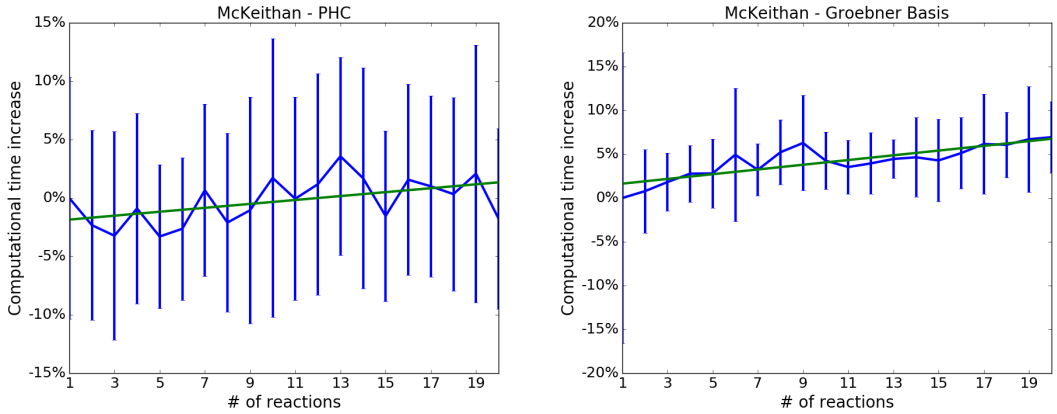


Figure 4.5: The polygon $P = \mathrm{conv}(\bar{A})$.



(a) Direct computation with PHCpack

(b) Computation of the Gröbner basis

Figure 4.6: A comparison of the runtime for solving the ED problem for the McKeithan model. Both methods seem to have an approximately constant run time; however, the Gröbner basis algorithm outperforms the numerical algebraic geometry approach, even when the fact that the triangular system still needs to be solved is accounted for.

volume of P is $V_2 = \mathrm{Vol}(P) = 2$, there are four edges (dimension one faces) so $V_1 = 4$, and there are four vertices giving $V_0 = 4$. Applying (4.11) gives

$$\mathrm{EDdegree}(X_{\bar{A}}) = \sum_{j=0}^{2} (-1)^{2-j}(2^{j+1} - 1) \cdot V_j = 6.$$

□

In a similar manner to the sequestration networks the ED problem can be solved numerically with PHCpack or by computing the Gröbner basis of the model. The findings are summarised in Figure 4.6 and show a nearly constant computation time. The slight increase in the observed time is likely due to extra computational overhead when working with polynomial systems in more variables.

4.2.4 Multimeric Pore-Forming Toxins

Pore forming toxins attack cells by assembling pores in the cell membrane from monomers. The pores cause the cells to leak, which eventually leads to cell death [Voskoboinik et al., 2006; Rosado et al., 2007; Iacovache et al., 2010]. A number of pore forming cytotoxins are employed by various bacteria such as Streptococcus pneumonia, Staphylococcus aureus, Escherichia coli and Myobacterium tuberculosis, but they are also used in the eurokaryotic immune system to kill pathogens and infected cells [Los et al., 2013].

For the calculation of this section the N-monomer pore model from Lee et al. [2016] is adapted, which follows the reaction scheme,

$$\begin{aligned} X_1 + X_i &\underset{l_i}{\overset{\kappa_i}{\rightleftharpoons}} X_{i+1}, \quad 1 \geq i \geq N-2, \\ X_1 + X_{N-1} &\xrightarrow{\kappa_0} X_N. \end{aligned} \tag{4.23}$$

In the current form the non-zero closure of the steady state variety of (4.23) is not a toric variety. To obtain a non-zero closure which is a toric variety a slight modification to the model is made. In the modified model the additional assumption is made that fully formed pores X_N have a finite lifetime and can open up again. This change results in the scheme

$$\begin{aligned} X_1 + X_i &\underset{l_i}{\overset{\kappa_i}{\rightleftharpoons}} X_{i+1}, \quad 1 \geq i \geq N-2, \\ X_1 + X_{N-1} &\underset{l_0}{\overset{\kappa_0}{\rightleftharpoons}} X_N. \end{aligned} \tag{4.24}$$

Since the ED degree is independent of the model parameters, (4.23) can be thought of as (4.24) in the limit of $l_0 \to 0$ or the lifetime of the pore $l_0^{-1} \to \infty$, which gives confidence that the modification still bears biological relevance.

From the reaction scheme the stoichiometric matrix can be found

$$\Gamma = (\underbrace{-\boldsymbol{e}_1 - \boldsymbol{e}_1 + \boldsymbol{e}_2, -\boldsymbol{e}_1 - \boldsymbol{e}_2 + \boldsymbol{e}_3, \cdots, -\boldsymbol{e}_1 - \boldsymbol{e}_{N-1} + \boldsymbol{e}_N,}_{\Gamma_1} | - \Gamma_1). \tag{4.25}$$

Further, the flux vector is given by

$$\boldsymbol{\nu}(\boldsymbol{x}) = (\kappa_1 x_1 x_1, \kappa_2 x_1 x_2, \ldots, \kappa_{N-2} x_1 x_{N-2}, \kappa_0 x_1 x_{N-1}, l_1 x_2, l_2 x_3, \ldots, l_{N-2} x_{N-1}, l_0 x_N)^T. \tag{4.26}$$

From the ODE system describing the dynamics of the model the steady state variety can be found. Next, in Theorem 4.2.6, the exponents of the parameterisation of the steady state variables are found and the ED degree is computed.

Theorem 4.2.6. *Let $V_{\mathfrak{N}}$ be the steady state variety of the N-site pore network $\mathfrak{N}$. Then, the ED degree is given by*

$$\text{EDdegree}\left(\overline{V_{\mathfrak{N}}^{\neq 0}}\right) = 3N - 2.$$

Proof. Let I_N be the ideal in $\mathbb{K}[x_1, \ldots, x_N]$ generated by $\Gamma\boldsymbol{\nu}(\boldsymbol{x})$. Computing a Gröbner basis of I_N (in the graded reverse lexicographic order) it can be seen that I_N is a prime ideal generated by binomials. Finding a matrix with kernel given by the set of exponents of I_N (interpreted as in (4.6)) it can be seen that $V_{\mathfrak{N}}$ is isomorphic to the affine *rational normal curve* (which is an affine toric variety). That is, $V_{\mathfrak{N}}^{\neq 0} \cong X_A$ where X_A is the affine toric variety defined by the $1 \times (N+1)$ integer matrix

$$A = \begin{pmatrix} N & N-1 & N-2 & N-3 & \cdots & 2 & 1 & 0 \end{pmatrix}.$$

Taking the projective closure of X_A reveals that $X_{\bar{A}}$ is the projective toric variety defined by the $2 \times (N+1)$ integer matrix

$$\bar{A} = \begin{pmatrix} N & N-1 & N-2 & N-3 & \cdots & 2 & 1 & 0 \\ 1 & 1 & 1 & 1 & \cdots & 1 & 1 & 1 \end{pmatrix},$$

i.e. $X_{\bar{A}}$ is the projective rational normal curve. The polytope $P = \text{conv}(\bar{A})$ is one dimensional and consists of a line with vertices 0 and N. This polytope is smooth, and has normalized volume N. Computing with this polytope it can be shown that the Chern-Mather volumes of P are $V_0 = 2$ (that is the number of vertices), and $V_1 = N = \text{Vol}(P)$ (that is the normalized volume of P, i.e the length of the line). Applying (4.11) gives

$$\text{EDdegree}(X_{\bar{A}}) = 3V_1 - V_0 = 3N - 2.$$

□

Remark 4.2.7. *It is shown in Example 1.3 of Helmer and Sturmfels [2016] that the usual Euclidean norm (i.e. where we set $\lambda_i = 1$ in (4.9)) gives the generic value of* $\text{EDdegree}(X_{\bar{A}}) = 3N - 2$ *for the projective rational normal curve.*

In a similar manner to the distributive phosphorylation networks the computational time rises exponentially with the number of monomers in a formed pore, see Figure 4.7.

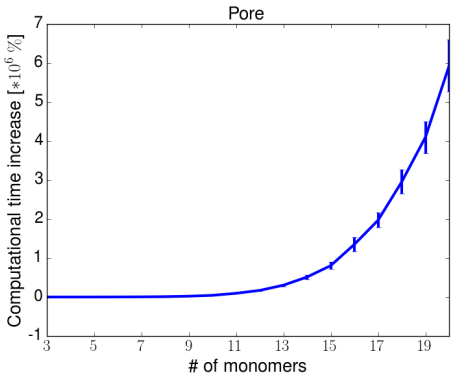


Figure 4.7: The wall time of lex Gröbner basis computation for the pore model. As expected from the ED degree the run time grows quickly, however, not linearly, with the number of monomers.

4.3 Discussion

Ultimately the algebraic complexity of the models studied in this chapter should be related back to biological features of the underlying reaction network, as there is no obvious connection between projective toric varieties and biology. Hence, in Table 4.3 some common metrics used to classify chemical reaction networks are collected such as their deficiency, their reversibility and their multistationarity. However, there is not enough data to see an obvious pattern of how the functional form of the ED degree relates to these network features.

It seems that more insight can be gained when the combinatorics of the "substrate" is considered. For the phosphorylation networks the substrates are proteins with N sites which can be in a phosphorylated or unphosphorylated state. A priori, this gives 2^N possible states of the substrate. These are achieved in the distributive network due to the constant docking and undocking (1 docking event per phosphorylation) of the phosphatases and kinases. In the processive network, however, there only exist $N+1$ possible states, completely unphosphorylated, phosphorylated up to the i^{th} site, and fully phosphorylated. It takes a minimum of one docking event to form the end product. A similar situation to the distributive network is encountered in the pore forming network. From the "seed monomer" there always exist 2 possible docking sites until the $N-1^{st}$ docking event when the pore is formed, giving a total of 2^{N-2} possible states of the pore. It is less clear what the "substrate" for the sequestration network is. However, since the ultimate goal of such networks is to eliminate certain chemical species we take the zero complex, $\emptyset$, as our product. It takes only one docking event to form the zero complex and there are $N-1$ reactions which can

form it. The zero complex itself can only exist in one state, however, bearing in mind that $\emptyset$ is just a modelling notation and that in the actual biological system the product of e.g. $X_1 + X_2$ and $X_2 + X_3$ may well be different the products of these reactions can be counted as different states. Hence, the combinatorial complexity of the sequestration network can be defined to be $N - 1$. The McKeithan model needs one docking event, $A + B \to X_1$, to form the initial product. The rest of the reaction network is comprised of dynamical steps only. However, in a similar fashion to the processive phosphorylation network, the "substrate" X_i can exist in N different states and therefore the combinatorial complexity of the McKeithan model is N.

Despite the limited number of models under investigation it can be conjectured from Table 4.3 that the functional form of the ED degree is intimately related to the combinatorial complexity of the "substrates" and even scales directly with the minimum number of docking events it takes to form the final product.

Model	Deficiency	Weakly reversible	Multistationary	Combinatorial complexity	# of docking events	ED degree
Processive	1	No	No	$N+1$	1	28
Distributive	variable	No	Yes	2^N	N	$23N+5$
Pore	0	Yes	No	2^{N-2}	$N-1$	$3N-2$
Sequestration	0	No	No	$N-1$	1	1
McKeithan	0	Yes	No	N	1	6

Table 4.3: Biological and chemical reaction network theory metrics for the models.

4.3.1 Restrictions and Extensions

Throughout the previous sections assumptions are made which solely serve the purpose of illustrating the mathematical concepts behind the approach presented in this chapter. However, in applications, especially when considering experimental data, these assumptions can be relaxed in a rigorous manner. In this section extensions to the approach presented in this chapter to multiple data points and how to address the common problem of immeasurable concentrations in network models are briefly discussed.

In the previous sections only one data point $\boldsymbol{u} \in \mathbb{R}^n$ is considered for mathematical simplicity. However, the approach can easily be generalised to a discrete set of data points by solving the Euclidean distance problem separately for each data point.Then, a global, real, positive minimum point on the steady state variety can be found for each data point $\boldsymbol{u}_q$ and their respective Euclidean distance δ_q. By applying an appropriate selection criterion such as $\max_q \delta_q < \epsilon$ the model can be tested for its validity. It is obvious that, unless the task is parallelised appropriately, the computational time of solving the ED problem is additive in the number of data points.

In real biological systems it is often not possible to measure the concentrations of all the chemical species in the model. One way to adapt our calculations is to compute an appropriate elimination ideal of the steady state ideal, which corresponds to a projection of the steady state variety, and proceed using the variety generated by the elimination ideal. More explicitly, suppose that $V_{\mathfrak{N}}$ in $\mathbb{C}^n$ is the steady state variety of a chemical reaction network $\mathfrak{N}$ and further suppose that only m, $m < n$, of the n coordinate values in the model $\mathfrak{N}$ can be measured. Without loss of generality it may be assumed that the first m coordinates of a data point $\boldsymbol{u} \in \mathbb{C}^n$ can be measured, while the remaining $n - m$ coordinates cannot. In this case the Euclidean distance problem for (the Zariski closure of) the projection of the steady state variety onto the first m coordinates could be studied, that is the ED problem for $\overline{\pi(V_{\mathfrak{N}})}$ where $\pi : \mathbb{C}^n \to \mathbb{C}^m$ is given by $\pi : (x_1, \ldots, x_n) \mapsto (x_1, \ldots, x_m)$ would be studied. In this case the following proposition shows that the ED degree of the projected model will still be bounded by the ED degree of $V_{\mathfrak{N}}$.

Proposition 4.3.1. *Let V be a projective variety in $\mathbb{P}^n$ and let π denote the projection map $\pi : \mathbb{P}^n \to \mathbb{P}^m$ with $m < n$. Then it holds that*

$$\text{EDdegree}\left(\overline{\pi(V)}\right) \leq \text{EDdegree}(V).$$

Proof. Let W be an arbitrary subvariety of $\mathbb{P}^n$. By Draisma et al. [2016, Theorem 5.4] it holds that

$$\text{EDdegree}(W) = \delta_0(W) + \cdots + \delta_n(W),$$

where the δ_i are the polar degrees of W. Also note that the polar degrees are non-negative by definition, i.e. $\delta_i(W) \geq 0$ for all i. By Piene [1978, Theorem 4.1] (and by the fact that the degree of the preimage of a projection map is equal to the degree of the map multiplied by the degree of the image, see, for example, [Mumford, 1995, Proposition 5.5]) it is true that

$$\delta_i\left(\overline{\pi(V)}\right) \leq \delta_i(V), \quad \text{for all } i = 0, \ldots, n.$$

Hence, putting this together, results in the relation

$$\text{EDdegree}\left(\overline{\pi(V)}\right) = \delta_0\left(\overline{\pi(V)}\right) + \cdots + \delta_n\left(\overline{\pi(V)}\right) \leq \delta_0(V) + \cdots + \delta_n(V) = \text{EDdegree}(V).$$

□

4.4 Conclusion

In this chapter the Euclidean Distance degree (ED degree) for a number of common chemical reaction networks with toric steady states is calculated. The ED degree was shown to be a concise model invariant which is independent of the parameter values and, therefore, the problem of model testing has the same complexity for (almost) any parameter values.

It was demonstrated that the ED degree can be used to quantify the overall algebraic complexity of finding points on the model closest to an observed data point. In general such points will be complex, however, it was shown in this chapter that biologically viable (real and positive) points are always contained in the solution set of the ED problem for toric models.

Further, it was shown that the ED degree is constant for many common biological models, namely, the processive multi-site phosphorylation network, the McKeithan kinetic proofreading network and sequestration networks. Thus, finding the global minimum to the optimisation problem (4.13) should exhibit the same algebraic complexity, independent of the number of reactions. Similarly, it was proved that the ED degree increases linearly for distributive multi-site phosphorylation networks and pore forming networks.

To illustrate the meaning of algebraic complexity in practice the ED problem was solved computationally using Gröbner bases and numerical algebraic geometry (NAG) techniques. It was confirmed that, indeed, the run time for computing the Gröbner bases stays constant for models with constant ED degree.

Care needs to be taken, however, when relating the functional form of the ED degree of a model back to other measures of "model complexity" such as the capability of a model to have multiple positive steady states. Indeed, the distributive network has been shown to have the capability of multistationarity, whereas the processive model does not. However, the pore forming network does not have multiple positive steady states for any choice of parameters. A pattern can be seen when comparing the combinatorial complexity to the ED degree, however, no rigorous connection between the two is derived in this chapter.

The combinatorial calculation of the ED degree for toric models can be many orders of magnitude faster than calculating its Gröbner basis. Knowing this value can also be used to optimize specially designed NAG algorithms since, a priori, the number of solution paths which need to be tracked by these methods is known. Future work could include a software package to calculate the ED degree for a large number

of biologically relevant networks. Furthermore, a more detailed study of non-toric models would be desirable.

Chapter 5

Graph-Theoretic Methods for Finding Quasi-Cycles in Non-spatial Models with Stochastic Inflow

"I have here only made a nosegay of culled flowers, and have brought nothing of my own but the thread that tied them together."

– Michel de Montaigne

This chapter is based on results presented in Adamer et al. [2017].

Dynamical systems with oscillatory solutions, limit cycles in the deterministic setting and quasi-cycles in stochastic systems, are ubiquitous in the physical and biological sciences; from predator-prey models [McKane and Newman, 2005; Wang and Chen, 1997; Yoshida et al., 2003; Lugo and McKane, 2008; Lotka, 1925] to mathematical biology [Murray, 2002, 2008; van Kampen, 1983] and the vast field of chemical reaction networks [Mincheva and Roussel, 2007; Feinberg, 1987, 1988; Michaelis and Menten, 1913].

Previous research highlights how resonant amplification of intrinsic noise in stochastic interaction networks with low particle numbers can lead to behaviour not anticipated from deterministic ordinary differential equation (ODE) models. In particular, cyclic behaviour, often termed 'quasi-cycles', may emerge in stochastic models where the deterministic counterpart does not show a Hopf bifurcation [McKane and Newman, 2005; Dauxois et al., 2009]. The aim of this chapter is to show how extrinsic noise, which arises from stochastic inflows discussed in 2.3, can also lead to quasi-cyclic behaviour. It is highlighted, that, although the model itself is deterministic

and described by ODEs, fluctuating inflows have the same qualitative effect as low particle number. However, the extrinsic stochastic effects have a smaller amplitude.

The main tools for investigating stochastic cycles in intrinsic noise models are based on the direct calculation of power spectra for the constituents of the network from a Langevin equation [Woolley et al., 2011b; van Kampen, 1983; M. L. Simpson et al., 2004], which demands knowledge of noise covariances. The determination of noise covariances requires extensive coarse graining, starting from a master equation formulation of the interaction system. Via weak noise expansions of the deterministic equations, and a Fokker-Planck equation, the covariances can be calculated. Eventually, coarse graining allows for the use of the simpler chemical Langevin equation [van Kampen, 1983]. In this chapter it is shown how power spectra are calculated for extrinsic noise systems, starting from the deterministic description and using the techniques of Section 2.3. In particular, it is shown that for stochastic inflow reactions only, the extrinsic noise power spectra differ form the intrinsic noise spectra only in the noise covariances, which are fixed by the microscopic description in the intrinsic model and are arbitrary in the extrinsic noise model.

In Dauxois et al. [2009] an approximation procedure was presented which focused on the eigenvalues of a matrix that the power spectrum depends on, to predict quasi-cycles in a stochastic system. While the eigenvalue method is fast and elegant it can lead to false positives when investigating the number of oscillation frequencies, named resonant modes. In this chapter a more exact procedure for obtaining the desired information, namely the number of resonant frequencies of a network, is presented which relies on results of real algebraic geometry and graph theory. Crucially, it is also shown that this method is independent of the noise model, intrinsic or extrinsic. The parameter ranges associated with the number of resonant modes are also found by using graph theoretical approaches developed for chemical reaction networks. The techniques presented in this chapter can be applied in a more general context than chemical reaction networks, namely, to any stochastic dynamical system which can be modelled by a linear Langevin equation.

There is a large body of literature combining graph theory and algebra for studying deterministic mathematical models. Often these techniques are used to make predictions of the dynamics of a model independent of its rate constants, such as the techniques introduced in Section 2.1. Furthermore, graph theoretical methods have also been employed to show how network features such as feedback cycles can lead to oscillations and multistationarity in chemical reaction networks [Mincheva and Roussel, 2007; Clarke, 1974; Angeli et al., 2010; Banaji and Craciun, 2010; Temkin et al.,

1996; Gleiss et al., 2001; van der Schaft et al., 2015; Radde et al., 2010]. Furthermore, a generalised theory of Turing patterns has been developed exploiting network features [Diego et al., 2018]. Graph theoretical methods provide an additional advantage over the approach in Feinberg [1987], that they allow one to explore the bifurcation structure of the network. Despite the apparent advantage of using graph theoretical methods for the investigation of dynamical capabilities of interaction networks the graph based investigation of stochastic models is still in its infancy.

In this chapter an alternative route for calculating the resonant frequencies (and their parameter ranges) of stochastically-driven oscillating systems is presented. The existing techniques of Sturm's theorem and the graph theoretic methods of Mincheva and Roussel [2007] are used and then combined to be applicable to power spectral methods. Instead of solving for the roots of a rational function of the power spectrum from the weak noise approximation, the maxima of this function are investigated. To do this, algebraic techniques (e.g. Sturm chains) and a graph theoretic formulation for finding the coefficients of the characteristic polynomial are adapted. Thereby a novel methodology is developed, which can be applied to systems with intrinsic and extrinsic noise without the necessity of a microscopic description. The autocatalytic networks studied in Dauxois et al. [2009], and Togashi and Kaneko [2001, 2003] are used to illustrate the use of the method.

This chapter is organised as follows. In Section 5.1 formal expressions for the power spectra for intrinsic and extrinsic noise are derived. Section 5.2 introduces Sturm chains and graph theoretic methods and shows how these can be applied to small autocatalytic networks. Section 5.3 covers the application of the graph theoretic methods to larger networks with intrinsic and extrinsic noise respectively and the results of this chapter are summarised in Section 5.4.

5.1 Power Spectra for Systems with Intrinsic or Extrinsic Noise

In this section formulae for the power spectra of non-spatial stochastic chemical reaction networks are described. Starting with intrinsic noise, which was already discussed in Subsection 2.2.2.1, a similar formulation for systems subject to extrinsic noise is developed.

5.1.1 The Intrinsic Noise Case

In Section 2.2 it was shown that in the weak noise limit the stochastic perturbation the steady state due to low particle numbers can be described by

$$d\boldsymbol{\delta x} = J\boldsymbol{\delta x}dt + b\,\boldsymbol{\xi}\sqrt{dt}, \tag{5.1}$$

which is called the Chemical Langevin Equation (CLE). Alternatively equation (5.1) can be written in a differential form

$$\frac{d\boldsymbol{\delta x}}{dt} = J\boldsymbol{\delta x} + \boldsymbol{\eta}, \tag{5.2}$$

which can be Fourier transformed using

$$\hat{f}(\omega) = \int_{-\infty}^{\infty} f(t)e^{-i\omega t}dt, \tag{5.3}$$

where $f(t)$ is any function of time. Hence,

$$\int_{-\infty}^{\infty} \frac{d\boldsymbol{\delta x}}{dt}e^{-i\omega t}dt = -i\omega\widehat{\boldsymbol{\delta x}}. \tag{5.4}$$

Rearranging and averaging over realisations [Woolley et al., 2011b] gives the power spectrum, equation (2.21),

$$P_{\boldsymbol{\delta x}} = \langle\widehat{\boldsymbol{\delta x}}\widehat{\boldsymbol{\delta x}}^{\dagger}\rangle = (J + i\omega\boldsymbol{I})^{-1}\langle\hat{\boldsymbol{\eta}}\hat{\boldsymbol{\eta}}^{\dagger}\rangle\left[(J + i\omega\boldsymbol{I})^{-1}\right]^{\dagger}. \tag{5.5}$$

Crucially, the power spectrum of the intrinsic noise is dependent on the noise covariance matrix $B = \langle\hat{\boldsymbol{\eta}}\hat{\boldsymbol{\eta}}^{\dagger}\rangle$, which is determined by the microscopic model and defined in (2.16b) and by the Jacobian of the deterministic system.

5.1.2 The Extrinsic Noise Case

The ideas of this subsection are adapted from Adamer et al. [2020]. In the extrinsic noise case stochastic fluctuations affect the parameters of the system and are not part of the intrinsic dynamics. Let a chemical reaction network with species concentrations $\boldsymbol{x} = (x_1, \ldots, x_n)^T$ and parameters $\boldsymbol{\kappa} = (\kappa_1, \ldots, \kappa_m)^T$ be described by the ODE system

$$\frac{d\boldsymbol{x}}{dt} = \boldsymbol{f}(\boldsymbol{\kappa}, \boldsymbol{x}) \equiv \boldsymbol{f}(\boldsymbol{x}), \tag{5.6}$$

where $\boldsymbol{f}$ are polynomial functions in $\boldsymbol{x}$, as discussed in Section 2.1. While extrinsic noise could affect any noise parameters, the simplifying assumption of this chapter is that only the inflow parameters describing reactions of the kind $\emptyset \to X_i$ are stochastic.

Possible physical justifications for this assumption are experimental fluctuations or stochastic subnetworks and both mechanisms are further discussed in Chapter 6.

Without loss of generality, let $\boldsymbol{\kappa'} = \kappa_1, \ldots, \kappa_\ell$ represent the (expectation values of the) reaction rates of the inflow reactions of the first ℓ species and assume that no other species has inflow reactions. A stochastic process $\boldsymbol{K}(t)$ describing the behaviour of the inflow reactions can be found via,

$$\boldsymbol{K}(t) = \boldsymbol{\kappa} + \frac{1}{\sqrt{\Omega}}\sqrt{B}\,\boldsymbol{\eta}, \tag{5.7}$$

where $\boldsymbol{\eta}$ is a vector of truncated Gaussian noise and B is the covariance matrix of the stochastic processes. The notation $\sqrt{B}$ denotes the matrix b such that $B = bb^T$. Note that b may not be unique. The parameter Ω represents the "strength" of the perturbation and further connections to the origin and significance of Ω are highlighted in Chapter 6. Note that $K(t)_i = \kappa_i \; \forall t$ and for all $i > \ell$. A more realistic model might use a non-negative distribution such as log-normal instead of a simple truncated Gaussian and an investigation of log-normal noise could form part of future work. In the remainder of the chapter it is assumed that the truncation is negligible, such that the moments of the truncated distribution can be approximated by the moments of the full Gaussian distribution. This assumption always holds for large enough values of Ω.

By writing the inflow stochastic process as $\boldsymbol{K'} = \boldsymbol{\kappa'} + 1/\sqrt{\Omega}\boldsymbol{\eta}$, the system of equations (5.6) becomes

$$\frac{d\boldsymbol{x}}{dt} = \boldsymbol{f}(\boldsymbol{x}) + \frac{1}{\sqrt{\Omega}}\boldsymbol{\eta}. \tag{5.8}$$

In a similar manner to the intrinsic noise it is assumed that the system (5.6) has one stable steady state only and, therefore, one can linearise the system by letting $\boldsymbol{x} \sim \boldsymbol{x}^* + \overline{\boldsymbol{\delta x}}$ to obtain

$$\frac{d\overline{\boldsymbol{\delta x}}}{dt} = J|_{\boldsymbol{x}=\boldsymbol{x}^*}\overline{\boldsymbol{\delta x}} + \frac{1}{\sqrt{\Omega}}\boldsymbol{\eta}, \tag{5.9}$$

where $J|_{\boldsymbol{x}=\boldsymbol{x}^*}$ is the Jacobian matrix of $\boldsymbol{f}(\boldsymbol{x})$ evaluated at the steady state and for notational convenience is abbreviated to J in the remainder of this chapter. One further assumption is made, namely about the scaling of the perturbation $\overline{\delta\boldsymbol{x}}$ with the parameter Ω controlling the magnitude of the stochastic input. Let $\overline{\delta\boldsymbol{x}} = \Omega^\alpha\delta\boldsymbol{x}$. Then, if $\alpha < -1/2$ and in the limit of $\Omega \to \infty$ the leading order term is the stochastic process $\boldsymbol{\eta}$ only, similarly, if $\alpha > -1/2$, then $\boldsymbol{\eta}$ could be neglected to leading order in Ω. Hence, letting $\alpha = -1/2$ and equation (5.9) simplifies to

$$\frac{d\boldsymbol{\delta x}}{dt} = J\boldsymbol{\delta x} + \boldsymbol{\eta}. \tag{5.10}$$

Equation (5.10) is mathematically *identical* to the CLE (5.1), and, therefore, the power spectra are described by (5.5). However, physically there is the crucial difference that the covariance matrix, B, is fixed by the microscopic dynamics in (5.1), whereas it is a completely arbitrary positive semi-definite matrix in the extrinsic noise case. Hence, it is possible to *choose* B to cater for different mechanistic assumptions in a model. The methods outlined in the sections below apply equally to the intrinsic and extrinsic noise cases and differences only appear in the simulations. In the examples presented in this chapter both cases are simulated and differences are highlighted when they appear.

5.2 Sturm Chains and Digraphs

In this section the power spectra are viewed from an algebraic perspective and Sturm chains are introduced as a tool to find real roots of a polynomial. Further, graph theoretic methods are used to derive conditions for quasi-cycles in stochastic systems. The results of this section are illustrated by example of the three species autocatalytic network.

5.2.1 Sturm Chains for Counting the Maxima of Power Spectra

To find the power spectrum of the ℓ^{th} species one takes the ℓ^{th} diagonal element of the matrix of power spectra introduced in (5.5). The power spectrum of the ℓ^{th} species in the network has the general form of a rational function in ω,

$$P_\ell(\omega^2) = \frac{Q_\ell(\omega^2)}{R(\omega^2)}, \tag{5.11}$$

with

$$R(\omega^2) = \det(J^2 + \omega^2 \boldsymbol{I}), \tag{5.12}$$

$$Q_\ell(\omega^2) = \left([\mathrm{adj}(J + i\omega \boldsymbol{I})]\langle \hat{\boldsymbol{\eta}}\hat{\boldsymbol{\eta}}^\dagger\rangle[\mathrm{adj}(J - i\omega \boldsymbol{I})]^T\right)_\ell, \tag{5.13}$$

where $\boldsymbol{I}$ is the identity matrix, $\mathrm{adj}(\cdot)$ is the adjugate matrix and $(\cdot)_\ell$ denotes the ℓ^{th} diagonal element. $R(\omega^2)$ and $Q_\ell(\omega^2)$ are polynomials of degree n and $n-1$, respectively, with n being the number of species in the network. Note that $R(\omega^2)$ reduces to the characteristic polynomial of J^2 if ω^2 is identified with $-\lambda$. Previous approaches proceeded by analysing all n rational functions of (5.11) to determine the exact shape of the power spectra, and, hence, prove the existence of maxima. In this chapter it

is shown how to determine the number of maxima and their parameter ranges by considering a single polynomial equation. Due to the similarities of the power spectra of the intrinsic and extrinsic noise cases the analysis of this chapter can be applied to both cases and significant quantitative differences arise only in simulations of the systems, when parameter values and correlation matrices are chosen.

Stochastic oscillations manifest themselves as peaks in the power spectra which are closely linked to resonances. In analogy with the damped harmonic oscillator define ω_R to be a resonant frequency, or resonant mode, such that $R(\omega_R^2)$ is at a minimum. This definition implies that the resonant frequencies are properties of the underlying network structure, represented by J^2, rather than the individual network constituents. Furthermore, this definition implies that every species in the network will have the same number of resonant modes, which is, of course, not true in general. In this chapter only networks with no disjoint subnetworks are analysed. Graph theoretically this condition translates into the graph of J, as defined in Section 5.2.2, being connected. If a network has disjoint subnetworks the analysis can be performed separately for each component of the graph of J. The polynomials $Q_k(\omega^2)$ can also suppress stochastic oscillations, but for the purpose of this chapter, the approximation of Dauxois et al. [2009] is used and the generic case where the number of modes is solely determined by $R(\omega^2)$ is assumed. This assumption is the resonance assumption where the power spectra show a peak which is larger than expected [Bartlett, 1957; Nisbet and Gurney, 2003]. Therefore, generically, the number of resonant modes is independent of the noise covariances $\langle \boldsymbol{\eta}\boldsymbol{\eta}^\dagger \rangle$, even though resonance in interaction networks is a stochastic effect.

To find the number of resonance frequencies and their parameter ranges the polynomial $R(\omega^2)$ is studied. At resonance the polynomial $R(\omega^2)$ has a minimum which translates into the condition

$$\frac{\mathrm{d}R(\omega^2)}{\mathrm{d}(\omega^2)} = R'(\omega^2) = 0, \tag{5.14}$$

and, since the angular frequency ω is a real number, all distinct, real, positive solutions to equation (5.14) are of interest. Note that this is also the condition of a maximum. However, exploiting the fact that $R(0) = \text{constant} \geq 0$ and $\lim_{\omega\to\infty} R(\omega^2) \to \infty$, it can be shown that for an even number of extrema there are as many minima as maxima and for an odd number there is one more minimum than there are maxima. Points of inflection are ignored in this chapter due to the very specific conditions on the parameters required. However, the appearance of inflection points in power spectra and their effect could form part of future work. A method to determine an

upper bound of real, positive solutions is given by "Descartes' rule of signs" [Struik, 2014], which states that the maximum number of real, positive roots of a polynomial is given by the number of sign changes of consecutive non-zero coefficients, if the terms of the polynomial are ordered with descending variable exponent. Descartes' rule, however, only gives an upper bound and counts multiple roots as distinct roots.

An exact root counting algorithm is given through the computation of Sturm sequences and the use of Sturm's theorem [Sturm, 1829]. For a univariate polynomial, $p(x)$, Sturm's theorem gives the number of distinct real roots in an interval $(a, b]$ with $a < b$. To apply Sturm's theorem a Sturm chain for $p(x)$ is computed,

$$\begin{aligned} p_0 &= p(x), \\ p_1 &= \tfrac{\mathrm{d}p(x)}{\mathrm{d}x} = p'(x), \\ p_2 &= -\mathrm{rem}(p_0, p_1), \\ &\vdots \\ p_i &= -\mathrm{rem}(p_{i-1}, p_{i-1}), \\ &\vdots \\ 0 &= -\mathrm{rem}(p_{m-1}, p_m), \end{aligned} \tag{5.15}$$

where $\mathrm{rem}(\cdot, \cdot)$ is the remainder of the polynomial long division. Sturm's theorem proceeds by considering the signs of the Sturm chain $p_0, p_1, \ldots, p_m$ evaluated at the points a and b. Similarly to Descartes' rule the number of sign changes of $p_0(a), p_1(a), \ldots, p_m(a)$ and $p_0(b), p_1(b), \ldots, p_m(b)$ is counted which will be denoted as $\sigma(a)$ and $\sigma(b)$. The number of distinct real roots is simply $\sigma(a) - \sigma(b)$. Letting $a = 0$ and $b = \infty$ gives the number of all positive, distinct, real roots. For small networks, especially the case $n = 2$, the number of real roots follows trivially from the quadratic formula and $\det(A + xI) = x^2 + \mathrm{Tr}(A)x + \det(A)$, where $Tr(A)$ is the trace. When turning to larger networks, however, Sturm chains become an invaluable tool.

Example 5.2.1 (Brusselator)**.** *The number of stochastic modes of the Brusselator model introduced in Example 2.3.1 is determined by the quadratic polynomial*

$$R(\omega^2) = \omega^4 + [(\kappa_2 - 1)^2 + \kappa_1^2(\kappa_1^2 - 2\kappa_2)]\omega^2 + \kappa_1^4,$$

which is the characteristic polynomial of the Jacobian matrix of the Brusselator with

$\lambda = -\omega^2$. *Constructing the Sturm chain gives*

$$\begin{aligned} p_0 &= \frac{dR(\omega^2)}{d\omega^2} = 2\omega^2 + (\kappa_2 - 1)^2 + \kappa_1^2(\kappa_1^2 - 2\kappa_2), \\ p_1 &= 2, \\ p_2 &= 0, \end{aligned}$$

which translates into the condition for resonances determined by $\sigma(0)$, $(\kappa_2 - 1)^2 + \kappa_1^2(\kappa_1^2 - 2\kappa_2) < 0$. *Indeed, this condition is simply the discriminant of the solution formula for a quadratic polynomial.*

5.2.1.1 Application to the Three-Species Autocatalytic Network

The methodology of this chapter is illustrated by example of the autocatalytic systems discussed in Dauxois et al. [2009], but the results presented in this chapter can be applied to any dynamical system with a single stable steady state. Autocatalytic reactions form an important class of chemical reaction networks and many biological systems can be modelled by autocatalytic reactions. The defining feature of autocatalytic networks is that one reaction product is the catalyst for some other reactions and the system follows the general reaction scheme [Dauxois et al., 2009]

$$\begin{aligned} X_i + X_{i+1} &\xrightarrow{r_{i+1}} 2X_{i+1}, \\ \emptyset &\xrightarrow{\alpha_i} X_i, \\ X_i &\xrightarrow{\beta_i} \emptyset, \end{aligned}$$

with,

$$X_{n+1} \equiv X_1,$$

for a set of chemical species $\{X_1, \ldots, X_n\}$ and $i = 1, \ldots, n$.

The intrinsic noise case was studied in Dauxois et al. [2009] where a chemical master equation for the autocatalytic system was derived using the stochastic law of mass action discussed in Section 2.2. Using a weak noise expansion [van Kampen, 1983], the deterministic equations for autocatalytic networks of n species were derived in Dauxois et al. [2009]

$$\frac{dx_i}{dt} = (r_i x_{i-1} - r_{i+1} x_{i+1}) x_i + \alpha_i \left(1 - \sum_{j=1}^{n} x_j\right) - \beta_i x_i, \tag{5.16}$$

where x_i denotes the concentration of the i^{th} species. Note that in this model it is assumed, that there is a finite amount of molecules in the system and, therefore, an

extra factor of $\left(1-\sum_{j=1}^{n} x_j\right)$ appears in the inflow term, Following the approaches of Dauxois et al. [2009], and Togashi and Kaneko [2003, 2001], the assumption that $r_i = r_j = r$, $\alpha_i = \alpha_j = \alpha$ and $\beta_i = \beta_j = \beta$ for all i, j is made. With these simplifications it can be shown that the system has a single steady state at

$$x_i^* = \frac{\alpha}{\beta + n\alpha} \equiv x^* \qquad \forall i. \tag{5.17}$$

A linear stability analysis shows that the steady state is stable for all parameter values [Dauxois et al., 2009].

For stochastic dynamics, noise covariance matrix of the intrinsic noise case, B, was found to be of the general form

$$B = \begin{pmatrix} b_0 & b_1 & 0 & 0 & \cdots & b_1 \\ b_1 & b_0 & b_1 & 0 & \cdots & \\ 0 & b_1 & b_0 & b_1 & \cdots & \\ \vdots & \vdots & \vdots & \vdots & \vdots & \vdots \\ b_1 & 0 & \cdots & 0 & b_1 & b_0 \end{pmatrix},$$

with,

$$\begin{aligned} b_0 &= 2r(x^*)^2 + \beta x^* + \alpha(1 - nx^*), \\ b_1 &= -r(x^*)^2, \end{aligned} \tag{5.18}$$

which is completely determined by the reaction rates $\boldsymbol{\kappa} = (\alpha, \beta, r)^T$.

In the extrinsic noise case the deterministic equations (5.16) are linearised, which leads to the Jacobian matrix as defined in Dauxois et al. [2009] and found in this chapter for the three species case and the five species network. Of main importance for extrinsic noise are the inflow parameters α_i. To linearise the inflow term $\alpha_i \left(1 - \sum_{j=1}^{n} x_j\right)$, let $\alpha_i = \mathbb{E}[\alpha_i] + 1/\sqrt{\Omega}\,\eta_i$ and $\boldsymbol{x} = \boldsymbol{x}^* + \overline{\boldsymbol{\delta x}}$, then

$$\alpha_i \left(1 - \sum_{j=1}^{n} x_j\right) = \mathbb{E}[\alpha_i] \left(1 - \sum_{j=1}^{n} x_j^* + \overline{\delta x_j}\right) + \frac{1}{\sqrt{\Omega}} \eta_i \left(1 - \sum_{j=1}^{n} x_j^* + \overline{\delta x_j}\right), \tag{5.19}$$

where the first term is part of the linearisation of the deterministic equations and the second term simplifies to

$$\frac{1}{\sqrt{\Omega}} \eta_i \left(1 - \sum_{j=1}^{n} x_j^* + \overline{\delta x_j}\right) \sim \frac{1}{\sqrt{\Omega}} \eta_i \left(1 - \sum_{j=1}^{n} x_j^*\right), \tag{5.20}$$

as $\overline{\delta x_j}$ is of order $1/\sqrt{\Omega}$ and, hence, $\overline{\delta x_j}(\eta_j/\sqrt{\Omega})$ is of higher order in Ω. Hence, the dynamical equations of the systems subject to extrinsic noise are the linearised deterministic equations with a extra term $\left(1 - \sum_{j=1}^{n} x_j^*\right) \boldsymbol{\eta}$.

An illustrative example of a small system is the $n = 3$ autocatalytic network. The three-species network is in fact the Rock-Paper-Scissors game for which stochastic simulations have been studied in Mobilia [2010]. In Section 5.3 it is shown that the same reasoning can easily be extended to larger networks.

The $n = 3$ autocatalytic network is described by the deterministic equations

$$\begin{aligned}
\dot{x}_1 &= rx_1(x_3 - x_2) + \alpha(1 - x_1 - x_2 - x_3) - \beta x_1, \\
\dot{x}_2 &= rx_2(x_1 - x_3) + \alpha(1 - x_1 - x_2 - x_3) - \beta x_2, \\
\dot{x}_3 &= rx_3(x_2 - x_1) + \alpha(1 - x_1 - x_2 - x_3) - \beta x_3,
\end{aligned} \tag{5.21}$$

with a steady state

$$x_i^* = \frac{\alpha}{\beta + 3\alpha}, \tag{5.22}$$

for every $i = \{1, 2, 3\}$ and, hence, the index is dropped. The Jacobian of (5.21) evaluated at the steady state is

$$J = \begin{pmatrix} -\alpha - \beta & -\alpha - \frac{\alpha r}{\beta+3\alpha} & -\alpha + \frac{\alpha r}{\beta+3\alpha} \\ -\alpha + \frac{\alpha r}{\beta+3\alpha} & -\alpha - \beta & -\alpha - \frac{\alpha r}{\beta+3\alpha} \\ -\alpha - \frac{\alpha r}{\beta+3\alpha} & -\alpha + \frac{\alpha r}{\beta+3\alpha} & -\alpha - \beta \end{pmatrix}, \tag{5.23}$$

and therefore $R(\omega^2)$ is a degree three polynomial. Following the reasoning of the previous section, the Sturm chain for the first derivative of $R(x) = x^3 + a_2x^2 + a_1x + a_0$ will need to be computed, namely

$$\begin{aligned}
p_0(x) &= 3x^2 + 2a_2x + a_1, \\
p_1(x) &= 6x + 2a_2, \\
p_2(x) &= \tfrac{a_2^2}{3} - a_1.
\end{aligned} \tag{5.24}$$

To find stochastic oscillations the Sturm chain needs to be evaluated at the points $x = 0$ and $x \to \infty$,

$$p(\infty) = (3, 6, \tfrac{a_2^2}{3} - a_1), \tag{5.25a}$$

$$p(0) = (a_1, 2a_2, \tfrac{a_2^2}{3} - a_1), \tag{5.25b}$$

and their sign changes need to be found. For stochastic resonance the difference of sign changes need to be to be either one or two. This follows from the fact that $R(-\infty) \to -\infty$ and $R(\infty) \to \infty$ and, therefore, a maximum exists if and only if a minimum exists too and ω^2 of the minimum will be larger than that of the maximum.

As only the minimum is of interest, at least one sign change is needed. Hence, for stochastic oscillations

$$\begin{aligned} a_1 &< 0, \\ a_2 &> 0, \end{aligned} \tag{5.26}$$

or,

$$\begin{aligned} a_1 &> 0, \\ a_2 &< 0, \\ \tfrac{a_2^2}{3} - a_1 &> 0. \end{aligned} \tag{5.27}$$

To relate the abstract notion of polynomial coefficients back to model parameters expressions for the coefficients a_i need to be computed.

From equations (5.26) and (5.27) it becomes apparent that often only specific coefficients of $R(\omega^2)$ need to be evaluated and the polynomial itself need not be found. Often, unless exact parameter ranges are needed, even fewer polynomial coefficients need to be considered due to some coefficients' inability to change sign, a feature easily identified from network motifs in the graph of J^2. In the next section a graph-based method to facilitate the finding of coefficients of $R(\omega^2)$ is outlined, which is based on [Mincheva and Roussel, 2007].

5.2.2 Graph Theoretic Approach

In Mincheva and Roussel [2007] a graph theoretic formula for the coefficients of the characteristic polynomial of the Jacobian of a chemical reaction network is given. A more general relation between the coefficients of a characteristic polynomial of a general square matrix A and the graph associated to A can be found in the earlier work of Maybee et al. [1989]. The ideas of Mincheva and Roussel [2007] and Maybee et al. [1989] are adapted in this chapter for stochastic systems. The squared Jacobian, J^2, which is always a square matrix, is used as an adjacency matrix for a directed graph $\mathcal{G}$. Note that for complete, directed graphs, the calculations of this subsection may be faster if done symbolically, however, if the graph is sparse, then graph theoretic methods can offer significant advantages for calculating (sums of) minors of matrices. Define the vertex set $\mathbb{V}(\mathcal{G}) = \{1, \ldots, n\}$ for an n species interaction network. Notice that, in contrast to the reasoning in Mincheva and Roussel [2007], there is no longer a one to one correspondence between the *vertex* i and the *chemical species* x_i as J^2 is considered rather than J. By definition there is an edge from vertex i to vertex j

if $J^2_{ji} \neq 0$. The convention used in Mincheva and Roussel [2007], and Maybee et al. [1989] is to only draw self loops if $A_{ii} > 0$, however, for convenience, a self loop is always drawn in this chapter, if $J^2_{ii} \neq 0$. It will become apparent that the choice to always draw self loops will only change the visual character of the graph but does not alter the calculations involved in any way. The reason for the convention in previous research was that often the diagonal elements A_{ii} had the same sign for any parameter values, e.g. the diagonal elements of (5.23) are always negative. As in this chapter the square of a matrix is considered, the diagonal elements will generically contain multiple terms and, hence, the sign will depend on the parameter values. Using these conventions, a vertex and an edge set can be defined, from which the directed graph for the $k = 3$ autocatalytic network can be drawn, as shown in Figure 5.1.

In graph theory a cycle c of length k in the graph $\mathcal{G}$ is defined as a series of distinct vertices $\{v_{i_1}, \ldots, v_{i_k}\}$ connected by edges $v_{i_1}v_{i_2}, v_{i_2}v_{i_3}, \ldots, v_{i_k}v_{i_1}$ [Harary, 1969]. For a cycle c denote $J^2[c] = (J^2)_{v_{i_2}v_{i_1}}(J^2)_{v_{i_3}v_{i_2}} \cdots (J^2)_{v_{i_1}v_{i_k}}$, which is the product of all the edge weights in the cycle. The cycles in an interaction graph such as Figure 5.1 will be the fundamental building blocks for this graph theoretic approach. The graph in Figure 5.1 has eight cycles, two of length three ($\{1,2,3\}$ and $\{3,2,1\}$), three of length two ($\{1,3\}$, $\{1,2\}$ and $\{2,3\}$) and three length one cycles which are the self loops. In the method presented in this chapter complete directed graphs only are handled, as, even though the Jacobian matrix of a chemical reaction system may be sparse, its square will generically be a dense matrix. Therefore, efficient enumeration of cycles will be a non-trivial limitation of this method. Computational experiments in SageMath [Stein et al., 2016] show that cycle enumeration for small graphs is fast, and is therefore not a time limiting step in the calculation of phase diagrams.

Using the directed cycles of a graph $\mathcal{G}$ as building blocks the concept of factors can be defined. A factor f_k of degree k of $\mathcal{G}$ is a collection of pairwise disjoint cycles covering k distinct vertices. The number of cycles in a factor f_k is denoted by $|f_k|$ which is called the cardinality of the factor. Hence, a graph can have multiple factors of the same degree, but with a vastly different number of cycles, e.g. the graph in Figure 5.1 has a factor of degree three $f_3^{(1)} = \{\{1,2,3\}\}$ with $|f_3^{(1)}| = 1$ and a factor of the same degree $f_3^{(2)} = \{\{1\},\{2\},\{3\}\}$ with $|f_3^{(2)}| = 3$. Other factors of degree three can be built from the cycles.

Consider the characteristic polynomial $p(x) = x^n + \sum_{i=0}^{(n-1)} a_i x^i$ of a matrix A. It is possible to adapt a graph theoretic formula to find the coefficients a_i derived in [Maybee et al., 1989] and applied to interaction networks in Mincheva and Roussel

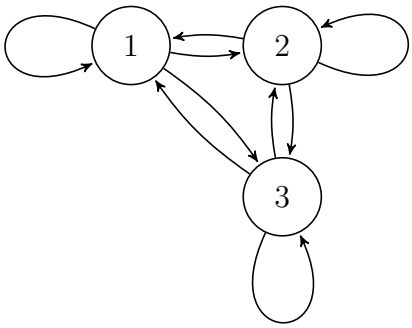


Figure 5.1: The directed graph associated with J^2 of the $n = 3$ autocatalytic network. The edges have weights: $1 \to 1 = 2 \to 2 = 3 \to 3 : (\alpha+\beta)^2+2(\alpha+\alpha r/(3\alpha+\beta))(\alpha-\alpha r/(3\alpha+\beta))$, $2 \to 1 = 3 \to 2 = 1 \to 3 : 2(\alpha+\beta)(\alpha+\alpha r/(3\alpha+\beta))+(\alpha-\alpha r/(3\alpha+\beta))^2$ and $3 \to 1 = 1 \to 2 = 2 \to 3 : (\alpha+\alpha r/(3\alpha+\beta))^2+2(\alpha+\beta)(\alpha-\alpha r/(3\alpha+\beta))$.

[2007]. If the graph associated to the matrix A is $\mathcal{G}$ then

$$a_{n-k} = \sum_{f_k \in \mathcal{G}} (-1)^{|f_k|+k} \prod_{c \in f_k} A[c] \qquad k = 1, \ldots, n \tag{5.28}$$

where in the case of stochastic networks $A = J^2$ and all other quantities are as previously defined.

While finding factors is trivial for small graphs, the task can become computationally intractable for larger networks with more than six vertices. This is mainly due to the fact that no efficient algorithms for finding all possible factors of a graph exist. Additionally, the complexity is increased as directed graphs are considered, which are generically complete. Finding all factors is the main bottleneck of the method.

Returning to equations (5.26) and (5.27) expressions for a_1 and a_2 and need to be calculated. Hence, all factors of degree two and one need to be found, which are summarised in Table 5.1. Therefore, by utilising equation (5.28), the expressions for the coefficients a_1 and a_2 are

$$a_2 = \frac{3(27\alpha^4+36\alpha^3\beta+24\alpha^2\beta^2+8\alpha\beta^3+\beta^4-2\alpha^2r^2)}{9\alpha^2+6\alpha\beta+\beta^2}, \tag{5.29}$$

$$\begin{aligned} a_1 = &\frac{3(486\alpha^6\beta^2+972\alpha^5\beta^3+837\alpha^4\beta^4+396\alpha^3\beta^5)}{81\alpha^4+108\alpha^3\beta+54\alpha^2\beta^2+12\alpha\beta^3+\beta^4}+ \\ &+\frac{3(108\alpha^2\beta^6+16\alpha\beta^7+\beta^8+3\alpha^4r^4)}{81\alpha^4+108\alpha^3\beta+54\alpha^2\beta^2+12\alpha\beta^3+\beta^4}- \\ &-\frac{18(27\alpha^6+36\alpha^5\beta+15\alpha^4\beta^2+2\alpha^3\beta^3)r^2)}{81\alpha^4+108\alpha^3\beta+54\alpha^2\beta^2+12\alpha\beta^3+\beta^4}. \end{aligned} \tag{5.30}$$

$\boldsymbol{k=1}$	**Cycles**	**Cardinality**
$f_1^{(1)}$	$\{1\}$	1
$f_1^{(2)}$	$\{2\}$	1
$f_1^{(3)}$	$\{3\}$	1
$\boldsymbol{k=2}$	**Cycles**	**Cardinality**
$f_2^{(1)}$	$\{\{1,3\}\}$	1
$f_2^{(2)}$	$\{\{1,2\}\}$	1
$f_2^{(3)}$	$\{\{2,3\}\}$	1
$f_2^{(4)}$	$\{\{1\},\{2\}\}$	2
$f_2^{(5)}$	$\{\{1\},\{3\}\}$	2
$f_2^{(5)}$	$\{\{2\},\{3\}\}$	2

Table 5.1: A summary of all relevant factors in the $n = 3$ autocatalytic network graph.

From the relations (5.26), (5.27), (5.29) and (5.30) a phase diagram of the system can be plotted by either simplifying the resulting set of inequalities using cylindrical algebraic decomposition [Arnon et al., 1984] or numerically, by substituting in parameter values. A summary of the phases of the $n = 3$ autocatalytic network can be found in Figure 5.2.

The trajectories of the $n = 3$ network were simulated in the intrinsic and extrinsic noise case using an Euler-Maruyama method [Kloeden and Platen, 1995] to integrate equation (5.1). In the intrinsic noise case the covariance matrix (5.18) was used with the parameters $\alpha = \beta = 0.1$, $r = 1$ and $\Omega = 5000$. The amplitude of oscillations reached about 10% of the steady state value as can be seen in Figure 5.3a and there was good agreement between the analytic power spectrum and the simulation as shown in Figure 5.3b.

In the extrinsic noise case the prefactor to the noise term $\boldsymbol{\eta}$, $\left(1 - \sum_{j=1}^{n} x_j^*\right)$, simplifies to 1/4, if $\alpha = \beta$. Hence, by choosing $B_{\text{ext}} = 1/16B$ the dynamics of the intrinsic noise is recovered. To best highlight the difference between extrinsic and intrinsic noise this choice was made and the parameters chosen were $\alpha = \beta = 6.0$, $r = 15.0$ and Ω was kept at 5000. While still in the oscillatory regime predicted by the set of inequalities (5.29)-(5.30), there are quantitative differences between the extrinsic and the intrinsic noise case. Most importantly, due to the limitation on the noise strength, owing to the fact that $\alpha > 0$ at all times, the amplitude of oscillations is greatly reduced to about 4% of the steady state value, as can be seen in Figure 5.3c. As a consequence, the total power in the system is much lower as highlighted

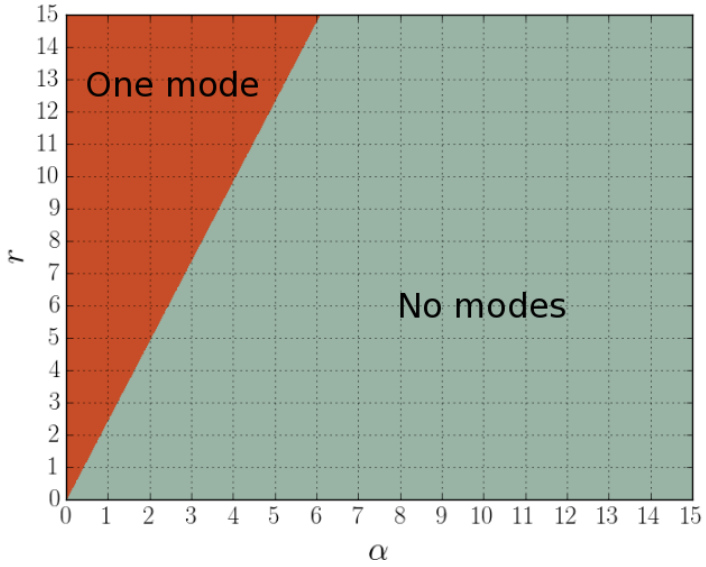
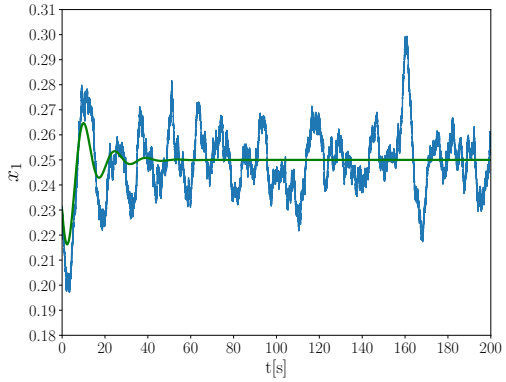


Figure 5.2: The phase diagram for the $\alpha = \beta$ slice of the parameter space of the $n = 3$ autocatalytic network computed from relations (5.26), (5.27), (5.29) and (5.30). There are two connected regions, one where stochastic oscillations are possible and one where the power spectrum is flat. Note that the two regimes are separated by a straight line.

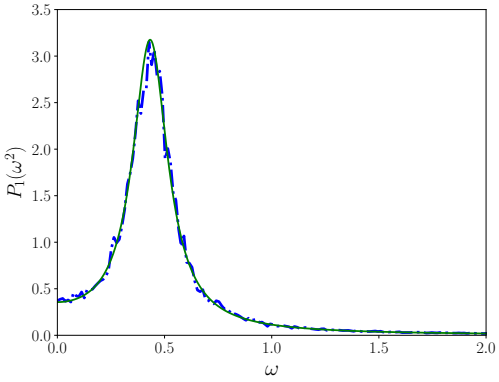
by the smaller $y-$axis values in Figure 5.3d, even though there is still a prominent peak in the spectrum.

5.3 Application to Larger Networks

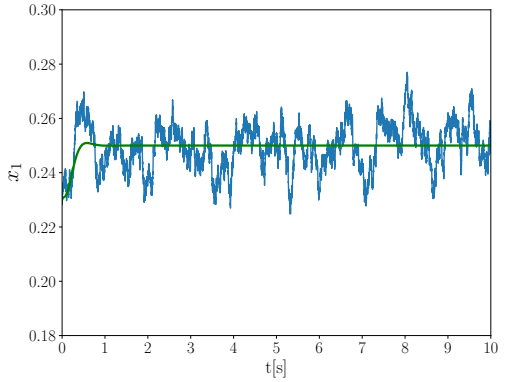
In this section it is illustrated that the method developed in this chapter can be applied with ease to larger networks by example of the $n = 5$ autocatalytic network. Traditional methods include the exact calculation of the power spectrum from the chemical Langevin equation [McKane and Newman, 2005] or approximations via the eigenvalues of the Jacobian matrix [Dauxois et al., 2009]. These tools have the capabilities of achieving the same results of finding the number of modes of a stochastic system, however they are subject to serious drawbacks. Analytic expressions for the exact power spectra of a network can be calculated quickly in symbolic packages such as Mathematica [Wolfram Research, Inc., 2010] or SageMath [Stein et al., 2016]. However, in the intrinsic noise case such a calculation involves knowledge of the correlations of the Markov processes η_i, $\langle \eta_i(t)\eta_j(t')\rangle = B_{ij}\delta(t-t')$, which are cumbersome to compute. Moreover, the full analytic form does not *a priori* give away any information about the number of stochastic modes of a system. To extract this information



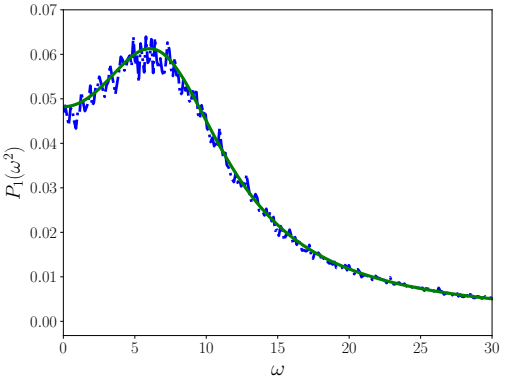
(a) An intrinsic noise trajectory with parameter values $\alpha = \beta = 0.1$, $r = 1.0$. The oscillating trajectory is the stochastic trajectory.



(b) The power spectrum of the intrinsic noise system with parameter values $\alpha = \beta = 0.1$, $r = 1.0$. The analytic curve was calculated from equation (14) in Dauxois et al. [2009] and the dotted line is the average power spectrum of 200 simulations.



(c) An extrinsic noise trajectory with parameter values $\alpha = \beta = 6.0$, $r = 15.0$. The oscillating trajectory is the stochastic trajectory.



(d) The power spectrum of the extrinsic noise system with parameter values $\alpha = \beta = 6.0$, $r = 15.0$. The analytic curve was calculated from equation (14) in Dauxois et al. [2009], and the dotted line is the average power spectrum of 500 simulations.

Figure 5.3: A comparison of the intrinsic and extrinsic noise behaviour of the three species autocatalytic networks with $\Omega = 5000$. The smooth, green curves represent the deterministic trajectories in subfigures 5.3a and 5.3c and the analytic spectra in subfigures 5.3b and 5.3d. Following [Toner and Grima, 2013], the spectra are normalised such that they have unit area.

one would need to analyse the full rational function that is the power spectrum. While this is at best impractical, it can often be impossible and approximations need to be used. One such approximation was outlined in Dauxois et al. [2009] and it focused on the pairs of complex conjugate eigenvalues of the Jacobian matrix. In Dauxois et al. [2009] it was argued that the system will have a stochastic resonance if there exists a complex conjugate pair of eigenvalues $\lambda_i,\ \lambda_i^*$ such that $\Im(\lambda_i)^2 - \Re(\lambda_i)^2 > 0$. While this is a quick and elegant method which also gives additional information about the relative intensities of resonances, it can lead to false positives. In particular, parameter regions for stochastic oscillations will be *smaller* than predicted as the approximation focuses on one factor of the characteristic polynomial of J^2 at a time. In practice, however, other factors can "destroy" the resonance. The method outlined in this chapter will be able to exactly predict the parameter regions and the number of stochastic resonances, however, there are limitations on the network size which are also discussed in this section.

The five species autocatalytic network is described by the equations

$$\begin{aligned}
\dot{x}_1 &= rx_1(x_5 - x_2) + \alpha(1 - x_1 - x_2 - x_3 - x_4 - x_5) - \beta x_1,\\
\dot{x}_2 &= rx_2(x_1 - x_3) + \alpha(1 - x_1 - x_2 - x_3 - x_4 - x_5) - \beta x_2,\\
\dot{x}_3 &= rx_3(x_2 - x_4) + \alpha(1 - x_1 - x_2 - x_3 - x_4 - x_5) - \beta x_3,\\
\dot{x}_4 &= rx_4(x_3 - x_5) + \alpha(1 - x_1 - x_2 - x_3 - x_4 - x_5) - \beta x_4,\\
\dot{x}_5 &= rx_5(x_4 - x_1) + \alpha(1 - x_1 - x_2 - x_3 - x_4 - x_5) - \beta x_5.
\end{aligned} \tag{5.31}$$

The steady state of the system is

$$x_i^* = \frac{\alpha}{\beta + 5\alpha}, \tag{5.32}$$

for every $i = \{1, \ldots, 5\}$. The Jacobian evaluated at the steady state is

$$J = \begin{pmatrix}
J_0 & J_1 & J_2 & J_2 & J_3\\
J_3 & J_0 & J_1 & J_2 & J_2\\
J_2 & J_3 & J_0 & J_1 & J_2\\
J_2 & J_2 & J_3 & J_0 & J_1\\
J_1 & J_2 & J_2 & J_3 & J_0
\end{pmatrix}, \tag{5.33}$$

with

$$\begin{aligned}
J_0 &= -\alpha - \beta,\\
J_1 &= -\alpha - \frac{r\alpha}{\beta + 5\alpha},\\
J_2 &= -\alpha,\\
J_3 &= \alpha + \frac{r\alpha}{\beta + 5\alpha}.
\end{aligned} \tag{5.34}$$

A linear stability analysis guarantees that system (5.31) is stable for any positive parameter values.

To determine the phase diagram one can follow the exact same procedure described above, namely:

1. compute the Sturm chain for a generic degree $n-1$ polynomial;
2. determine sets of inequalities on the Sturm coefficients to give resonances;
3. compute the relevant coefficients of the polynomial using graph theoretic methods;
4. use the information from steps 2 and 3 to plot a phase diagram.

In practice, however, this turns out to be impractical due to the vast number of sets of inequalities involved in step two, in addition to the quickly rising number of cycles and factors involved in step three. Furthermore, the explicit expressions for the Sturm coefficients can be cumbersome to work with. While it is possible to do step three on a computer, the inequalities involved in step two need to be formulated by hand. Therefore, to optimise the procedure for automation the following algorithm is used:

1. compute the Sturm chain for a generic degree $n-1$ polynomial;
2. compute the relevant coefficients of the polynomial using symbolic or graph theoretic methods, depending on the sparseness of the J^2 matrix;
3. substitute parameter values and compute the number of real, positive roots;
4. use this information to find the number of stochastic modes;
5. plot the phase diagram.

Step four is necessary due to the fact that a real, positive root could indicate a maximum or a minimum of $R(\omega^2)$. This second algorithm can easily be implemented on a computer and phase diagrams can be calculated quickly. The only input required is a Jacobian evaluated at the steady state. The method was implemented in SageMath to plot a phase diagram for the $n = 5$ autocatalytic network in the $\alpha = \beta$ plane. The results are summarised in Figure 5.4. There are three regions in the phase diagram with two, one and no stochastic modes. As in the three species case an Euler-Maruyama integration of equation (5.1) was performed for the intrinsic and extrinsic noise scenario respectively in the two-resonance regime.

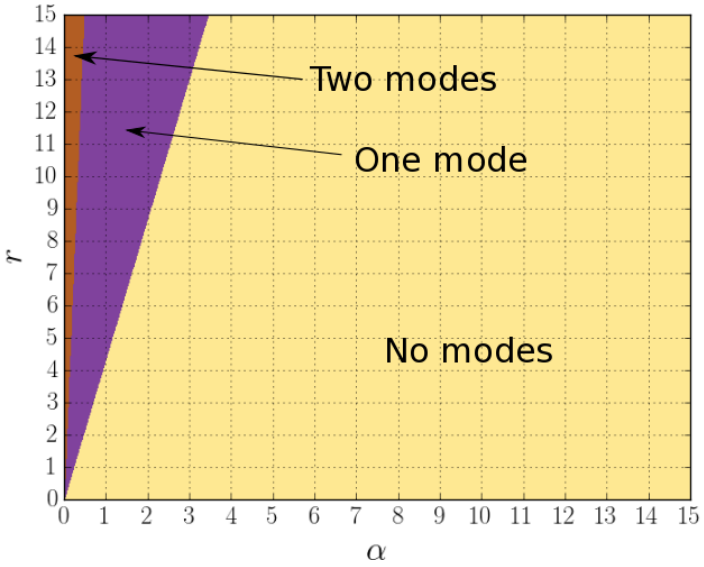


Figure 5.4: The phase diagram for the $\alpha = \beta$ slice of the parameter space of the $n = 5$ autocatalytic network. Three connected regions were identified, one where there are two stochastic modes, one with only one mode and where no oscillations are possible.

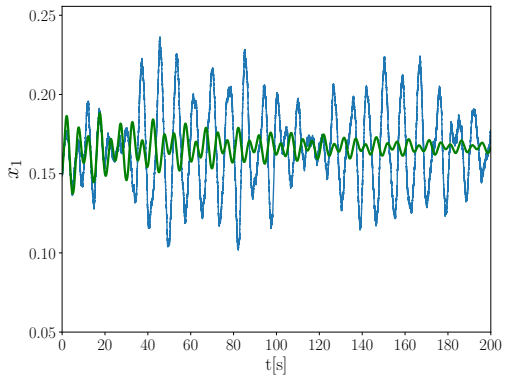
The results of the intrinsic noise simulation are summarised in Figure 5.5a and 5.5b and show the beating pattern in the stochastic trajectory that is expected from two oscillation frequencies.

The results of the extrinsic noise simulation are shown in Figure 5.5c and 5.5d. To highlight the fact that arbitrary correlation matrices can be chosen the correlation matrix for this simulation was

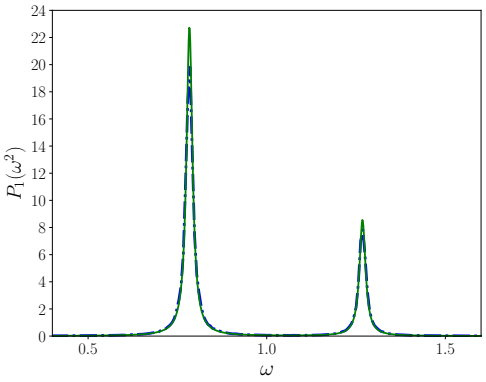
$$B = \begin{pmatrix} 0.0036 & 0 & 0 & 0 & 0 \\ 0 & 0.0036 & 0 & 0 & 0 \\ 0 & 0 & 0.0036 & 0 & 0 \\ 0 & 0 & 0 & 0.0036 & 0 \\ 0 & 0 & 0 & 0 & 0.0036 \end{pmatrix}, \tag{5.35}$$

and the prefactor to $\boldsymbol{\eta}$ simplifies to $1/6$. The parameter Ω was kept at 5000 and the other model parameters were $\alpha = \beta = 0.1$ and $r = 40.0$. Similarly to the three species case there were quantitative rather than qualitative differences, e.g. reduced oscillation amplitude, in the simulations. The origin of these differences is partly the restriction to $\alpha > 0$ at all times.

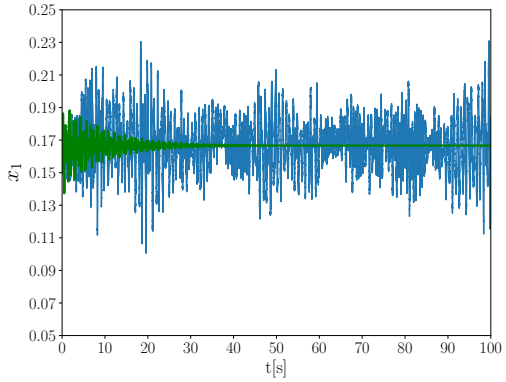
In principle the method presented in this paper could be applied to networks of arbitrary number of species, however, there are a number of problems one encounters in networks with more species. The first problem is of a fundamental nature and was already discussed in Subsection 5.2.2, namely the fact that the graphs encountered are



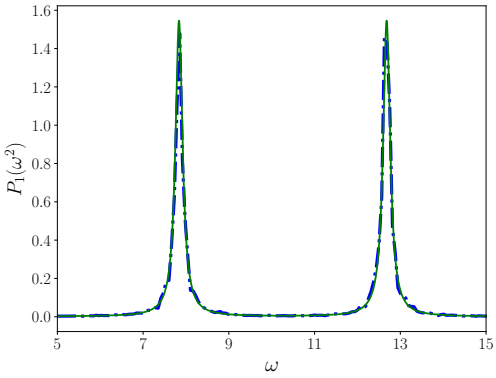
(a) A trajectory of the intrinsic noise system with parameter values $\alpha = \beta = 0.01$, $r = 4.0$ and $\Omega = 10000$. The oscillatory curve is the stochastic trajectory.



(b) The power spectrum of the intrinsic noise system with parameter values $\alpha = \beta = 0.01$, $r = 4.0$ and $\Omega = 10000$. The dotted blue line is the average power spectrum of 500 simulations.



(c) A trajectory of the extrinsic noise model with parameter values $\alpha = \beta = 0.1$, $r = 40.0$ and $\Omega = 5000$. The oscillatory curve is the stochastic trajectory.



(d) The power spectrum of the extrinsic noise model with parameter values $\alpha = \beta = 0.1$, $r = 40.0$ and $\Omega = 5000$. The dotted blue line is the average power spectrum of 40 simulations.

Figure 5.5: A comparison of the intrinsic and extrinsic noise behaviour of the five species autocatalytic networks. The smooth, green curves represent the deterministic trajectories in subfigures 5.5a and 5.5c and the analytic spectra in subfigures 5.5b and 5.5d. Following [Toner and Grima, 2013], the spectra are normalised such that they have unit area.

normally complete, directed graphs and finding the factors of such a graph is a non-trivial task. In general, (symbolically) computing minors of matrices with general polynomial or rational entries of is highly non-trivial. The second issue is to do with numerical errors during computations. Substituting parameter values into the Sturm coefficients requires extensive floating point arithmetic and when the Sturm coefficients are small, numerical errors will change the result. While the method should generally be robust, as only signs and sign changes are needed, as soon as one coefficient is small, numerical fluctuations will become significant.

5.4 Conclusion

Numerous dynamical systems, which appear stable in a deterministic regime, can exhibit oscillatory behaviour when model stochasticity is accounted for. Such stochastically driven oscillations are likely to be missed in many applications.

In the first part of this chapter, a theory for extrinsic noise in coupled chemical reactions was developed. To this end, a stochastic process, which governs the parameters of the inflow reactions of the network, was defined. The process was modelled by a truncated Gaussian distribution and it was shown, how under this assumption the formulas for the Langevin equations and power spectra of the intrinsic and extrinsic noise systems were identical.

In the second part of this chapter, simple and general graph theoretic tools were developed, which allow for ODE systems to be analysed as to the possibility of the occurrence of quasi-cycles. It was shown how Sturm's theorem can be applied to the denominator of a rational function which determines the power spectrum of the stochastic chemical reaction network. This resulted in conditions for the exact number of stochastic resonance modes or quasi-cycle frequencies. The set of inequalities thus obtained was then studied further by transforming the conditions on polynomial coefficients to constraints on parameters values. To this end, the graph theoretic formulas developed for deterministic systems were modified and applied to the directed graph defined by the squared Jacobian matrix. Finally, sample trajectories, the averaged power spectra and the phase diagrams for two autocatalytic systems were computed numerically. It was shown that, despite the different physical mechanisms involved and the arbitrary correlation matrices in the extrinsic noise case, the same qualitative features arise in both models.

While a simple and powerful technique, the task of finding factors leads to a hard combinatorial problem, which limits the system size to about 10 species. Further

limitations are the numerical inaccuracies which propagate through the system when the symbolic expressions are evaluated. These inaccuracies can lead to a sign change in the polynomial coefficients and, hence, a false number of resonant modes. This fact further limits the feasible system size to about 8 species. Future research could target these limitations by developing efficient algorithms for finding factors in graphs and, potentially circumvent the numerical fluctuations. The next chapter, Chapter 6, extends the application of power spectra methods to stochastic spatial systems subject to extrinsic noise such as deterministic Turing patterns with stochastic inflows.

Chapter 6

Coloured Noise From Stochastic Inflows in Reaction-Diffusion Systems

> *"The idea would be in my mind - and I know it sounds strange - is that the most important advances in medicine would be made not by new knowledge in molecular biology, because that's exceeding what we can even use. It'll be made by mathematicians, physicists, computer scientists, figuring out a way to get all that information together."*
>
> – Patrick Soon-Shiong

This chapter is based on work published by Adamer et al. [2020].

One of the central challenges in mathematical biology is understanding mechanisms involved in developmental processes. Within the context of developmental biology, the emergence of large scale spatial structure, has often been theoretically explored through the common framework of deterministic partial differential equations defining reaction-diffusion systems [Murray, 2008; Hochberg et al., 2003; Turing, 1952]. While current models may explain a variety of phenomena in development, they can also suffer from over-simplification [McKane et al., 2014]. Further, there is the caveat that finding theoretical models, both consistent with mechanism-based knowledge and capable of predicting observed patterns, is a highly complex task. Many such models suffer from both, model and parameter fine tuning [Butler and Goldenfeld, 2011; Xavier, 2013].

Furthermore, models that describe pattern formation assume that their parameters are constant. However, as described in Chapter 2, this deterministic assumption is not suitable in certain situations. Some systems are better suited towards a stochastic

approach; in particular, when a system is coupled to external and stochastic drivers, the parameter values can change. The stochastic driving force is often represented by stochastic parameters, as outlined in Chapter 2. A parameter is drawn from a certain distribution at each time step or spatial point, and referred to as extrinsic noise below. This contrasts with most previous work on stochastic pattern formation, referred to as intrinsic noise, which assumes low copy number and it does not model external drivers as the source of noise [Schumacher et al., 2013; McKane and Newman, 2005; McKane et al., 2014; Biancalani et al., 2011; Woolley et al., 2012, 2011a].

As mentioned in Chapter 2, the structure of intrinsic noise can often be highly constrained and, in particular, uncorrelated in time, leading to white noise systems. Nevertheless, even with the constraints of intrinsic noise, there is a rich diversity of noise-induced phenomena, such as spatio-temporal pattern formation [Schumacher et al., 2013; Woolley et al., 2012], and other manifestly stochastic behaviour such as outlined in Chapter 1.

However, when the source of the noise is external, other forms of noise are permissible. In particular, the defining special properties of white noise may in general be relaxed. Hence, stochastic forcing can emerge with non-trivial temporal correlations, often termed *coloured noise*. The objective of this chapter is to show how extrinsic noise influences spatio-temporal reaction-diffusion patterns and, in particular, to develop power spectral methods to analyse the impact of coloured noise. In this chapter it is assumed that the effects of intrinsic noise are negligible and only the extrinsic noise provides a stochastic perturbation of the system. Therefore, in contrast to intrinsic noise models, the common description of a stochastic chemical reaction network as a continuous time Markov chain (and its computational solution via the Gillespie algorithm [Gillespie, 1977]) cannot typically be applied.

To proceed, the biological system is abstracted to a chemical reaction network and techniques from the mathematical modelling of chemical reaction networks can be used. However, for biological interpretations it is imperative to remember that many cellular processes are governed by biochemical reactions [Alberts et al., 2007] and, hence, can be described by chemical reaction networks. To proceed, as briefly remarked in Chapter 1 and Chapter 2, let deterministic pattern formation in biological systems with n interacting biochemical species take the reaction diffusion form, [Turing, 1952; Murray, 2008]

$$\frac{\partial \boldsymbol{x}}{\partial t} = \boldsymbol{D}\frac{\partial^2 \boldsymbol{x}}{\partial s^2} + \boldsymbol{f}(\boldsymbol{x}), \tag{6.1}$$

in one spatial dimension s, and $\boldsymbol{x} \in \mathbb{R}^n_{\geq 0}$ is a vector of n chemical concentrations. The models considered require the term $\boldsymbol{f}(\boldsymbol{x}) = (f_1(\boldsymbol{x}), \ldots, f_n(\boldsymbol{x}))^T$ to be a vector of rational functions. The rational functions describe the underlying reaction network between the species and $\boldsymbol{D}(\partial^2\boldsymbol{x}/\partial s^2)$ with $\boldsymbol{D} = \text{diag}(D_1, \ldots, D_n)$ describes the diffusion of $\boldsymbol{x}$. Let there be m chemical reactions in the spatially homogeneous system whose dynamics are described by $d\boldsymbol{x}/dt = \boldsymbol{f}(\boldsymbol{x})$. Each reaction is parameterised by a rate constant $\kappa_i > 0$ and, therefore, a vector of rate constants $\boldsymbol{\kappa} = (\kappa_1, \ldots, \kappa_m) \in \mathbb{R}^m_{>0}$ can be defined. Throughout this chapter the analysis is restricted to mass action kinetics (see Chapter 2), rendering $\boldsymbol{f}(\boldsymbol{x})$ a vector of polynomials and homogeneous Neumann boundary conditions are used,

$$\left.\frac{\partial \boldsymbol{x}}{\partial s}\right|_{s=0,L} = 0\,, \tag{6.2}$$

where L is the domain length. Note that, although the analysis of this chapter is only applied to systems of one spatial dimension, the theory can easily be extended to an arbitrary number of spatial dimensions. Counter-intuitively, it has been shown that under certain conditions [Murray, 2008] diffusion can drive an otherwise spatially uniform stable state to instability. Such unstable systems, which can form stable patterns, such as stripes or spots, are called *Turing Systems* [Turing, 1952; Woolley et al., 2017] and previous results have been discussed in Section 1.2 of Chapter 1. Crucially, Turing theory is a local theory with two species $\boldsymbol{x} = (x_1, x_2)^T$ and the system $\boldsymbol{f}(\boldsymbol{x})$ is at a steady state $\boldsymbol{x} = \boldsymbol{x}^*$ such that $\boldsymbol{f}(\boldsymbol{x}^*) = 0$. Despite the original work only considering two species, the analysis can be generalised to n species. By linearising equation (6.1) around the steady state $\boldsymbol{x} = \boldsymbol{x}^* + \boldsymbol{\delta x}$ the Jacobian matrix of the two-species system is obtained

$$J = \begin{pmatrix} f_{1x_1} & f_{1x_2} \\ f_{2x_1} & f_{2x_2} \end{pmatrix}, \tag{6.3}$$

where $f_{ix_j} = \partial f_i/\partial x_j|_{\boldsymbol{x}=\boldsymbol{x}^*}$. Further, for patterns, solutions of the form $\boldsymbol{\delta x} = \boldsymbol{x}_0 e^{iks+\lambda t}$ are sought and, hence, equation (6.1) is transformed to

$$0 = (-\lambda - k^2\boldsymbol{D} + J)\boldsymbol{\delta x}. \tag{6.4}$$

For non-trivial solutions it is required that the determinant $\det(-\lambda - k^2\boldsymbol{D} + J) = 0$. Therefore, by computing the Turing conditions, which state that

(i) the non-spatial system has a stable steady state (eigenvalues of J have a real part less than zero) and

(ii) the spatial system has a growing perturbation to the homogeneous solution (the real part of some λ which solves $\det(-\lambda - k^2\boldsymbol{D} + J) = 0$ is larger than zero),

the inequalities for pattern formation are obtained. Explicitly, they read

$$f_{1x_1} + f_{2x_2} < 0, \tag{6.5a}$$

$$f_{1x_1}f_{2x_2} - f_{2x_1}f_{1x_2} > 0, \tag{6.5b}$$

$$D_1 f_{2x_2} + D_2 f_{1x_1} > 2\sqrt{D_1 D_2}\sqrt{f_{1x_1}f_{2x_2} - f_{2x_1}f_{1x_2}} > 0. \tag{6.5c}$$

Parameters obeying these inequalities are said to be in the Turing regime. However, as mentioned in Section 1.2 of Chapter 1, patterns are also possible outside the Turing regime when stochastic fluctuations are considered.

To avoid the complications of bistable dynamics, and, later, the stochastic analogues such as switching between steady states in the general equation (6.1), the constraint that the spatially homogeneous solution has a unique stable steady state, $\boldsymbol{x}^*$, such that $\boldsymbol{f}(\boldsymbol{x}^*) = 0$ is imposed in this chapter. To find models which have this property techniques from real algebraic geometry [Müller et al., 2016] are used which provides simple tools to ensure there exists only a single steady state in a model.

Fundamentally, the application of a set of partial differential equation (PDE) models for a biochemical reaction system assumes that the species of interest are in high enough concentration to allow continuum modelling. By contrast, when the number of particles in the biological system is low, intrinsic stochasticity of the system must be included in the model [Schumacher et al., 2013; Woolley et al., 2012; McKane and Newman, 2005; McKane et al., 2014; Biancalani et al., 2011], which typically yields studies that investigate the impact of white noise.

However, as mentioned, stochasticity in biological systems can also arise from extrinsic noise and temporal variations in parameter values [Picco et al., 2017]. Thus, instead, the deterministic system is generalised to include *stochastic* parameter values. In a similar manner to the results of Chapter 5, the focus lies on the effect of stochastic fluctuations in the constant term, the "inflow" term, of the chemical reaction network $\boldsymbol{f}(\boldsymbol{x})$. As the extrinsic noise can arise from a vast number of different mechanisms, such as varying experimental conditions [Lenive et al., 2016], it is largely free of microscopic constraints, especially the absence of temporal correlation. However, the impact of correlated extrinsic noise has, to the extent the literature review can reveal, received little theoretical modelling attention. Thus, the aim of this chapter is to develop a framework to study extrinsic coloured noise forcing of the above deterministic system for pattern formation in biologically motivated scenarios and

to analyse how temporal correlation in noise, as described by colour, impacts self-organisation properties.

The chapter is organised as follows. In Section 6.1 the required notions of real algebraic geometry to select a class of models relevant to the framework of this chapter is introduced, i.e. those models whose number of steady states is unaltered by changes in parameter values, temporal or otherwise. Further, stochastic inflow parameters are introduced and their connection to coloured noise is described. In particular, noise arising from stochastic subnetworks and varying experimental conditions is discussed. In Section 6.2 the impact of noise colouring on the spatio-temporal patterns formed is highlighted by example of the Schnakenberg system. The numerical results are discussed in Section 6.3, where the distinguishable differences between the various noise colours are highlighted. The results are summarised in Section 6.4.

6.1 Theoretical Results

In this section the theoretical background of this chapter is introduced.

6.1.1 Sign Conditions for Monostationarity

The methods of this chapter are based on the work of Müller et al. [2016] and can be applied to any polynomial system arising from chemical reaction networks with mass action kinetics as introduced in Section 2.1.

In this chapter the influence of noise on reaction-diffusion systems that are able to produce patterns in a well-defined parameter region is studied. Critically, it will be shown that coloured noise is able to have both a constructive influence outside of this previously defined parameter region (i.e. the noise stabilises patterns where no patterns are expected deterministically), as well as a destructive influence on patterns which normally would arise. In particular, it is desirable to exclude the intrinsically stochastic effect of *stochastic switching*, which occurs for a system that has multiple steady states in some parameter region. Stochastic switching describes the phenomenon that a chemical reaction network can jump from one steady state to another when subject to finite stochastic perturbations. Hence, the resulting steady state distribution is multimodal. To avoid this scenario, a network structure based tool described in Müller et al. [2016] is used which allows for a priori exclusion of multistationarity.

Take a chemical reaction network $\mathfrak{N}$ with n species and embed its complexes and reactions into $\mathbb{R}^n$. For a reaction $C_i \to C_j$ let C_i be the reactant complex and C_j

the product complex. Then, define the matrices $M_1 = (\boldsymbol{r}_1\boldsymbol{r}_2\cdots\boldsymbol{r}_m)$ for $\boldsymbol{r}_i \in \mathcal{R}$ and $M_2^T = (\boldsymbol{b}_1\boldsymbol{b}_2\cdots\boldsymbol{b}_r)$ where $\{\boldsymbol{b}_i\}$ is the set of reactant complex vectors of $\mathfrak{N}$. Let $\text{diag}(\kappa_1,\ldots,\kappa_m)$ be the diagonal matrix of reaction constants. Using the law of mass action the dynamics of the species concentrations can be described by

$$\frac{d\boldsymbol{x}}{dt} = \boldsymbol{f}(\boldsymbol{x}) = M_1\,\text{diag}(\kappa_1,\ldots,\kappa_m)\,\boldsymbol{x}^{M_2} \tag{6.6}$$

where $\boldsymbol{x}^{M_2} = (x_1^{b_{11}}x_2^{b_{12}}\cdots x_n^{b_{1n}},\ldots,x_1^{b_{m1}}x_2^{b_{m2}}\cdots x_n^{b_{mn}})^T$. Note that the reactant complexes and the reactions are structural properties of the reaction graph. Further, let $\boldsymbol{a} \in \mathbb{R}^n$ and define its sign vector $\sigma(\boldsymbol{a}) = \{-,0,+\}^n$ by applying the sign function to each component of $\boldsymbol{a}$. Therefore, the i^{th} component of the sign vector $\sigma(\boldsymbol{a})_i = \text{sign}(a_i) \in \{+,0,-\}$.

The link from network structure to multistationarity is formed via the injectivity of the map $\boldsymbol{f}(\boldsymbol{x})$ and summarised in Theorem 6.1.1, which is a corollary of Müller et al. [2016, Theorem 1.4]. If $\boldsymbol{f}(\boldsymbol{x})$ is injective then there exists a unique vector $\boldsymbol{x}^* \in \mathbb{R}^n$ such that $\boldsymbol{f}(\boldsymbol{x}^*) = 0$. In other words the network is monostationary. Note that there exists an extensive body of literature on injectivity of polynomial maps associated to chemical reaction networks and some of the most important results are summarised in Banaji and Pantea [2016].

Theorem 6.1.1. *Let $\boldsymbol{f}(\boldsymbol{x}) : \mathbb{R}^n_{>0} \to \mathbb{R}^n$ be a polynomial map $\boldsymbol{f}(\boldsymbol{x}) = M_1\text{diag}(\boldsymbol{\kappa})\boldsymbol{x}^{M_2}$, where $M_1 \in \mathbb{R}^{n\times m}$, $M_2 \in \mathbb{R}^{m\times n}$ and $\text{diag}(\boldsymbol{\kappa})$ is a diagonal matrix with κ_i as its i^{th} diagonal element. Then, $\boldsymbol{f}(\boldsymbol{x})$ is injective for all $\kappa_1,\ldots,\kappa_m \in \mathbb{R}_{>0}$ if*

$$\ker(M_2) = \{0\} \text{ and } \sigma(\ker(M_1)) \cap \sigma(\text{im}(M_2)) = \{0\}\,.$$

Note that this condition depends on the network structure, specifically, the spaces spanned by the kernel of the reaction matrix, M_1, and the image of the source complex matrix, M_2, but not on the parameter values.

6.1.2 Stochastic Inflow in Chemical Reaction Networks

It is now shown how chemical reaction networks that satisfy injectivity (preclusion of multistationarity) can be applied to consider parameter stochasticity, especially, to the case of stochastic inflows. In particular, this subsection extends the results of Chapter 5 and serves to demonstrate the mathematical equivalence between stochastic inflows and spatial intrinsic noise systems but also to introduce a novel way of modelling extrinsic noise in spatial chemical reaction networks.

Much effort in the chemical reaction network theory literature has been made to investigate "fully open systems", these are chemical reaction networks in which every species has an inflow and an outflow reaction [Banerjee and Bhattacharyya, 2014; Joshi and Shiu, 2015; Félix et al., 2016; Banaji and Pantea, 2018]. By contrast, here the nature of the model is changed by generalising the inflow rate constants to stochastic processes, rather than simply adding inflow processes as deterministic reactions. It should be noted that despite the name it is not assumed that these reactions are inflows into the domain of simulation, rather, the inflow reactions correspond to the creation of particles from some other process which happens *throughout the domain*. Sometimes these inflow reactions are the called"inputs" in engineering applications and the concentrations are the "outputs" and, therefore the study of chemical reaction networks with varying inflows can be rephrased into a study of the "input-output" relation as has been the approach in previous work [Frank, 2013].

Consider a chemical reaction network $\mathfrak{N}$. An *inflow* reaction for species X_i is manifested in the reaction graph as

$$\emptyset \xrightarrow{\kappa_{\text{in}}} X_i \ .$$

Usually, chemical reaction network theory assumes the rate constant κ_{in} to be constant in time (and space). However, the zero complex, $\emptyset$, symbolises a process not included in the model such as the the production of X_i by another network, which is called an "auxiliary network" in this chapter, or a mechanical addition of X_i to an experimental setup. Both mechanisms are often subsumed into $\emptyset$ and usually approximated as constant or "perfect" inflow, however, they can exhibit intricate dynamics. The dynamics of "non-perfect" inflows are modelled by a stochastic process whose origin can be two-fold.

(a) *Experimental fluctuations*: In chemical engineering it is assumed that inflow of chemicals into a reactor is a perfectly deterministic process, however, due to mechanical or other experimental imperfections the inflow into a reaction can vary stochastically. This renders the influx parameter κ_{in} into a stochastic process $K_{\text{in}}(t)$.

(b) *Stochastic sub-systems*: It is often assumed that the inflow into the (deterministic) reaction diffusion system is provided by the output of another chemical reaction network (with a unique fixed point). When the number of particles in the *auxiliary network* is large the system will be in a steady state and the inflow rate κ_{in} will simply be proportional to the steady state value of a species of the

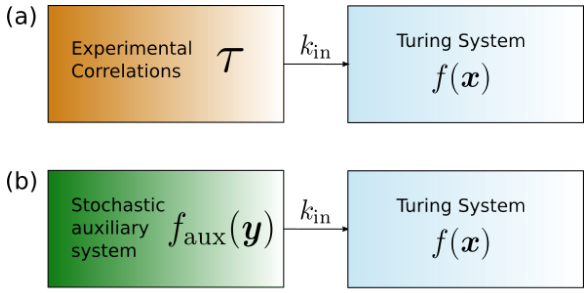


Figure 6.1: The two mechanisms contributing to stochastic inflows. The boxes on the left are usually treated as black boxes resulting in some constant inflow modelled by the parameter k_{in}. The difference between experimental fluctuations, symbolised by a correlation τ in (a) and auxiliary networks described by $f_{\text{aux}}(\boldsymbol{y})$ in case (b) is highlighted.

auxiliary system. However, when the particle number in the auxiliary system is low, stochastic fluctuations cannot be ignored and, while still proportional to the concentration of a species in the subsystem, the actual influx parameter κ_{in} will again be a stochastic process $K_{\text{in}}(t)$.

Whereas the two sources of parameter noise are conceptually different, their mathematical description is the same. Consider a stochastic process $K(t)$ with an underlying distribution $\mathcal{D}(t)$. Therefore, at every time, t, K is given by $K(t) \sim \mathcal{D}(t)$. To be biologically relevant (i.e. to ensure all chemical concentrations are non-negative at every t) it is required that $\mathcal{D} = 0$ for all $K(t) < 0$ and, the distribution $\mathcal{D}$ needs to be continuous almost everywhere. To simplify the following mathematical analysis the distribution of $K(t)$ is approximated as a *truncated Gaussian*, since it is desirable to connect the analysis to the intrinsic noise case. Future work could focus on other non-negative distributions, such as the log-normal distribution, on a continuous probability space. The process $K(t)$ can be described as

$$K(t) = \kappa + \frac{b}{\sqrt{\Omega}}\eta,$$

and

$$\begin{aligned} \langle \eta(t) \rangle &\approx 0, \\ \langle \eta(t)\eta(t') \rangle &= g(t, t'). \end{aligned} \tag{6.7}$$

where η follows a (truncated) Gaussian distribution whose non-truncated mean is exactly zero. It is assumed that the truncation is small, such that in analytic calculations the truncated moments can be approximated by the full moments of η. The

quantities Ω and b are positive constants. In the remainder of this chapter it will be shown how various functions $g(t,t')$ can arise in mathematical modelling, especially when stochastic auxiliary networks are considered.

The parameter Ω can be further connected to physical quantities of the underlying chemical reaction network by again considering the sources of stochastic inflow. Assume that the origin of the stochastic inflow are stochastic auxiliary networks or experimental imperfections. Therefore, in the limit of either a perfect experiment or a deterministic auxiliary network the inflow should be deterministic and $\langle (K(t)-\kappa)(K(t')-\kappa)\rangle = 0$ implying $\Omega \to \infty$. For stochastic auxiliary networks the quantity Ω which parameterises the size of the stochastic fluctuations can be related to the *system size* [van Kampen, 1983]. Similarly to the system size expansion, it is required that Ω is sufficiently large. Large Ω helps to maintain a positive solution of the stochastic partial differential equation, although, positivity cannot be guaranteed when the noise is correlated. Positivity of solutions is vital in biological systems as the variables represent concentrations of chemical species which cannot be negative. The parameter Ω regulates the noise to give positive solutions to the governing equations, however, no rigorous bounds on the minimal size are derived.

Next, consider a chemical reaction network $\mathfrak{N}$ in which a subset of species has an inflow reaction. Denote the set of species with (stochastic) inflow by $\mathcal{S}_{\text{in}} \subseteq \mathcal{S}$. If there is more than one (stochastic) inflow $|\mathcal{S}_{\text{in}}| > 1$ the stochastic process will be a multi-dimensional version of (6.7). Further, assume that the stochastic process has a spatial dependence. The description of the stochastic process outlined in this section still applies in this case, if $\boldsymbol{K}_{\text{in}}(s,t)$ is taken to be the vector of stochastic inflows such that

$$\boldsymbol{K}_{\text{in}}(s,t) = \boldsymbol{\kappa}_{\text{in}} + \frac{1}{\sqrt{\Omega}}\boldsymbol{\eta}(s,t)$$

with

$$\begin{aligned} \langle \boldsymbol{\eta}(s,t)\rangle &\approx 0 \\ \langle \boldsymbol{\eta}(s,t)\boldsymbol{\eta}^T(s',t')\rangle &= B(s,s')G(t,t') \\ &= \{B_{ij}(s,s')G_{ij}(t,t')\} \end{aligned} \tag{6.8}$$

where $B(s,s')$ represents the potential spatial covariances between the stochastic inflows and $G(t,t')$ models the temporal correlations.

Since the assumptions have made the inflow process additive and uncoupled to the species, the stochastic reaction network can be described by the system of stochastic

partial differential equations (SPDEs)

$$\frac{\partial \boldsymbol{x}}{\partial t} = D\frac{\partial^2 \boldsymbol{x}}{\partial s^2} + \boldsymbol{f}(\boldsymbol{x}) + \frac{1}{\sqrt{\Omega}}\boldsymbol{\eta}\,, \tag{6.9}$$

where $\boldsymbol{\eta}$ is a vector of stochastic processes such that its support is $supp(\boldsymbol{\eta}) = \mathcal{S}_{\text{in}}$.

Note that in this limit randomising inflows leaves $\mathfrak{N}$ as well as $\boldsymbol{f}(\boldsymbol{x})$ invariant, and hence, the steady state structure of the system is invariant; i.e. if $\boldsymbol{f}(\boldsymbol{x})$ is initially an injective function, then adding stochasticity will not change this injectivity.

The assumption of rate constants being stochastic processes rather than constants can be extended to non-inflow reactions too. However, equation (6.9) will have extra terms of multiplicative noise. In the next section perturbations to the steady state are studied whose scaling will render the study of non-inflow stochastic rate constants a trivial extension to the analysis. Further, note that in Chapter 5 a similar argument was used to neglect the non-linear terms in the inflow of autocatalytic networks.

Finally, it should be added that in this chapter it is assumed that in the system under study intrinsic noise is negligible compared to the effects of extrinsic noise. However, if intrinsic noise was to be included, the inflow rate constants could be modified in a chemical master equation, which could be simplified using a weak noise expansion. Care needs to be taken, however, when judging system sizes as the external system size, here denoted as Ω, may be considerably different from the intrinsic system size.

6.2 Power Spectra for Stochastic Inflows

To fully classify the patterns arising from the addition of stochastic inflows the power spectra of the patterns are calculated. Power spectra are an analytic tool showing which spatial and temporal frequencies are present in a pattern [Adamer et al., 2017; Schumacher et al., 2013; Woolley et al., 2011c] and non spatial spectra are studied in Chapter 5. Peaks in power spectra give information about dominant frequencies and, hence, about oscillatory behaviour of a system in space and time.

First, linearise equation (6.9) about the fixed point $\boldsymbol{x} \sim \boldsymbol{x}^* + \overline{\delta \boldsymbol{x}}$, where $\overline{\delta \boldsymbol{x}}$ represent small perturbations; these should decay in the deterministic limit as the system will be selected to converge to the steady state outside the Turing parameter regime. In particular, inside the Turing regime the system is assumed to converge to a stable pattern rather than a stable state which is not considered in this chapter. Hence, the

analysis is valid only *outside* the Turing pattern regime. Substituting the linearisation ansatz into equation (6.9) and keeping lowest order terms only the equation,

$$\frac{\partial \overline{\delta \boldsymbol{x}}}{\partial t} = D\frac{\partial^2 \overline{\delta \boldsymbol{x}}}{\partial s^2} + J|_{\boldsymbol{x}=\boldsymbol{x}^*}\overline{\delta \boldsymbol{x}} + \frac{1}{\sqrt{\Omega}}\boldsymbol{\eta}\,, \tag{6.10}$$

is obtained where $J|_{\boldsymbol{x}=\boldsymbol{x}^*}$ is the Jacobian of $\boldsymbol{f}(\boldsymbol{x})$ evaluated at the fixed point $\boldsymbol{x}^*$, which for notational convenience will be denoted as J.

In a similar manner to Chapter 5 one further assumption is made, namely about the scaling of the perturbation $\overline{\delta \boldsymbol{x}}$ with the parameter Ω controlling the magnitude of the stochastic input. By the same reasoning as outlined in Chapter 5, let $\alpha = -1/2$ and equation (6.10) simplifies to

$$\frac{\partial \delta \boldsymbol{x}}{\partial t} = D\frac{\partial^2 \delta \boldsymbol{x}}{\partial s^2} + J\delta \boldsymbol{x} + \boldsymbol{\eta}\,. \tag{6.11}$$

The reasoning behind choosing $\alpha = -1/2$ is analogous to the reasoning of the scaling in the weak noise expansion of van Kampen [van Kampen, 1983], especially the requirement that in the limit $\Omega \to \infty$ the noise correlations are zero. However, the system size in the extrinsic noise case is imposed by an external mechanism such as a non-modelled stochastic network with system size Ω.

The scaling of the perturbations to the steady state determines a hierarchy on the terms of equation (6.9) and in the case of non-inflow stochastic rate constants all multiplicative noise terms are linearised to additive terms with all non-trivial multiplicative perturbations only manifesting at higher order (e.g. see the autocatalytic system of Chapter 5).

Note that equation (6.11) is mathematically equivalent to a chemical Langevin equation of compartmentalised diffusion in the limit of the compartment size, Δ_s, going to zero [Smith, 1985]. However, in the derivation of this chapter the source of the noise is *extrinsic*. To emphasise the mathematical connection with intrinsic noise it is convenient, to discretise equation (6.11) into a finite number of compartments, such that for an n species network with $\mathcal{K}$ compartments

$$\delta \boldsymbol{x} = [\delta x_1, \ldots, \delta x_{\mathcal{K}}, \delta x_{\mathcal{K}+1}, \ldots, \delta x_{2\mathcal{K}}, \ldots, \delta x_{n\mathcal{K}}]^T\,, \tag{6.12a}$$

$$\boldsymbol{\eta} = [\eta_1, \ldots, \eta_{\mathcal{K}}, \eta_{\mathcal{K}+1}, \ldots, \eta_{2\mathcal{K}}, \ldots, \eta_{n\mathcal{K}}]^T\,, \tag{6.12b}$$

$$s \approx s_i = i\Delta_s \quad \text{where } i = \{1, \ldots, \mathcal{K}\}\,, \Delta_s = L/\mathcal{K}\,, \tag{6.12c}$$

$$\frac{\partial^2 \delta \boldsymbol{x}(s)}{\partial s^2} \approx \frac{\delta \boldsymbol{x}(s_i + \Delta_s) + \delta \boldsymbol{x}(s_i - \Delta_s) - 2\delta \boldsymbol{x}(s_i)}{(\Delta_s)^2}\,, \tag{6.12d}$$

and the matrices D and J turn into block matrices such that

$$D = \begin{pmatrix} [D_1]_{\mathcal{K}\times\mathcal{K}} & 0 & 0 & \cdots \\ 0 & [D_2]_{\mathcal{K}\times\mathcal{K}} & 0 & \cdots \\ \vdots & \vdots & \vdots & \ddots \end{pmatrix} . \tag{6.13}$$

The ij^{th} block of J is $J_{ij}\boldsymbol{I}_{\mathcal{K}\times\mathcal{K}}$, where $\boldsymbol{I}_{\mathcal{K}\times\mathcal{K}}$ is the $\mathcal{K}\times\mathcal{K}$ identity matrix, to give

$$J = \begin{pmatrix} [J_{11}]_{\mathcal{K}\times\mathcal{K}} & [J_{12}]_{\mathcal{K}\times\mathcal{K}} & \cdots \\ [J_{21}]_{\mathcal{K}\times\mathcal{K}} & [J_{22}]_{\mathcal{K}\times\mathcal{K}} & \cdots \\ [J_{31}]_{\mathcal{K}\times\mathcal{K}} & [J_{32}]_{\mathcal{K}\times\mathcal{K}} & \cdots \\ \vdots & \vdots & \ddots \end{pmatrix} . \tag{6.14}$$

Compartmentalisation results in a system of $n\mathcal{K}$ coupled SDEs

$$d\delta\boldsymbol{x} = A\delta\boldsymbol{x}\, dt + \boldsymbol{\eta}\, dt\,, \tag{6.15}$$

with $A = D/\Delta_s^2 + J$, $\langle\eta_i(t)\rangle = 0$ and $\langle\eta_i(t)\eta_j(t')\rangle = B_{ij}G_{ij}(t,t')$. Note that after compartmentalisation $B(s,s')$ is a block matrix of n^2 $\mathcal{K}\times\mathcal{K}$ matrices, describing the spatial auto-correlation of each species and the spatial correlations between species.

To calculate the power spectra of the system the discrete cosine transform [Briggs and Henson, 1995] is introduced

$$f_k = \Delta_s \sum_{j=1}^{\mathcal{K}} \cos[k\Delta_s(j-1)] f(s_j)\,. \tag{6.16}$$

The cosine transform incorporates the Neumann (no flux) boundary conditions, which are commonly used for reaction-diffusion systems, however, other homogeneous boundary conditions can easily be implemented [Briggs and Henson, 1995]. Due to the boundary conditions it is required that $k = m\pi/l$ with $m \in \{0,1,2,\dots\}$. The integer m will be referred to as the *spatial mode*. Note that the use of $(j-1)$ instead of j is due to the fact that the compartment labelling starts at $j = 1$. Hence, by applying the spatial Fourier transform the system of $n\mathcal{K}$ coupled SDEs (6.15) is reduced to a system of n coupled SDEs

$$d\delta\boldsymbol{x}_k = A_k\delta\boldsymbol{x}_k\, dt + \boldsymbol{\eta}_k\, dt\,. \tag{6.17}$$

Finally, applying the temporal Fourier transform

$$\hat{f}(\omega) = \int_{-\infty}^{\infty} f(t)e^{-i\omega t}dt\,, \tag{6.18}$$

an expression is obtained for $\delta\hat{\boldsymbol{x}}_k(\omega)$, and one has

$$\delta\hat{\boldsymbol{x}}_k(\omega) = \left[-A_k - i\omega\right]^{-1} \hat{\boldsymbol{\eta}}_k(\omega) \,. \tag{6.19}$$

Note that the Fourier transform always exists if the system is considered to have a fixed point [Woolley et al., 2011b]. Therefore, the power spectra of the pattern, $P_{\delta x}(k,\omega)$, can be expressed as the diagonal elements of

$$\langle \delta\hat{\boldsymbol{x}}_k(\omega)\delta\hat{\boldsymbol{x}}_k^\dagger(\omega)\rangle = \Phi^{-1} \underbrace{\langle \hat{\boldsymbol{\eta}}_k(\omega)\hat{\boldsymbol{\eta}}_k^\dagger(\omega)\rangle}_{N} \left(\Phi^{-1}\right)^\dagger \,, \tag{6.20}$$

where the matrix Φ is defined by

$$\Phi = -\left[A_k + i\omega\right] \,, \tag{6.21}$$

and $\dagger$ denotes the hermitian conjugate of a matrix. In order to be guaranteed real power spectra the identity $N = N^\dagger$ needs to hold. In the case of Gaussian noise it can be shown that

$$N = \mathcal{F}_{\cos}\left(\mathcal{F}(BG(t,t'))\right) , \tag{6.22}$$

where $\mathcal{F}_{\cos}$ denotes the cosine transform and $\mathcal{F}$ the temporal Fourier transform. Note that when all temporal correlations are equal such that $G_{ij}(t,t') = g(t,t')$ the transform factor becomes

$$N = \mathcal{F}_{\cos}\left(B\right)\mathcal{F}(g(t,t')) = B_k P_{\text{Correlations}}(\omega) \,, \tag{6.23}$$

where $P_{\text{Correlations}}$ is the power spectrum of the correlation function $g(t,t')$ and B_k is the $n \times n$ matrix of covariances. For white noise take $\boldsymbol{\eta}\, dt = \boldsymbol{\xi}\sqrt{dt}$ to reduce (6.15) to the Itô form

$$d\delta\boldsymbol{x} = A\delta\boldsymbol{x}\, dt + \boldsymbol{\xi}\sqrt{dt} \,, \tag{6.24}$$

with $\langle\boldsymbol{\xi}(t)\rangle = 0$ and $\langle\xi_i(t)\xi_j(t')\rangle = B_{ij}\delta(t-t')$ and, therefore, $P_{\text{Correlations}} = 1$. Hence, it can be seen that for white noise the power spectra are

$$\begin{aligned}\langle \delta\hat{\boldsymbol{x}}_k(\omega)\delta\hat{\boldsymbol{x}}_k^\dagger(\omega)\rangle &= \left[\Phi^{-1}\langle \hat{\boldsymbol{\eta}}_k(\omega)\hat{\boldsymbol{\eta}}_k^\dagger(\omega)\rangle \left(\Phi^{-1}\right)^\dagger\right] = \\ &= \left[\Phi^{-1} B_k \left(\Phi^{-1}\right)^\dagger\right] = P_{\text{white}} \,.\end{aligned} \tag{6.25}$$

For general temporal correlations $g(t,t')$ it holds that

$$\begin{aligned}\langle \delta\hat{\boldsymbol{x}}_k(\omega)\delta\hat{\boldsymbol{x}}_k^\dagger(\omega)\rangle &= \left[\Phi^{-1} B_k P_{\text{Correlations}} \left(\Phi^{-1}\right)^\dagger\right] = \\ &= P_{\text{white}} P_{\text{Correlations}} \,,\end{aligned} \tag{6.26}$$

such that the spectra of the noise colour appear as a multiplicative factor modulating the white noise spectra.

6.2.1 Application to the Schnakenberg System

The analysis of this chapter is illustrated via the example of the Schnakenberg kinetics. The Schnakenberg system is an $n = 2$ species reaction-diffusion system which, despite its apparent simplicity, exhibits a wealth of different behaviours in the deterministic [Iron et al., 2004; Maini et al., 2012; Ward and Wei, 2002; Flach et al., 2007] as well as stochastic [Schumacher et al., 2013; Woolley et al., 2011c; Schnakenberg, 1979] regime. The Schnakenberg system is a network in which every species has an inflow reaction and, hence, both species can be subject to stochastic inflow. Therefore, the Schnakenberg system is a perfect candidate to highlight the effects of coloured noise computationally and illustrate how the above analysis can be applied in practice. The system follows the reaction scheme

$$X_2 \xleftarrow{\kappa_2} \emptyset \underset{\kappa_{-1}}{\overset{\kappa_1}{\rightleftharpoons}} X_1 \,, \qquad\qquad 2X_1 + X_2 \xrightarrow{\kappa_3} 3X_1 \,. \tag{6.27}$$

The dynamics of the Schnakenberg system is described by the system of PDEs

$$\begin{aligned} \frac{\partial x_1}{\partial t} &= D_1 \frac{\partial^2 x_1}{\partial s^2} + \kappa_1 - \kappa_{-1} x_1 + \kappa_3 x_1^2 x_2, \\ \frac{\partial x_2}{\partial t} &= D_2 \frac{\partial^2 x_2}{\partial s^2} + \kappa_2 - \kappa_3 x_1^2 x_2. \end{aligned} \tag{6.28}$$

First, the potential multistationarity in the Schnakenberg system is investigated by formulating the matrices M_1 and M_2,

$$M_1 = \begin{pmatrix} 1 & -1 & 0 & 1 \\ 0 & 0 & 1 & -1 \end{pmatrix} \qquad \text{and} \qquad M_2 = \begin{pmatrix} 0 & 0 \\ 1 & 0 \\ 0 & 0 \\ 2 & 1 \end{pmatrix}. \tag{6.29}$$

It is easy to assert that $\ker(M_2) = \{0\}$. Further, it can be shown that

$$\sigma(\ker(M_1)) = \{(+,+,0,0)^T, (-,0,+,+)^T\}$$

and

$$\sigma(\mathrm{im}(M_2)) = \{(0,+,0,+)^T, (0,0,0,+)^T\}\,. \tag{6.30}$$

Hence, applying the injectivity criterion of Theorem 6.1.1, it can be seen that the Schnakenberg system is monostationary for all positive parameter values and, therefore, stochastic fluctuations in the inflow parameters cannot trigger stochastic switching between steady states.

Next, consider stochastic inflows which result in $\kappa_i \to \kappa_i + 1/\sqrt{\Omega}\,\eta_i$ for $i \in \{1,2\}$ and the equations

$$\begin{aligned}\frac{\partial x_1}{\partial t} &= D_1\frac{\partial^2 x_1}{\partial s^2} + \kappa_1 - \kappa_{-1}x_1 + \kappa_3 x_1^2 x_2 + \frac{1}{\sqrt{\Omega}}\eta_1,\\ \frac{\partial x_2}{\partial t} &= D_2\frac{\partial^2 x_2}{\partial s^2} + \kappa_2 - \kappa_3 x_1^2 x_2 + \frac{1}{\sqrt{\Omega}}\eta_2.\end{aligned} \tag{6.31}$$

Linearising equations (6.31) about the steady state $x_1^* = (\kappa_1+\kappa_2)\kappa_{-1}^{-1}$, $x_2^* = \kappa_2\kappa_{-1}^2\kappa_3^{-1}(\kappa_1+\kappa_2)^{-2}$ and discretising space, a system of linear stochastic differential equations is obtained, similar to the ones arising from the study of intrinsic noise [Schumacher et al., 2013],

$$\frac{d\boldsymbol{x}}{dt} = A\boldsymbol{x} + \boldsymbol{\eta}, \tag{6.32}$$

with

$$A = \begin{pmatrix}\boldsymbol{a} & \boldsymbol{b}\\ \boldsymbol{c} & \boldsymbol{d}\end{pmatrix}, \tag{6.33}$$

where $\boldsymbol{a}, \boldsymbol{d}$ are tridiagonal matrices with diagonal elements

$$\begin{aligned}a_0 &= -2D_1/\Delta_s^2 - \kappa_{-1} + 2\kappa_3 x_1^* x_2^*,\\ d_0 &= -2D_2/\Delta_s^2 - \kappa_3 x_1^{*2},\end{aligned} \tag{6.34}$$

and off-diagonal (sub- and super-diagonal) elements

$$\begin{aligned}a_1 &= D_1/\Delta_s^2 \equiv d_u,\\ d_1 &= D_2/\Delta_s^2 \equiv d_v.\end{aligned} \tag{6.35}$$

The matrices $\boldsymbol{b}$ and $\boldsymbol{c}$ are diagonal matrices with entries

$$\begin{aligned}b_0 &= \kappa_3 x_1^{*2},\\ c_0 &= -2\kappa_3 x_1^* x_2^*.\end{aligned} \tag{6.36}$$

Note that the vector $\boldsymbol{x}$ has $2\mathcal{K}$ components. There are $\mathcal{K}$ components for species x_1 and $\mathcal{K}$ components for species x_2.

Hence, Fourier transforming equation (6.32) in space and time the power spectra can be computed,

$$P(k,\omega) = [A_k + i\omega]^{-1}\left\langle\hat{\eta}_k(\omega)\hat{\eta}_k^\dagger(\omega)\right\rangle\left([A_k + i\omega]^{-1}\right)^\dagger, \tag{6.37}$$

with

$$A_\kappa = \begin{pmatrix}a_0 + 2a_1\cos k\Delta_s & b_0\\ c_0 & d_0 + 2d_1\cos k\Delta_s\end{pmatrix}. \tag{6.38}$$

In the following section the effect of various noise correlations on the power spectra, and, hence, the patterns generated will be discussed.

Colour	Correlation Function	Effect	Possible Origin	Section
White	1	N/A	intrinsic	6.3.2
Ornstein-Uhlenbeck	$1/\left(\omega^2\tau^2+1\right)$	suppresses small ω	experimental apparatus	6.3.3
Red	$1/\omega^2$	excites small ω	deterministic	6.3.4
Predator-Prey	$\left(\alpha+\beta\omega^2\right)/\left(\omega^4+\gamma\omega^2+\delta\right)$	induces oscillations	stochastic subsystems	6.3.5

Table 6.1: An overview of the main results on various noise colours.

6.3 Computational Results

In this section the computational patterns generated by a Turing system with coloured noise are highlighted.

6.3.1 Numerical Methods

The system of SDEs (6.15) is simulated by an Euler-Maruyama scheme [Kloeden and Platen, 1995; Milshtein and Tretyakov, 1994] with time step Δt such that

$$\boldsymbol{x}(t+\Delta t)=\boldsymbol{x}(t)+A\boldsymbol{x}\Delta t+\boldsymbol{\eta}\Delta t. \tag{6.39}$$

The important step of the integration is to find the correct vector $\boldsymbol{\eta}$.

The white noise and Ornstein-Uhlenbeck noise are generated by an auxiliary noise process. In particular, at teach time step the white noise is sampled from a multivariate Gaussian distribution

$$\boldsymbol{\eta}\Delta t\sim\mathcal{N}(0,B\Delta t).$$

The Ornstein-Uhlenbeck process is a generated by the stochastic differential equation

$$\frac{d\boldsymbol{\eta}}{dt}=-\frac{1}{\tau}\boldsymbol{\eta}+\frac{\sqrt{B}}{\tau}\boldsymbol{\xi},$$

where $\boldsymbol{\xi}$ is a standard white noise vector. Therefore, at time t the vector $\boldsymbol{\eta}(t)$ is added to the system of SDEs. The Ornstein-Uhlenbeck "auxiliary equation" is integrated by an Euler-Maruyama scheme as originally described in Milshtein and Tretyakov [1994].

To simulate power law noise for which, in general, no auxiliary SDE exists, inverse transforms [Timmer and Koenig, 1995] are used. To generate a vector $\boldsymbol{\eta}(t)$ with correlations $\langle\boldsymbol{\eta}(t)\boldsymbol{\eta}^T(t')\rangle=Bg(t-t')$, first the fact is used that $\boldsymbol{\eta}=\sqrt{B}\boldsymbol{\xi}$ where $\boldsymbol{\xi}$ may be correlated in time but not in space, i.e. $\langle\boldsymbol{\xi}(t)\boldsymbol{\xi}^T(t')\rangle=\delta_{ij}g(t-t')$. Then, let the power spectrum of ξ_i be $1/\omega^\alpha$ as described in subsection 6.3.4 and use the

algorithm of Timmer and Koenig [1995] to create a time series. Multiplication of $\boldsymbol{\xi}(t)$ with $\sqrt{B}$ gives the desired noise process, $\boldsymbol{\eta}(t)$, which can be added to the SDE system.

Auxiliary networks as in 6.3.5 can be simulated by either method and in this chapter the auxiliary network input is generated by using the inverse transforms technique.

6.3.2 White Noise

First, extrinsic white noise is considered. In this special case the noise vector $\boldsymbol{\eta}$ is just a Wiener process with correlation matrix B. This case is mathematically identical to the case of intrinsic noise in the weak noise limit as studied in Schumacher et al. [2013]. The main differences between intrinsic noise and the parameter noise considered in this chapter are the amplitude of the noise and the exact forms of the covariances of the stochastic processes $\boldsymbol{\eta}$.

Both approximations (the weak noise limit, as well as the "truncated Gaussian" approximation) assume that the stochastic effect is a perturbation to the deterministic limit. However, as derived in Schumacher et al. [2013], the covariance matrix of the stochastic processes $\boldsymbol{\eta}$ is determined by the microscopic processes whereas for extrinsic noise, whose origin can be manifold, the covariance matrix is arbitrary. For mathematical simplicity the covariance matrix

$$B_\kappa = \begin{pmatrix} 1 & 1 \\ 1 & 1 \end{pmatrix}, \tag{6.40}$$

is chosen.

Throughout the remainder of this chapter the parameter values are fixed to

$$\begin{aligned} \kappa_1 &= \kappa_2 = 10.0, \\ \kappa_3 &= 0.01, \\ \kappa_{-1} &= 20.0, \\ L &= 0.1, \\ \mathcal{K} &= 40, \end{aligned}$$

with diffusion coefficients

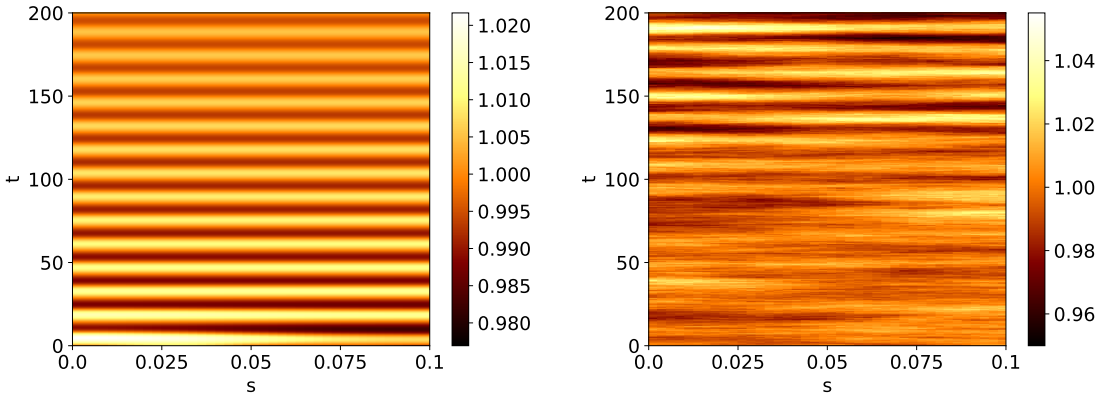
$$\begin{aligned} D_1 &= 10^{-4}, \\ D_2 &= 10^{-2}, \end{aligned} \tag{6.41}$$

which results in steady state concentrations of $x_1^* = 1$, $x_2^* = 1000$. The parameters chosen are not generic, but they represent a particularly interesting point in parameter space. The parameters are in the (stable) oscillatory regime of the Schnakenberg system and outside the Turing space. The main function of the noise will be to temporarily move the system into the Turing regime. Note that the system has large inflows (and outflows) compared to the chemical reaction parameterised by k_3 which allows for larger variations in the noise translating into larger pattern amplitudes. The modifications to the power spectra due to coloured noise are generic and apply to all points in parameter space. However, the visibility of these modifications depends on the point in parameter space and the correlation matrix. Similarly, the results on amplitude of the patterns are parameter-dependent. To simulate the system, the space is discretised into 40 compartments of width $\Delta_s = 0.0025$ (which gives the total domain length of $L = 0.1$).

Figure 6.2 illustrates equation (6.27) simulated deterministically in 6.2a, equation (6.32) simulated stochastically in 6.2b and the power spectra extracted in 6.2c. The power spectrum shows the temporal frequencies, ω, and spatial modes, m, present in the pattern. The amplitude of the oscillations is about 3% of the steady state value for species x_1 whereas for species x_2 it is much lower. Therefore, it is assumed that any patterning of x_2 is not generally measurable and, hence, the focus of attention is on x_1. The prominent temporal oscillations with no spatial dependency manifest themselves as a sharp peak in the power spectrum. This is due to the fact that the chosen parameter point is in the oscillatory regime of the Schnakenberg model. Upon close inspection slight spatial variations in the pattern of x_1 can be seen, but with white noise these are not very pronounced. In the following sections it is shown how noise colour can enhance spatial modes, create additional oscillations or even create a stable pattern.

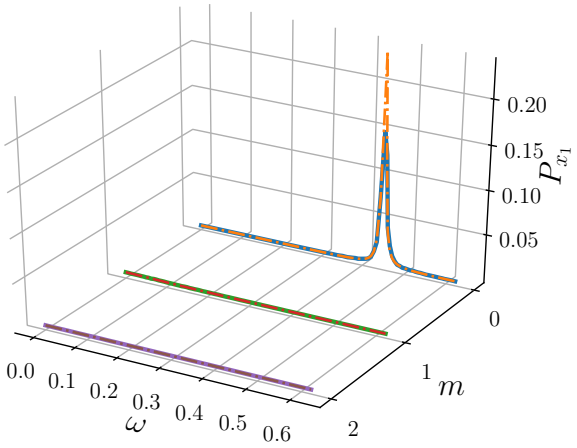
6.3.3 Ornstein-Uhlenbeck Noise

Next, the effect of exponentially correlated noise also known as Ornstein-Uhlenbeck noise [Hänggi and Jung, 1994] is investigated. This stochastic process has a finite correlation time τ which can be interpreted as a response time. Consider an experiment in which the inflow rate is highly sensitive to the ambient temperature. Further, suppose this temperature undergoes random fluctuations about a regulated mean value. Therefore, the correlation time τ could represent the average response time of the temperature regulator.



(a) The deterministic solution of the Turing system at the given parameter point.

(b) A stochastic realisation with white noise.



(c) The power spectra of the analytical calculations (dashed lines) and their simulated curves averaged over 50 realisations of length $T = 1000$ and subsystem size $\Omega = 5000$. The differences in peak height are attributed to the finite time steps used.

Figure 6.2: An overview of the deterministic and white noise behaviour of the Schnakenberg system with parameters as in (6.41). The peak in 6.2c at zero spatial mode, $m = 0$, indicates temporal oscillations which result from deterministic limit cycle oscillations. Due to the choice of reaction kinetics the temporal oscillations of species x_1 and x_2 are in phase.

The simplification is made that all the temporal correlations in equation (6.8) originate from Ornstein-Uhlenbeck processes with the same correlation time, τ, such that

$$g_{ij}(t,t') = g(t,t') = \frac{1}{2\tau} e^{-\frac{|t-t'|}{\tau}}. \tag{6.42}$$

Hence, it follows that

$$\langle \hat{\eta}_k(\omega) \hat{\eta}_k(\omega)^\dagger \rangle = B_k \frac{1}{\omega^2\tau^2 + 1} \tag{6.43}$$

where B_k is the same matrix as in the white noise case and, therefore,

$$P(k,\omega)_{\text{Ornstein-Uhlenbeck}} = P(k,\omega)_{\text{white}}/(\omega^2\tau^2 + 1).$$

Hence, the noise colouring will dampen temporal frequencies of $\omega \neq 0$ and, therefore, stabilise the pattern. Consequentially, in systems subject to Ornstein-Uhlenbeck noise it is expected that any stationary patterns, that may be hidden due to transient noise effects, are more prominent. The Schnakenberg system with Ornstein-Uhlenbeck noise is simulated and the resulting patterns and power spectra are plotted in Figure 6.3. The pattern of x_2 has the same characteristic as in the white noise case, except for a smaller amplitude. Interestingly, x_1 shows a very different behaviour to the white noise case. Clear spatial structures can be seen, in particular, the phenomenon of polarity switching [Woolley et al., 2011c; Schumacher et al., 2013]. However, in the novel case of Ornstein-Uhlenbeck noise only one species switches, while the other stays spatially nearly homogeneous. A Turing pattern of mode $m = 1$ is generated with a given polarity, namely, a minimum at $s = 0$ and a maximum at $s = L$ or vice versa. Polarity switching describes the inherently stochastic phenomenon of a sudden change in polarity as can be observed in Figure 6.3. The temporal oscillations, although still present, are reduced to a practically unobservable level. This is attributed to the fact that the exponential noise correlations dampen the oscillations present in the white noise system.

6.3.4 Power Law Noise

Power law noise is defined here as a stochastic process whose frequency distribution follows a power law in Fourier space

$$P_{\text{power}} = \frac{1}{\omega^\alpha}. \tag{6.44}$$

Various types of power law noise are common in engineering and are defined by the colours summarised in Table 6.2. In this chapter red noise, white noise (subsection

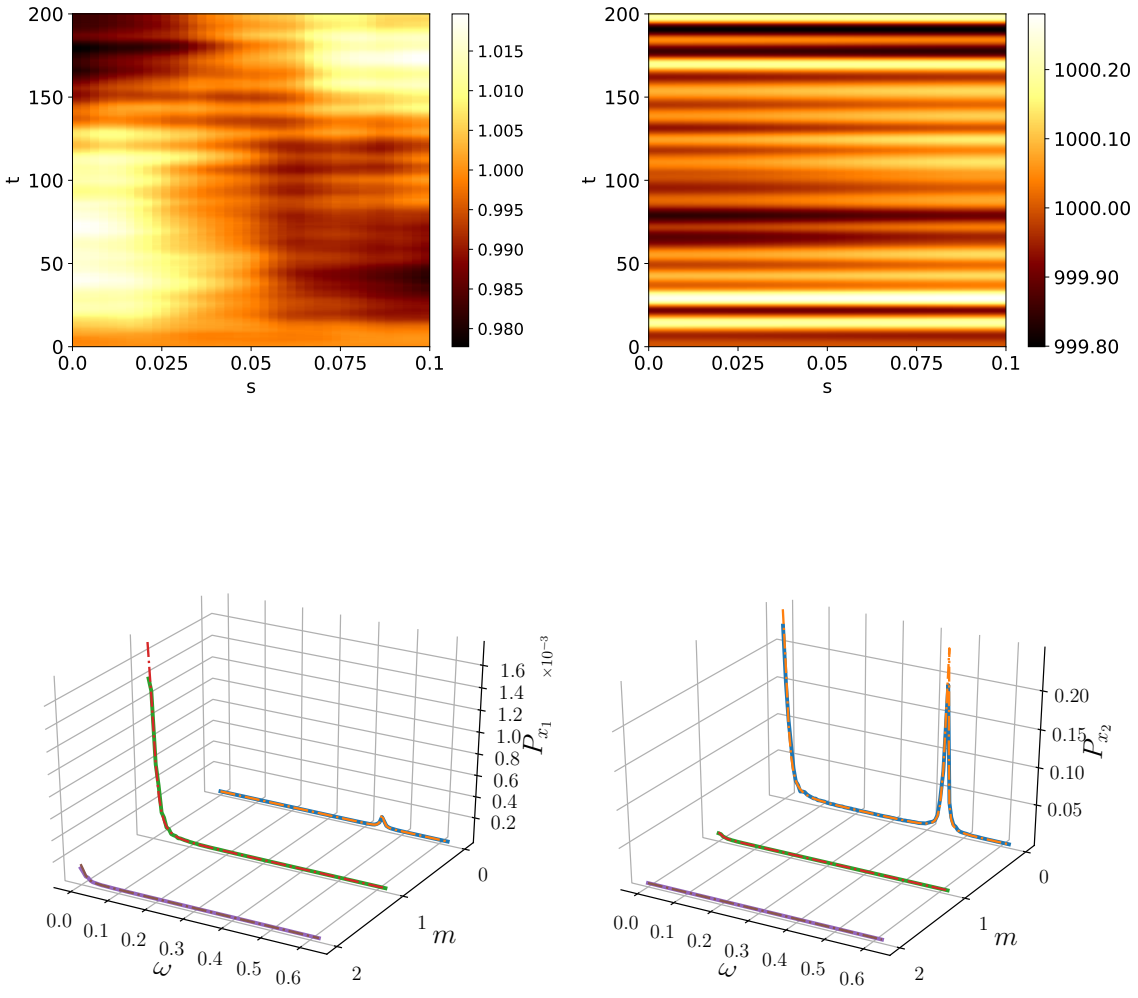


Figure 6.3: Patterns and power spectra for the species x_1 (left) and x_2 (right) with noise generated by an Ornstein-Uhlenbeck process and $\tau = 100$. Spatial patterns become visible in the Ornstein-Uhlenbeck case which can be attributed to its dampening effect on temporal oscillations. This can be observed as a visible excitation of the $m = 1$ mode in the power spectrum of x_1 with the dashed line representing the analytical prediction. The well-known phenomenon of polarity switching [Schumacher et al., 2013] is observed in the pattern of x_1. The spectra were averaged over 50 repetitions with $T = 1000$ and subsystem size $\Omega = 100$.

Colour	α
Red	$\alpha = 2$
Pink	$\alpha = 1$
White	$\alpha = 0$
Blue	$\alpha = -1$
Violet	$\alpha = -2$

Table 6.2: The various colours of power law noise. In this chapter the focus lies on red and violet noise.

6.3.2) and violet noise are studied to illustrate the effects of a positive, zero and negative exponent, α.

Red noise amplifies small temporal frequencies with $1/\omega^2 \to \infty$ as $\omega \to 0$. Therefore, the zero frequency behaviour dominates the pattern. As can be seen in Figures 6.4a and 6.4c, due to the amplification of small ω, the pattern becomes stable, even though the amplitude grows beyond the biologically viable (non-negative) bound indicating that non-linear effects need to be considered in the model. To investigate the red noise further, the noise vector $\boldsymbol{\eta}$ is investigated. For the simulation times chosen, $T = 1000$, the noise vector is independent of the time t such that each η_i has a constant, but random value. Hence, the effect of red noise is deterministic and equation (6.32) is just a linear ordinary differential equation with a constant drift term. After applying the spatial Fourier transform the equation

$$\frac{d\boldsymbol{\delta x}_k}{dt} = A_\kappa \boldsymbol{\delta x}_k + \boldsymbol{\eta}_k, \tag{6.45}$$

is obtained and, denoting the eigenvalues and eigenvectors of A_k as $\lambda_1(k)$, $\lambda_2(k)$ and $\boldsymbol{\nu}_1(k)$, $\boldsymbol{\nu}_2(k)$ respectively, the linear equation can be solved to give

$$\boldsymbol{\delta x}_k(t) = c_1 \boldsymbol{\nu}_1(k) e^{\lambda_1(k)t} + c_2 \boldsymbol{\nu}_2(k) e^{\lambda_2(k)t} - A_k^{-1} \boldsymbol{\eta}_k, \tag{6.46}$$

where c_1 and c_2 are constants determined by the initial conditions. Investigating the spatial mode $m = 0$, which corresponds to perturbations to the non-spatial deterministic system, it can be found that the eigenvalues are complex with negative real part. These eigenvalues correspond to the dynamics of a stable spiral and, therefore, transient oscillations around $\omega \approx 0.5$, the deterministic oscillation frequency, are expected. Indeed, it can be seen in Figure 6.4b that transient oscillations are present and in order to calculate the power spectrum accurately only the time points in $t \in [800, 1000]$ are used. If the entire data were used for the calculation of the power spectra a peak at $\omega \approx 0.5$ would appear, which is not accounted for in the

analytic spectrum. The same caveat does not apply to other coloured noise processes due to the constantly varying perturbations to the steady state.

To illustrate the behaviour of the system on the other end of the colour spectrum, and to highlight the limits of the analysis, violet noise was simulated, which stabilised the temporal oscillations further and, due to large power at large ω, drove the oscillation amplitude in the linear treatment to non-biologically viable values. Again, this indicates that violet noise cannot be treated in biological applications with a simple linear theory, but a full non-linear theory must be used. For violet noise the effect of the truncation of the Gaussian became too large to get an accurate prediction of the power spectra as can be seen in Figure 6.5. Further, while noise colours with positive exponent are actively studied in biology [Szendro et al., 2001], the potential emergence of blue or violet noise in biological systems is not clear.

6.3.5 Stochastic Auxiliary Networks

Now, the second major source of random inflows is studied, namely the dependence on a stochastic auxiliary network. An auxiliary network is a chemical reaction network which provides an input into the Turing system (see Figure 6.6). The auxiliary network is connected to the main network only via an inflow reaction and, if the auxiliary network reaches a steady state, it can be subsumed into the zero complex for practical modelling. If, however, the auxiliary network exhibits more complex dynamics such as deterministic or stochastic oscillations, then it needs to be treated as a part of the main network. In this subsection the focus lies on auxiliary networks which are deterministically stable, but show stochastic quasi-cycles. The dynamics of such systems are modelled by using a correlated stochastic inflow parameter as outlined in section 6.1.2.

As an illustrative example the predator-prey system, described in McKane and Newman [2005], is used,

$$\begin{aligned} Y_1 &\xrightarrow{d_1} \emptyset \xleftarrow{d_2} Y_2, \\ 2Y_1 &\xleftarrow{p_1} Y_1 + Y_2 \xrightarrow{p_2} Y_1. \end{aligned} \tag{6.47}$$

In McKane and Newman [2005] it was shown that in the deterministic regime the system (6.47) has exactly one attractor for any choice of rate constants. Hence, if the inflow parameters κ_1 and κ_2 are proportional to the concentration of Y_1, they will have a constant value. However, when the copy numbers of Y_1 and Y_2 are small and stochastic fluctuations are important the predator-prey model (6.47) can exhibit

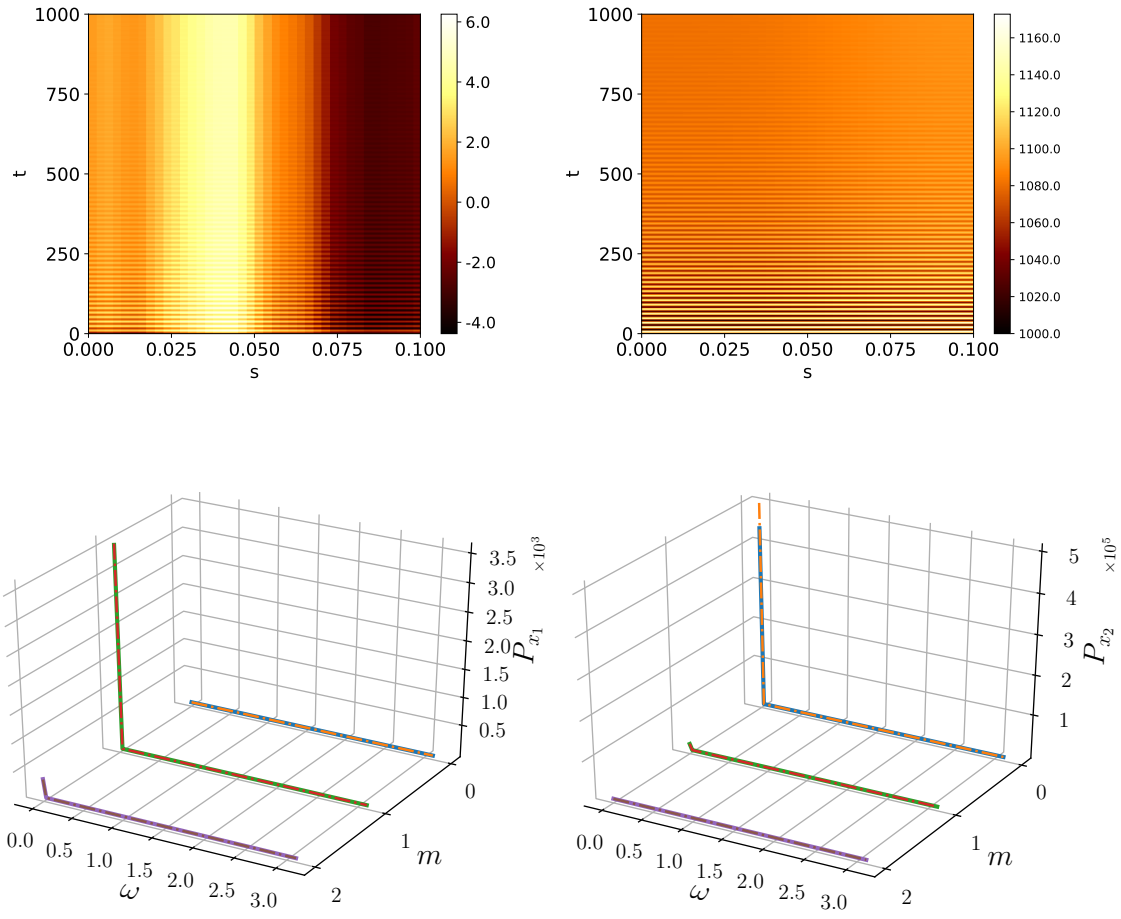


Figure 6.4: Patterns and power spectra for the species x_1 (left) and x_2 (right) with noise generated by a red noise process. As predicted, the spectra are dominated by the behaviour at $\omega = 0$, which amounts to the stabilisation of a particular spatial mode. The species concentrations, however, go negative indicating that a full non-linear model needs to be used. The spectra were averaged over 50 repetitions with simulation time $T = 200$ after a burn-in of 800 seconds. The subsystem size was $\Omega = 5000$.

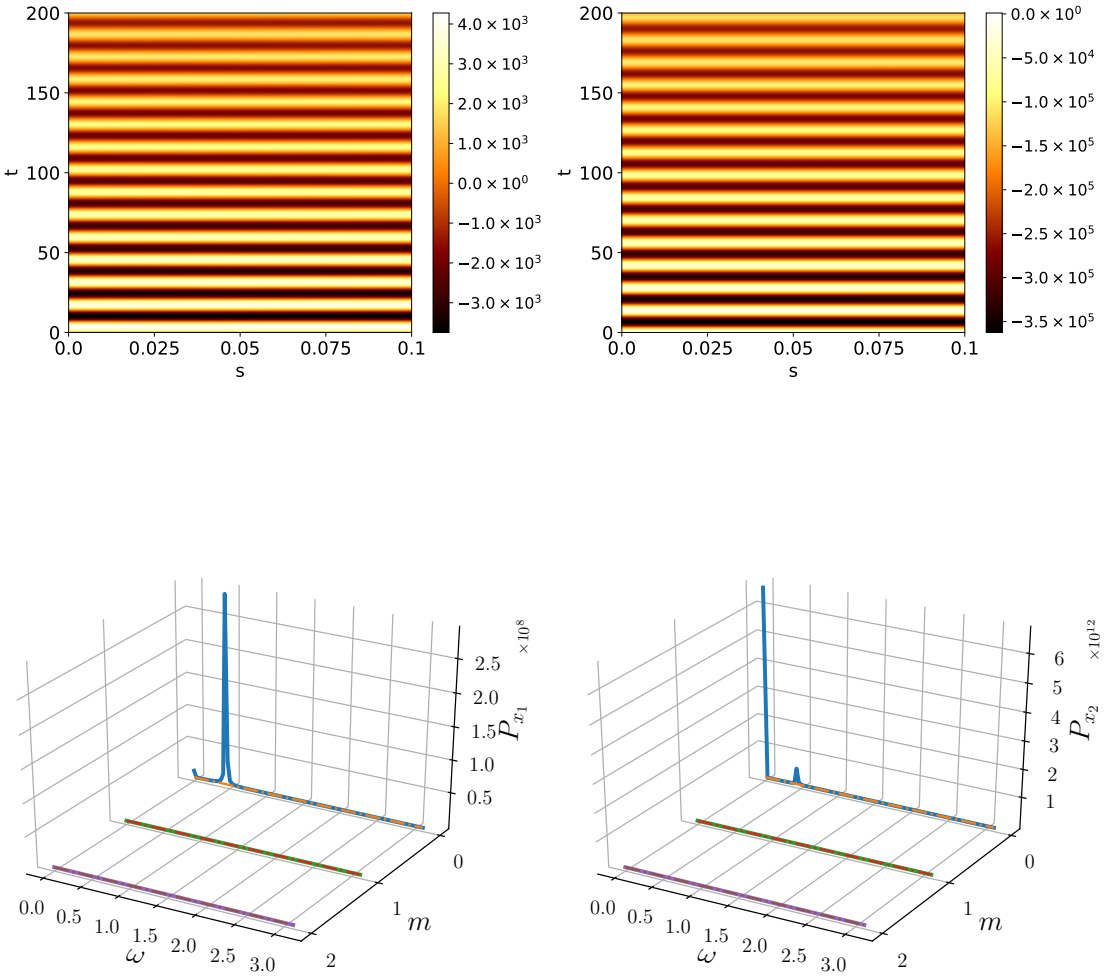


Figure 6.5: Patterns and power spectra for x_1 (left) and x_2 (right) with noise generated by a violet noise process. The discrepancy in the power spectra originates from the truncation of the Gaussian process. The negative species concentrations indicate that a non-linear theory needs to be used to fully model a violet noise system. The spectra were averaged over 50 repetitions with simulation time $T = 200$. The subsystem size was $\Omega = 5000$.

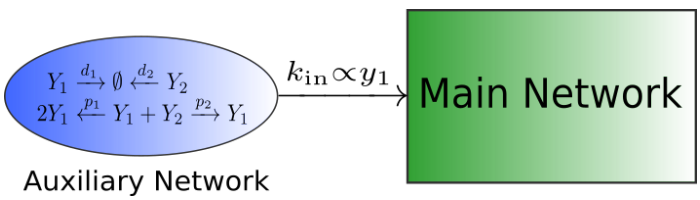


Figure 6.6: A schematic of an auxiliary network and its input to the main system. This is a specific example of scenario (b) of Figure 6.1.

so-called "quasi-cycles" which are stochastic analogue of limit-cycles and manifest themselves as peaks in the power spectra.

Consider this "predator-prey noise" in a Schnakenberg system. Suppose the inflows κ_1 and κ_2 in the Schnakenberg system depend on the presence of the chemical species Y_1, such that $k_1 \propto y_1$ and $k_2 \propto y_1$, where y_1 denotes the concentration of Y_1. Again, assume $g_{ij}(t,t') = g(t,t')$ for mathematical simplification. In Fourier space the power spectrum of Y_1 is

$$P_{\text{Predator-Prey}} = \frac{\alpha + \beta\omega^2}{(\omega^2 + \Omega_0^2) + \Gamma^2\omega^2}, \tag{6.48}$$

where α, β, Ω_0 and Γ are reaction parameters of the predator-prey system and their values are taken from McKane and Newman [2005] to be, $\alpha = 0.000384$, $\beta = \Gamma = 0.04$, and $\Omega_0^2 = 0.016$.

Equation (6.48) has a peak at $\omega \sim 0.06$, hence, peaks at a similar frequency for each non-zero spatial mode are expected in the power spectrum of the Schnakenberg system. The resulting patterns and the corresponding averaged power spectra are presented in Figure 6.7. The power spectra gained a second peak in the $m = 0$ mode and peak in all modes $m > 0$ at $\omega \sim 0.06$. Therefore, it can be seen that a deterministic parent system can inherit the dynamics of a stochastic auxiliary network and mix it with its own intrinsic dynamics.

6.3.6 Mixed Noise

Next, the case of mixing noise processes is investigated. In particular, an Ornstein-Uhlenbeck process, which has a different correlation time for x_1 and x_2, τ_1 and τ_2, respectively, is considered. In order to recover the white noise case for species two, let $\tau_2 \to 0$.

Therefore, introduce the auxiliary normal stochastic processes ξ which leads to the description of the spatial modes of the noise η_κ by Hänggi and Jung [1994]

$$\frac{d\eta_k}{dt} = -\begin{pmatrix} \frac{1}{\tau_1} & 0 \\ 0 & \frac{1}{\tau_2} \end{pmatrix} \eta_k + \begin{pmatrix} \frac{1}{\tau_1} & 0 \\ 0 & \frac{1}{\tau_2} \end{pmatrix} b_k \xi, \tag{6.49}$$

where b_k is a 2×4 matrix satisfying $b_k b_k^T = B_k$. Fourier transform equation (6.49) and define the matrix,

$$\phi = \begin{pmatrix} \frac{1}{\tau_1} + i\omega & 0 \\ 0 & \frac{1}{\tau_2} + i\omega \end{pmatrix} \tag{6.50}$$

to give

$$\hat{\eta}_k = \phi^{-1} \begin{pmatrix} \frac{1}{\tau_1} & 0 \\ 0 & \frac{1}{\tau_2} \end{pmatrix} b_k \hat{\xi}. \tag{6.51}$$

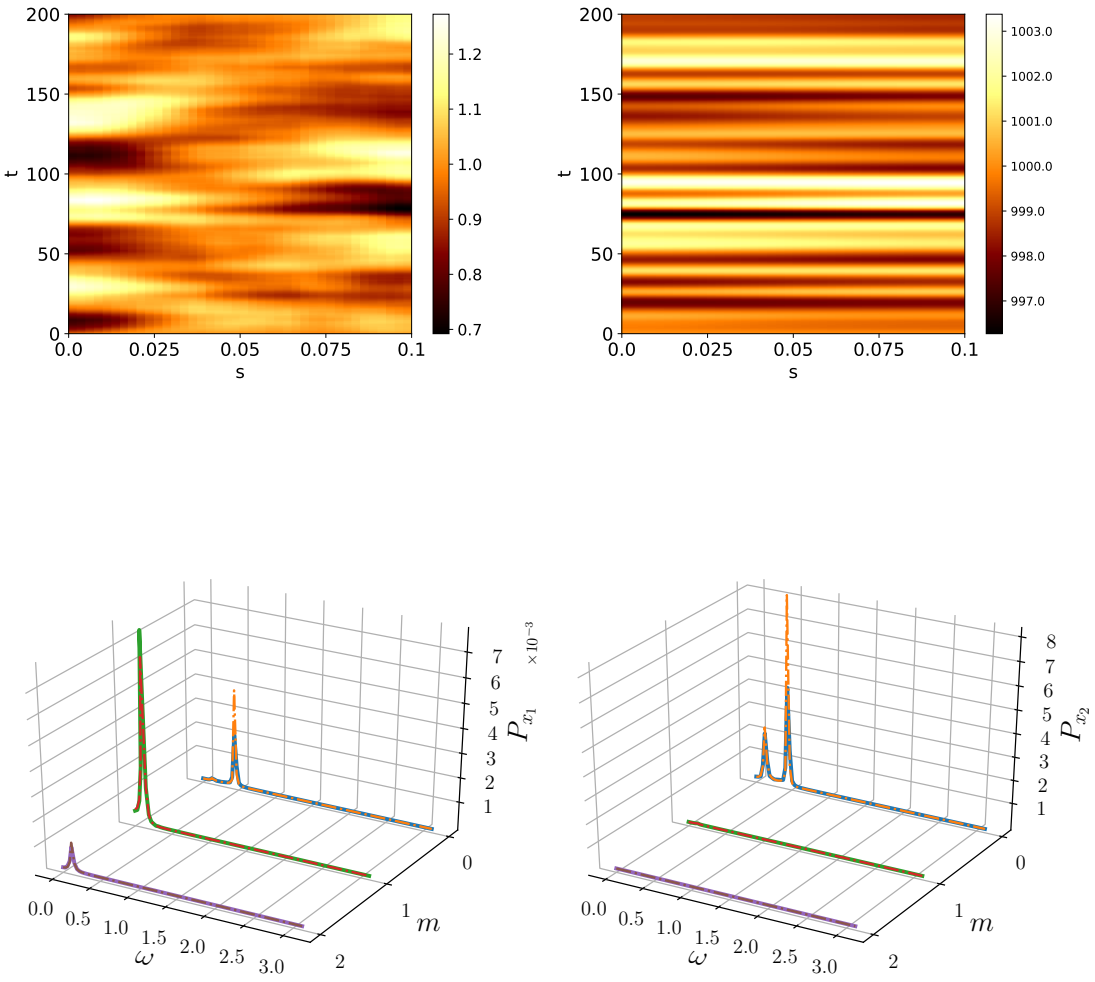


Figure 6.7: The power spectra for the species x_1 (left) and x_2 (right) with noise generated by a stochastic predator-prey network [McKane and Newman, 2005]. The power spectra inherited a second peak from the subsystem which activates oscillatory modes on top of the deterministic oscillation frequency. The spectra were averaged over 50 repetitions and simulation time $T = 200$ with m indexing the spatial mode. The subsystem size was $\Omega = 100$.

Letting $\tau_2 \to 0$ and computing the covariance matrix gives

$$N = \langle \hat{\eta}_k(\omega)\hat{\eta}_k(\omega)^\dagger \rangle = \begin{pmatrix} B_{k,11}\frac{1}{1+\omega^2\tau_1^2} & B_{k,12}\frac{1}{1+i\omega\tau_1} \\ B_{k,12}\frac{1}{1-i\omega\tau_1} & B_{k,22} \end{pmatrix}, \tag{6.52}$$

where $B_{k,ij}$ are the ij^{th} elements of the B_k matrix. Note that N is hermitian and therefore real power spectra for the patterns of x_1 and x_2 are expected.

Simulating equation (6.11) with the noise process described by (6.49) gives rise to the mixed patterns seen in Figure 6.8. Note that computationally the limit $\tau_2 \to 0$ is equal to setting τ_2 to the time step dt. The patterns of both species appear similar to the pure Ornstein-Uhlenbeck patterns, however, with reduced amplitude.

6.3.7 Reduced Stochastic Inflows

In the final subsection the case of only species x_1 being subjected to stochastic inflows is investigated. The species x_2 is assumed to only have deterministic inflow at a rate κ_2 and $\eta_2 = 0$. Hence, the correlation matrix N will be reduced to

$$N = \begin{pmatrix} \langle \hat{\eta}_{1k}\hat{\eta}_{1k}^* \rangle & 0 \\ 0 & 0 \end{pmatrix}. \tag{6.53}$$

In the noise processes studied in this chapter the behaviour of the species is virtually unchanged and the patterning is robust with respect to disregarding cross-correlations.

6.4 Conclusion

In this chapter the effect of stochastic inflows on a deterministic reaction-diffusion system was investigated. The class of networks considered was restricted to monostationary systems and results from the injectivity theory of polynomial maps were used to show how monostationarity is related to network structure. Further, a stochastic process for a perturbation to an inflow reaction was introduced. After linearising, the power spectra for arbitrary noise colours were computed and it was shown that in simple cases the correlated power spectra can be derived as a multiplicative factor. The remainder of the chapter consisted of applying the analysis to the Schnakenberg system and highlighting the effects various noise colours can have on a reaction-diffusion system.

The results from the white noise analysis were briefly restated before proceeding to add coloured noise and then demonstrating its effect by computing the power spectra. It was shown that, depending on the nature of the correlations, coloured noise

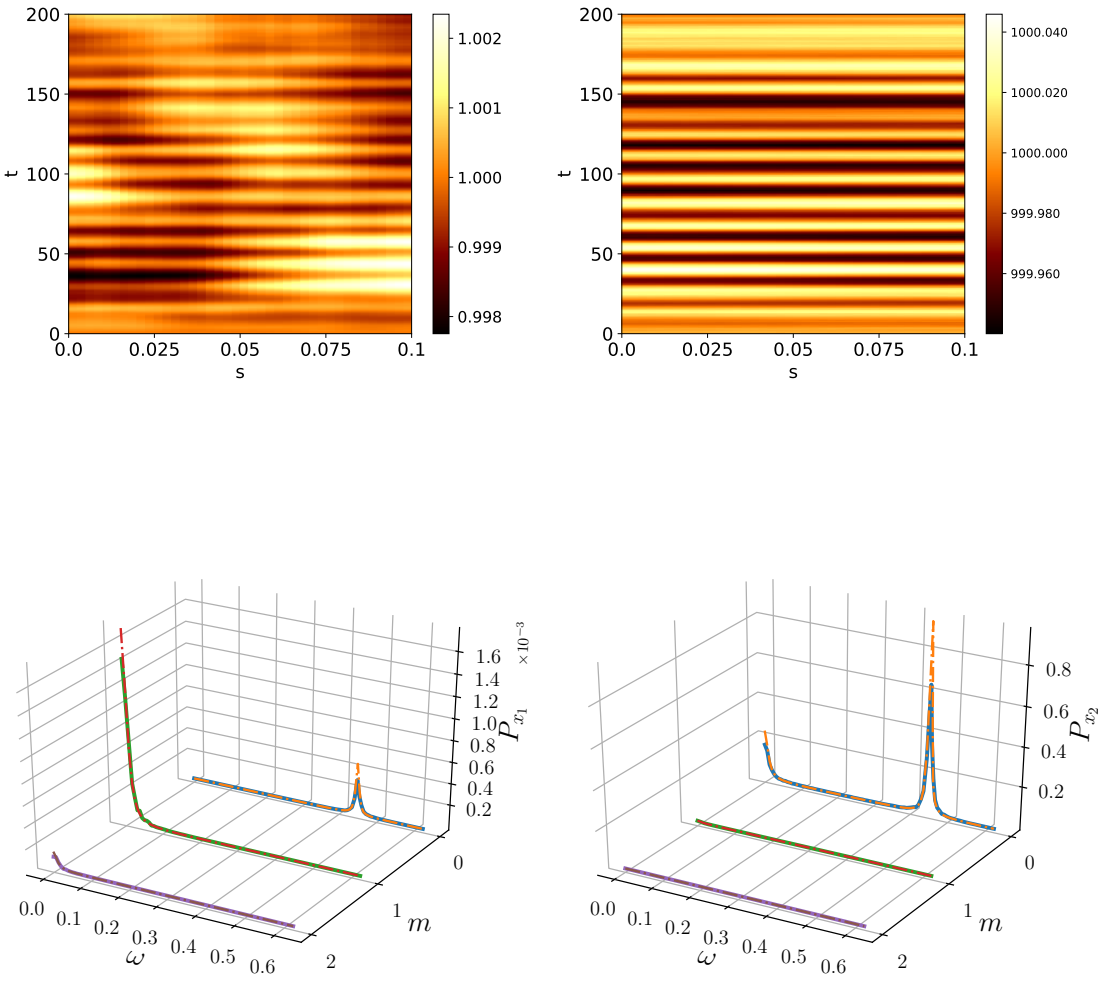


Figure 6.8: The patterns generated for the species x_1 (left) and x_2 (right) with Ornstein-Uhlenbeck noise and $\tau = 100$ for x_1 and x_2 with white noise.The patterns are phenomenologically similar to the Ornstein-Uhlenbeck patterns, however, with reduced amplitude. The power spectrum of x_2 is a mixture of white noise and Ornstein-Uhlenbeck noise. The power spectra were averaged over 50 simulations with simulation time $T = 1000$ and subsystem size $\Omega = 5000$.

as a multiplicative factor will suppress or excite temporal frequencies at all spatial modes. Ornstein-Uhlenbeck noise has a Lorentzian frequency distribution and, therefore, suppresses positive frequencies. Power law noise can either completely stabilise or destabilise the pattern depending on the sign of the exponent, α. This is due to the fact that for positive α temporal frequencies at $\omega = 0$ go to infinity and, therefore, all oscillations are suppressed, which results in a stable pattern that resembles a pattern arising from simulations inside the Turing regime. For the simulation times used in this chapter, the noise vector was actually constant, and, therefore, deterministic methods could be used to study the stabilising effect of pink or red noise. The opposite is the case for negative α, where the frequency contribution in the power spectrum increases as ω increases and oscillations are enhanced. However, certain aspects of the red, blue, or violet noise cases cannot be explained by the simple analytic prediction. The biological significance and the correct analytic description of blue/violet noise could form a part of further work.

When turning to stochastic auxiliary networks it can be seen that the reaction-diffusion system can inherit traits of the dynamics of the auxiliary network. In particular, it was shown that when the auxiliary network exhibits a predator-prey dynamic with stochastic oscillations, these oscillations can still be observed in the deterministic main network. The range of applications was concluded by considering mixed noise with Ornstein-Uhlenbeck input for species x_1 and white noise for species x_2. In this case, the system behaves similar to a system with pure Ornstein-Uhlenbeck dynamics and differences can only be found by a power spectral analysis. Finally, it was observed that, in the cases considered, when only one species experiences stochastic inflow the patterns created are, except for potential special cases, similar to the ones when the inflow to both species is randomised. However, the extent to which such results may hold in general is subject to further investigation.

Further directions could also include attempting to relate these studies to potential mechanisms of left-right symmetry breaking amplification in developmental biology. In particular, the impact of induced Nodal production on one side of the embryonic node, which is hypothesised to be driven by ciliary fluid flows, is also highly error-prone [Blum et al., 2014]. It is generally asserted that the resulting interactions of the gene products Nodal and Lefty, which are major contenders as Turing morphogens [Müller et al., 2012; Chen and Schier, 2002; Schier, 2003], amplify this initial error-prone signal to generate robust patterning, driving downstream developmental left-right asymmetry. However, the ability of Turing systems to amplify the spatially localised, error-prone, and thus stochastic, influx of activator morphogen [Blum et al.,

2014, Figure 2] to induce a robust symmetry breaking self-organisation, as well as any additional constraints required to do so, is theoretically untested. Thus examining the mechanistic basis of these postulates in this critical developmental biological process provides a fundamental application for the theoretical foundations developed here.

Chapter 7

Discussion and Future Research

"Das Glück der letzten Schritte auf einen Gipfel, den man sich jahrelang gewünscht hat, ist nicht beschreibbar."

– Oswald Oelz

Since the 1970s chemical reaction network theory has been used to derive general properties of reaction networks, such as their mono- or multistationarity, their ability for oscillations and their identifiability. Recent research has expanded its framework from non-spatial deterministic systems to spatial systems and even stochastic systems with intrinsic noise. In this Thesis, the algebraic approach to chemical reaction network theory was expanded and a novel perspective on the source of stochasticity in reaction models was introduced to study chemical reaction networks subject to extrinsic noise. To this end, the distinction was made between constant extrinsic noise, which manifests itself in unknown parameters and extrinsic noise as stochastic rate constants. This feature is often built into chemical reaction network theory, however hardly addressed from a stochastic modelling viewpoint. Further, time-varying extrinsic noise was considered, which can be shown to be similar, qualitatively, to intrinsic noise.

7.1 Summary of Thesis Results

Chapter 2 introduced the necessary mathematical tools for modelling the dynamics of chemical reaction networks and studying them from an algebraic viewpoint. Essential notions of chemical reaction network theory were introduced, such as the multiset definition with species, complexes and reactions. It was demonstrated how the law of mass action enables the conversion of a static network description to a polynomial dynamical system. Together with the concepts of reversibility and deficiency, dynamical properties were studied. Notions of commutative algebra, such as

Hilbert's Nullstellensatz and basis theorem, and algebraic geometry, such as varieties, irreducibility and associated primes were introduced to study the steady state properties of chemical reaction networks. Further, stochastic modelling frameworks were covered, especially Chemical Langevin Equations and power spectra. The chapter was concluded by outlining the two types of extrinsic noise studied in this thesis and introducing the mathematical assumptions used.

Chapters 3 and 4 focused on chemical reaction networks with arbitrary rate constants. The main goal was to find algebraic invariants which are independent of model parameters.

Chapter 3 studied families of graphs defining chemical reaction networks. In particular, if the families were assumed to have toric steady states for all family members, then their steady state invariants have particularly favourable properties independent of the model parameters. It was shown that the matrices describing the monomial parameterisations at steady state are submatrices of each other and, hence, that the associated matroids are submatroids. Furthermore, binomials were found which evaluate to zero at each positive steady state and, hence, it was shown that the variety generated by these polynomials agrees on the positive orthant with the steady state variety. From there, these binomials were used to study the problems of model rejection and parameter fitting. A main result of the chapter was the proof that multistationarity lifts from smaller members of the family to its larger members.

In Chapter 4 a parameter-independent invariant was studied, the Euclidean Distance (ED) degree. The ED degree describes the complexity of models and estimates the difficulty of model selection. The ED degree is independent of the model parameters and, therefore, robust even in the context of external noise. It was shown that for toric models a real, positive minimum can always be found. Closed form formulas were developed for several models with a varying number of reaction sites, some of which are families as described in the previous chapter. It was shown that for some models the ED degree stays constant, independent of the number of sites and for other models the ED degree rises linearly. A connection between the number of bi-molecular reactions and ED degree was theorised, but not proved.

Chapters 5 and 6 studied time-varying extrinsic noise and, in particular, stochastic inflow reactions. In both chapters a close connection between intrinsic and extrinsic noise was established.

In Chapter 5 the inflow reaction to an autocatalytic system was modelled by a stochastic rate constant and a general stochastic process for stochastic model parameters was outlined. It was shown that, under certain scaling assumptions, the extrinsic

noise model is mathematically equivalent to the intrinsic noise model, which was studied in previous research. A second result of the chapter was to introduce a graph theoretic method for counting the number of resonant modes in stochastic chemical reaction networks. It was applied to the autocatalytic networks and phase diagrams were plotted. In particular, it was shown that the phase diagrams for intrinsic and extrinsic noise models are identical as they only depend on the squared Jacobian matrix of the associated deterministic system. Simulations showed the quantitative differences between extrinsic and intrinsic noise models, in particular, the smaller oscillation amplitude in extrinsic noise systems.

Chapter 6 extended the framework of stochastic inflows to spatial systems subject to correlated noise. The first result of the chapter was the application of injectivity methods to find systems with only one steady state. This is important, as pattern forming systems and stochastic systems described by a Chemical Langevin Equation are treated in general by local theories and stochastic switching between steady states leads to unpredicted behaviour. It was shown that correlated, or coloured, extrinsic noise appears as a modulating factor in the power spectra of spatial systems. Further, it was highlighted that, depending on the noise colour, correlated noise can create patterns, destroy patterns or even induce oscillations. The source of the extrinsic fluctuations was taken to either be stochastic auxiliary networks in multi-scale models or experimental fluctuations. The analytic results were verified by example of the Schnakenberg system.

7.2 Further Work

Chapter 3 provides a collection of algebraic results which, in conjunction with perfect data, allow for parameter estimation and model rejection of large classes of biological models. An obvious further step in the analysis presented in that chapter would be the extension of these results to noisy data and to build a statistical theory to complement the algebraic results in a similar fashion to [MacLean et al., 2015]. The statistical theory could then be applied to steady state data of real world biological systems. A good candidate would be kinetic proofreading models. The most basic model, the McKeithan model, has been studied in this thesis and was shown to be toric for any number of reaction sites. However, there exist more complex models building on the McKeithan model, e.g. Dushek and van der Merwe [2014], which could form a promising set of candidate families for testing the framework. Further, in that chapter a sufficient condition for multistationarity was given, however, the

maximum number of steady states has a lower bound of 2 (if there was one positive steady state the network would by definition not be multistationary). It is known for phosphorylation networks that the maximum number of steady states rises linearly across the family. Inspired by this result, a general theorem on the maximum number of steady states in a family would be desirable. A further direction could be to investigate the definition of a family given in Chapter 3 in the context of the network modifications presented in Banaji and Pantea [2018]. In particular, a proof that any family construction as defined in Chapter 3 can be achieved by a series of network modifications as outlined in Banaji and Pantea [2018] could lead to novel insights not only into the steady state behaviour, but also the dynamics of the networks such as oscillations or stability of the steady states.

A possible future direction, which is tangentially related to the results of Chapter 3, is the study of extinction components, that is, irreducible components contained in one or more coordinate axes. Supposing a trajectory in a chemical reaction network is not constrained to stay in the positive orthant, but can enter the boundary, then extinction steady states are an important factor of the long term behaviour of the network. Hence, a systematic algebraic study of the extinction components of the steady state variety needs to be conducted.

Chapter 4 provided a proof-of-principle study of the application of the ED degree to chemical reaction networks, however, many open questions exist. For example, why does the ED degree rise linearly for some models and stay constant for other? A potential answer could combine the insights of Chapter 3 and Chapter 4 to obtain results on the degree of the toric varieties. A natural extension is the question as to which model features let the ED degree grow faster than linear? In Chapter 4 only models with mono- and bi-molecular reactions were studied and it is likely that multi-molecular reactions have a drastic impact on the functional form of the ED degree. Another possible future research direction is the design of custom methods tailored to the computation of real, positive minima.

Chapter 5 introduces stochastic resonance modes and stochastic rate constants. The phase diagrams calculated in that chapter were a refinement of the criteria of [Dauxois et al., 2009]. However, due to the fact that only the denominator of a rational function was studied, there are still false negatives. A possible future research direction is the study of the numerator of the power spectra in order to obtain even sharper criteria for resonances. Another part of future research could be the study of inflection points of the denominator of power spectra via resultants. Currently

it is assumed that inflection points do not occur for almost all choices of parameters, however, a rigorous proof of this claim should be provided. Further, in order to obtain analytic boundaries in parameter space for resonances, computationally intensive methods such as cylindrical algebraic decomposition (CAD) need to be used and finding algebraic methods circumventing CAD is highly desirable. A bottleneck in the algorithm for calculating the phase diagrams is finding the factors of a graph. Currently this is done by brute force methods, and development of a more efficient algorithm for symbolic calculation of minors of large, dense matrices could be one step to push the methods of Chapter 5 to larger networks. The largest source of error in the computational approach used in Chapter 5 is the substitution of numerical values into complicated rational functions and small numerical errors can propagate to a sign change in a polynomial coefficient. Hence, in particular for parameter checking, which is used, for example, in the bootstrap sampling for calculating a phase diagram, a new method which does not rely on symbolic calculations of the graph factors should be developed. There is also a wealth of future research directions relating to parameters as the source of noise. Although it was assumed that only inflow parameters were noisy, this restriction can easily be removed in an analytic framework and the algebraic and stochastic theory of chemical reaction networks with *every* parameter represented by a stochastic process is barely developed. To this end, the modelling of the noise stochasticity should be expanded to other positive probability distributions such as a log-normal or a gamma distribution. This would allow for more realistic modelling of noise processes as it removes the artificial truncation step, however, analytic predictions are harder to make.

Chapter 6 extends the question of stochastic parameters to spatial systems and, while there exists substantial overlap in possible future research directions with chapter 5, the implication that Turing patterns might have extrinsic origin could offer a starting point of experimental collaborations to show the existence of extrinsic Turing patterns. As stated in the conclusion of Chapter 6, further directions could also include attempting to extend the study to other symmetry breaking mechanisms in biology, such as the left-right symmetry breaking amplification in developmental biology. Extrinsic noise can also play a role in chemical systems and, in particular, experimental proof of the theoretical results in this thesis could be obtained by studying a number of controllable chemical reactions [Chen et al., 2013; Lengyel and Epstein, 1992]. Another possibility would be the joint modelling of intrinsic and extrinsic noise and the study of their respective effects.

References

Adamer, M. F., Harrington, H. A., Gaffney, E. A., and Woolley, T. E. (2020). Coloured noise from stochastic inflows in reaction-diffusion systems. *Bull. Math. Biol.*, 82(4):1–28.

Adamer, M. F. and Helmer, M. (2019a). Complexity of model testing for dynamical systems with toric steady states. *Adv. Appl. Math.*, 110:42 – 75.

Adamer, M. F. and Helmer, M. (2019b). Steady state invariants and multistationarity for families of toric reaction networks. *arXiv e-prints*, page arXiv:1906.03931.

Adamer, M. F., Woolley, T. E., and Harrington, H. A. (2017). Graph-facilitated resonant mode counting in stochastic interaction networks. *Jour. Roy. Soc. Interface*, 14(137):20170447.

Alberts, B., Johnson, A., Lewis, J., Raff, M., Roberts, K., and Walter, P. (2007). *Molecular biology of the cell: Reference edition*. Garland Science.

Anderson, D. F., Cappelletti, D., Koyama, M., and Kurtz, T. G. (2018). Non-explosivity of stochastically modeled reaction networks that are complex balanced. *Bull. Math. Biol.*, 80(10):2561–2579.

Anderson, D. F., Cappelletti, D., and Kurtz, T. G. (2017). Finite time distributions of stochastically modeled chemical systems with absolute concentration robustness. *SIAM Jour. Appl. Dyn. Sys.*, 16(3):1309–1339.

Anderson, D. F., Craciun, G., and Kurtz, T. G. (2010). Product-form stationary distributions for deficiency zero chemical reaction networks. *Bull. Math. Biol.*, 72(8):1947–1970.

Anderson, D. F., Enciso, G. A., and Johnston, M. D. (2014). Stochastic analysis of biochemical reaction networks with absolute concentration robustness. *Jour. Roy. Soc. Interface*, 11(93):20130943.

Angeli, D., Banaji, M., and Pantea, C. (2013). Combinatorial approaches to hopf bifurcations in systems of interacting elements. *Comm. Math. Sci.*, 12(6):1101–1133.

Angeli, D., De Leenheer, P., and Sontag, E. (2010). Graph-theoretic characterizations of monotonicity of chemical networks in reaction coordinates. *Jour. Math. Biol.*, 61(4):581–616.

Angeli, D., De Leenheer, P., and Sontag, E. D. (2007). A petri net approach to the study of persistence in chemical reaction networks. *Math. Biosciences*, 210(2):598–618.

Aoki, K., Yamada, M., Kunida, K., Yasuda, S., and Matsuda, M. (2011). Processive phosphorylation of erk map kinase in mammalian cells. *PNAS*, 108(31):12675–12680.

Arnon, D., Collins, G., and McCallum, S. (1984). Cylindrical algebraic decomposition I: the basic algorithm. *SIAM J. Comput.*, 13(4):865–877.

Ashyraliyev, M., Fomekong-Nanfack, Y., Kaandorp, J. A., and Blom, J. G. (2009). Systems biology: parameter estimation for biochemical models. *The FEBS journal*, 276(4):886–902.

Aubol, B. E., Chakrabarti, S., Ngo, J., Shaffer, J., Nolen, B., Fu, X.-D., Ghosh, G., and Adams, J. A. (2003). Processive phosphorylation of alternative splicing factor/splicing factor 2. *PNAS*, 100(22):12601–12606.

Baez, J. C. and Pollard, B. S. (2017). A compositional framework for reaction networks. *Rev. Math. Phys.*, 29(09):1750028.

Baker, R. E., Gaffney, E. A., and Maini, P. K. (2008). Partial differential equations for self-organization in cellular and developmental biology. *Nonlinearity*, 21(11):R251.

Banaji, M. (2018). Inheritance of oscillation in chemical reaction networks. *Appl. Math.and Comp.*, 325:191–209.

Banaji, M. and Craciun, G. (2010). Graph-theoretic criteria for injectivity and unique equilibria in general chemical reaction systems. *Adv. Appl. Math.*, 44(2):168–184.

Banaji, M. and Pantea, C. (2016). Some results on injectivity and multistationarity in chemical reaction networks. *SIAM Jour. Appl. Dyn. Sys.*, 15(2):807–869.

Banaji, M. and Pantea, C. (2018). The inheritance of nondegenerate multistationarity in chemical reaction networks. *SIAM Jour. Appl. Math.*, 78(2):1105–1130.

Banerjee, K. and Bhattacharyya, K. (2014). Open chemical reaction networks, steady-state loads and braess-like paradox. *ArXiv e-prints*.

Barajas-Solano, D. A. and Tartakovsky, A. M. (2016). Probabilistic density function method for nonlinear dynamical systems driven by colored noise. *Phys. Rev. E*, 93(5):052121.

Barrio, R. A., Varea, C., Aragón, J. L., and Maini, P. K. (1999). A two-dimensional numerical study of spatial pattern formation in interacting turing systems. *Bull. Math. Biol.*, 61(3):483–505.

Bartlett, M. S. (1957). Measles periodicity and community size. *Journal of the Royal Statistical Society. Series A (General)*, 120(1):48–70.

Bates, D. J., Hauenstein, J. D., Sommese, A. J., and Wampler, C. W. (2006). Bertini: Software for numerical algebraic geometry.

Biancalani, T., Fanelli, D., and Di Patti, F. (2010). Stochastic turing patterns in the brusselator model. *Phys. Rev. E*, 81(4):046215.

Biancalani, T., Galla, T., and McKane, A. J. (2011). Stochastic waves in a brusselator model with nonlocal interaction. *Phys. Rev. E*, 84:026201.

Bihan, F., Dickenstein, A., and Giaroli, M. (2018). Lower bounds for positive roots and regions of multistationarity in chemical reaction networks. *arXiv preprint arXiv:1807.05157*.

Blanchard, S. C., Gonzalez Jr, R. L., Kim, H. D., Chu, S., and Puglisi, J. D. (2004). trna selection and kinetic proofreading in translation. *Nature Struct. & Mol. Biol.*, 11(10):1008.

Blum, M., Feistel, K., Thumberger, T., and Schweickert, A. (2014). The evolution and conservation of left-right patterning mechanisms. *Development*, 141(8):1603–1613.

Briggs, W. and Henson, V. (1995). *The DFT: An Owner's Manual for the Discrete Fourier Transform*. Society for Industrial and Applied Mathematics.

Burack, W. R. and Sturgill, T. W. (1997). The activating dual phosphorylation of mapk by mek is nonprocessive. *Biochem.*, 36(20):5929–5933.

Butler, T. and Goldenfeld, N. (2011). Robust ecological pattern formation induced by demographic noise. *Phys. Rev. E*, 84:011112.

Cao, Y. and Erban, R. (2014). Stochastic turing patterns: Analysis of compartment-based approaches. *Bull. Math. Biol.*, 76(12):3051–3069.

Cappelletti, D. and Joshi, B. (2018). Graphically balanced equilibria and stationary measures of reaction networks. *SIAM Jour. Appl. Dyn. Sys.*, 17(3):2146–2175.

Cappelletti, D., Ortiz-Munoz, A., Anderson, D., and Winfree, E. (2018). Stochastic chemical reaction networks for robustly approximating arbitrary probability distributions. *arXiv preprint arXiv:1810.02854*.

Cappelletti, D. and Wiuf, C. (2016). Product-form poisson-like distributions and complex balanced reaction systems. *SIAM Jour. Appl. Math.*, 76(1):411–432.

Cappelletti, D. and Wiuf, C. (2017). Uniform approximation of solutions by elimination of intermediate species in deterministic reaction networks. *SIAM Jour. Appl. Dyn. Sys.*, 16(4):2259–2286.

Casanellas, M., Fernández-Sánchez, J., and Michałek, M. (2017). Local equations for equivariant evolutionary models. *Adv. in Math.*, 315:285–323.

Chen, Y. and Schier, A. F. (2002). Lefty proteins are long-range inhibitors of squint-mediated nodal signaling. *Curr. Biol.*, 12(24):2124–2128.

Chen, Y.-J., Dalchau, N., Srinivas, N., Phillips, A., Cardelli, L., Soloveichik, D., and Seelig, G. (2013). Programmable chemical controllers made from dna. *Nature Nanotech.*, 8(10):755.

Chis, O.-T., Banga, J. R., and Balsa-Canto, E. (2011). Structural identifiability of systems biology models: a critical comparison of methods. *PloS one*, 6(11):e27755.

Clarke, B. L. (1974). Graph theoretic approach to the stability analysis of steady state chemical reaction networks. *Jour. Chem. Phys.*, 60(4):1481–1492.

Cohen, P. (2001). The role of protein phosphorylation in human health and disease. *Eur. Jour. Biochem.*, 268(19):5001–5010.

Compagnoni, M., Canclini, A., Bestagini, P., Antonacci, F., Sarti, A., and Tubaro, S. (2015). Tdoa denoising for acoustic source localization. *CoRR, vol. abs/1509.02380*.

Compagnoni, M., Notari, R., Antonacci, F., and Sarti, A. (2014). A comprehensive analysis of the geometry of tdoa maps in localization problems. *Inv. Prob.*, 30(3):035004.

Condat, L. and Hirabayashi, A. (2014). Cadzow denoising upgraded: A new projection method for the recovery of dirac pulses from noisy linear measurements. *STSIP*, 14(1):17–47.

Conradi, C., Feliu, E., Mincheva, M., and Wiuf, C. (2017). Identifying parameter regions for multistationarity. *PLoS Comp. Biol.*, 13(10):e1005751.

Conradi, C., Iosif, A., and Kahle, T. (2018). Multistationarity in the space of total concentrations for systems that admit a monomial parametrization. *arXiv preprint arXiv:1810.08152*.

Conradi, C., Saez-Rodriguez, J., Gilles, E.-D., and Raisch, J. (2005). Using chemical reaction network theory to discard a kinetic mechanism hypothesis. *IEE Proc. Sys. Biol.*, 152(4):243–248.

Conradi, C. and Shiu, A. (2015). A global convergence result for processive multisite phosphorylation systems. *Bull. Math. Biol.*, 77(1):126–155.

Conradi, C. and Shiu, A. (2018). Dynamics of post-translational modification systems: recent progress and future directions. *Biophys. Jour.*, 114(3):507–515.

Cox, D., Little, J., and O'Shea, D. (2013). *Ideals, varieties, and Algorithms*. Springer Science & Business Media.

Cox, D. A., Little, J., and O'shea, D. (2006). *Using Algebraic Geometry*, volume 185. Springer Science & Business Media.

Cox, D. A., Little, J. B., and Schenck, H. K. (2011). *Toric Varieties*. American Mathematical Society.

Craciun, G., Dickenstein, A., Shiu, A., and Sturmfels, B. (2009a). Toric dynamical systems. *Jour. Symb. Comp.*, 44(11):1551–1565.

Craciun, G., Kim, J., Pantea, C., and Rempala, G. A. (2013a). Statistical model for biochemical network inference. *Commun. Stat.-Sim. Comp.*, 42(1):121–137.

Craciun, G., Nazarov, F., and Pantea, C. (2013b). Persistence and permanence of mass-action and power-law dynamical systems. *SIAM Jour. Appl. Math.*, 73(1):305–329.

Craciun, G. and Pantea, C. (2008). Identifiability of chemical reaction networks. *Journal of Mathematical Chemistry*, 44(1):244–259.

Craciun, G., Pantea, C., and Rempala, G. A. (2009b). Algebraic methods for inferring biochemical networks: a maximum likelihood approach. *Comp. Biol. and Chem.*, 33(5):361–367.

Dauxois, T., Di Patti, F., Fanelli, D., and McKane, A. J. (2009). Enhanced stochastic oscillations in autocatalytic reactions. *Phys. Rev. E*, 79(3):036112.

De Kepper, P., Epstein, I. R., Kustin, K., and Orban, M. (1982). Systematic design of chemical oscillators. part 8. batch oscillations and spatial wave patterns in chlorite oscillating systems. *Jour. Phys. Chem.*, 86(2):170–171.

Deshaies, R. J. and Ferrell Jr, J. E. (2001). Multisite phosphorylation and the countdown to s phase. *Cell*, 107(7):819–822.

Dickenstein, A. (2016). Biochemical reaction networks: An invitation for algebraic geometers. In *Mathematical Congress of the Americas*, volume 656, pages 65–83. American Mathematical Soc.

Dickenstein, A., Pérez-Millán, M., Shiu, A., and Tang, X. (2019). Multistationarity in structured reaction networks. *Bull. Math. Biol.*, pages 1–55.

Diego, X., Marcon, L., Müller, P., and Sharpe, J. (2018). Key features of turing systems are determined purely by network topology. *Phys. Rev. X*, 8(2):021071.

Domijan, M. (2008). *Mathematical aspects of chemical reaction networks*. PhD thesis, University of Warwick.

Draisma, J., HorobeŢ, E., Ottaviani, G., Sturmfels, B., and Thomas, R. R. (2016). The euclidean distance degree of an algebraic variety. *Found. Comp. Math.*, 16(1):99–149.

Drescher, K., Goldstein, R. E., and Tuval, I. (2010). Fidelity of adaptive phototaxis. *PNAS*, 107(25):11171–11176.

Dushek, O. and van der Merwe, P. A. (2014). An induced rebinding model of antigen discrimination. *Trends Immunol.*, 35(4):153–158.

Eisenbud, D. and Sturmfels, B. (1996). Binomial ideals. *Duke Math. Jour.*, 84(1):1–45.

Elowitz, M. B., Levine, A. J., Siggia, E. D., and Swain, P. S. (2002). Stochastic gene expression in a single cell. *Science*, 297(5584):1183–1186.

Engblom, S. (2009). Spectral approximation of solutions to the chemical master equation. *Jour. Comp. and Appl. Math.*, 229(1):208–221.

Erban, R. and Chapman, J. (2009). Stochastic modelling of reaction–diffusion processes: algorithms for bimolecular reactions. *Phys. Biol.*, 6(4):046001.

Erban, R., Chapman, J., and Maini, P. K. (2007). A practical guide to stochastic simulations of reaction-diffusion processes. *arXiv preprint arXiv:0704.1908*.

Escudero, C. (2009). Stochastic growth equations on growing domains. *Jour. Stat. Mech.*, 2009(07):P07020.

Farina, M., Findeisen, R., Bullinger, E., Bittanti, S., Allgower, F., and Wellstead, P. (2006). Results towards identifiability properties of biochemical reaction networks. In *Proc. IEEE Conf. Dec. Contr.*, pages 2104–2109. IEEE.

Faugere, J.-C., Gianni, P., Lazard, D., and Mora, T. (1993). Efficient computation of zero-dimensional gröbner bases by change of ordering. *Jour. Symb. Comp.*, 16(4):329–344.

Feinberg, M. (1987). Chemical reaction network structure and the stability of complex isothermal reactors—i. the deficiency zero and deficiency one theorems. *Chem. Eng. Sci.*, 42(10):2229–2268.

Feinberg, M. (1988). Chemical reaction network structure and the stability of complex isothermal reactors-ii. multiple steady states for networks of deficiency one. *Chem. Eng. Sci.*, 43(1):1–25.

Feinberg, M. (1995). The existence and uniqueness of steady states for a class of chemical reaction networks. *Arch. Rat. Mech. Anal.*, 132(4):311–370.

Feliu, E. and Wiuf, C. (2013). Simplifying biochemical models with intermediate species. *Jour. Roy. Soc. Interface*, 10(87):20130484.

Félix, B., Shiu, A., and Woodstock, Z. (2016). Analyzing multistationarity in chemical reaction networks using the determinant optimization method. *Appl. Math. Comput.*, 287-288:60–73.

Ferrell, J. E. and Bhatt, R. R. (1997). Mechanistic studies of the dual phosphorylation of mitogen-activated protein kinase. *Jour. Biol. Chem.*, 272(30):19008–19016.

Filippi, S., Barnes, C., Kirk, P., Kudo, T., McMahon, S., Tsuchiya, T., Wada, T., Kuroda, S., and Stumpf, M. (2015). Origins of cell-to-cell variability, kinetic proofreading and the robustness of mapk signal transduction. *bioRxiv*, page 021790.

Flach, E. H., Schnell, S., and Norbury, J. (2007). Turing pattern outside of the turing domain. *Appl. Math. Lett.*, 20(9):959–963.

Flockerzi, D., Holstein, K., and Conradi, C. (2014). N-site phosphorylation systems with 2n-1 steady states. *Bull. Math. Biol.*, 76(8):1892–1916.

Fløystad, G., Kileel, J., and Ottaviani, G. (2018). The chow form of the essential variety in computer vision. *Jour. of Symb. Comp.*, 86:97–119.

Fox, R. F. (1986a). Functional-calculus approach to stochastic differential equations. *Phys. Rev. A*, 33(1):467.

Fox, R. F. (1986b). Uniform convergence to an effective fokker-planck equation for weakly colored noise. *Phys. Rev. A*, 34(5):4525.

Frank, S. A. (2013). Input-output relations in biological systems: measurement, information and the hill equation. *Biol. Direct*, 8:31.

Friedland, S. and Stawiska, M. (2013). Best approximation on semi-algebraic sets and k-border rank approximation of symmetric tensors. *arXiv preprint arXiv:1311.1561*.

Friedland, S. and Stawiska, M. (2014). Some approximation problems in semi-algebraic geometry. *arXiv preprint arXiv:1412.3178*.

Fulton, W. (1993). *Introduction to Toric Varieties*. Princeton University Press.

García-Ojalvo, J. and Sancho, J. M. (1994). Colored noise in spatially extended systems. *Phys. Rev. E*, 49(4):2769.

García-Ojalvo, J. and Sancho, J. M. (1996). External fluctuations in a pattern-forming instability. *Phys. Rev. E*, 53(6):5680.

Gardiner, C. W. (1985). *Handbook of Stochastic Methods*, volume 3. Springer Berlin.

Gelfand, I. M., Kapranov, M., and Zelevinsky, A. (2008). *Discriminants, Resultants, and Multidimensional Determinants*. Springer Science & Business Media.

Gerstl, M. P., Müller, S., Regensburger, G., and Zanghellini, J. (2018). Flux tope analysis: studying the coordination of reaction directions in metabolic networks. *Bioinf.*, 35(2):266–273.

Gierer, A. and Meinhardt, H. (1972). A theory of biological pattern formation. *Kybernetik*, 12(1):30–39.

Gillespie, D. T. (1976). A general method for numerically simulating the stochastic time evolution of coupled chemical reactions. *J. Comput. Phys.*, 22(4):403–434.

Gillespie, D. T. (1977). Exact stochastic simulation of coupled chemical reactions. *Jour. Phys. Chem.*, 81(25):2340–2361.

Gillespie, D. T. (1992). A rigorous derivation of the chemical master equation. *Physica A*, 188(1-3):404–425.

Gillespie, D. T. (2007). Stochastic simulation of chemical kinetics. *Annu. Rev. Phys. Chem.*, 58:35–55.

Gleiss, P. M., Stadler, P. F., Wagner, A., and Fell, D. A. (2001). Relevant cycles in chemical reaction networks. *Adv. Comp. Sys.*, 4(02n03):207–226.

Goldbeter, A. and Koshland, D. E. (1981). An amplified sensitivity arising from covalent modification in biological systems. *PNAS*, 78(11):6840–6844.

Goldbeter, A. and Koshland, D. E. (1984). Ultrasensitivity in biochemical systems controlled by covalent modification. interplay between zero-order and multistep effects. *Jour. Biol. Chem.*, 259(23):14441–14447.

Grimmet, G. R. and Stirzaker, D. R. (1982). *Probability statistics and random processes*. Oxford University Press.

Gross, E., Davis, B., Ho, K. L., Bates, D. J., and Harrington, H. A. (2016a). Numerical algebraic geometry for model selection and its application to the life sciences. *Roy.Soc. Interface*, 13(123):20160256.

Gross, E., Harrington, H. A., Meshkat, N., and Shiu, A. (2018). Joining and decomposing reaction networks. *arXiv preprint arXiv:1810.05575*.

Gross, E., Harrington, H. A., Rosen, Z., and Sturmfels, B. (2016b). Algebraic systems biology: a case study for the Wnt pathway. *Bull. Math. Biol.*, 78(1):21–51.

Gual, P., Le Marchand-Brustel, Y., and Tanti, J.-F. (2005). Positive and negative regulation of insulin signaling through irs-1 phosphorylation. *Bioch.*, 87(1):99–109.

Gunawardena, J. (2003). Chemical reaction network theory for in-silico biologists. *Notes available for download at http://vcp. med. harvard. edu/papers/crnt. pdf*.

Gürsoy, G., Terebus, A., Cao, Y., and Liang, J. (2016). Stochastic focusing and defocusing in biological reaction networks: Lessons learned from accurate chemical master equation (acme) solutions. *Biophys. Jour.*, 110(3):316a.

Hänggi, P. and Jung, P. (1994). Colored noise in dynamical systems. *Adv. Chem. Phys.*, 89:239–326.

Hansen, M. C. and Wiuf, C. (2018). Existence of a unique quasi-stationary distribution for stochastic reaction networks. *arXiv preprint arXiv:1808.06833*.

Harary, F. (1969). *Graph Theory*. Addison-Wesley, Reading.

Harary, F. (2005). *Structural Models: An Introduction to the Theory of Directed Graphs*. John Wiley & Sons Inc.

Harrington, H. A., Ho, K. L., and Meshkat, N. (2016). Differential algebra for model comparison. *arXiv preprint arXiv:1603.09730*.

Harrington, H. A., Ho, K. L., Thorne, T., and Stumpf, M. P. H. (2012). Parameter-free model discrimination criterion based on steady-state coplanarity. *PNAS*, 109(39):15746–15751.

Hartshorne, R. (2013). *Algebraic geometry*, volume 52. Springer Science & Business Media.

Helmer, M. and Sturmfels, B. (2016). Nearest points on toric varieties. *arXiv preprint arXiv:1603.06544*.

Hochberg, D., Lesmes, F., Morán, F., and Pérez-Mercader, J. (2003). Large-scale emergent properties of an autocatalytic reaction-diffusion model subject to noise. *Phys. Rev. E*, 68(6):066114.

Holstein, K., Flockerzi, D., and Conradi, C. (2013). Multistationarity in sequential distributed multisite phosphorylation networks. *Bull. Math. Biol.*, 75(11):2028–2058.

Hopfield, J. J. (1974). Kinetic proofreading: a new mechanism for reducing errors in biosynthetic processes requiring high specificity. *PNAS*, 71(10):4135–4139.

Horn, F. (1972). Necessary and sufficient conditions for complex balancing in chemical kinetics. *Arch. Rat. Mech. Anal.*, 49(3):172–186.

Horn, F. and Jackson, R. (1972). General mass action kinetics. *Arch. Rat. Mech. Anal.*, 47(2):81–116.

Iacovache, I., Bischofberger, M., and van der Goot, F. G. (2010). Structure and assembly of pore-forming proteins. *Curr. Opin. Struct. Biol.*, 20(2):241–246.

Iron, D., Wei, J., and Winter, M. (2004). Stability analysis of turing patterns generated by the schnakenberg model. *J. Math. Biol.*, 49(4):358–390.

Isaacson, S. A. (2009). The reaction-diffusion master equation as an asymptotic approximation of diffusion to a small target. *SIAM Jour. Appl. Math.*, 70(1):77–111.

Jolliffe, I. (2011). *Principal Component Analysis*. Springer.

Joshi, B. (2013). A detailed balanced reaction network is sufficient but not necessary for its markov chain to be detailed balanced. *arXiv preprint arXiv:1312.4196*.

Joshi, B. and Shiu, A. (2012). Simplifying the jacobian criterion for precluding multistationarity in chemical reaction networks. *SIAM Jour. Appl. Math.*, 72(3):857–876.

Joshi, B. and Shiu, A. (2013). Atoms of multistationarity in chemical reaction networks. *Jour. Math. Chem.*, 51(1):153–178.

Joshi, B. and Shiu, A. (2015). A survey of methods for deciding whether a reaction network is multistationary. *Mathematical Modelling of Natural Phenomena*, 10(5):47–67.

Kang, H.-W., Zheng, L., and Othmer, H. G. (2012). A new method for choosing the computational cell in stochastic reaction–diffusion systems. *Jour. Math. Biol.*, 65(6-7):1017–1099.

Karp, R. L., Millán, M. P., Dasgupta, T., Dickenstein, A., and Gunawardena, J. (2012). Complex-linear invariants of biochemical networks. *Journal of theoretical biology*, 311:130–138.

Kim, H. and Gelenbe, E. (2012). Stochastic gene expression modeling with hill function for switch-like gene responses. *IEEE Comp. Biol. and Bioinfor.*, 9(4):973–979.

Kloeden, P. E. and Platen, E. (1995). *Numerical solution of stochastic differential equations*. Springer-Verlag.

Kurtz, T. G. (1972). The relationship between stochastic and deterministic models for chemical reactions. *Jour. Chem. Phys.*, 57(7):2976–2978.

Lang, S. (2002). *Algebra*. Springer.

Lee, A. A., Senior, M. J., Wallace, M. I., Woolley, T. E., and Griffiths, I. M. (2016). Dissecting the self-assembly kinetics of multimeric pore-forming toxins. *Jour. Roy. Soc. Interface*, 13(114):20150762.

Lengyel, I. and Epstein, I. R. (1992). A chemical approach to designing turing patterns in reaction-diffusion systems. *PNAS*, 89(9):3977–3979.

Lenive, O., Kirk, P. D. W., and Stumpf, M. P. H. (2016). Inferring extrinsic noise from single-cell gene expression data using approximate bayesian computation. *BMC Sys. Biol.*, 10(1):81.

Lin, C.-M., Jiang, T. X., Baker, R. E., Maini, P. K., Widelitz, R. B., and Chuong, C.-M. (2009). Spots and stripes: pleomorphic patterning of stem cells via p-erk-dependent cell chemotaxis shown by feather morphogenesis and mathematical simulation. *Dev. Biol.*, 334(2):369–382.

Los, F. C. O., Randis, T. M., Aroian, R. V., and Ratner, A. J. (2013). Role of pore-forming toxins in bacterial infectious diseases. *Microbiol. Mol. Biol. Rev.*, 77(2):173–207.

Lotka, A. J. (1925). *Elements of Physical Biology*. Williams & Wilkins Co., Baltimore.

Lugo, C. A. and McKane, A. J. (2008). Quasicycles in a spatial predator-prey model. *Phys. Rev. E*, 78(5):051911.

M. L. Simpson, C. D. Cox, and G. S. Sayler (2004). Frequency domain chemical langevin analysis of stochasticity in gene transcriptional regulation. *J. Theor. Biol.*, 229(3):383–394.

Ma, C.-T., Velazquez-Dones, A., Hagopian, J. C., Ghosh, G., Fu, X.-D., and Adams, J. A. (2008). Ordered multi-site phosphorylation of the splicing factor asf/sf2 by srpk1. *Jour. Mol. Biol.*, 376(1):55–68.

MacLean, A. L., Rosen, Z., Byrne, H. M., and Harrington, H. A. (2015). Parameter-free methods distinguish wnt pathway models and guide design of experiments. *PNAS*, 112(9):2652–2657.

Maini, P. K., Woolley, T. E., Baker, R. E., Gaffney, E. A., and Lee, S. S. (2012). Turing's model for biological pattern formation and the robustness problem. *Interface Foc.*, 2(4):487–496.

Matheson, I., Walls, D. F., and Gardiner, C. W. (1975). Stochastic models of firstorder nonequilibrium phase transitions in chemical reactions. *Jour. Stat. Phys.*, 12(1):21–34.

Maybee, J. S., Olesky, D. D., van Den Driessche, P., and Wiener, G. (1989). Matrices, digraphs, and determinants. *SIAM J. Matrix Anal. A.*

McKane, A. J., Biancalani, T., and Rogers, T. (2014). Stochastic pattern formation and spontaneous polarisation: the linear noise approximation and beyond. *Bull. of Math. Biol.*, 76(4):895–921.

McKane, A. J. and Newman, T. J. (2005). Predator-prey cycles from resonant amplification of demographic stochasticity. *Phys. Rev. Lett.*, 94(21):218102.

Mckeithan, T. W. (1995). Kinetic proofreading in t-cell receptor signal transduction. *PNAS*, 92(11):5042–5046.

Meshkat, N., Anderson, C., and DiStefano III, J. J. (2011). Finding identifiable parameter combinations in nonlinear ode models and the rational reparameterization of their input–output equations. *Math. Biosci.*, 233(1):19–31.

Meshkat, N., Eisenberg, M., and DiStefano III, J. J. (2009). An algorithm for finding globally identifiable parameter combinations of nonlinear ode models using gröbner bases. *Math. Biosci.*, 222(2):61–72.

Meshkat, N., Rosen, Z., and Sullivant, S. (2018). Algebraic tools for the analysis of state space models. In *The 50th Anniversary of Gröbner Bases*, pages 171–205. Mathematical Society of Japan.

Meshkat, N. and Sullivant, S. (2014). Identifiable reparametrizations of linear compartment models. *Jour. Symb. Comp.*, 63:46–67.

Michaelis, L. and Menten, M. L. (1913). Die Kinetik der Invertinwirkung. *Biochem. Z.*, 49:333–369.

Míguez, D. G., Dolnik, M., Munuzuri, A. P., and Kramer, L. (2006). Effect of axial growth on turing pattern formation. *Physical review letters*, 96(4):048304.

Millán, M. P., Dickenstein, A., Shiu, A., and Conradi, A. (2012). Chemical reaction systems with toric steady states. *Bull. Math. Biol.*, 74(5):1027–1065.

Miller, S. and Childers, D. (2012). *Probability and Random Processes: With Applications to Signal Processing and Communications*. Academic Press.

Milshtein, G. N. and Tretyakov, M. V. (1994). Numerical solution of differential equations with colored noise. *J. Stat. Phys.*, 774(3).

Mincheva, M. and Craciun, G. (2008). Multigraph conditions for multistability, oscillations and pattern formation in biochemical reaction networks. *Proc. IEEE*, 96(8):1281–1291.

Mincheva, M. and Roussel, M. R. (2006). A graph-theoretic method for detecting potential turing bifurcations. *Journ. Chem. Phys.*, 125(20):204102.

Mincheva, M. and Roussel, M. R. (2007). Graph-theoretic methods for the analysis of chemical and biochemical networks. I. multistability and oscillations in ordinary differential equation models. *J. Math. Biol.*, 55(1):61–86.

Mincheva, M. and Siegel, D. (2004). Stability of mass action reaction–diffusion systems. *Nonl. Anal.*, 56(8):1105–1131.

Mittmann, J. (2013). *Independence in algebraic complexity theory*. PhD thesis, Universitäts-und Landesbibliothek Bonn.

Mobilia, M. (2010). Oscillatory dynamics in rock-paper-scissors games with mutations. *J. Theor. Biol.*, 264(1):1–10.

Mohamed, F., Pantea, C., and Tudorascu, A. (2018). Chemical reaction-diffusion networks: convergence of the method of lines. *Jour. Math. Chem.*, 56(1):30–68.

Müller, P., Rogers, K. W., Jordan, B. M., Lee, J. S., Robson, D., Ramanathan, S., and Schier, A. F. (2012). Differential diffusivity of nodal and lefty underlies a reaction-diffusion patterning system. *Science*, 336(6082):721–724.

Müller, S., Feliu, E., Regensburger, G., Conradi, C., Shiu, A., and Dickenstein, A. (2016). Sign conditions for injectivity of generalized polynomial maps with applications to chemical reaction networks and real algebraic geometry. *Found. Comput. Math.*, 16(1):69–97.

Mumford, D. (1995). *Algebraic Geometry I: Complex Projective Varieties*. Springer Science & Business Media.

Mumford, D. (1999). *The Red Book of Varieties and Schemes*, volume 1358. Springer Science & Business Media.

Munsky, B. and Khammash, M. (2006). The finite state projection algorithm for the solution of the chemical master equation. *Jour. Chem. Phys.*, 124(4):044104.

Murray, J. D. (1982). Parameter space for turing instability in reaction diffusion mechanisms: a comparison of models. *Jour. Theor. Biol.*, 98(1):143–163.

Murray, J. D. (2002). *Mathematical Biology: I. An Introduction*. Springer, 2nd edition.

Murray, J. D. (2008). *Mathematical Biology II - Spatial Models and Biomedical Applications*, volume 18 of *Interdisciplinary Applied Mathematics*. Springer-Verlag, New York, 3 edition.

Murray, J. D. and Oster, G. F. (1984). Cell traction models for generating pattern and form in morphogenesis. *Jour. Math. Biol.*, 19(3):265–279.

Mycielska, M. E. and Djamgoz, M. B. A. (2004). Cellular mechanisms of direct-current electric field effects: galvanotaxis and metastatic disease. *J. Cell. Sci.*, 117(9):1631–1639.

Nagase, T., Nagase, M., Machida, M., and Yamagishi, M. (2007). Hedgehog signaling. *Annal. NY Acad. Sci.*, 1101(1):412–438.

Nash, P., Tang, X., Orlicky, S., Chen, Q., Gertler, F. B., Mendenhall, M. D., Sicheri, F., Pawson, T., and Tyers, M. (2001). Multisite phosphorylation of a cdk inhibitor sets a threshold for the onset of dna replication. *Nature*, 414(6863):514.

Nisbet, R. M. and Gurney, W. (2003). *Modelling fluctuating populations: reprint of first Edition (1982)*. Blackburn Press.

Noy, M. and Ribó, A. (2004). Recursively constructible families of graphs. *Adv. Appl. Math.*, 32(1-2):350–363.

Ottaviani, G., Spaenlehauer, P.-J., and Sturmfels, B. (2014). Exact Solutions in Structured Low-Rank Approximation. *SIAM Jour. Mat. Anal. and Appl.*, 4:1521–1542.

Oxley, J. G. (2006). *Matroid Theory*, volume 3. Oxford University Press, USA.

Palsson, B. Ø. (2006). *Systems Biology: Properties of Reconstructed Networks*. Cambridge university press.

Pérez-Millán, M. and Dickenstein, A. (2018). The structure of messi biological systems. *SIAM Jour. Appl. Dyn. Sys.*, 17(2):1650–1682.

Picco, N., Sahai, E., Maini, P. K., and Anderson, A. R. A. (2017). Integrating models to quantify environment-mediated drug resistance. *Cancer Research*, 77(19):5409–5418.

Piene, R. (1978). Polar classes of singular varieties. *Annales Scientifiques de l'Ecole Normale Superieure*, 11(2):247–276.

Plesa, T., Erban, R., and Othmer, H. G. (2018). Noise-induced mixing and multimodality in reaction networks. *Europ. Jour. Appl. Math.*, pages 1–25.

Radde, N., Bar, N. S., and Banaji, M. (2010). Graphical methods for analysing feedback in biological networks–a survey. *Int. Jour. Sys. Sci.*, 41(1):35–46.

Roberts, R., Timchenko, N. A., Miller, J. W., Reddy, S., Caskey, C. T., Swanson, M. S., and Timchenko, L. T. (1997). Altered phosphorylation and intracellular distribution of a (cug) n triplet repeat rna-binding protein in patients with myotonic dystrophy and in myotonin protein kinase knockout mice. *PNAS*, 94(24):13221–13226.

Rosado, C. J., Buckle, A. M., Law, R. H. P., Butcher, R. E., Kan, W.-T., Bird, C. H., Ung, K., Browne, K. A., Baran, K., and Bashtannyk-Puhalovich, T. A. a. (2007). A common fold mediates vertebrate defense and bacterial attack. *Science*, 317(5844):1548–1551.

Rosen, Z. (2014). Computing algebraic matroids. *arXiv preprint arXiv:1403.8148*.

Rosen, Z. (2015). *Algebraic Matroids in Applications*. PhD thesis, UC Berkeley.

Rubinstein, B. Y., Mattingly, H. H., Berezhkovskii, A. M., and Shvartsman, S. Y. (2016). Long-term dynamics of multisite phosphorylation. *Mol. Biol. of the Cell*, 27(14):2331–2340.

Sadeghimanesh, A. H. and Feliu, E. (2018). The multistationarity structure of networks with intermediates and a binomial core network. *arXiv preprint arXiv:1808.07548*.

Sage, A., Tintut, Y., Garfinkel, A., and Demer, L. (2009). Systems biology of vascular calcification. *Trends Cardiov. Med.*, 19(4):118–123.

Sage Developer Team (2016). Sagemath.

Sagués, F., Sancho, J. M., and García-Ojalvo, J. (2007). Spatiotemporal order out of noise. *Rev. Mod. Phys.*, 79(3):829.

Salazar, C. and Höfer, T. (2009). Multisite protein phosphorylation – from molecular mechanisms to kinetic models. *The FEBS Journal*, 276(12):3177–3198.

Sato, K., Ito, Y., Yomo, T., and Kaneko, K. (2003). On the relation between fluctuation and response in biological systems. *PNAS*, 100(24):14086–14090.

Scarsoglio, S., Laio, F., D'Odorico, P., and Ridolfi, L. (2011). Spatial pattern formation induced by gaussian white noise. *Math. Biosci.*, 229(2):174–184.

Schier, A. F. (2003). Nodal signaling in vertebrate development. *Annu. Rev. Cell Dev. Biol.*, 19(1):589–621.

Schnakenberg, J. (1979). Simple chemical reaction systems with limit cycle behaviour. *Jour. Theor. Biol.*, 81(3):389–400.

Schumacher, L. J., Woolley, T. E., and Baker, R. E. (2013). Noise-induced temporal dynamics in turing systems. *Phys. Rev. E*, 87(4):042719.

Shinar, G. and Feinberg, M. (2010). Structural sources of robustness in biochemical reaction networks. *Science*, 327(5971):1389–1391.

Sick, S., Reinker, S., Timmer, J., and Schlake, T. (2006). Wnt and dkk determine hair follicle spacing through a reaction-diffusion mechanism. *Science*, 314(5804):1447–1450.

Smith, G. D. (1985). *Numerical solution of partial differential equations, Finite difference methods*. Clarendon Press.

Snijder, B. and Pelkmans, L. (2011). Origins of regulated cell-to-cell variability. *Nature Rev. Mol. Cell Biol.*, 12(2):119.

Sontag, E. D. (2001). Structure and stability of certain chemical networks and applications to the kinetic proofreading model of t-cell receptor signal transduction. *IEEE Trans. Aut. Cont.*, 46(7):1028–1047.

Stegeman, A. and Friedland, S. (2017). On best rank-2 and rank-(2,2,2) approximations of order-3 tensors. *Lin. and Multilin. Alg.*, 65(7):1289–1310.

Stein, W. A. et al. (2016). *Sage Mathematics Software (Version 7.2)*. The Sage Development Team. `http://www.sagemath.org`.

Struik, D. J. (2014). *A Source Book in Mathematics, 1200-1800*. Princeton University Press.

Sturm, J. C. F. (1829). Mémoire sur la résolution des équations numériques. *Bull. des Sci. Férussac*, 11:419–425.

Sturmfels, B. (1996). *Gröbner Bases and Convex Polytopes*, volume 8. American Mathematical Society.

Swain, P. S., Elowitz, M. B., and Siggia, E. D. (2002). Intrinsic and extrinsic contributions to stochasticity in gene expression. *PNAS*, 99(20):12795–12800.

Szendro, P., Vincze, G., and Szasz, A. (2001). Bio-response to white noise excitation. *Electro- and Magnetobiology*, 20(2):215–229.

Temkin, O. N., Zeigarnik, A. V., and Bonchev, D. G. (1996). *Chemical reaction networks: a graph-theoretical approach*. CRC Press.

Timmer, J. and Koenig, M. (1995). On generating power law noise. *Astronomay and Astrophysics*, 300:707.

Togashi, Y. and Kaneko, K. (2001). Transitions induced by the discreteness of molecules in a small autocatalytic system. *Phys. Rev. Lett.*, 86(11):2459–2462.

Togashi, Y. and Kaneko, K. (2003). Alteration of chemical concentrations through discreteness-induced transitions in small autocatalytic systems. *J. Phys. Soc. Jpn.*, 72(1):62–68.

Toner, D. L. K. and Grima, R. (2013). Molecular noise induces concentration oscillations in chemical systems with stable node steady states. *J. Chem. Phys.*, 138(5):055101.

Trager, M., Hebert, M., and Ponce, J. (2015). The joint image handbook. In *Proc. IEEE int. conf. on comp. vis.*, pages 909–917.

Turing, A. M. (1952). The chemical basis of morphogenesis. *Bull. Math. Biol.*, 52(1-2):153–197.

van der Schaft, A., Rao, S., and Jayawardhana, B. (2015). Complex and detailed balancing of chemical reaction networks revisited. *Jour. Math. Chem.*, 53(6):1445–1458.

van Kampen, N. G. (1983). *Stochastic Processes in Physics and Chemistry*. Elsevier.

Van Vu, T. and Hasegawa, Y. (2019a). An algebraic method to calculate parameter regions for constrained steady-state distribution in stochastic reaction networks. *Chaos*, 29(2):023123.

Van Vu, T. and Hasegawa, Y. (2019b). Diffusion-dynamics laws in stochastic reaction networks. *Phys. Rev. E*, 99(1):012416.

Velazquez-Dones, A., Hagopian, J. C., Ma, C.-T., Zhong, X.-Y., Zhou, H., Ghosh, G., Fu, X.-D., and Adams, J. A. (2005). Mass spectrometric and kinetic analysis of asf/sf2 phosphorylation by srpk1 and clk/sty. *Jour. Biol. Chem.*, 280(50):41761–41768.

Verschelde, J. (1999). Algorithm 795: Phcpack: A general-purpose solver for polynomial systems by homotopy continuation. *ACM Transactions on Mathematical Software (TOMS)*, 25(2):251–276.

Vlysidis, M. and Kaznessis, Y. (2018). On differences between deterministic and stochastic models of chemical reactions: Schlögl solved with zi-closure. *Entropy*, 20(9):678.

Voskoboinik, I., Smyth, M. J., and Trapani, J. A. (2006). Perforin-mediated target-cell death and immune homeostasis. *Nat. Rev. Immunol.*, 6(12):940.

Waas, W. F., Lo, H.-H., and Dalby, K. N. (2001). The kinetic mechanism of the dual phosphorylation of the atf2 transcription factor by p38 mitogen-activated protein (map) kinase α implications for signal/response profiles of map kinase pathways. *Jour. Biol. Chem.*, 276(8):5676–5684.

Walter, E. (2014). *Identifiability of parametric models*. Elsevier.

Wang, W. and Chen, L. (1997). A predator-prey system with stage-structure for predator. *Comput. Math. with Appl.*, 33(8):83–91.

Ward, M. J. and Wei, J. (2002). The existence and stability of asymmetric spike patterns for the schnakenberg model. *Stud. Appl. Math.*, 109(3):229–264.

Weber, M. F. and Frey, E. (2017). Master equations and the theory of stochastic path integrals. *Rep. Prog. Phys.*, 80(4):046601.

Wei, J. (1999). On single interior spike solutions of the gierer–meinhardt system: uniqueness and spectrum estimates. *Europ. Jour. Appl. Math.*, 10(4):353–378.

Wolfram Research, Inc. (2010). *Mathematica 11.0*. `https://www.wolfram.com`.

Woolley, T. E., Baker, R. E., Gaffney, E. A., and Maini, P. K. (2011a). Influence of stochastic domain growth on pattern nucleation for diffusive systems with internal noise. *Phys. Rev. E*, 84(4):041905.

Woolley, T. E., Baker, R. E., Gaffney, E. A., and Maini, P. K. (2011b). Power spectra methods for a stochastic description of diffusion on deterministically growing domains. *Phys. Rev. E*, 84(2):021915.

Woolley, T. E., Baker, R. E., Gaffney, E. A., and Maini, P. K. (2011c). Stochastic reaction and diffusion on growing domains: understanding the breakdown of robust pattern formation. *Phys. Rev. E*, 84(4):046216.

Woolley, T. E., Baker, R. E., Gaffney, E. A., Maini, P. K., and Seirin-Lee, S. (2012). Effects of intrinsic stochasticity on delayed reaction-diffusion patterning systems. *Phys. Rev. E*, 85(5):051914.

Woolley, T. E., Baker, R. E., and Maini, P. K. (2017). Turing's theory of morphogenesis: where we started, where we are and where we want to go. In *The Incomputable*, pages 219–235. Springer.

Xavier, D. (2013). *On the theory of cell migration: durotaxis and chemotaxis*. PhD thesis, Universitat Politcnica de Catalunya.

Yochelis, A., Tintut, Y., Demer, L. L., and Garfinkel, A. (2008). The formation of labyrinths, spots and stripe patterns in a biochemical approach to cardiovascular calcification. *New Jour. Phys.*, 10(5):055002.

Yoshida, T., Jones, L. E., Ellner, S. P., Fussmann, G. F., and Hairston, N. G. (2003). Rapid evolution drives ecological dynamics in a predator–prey system. *Nature*, 424(6946):303–306.

Yu, P. Y. and Craciun, G. (2018). Mathematical analysis of chemical reaction systems. *Israel Jour. Chem.*, 58(6-7):733–741.

Ziegler, G. M. (2012). *Lectures on Polytopes*, volume 152. Springer Science & Business Media.